The Role of Phosphatidylglycerol in Streptomycete Growth and Development

By

Maeidh Awad Alotaibi

A thesis submitted in fulfilment of the requirements for the degree of Doctor of Philosophy in Strathclyde Institute of Pharmacy and Biomedical Sciences

2015

Declaration

“This thesis is the result of the author’s original research. It has been composed by the author and has not been previously submitted for examination which has led to the award of a degree”.

Signed:

Date:

Acknowledgements

As always, all praises and thanks to Allah almighty for all strengths and blessings in completing this thesis. After that I am very grateful to my supervisor Dr. Paul Herron for his excellent supervision and continuous support. Always his positive feedback and suggestions during the thesis work have led to the success of this project. I can't thank him enough for encouraging me to continue in the right direction. I benefited a lot from his professional and academic experience which helped me to enhance my thesis. I also would like to thank Dr. Nicholas Tucker for his great advice in times of need.

Also, I'd like to thank all my microbiology group mates from the past and the present specially Leena, John, Zhenyu, Alison, Charles, Tia, Sara, Richard, Andy, Jana, Florence and Richard. Without their assistance and kindness, this success would not have been achieved.

I am very thankful for the government of Saudi Arabia for awarding me a scholarship allowing me such an opportunity to gain knowledge and experience as well as achieve my life's dream. Unforgettably, it is such wonderful experiences, for me and my family to experience different lifestyle and cold weather. Also I'm very grateful to all friends whom I met in Glasgow for their friendship and companionship.

I would like to thank my father and my mother who have supported me by doing everything they could for the whole my life of education; they are the source of my strength and success. Many thanks also go to my supportive brothers and sisters who encouraged me to achieve my dreams. Special thanks would be for my beloved wife, I'm very speechless to thank her for her patience and support during the time of my study, I can only say thank you very much from the bottom of my heart, also to my little daughters who made my life colourful during the hard time of the study. Lastly, for the memory of my little angel MALAK who is still alive in my heart, this thesis is dedicated to her.

Abstract

Phosphatidylglycerol (PG) is an important component of membranes and is found in bacteria. As Streptomycetes have a large amount of the PG in their cell membranes, in this study we have focused on the gene *SCO5753* (*pgsA*) from the model organism *Streptomyces coelicolor*, whose product is predicted to synthesize PG the precursor of CL. Mutations in the phosphatidylglycerol-3-phosphate synthase (*PgsA*) operon were introduced by using the procedure for *in vitro* transposon mutagenesis, and gene disruptions in the *pgsA* operon could not be achieved which indicated the essentiality of this operon in *S. coelicolor* development and growth. This gene was inserted under the control of an inducible promoter *tipA*, to understand the effect of over production of PG in *Streptomyces*. It showed poor development of growth on agar, except if provided with expression of the promoter. The importance of PG in the osmotic adaptation of wild type *S. coelicolor* culture was investigated. Phospholipids were extracted and the appearance of spots on thin layer chromatography plates (TLC) after separation by chloroform/methanol/acetic acid/water (80/12/15/4) showed that the proportion of PG increased during growth of these bacteria in media containing high amounts of KCl within 24 hours.

Table of Contents

List of Figures

List of Tables

List of Symbols and Abbreviations

~:	More or less
°C:	Degress Celsius
3MA:	Minimal medium & mannitol
A:	Adenine
Am:	Apramycin
Ap:	Ampicillin
BLAST:	Basic local alignment tool
Bp:	Base pairs
C:	Cytosine
CDP-DAG:	Cytidine-diphosphate-diacylglycerol
Chp:	Chaplin
CI	Confidence Interval
CL:	Cardiolipin
Cls:	Cardiolipin synthase
EDTA:	Ethylendiaminotetraacetic acid
EGFP:	Enhanced green fluorescent protein
Etbr:	Ethidium bromide
g:	Gram
G:	Guanine
Hyg:	Hygromycin
k:	Kilo
Kb:	Kilobase
Km:	Kanamycin
L:	Litre
LB:	Luria Bertani
M:	Molar
ml:	Milliliters
mM:	Millimolar
NA:	Naldixic acid
ng:	Nanogrames

OD:	Optical density
PA:	Phosphatidic acid
PCR:	Polymerase chain reaction
PE:	Phosphatidylethanolamine
PG:	Phosphatidylglycerol
PG3P	Phosphatidylglycerol-3-phosphate
PgP:	Phosphatidylglycerol phosphate phosphatase
PgsA:	Phosphatidylglycerol-3-phosphate synthase
PI:	Phosphatidylinositol
pmol:	Picamolar
RNase:	Ribonuclease
rpm:	Revolutions per minute
SAM	*S*-Adenosyl methionine
SDS:	Sodium deodecyl sulphate
SDW:	Sterile distilled water
SEM	Standard error of mean
sp:	Species
Spec:	Spectinomycin
T:	Thymine
Tet:	Tetracycline
TLC:	Thin layer chromatography
Tm:	Melting temperature
Tris:	Trishydroxymethylaminomethane
Tsr:	Thiostrepton
U:	Uracil
v/v:	Volume to volume ratio
V:	Volt
w/v:	Weight to volume ratio
w/w:	Weight to weight ratio
W:	Watt
WGA:	Wheat germ agglutinin
X-gal:	5-Bromo-4-chloro-3-indoyl-β-D-galactoside

YEME:	Yeast extract-malt extract medium
α:	Alpha
β:	Beta
Δ:	Mutant
λ:	Lambda
µ:	Micro
µg:	Micrograms
µl:	Microliters
µm:	Micrometres
σ:	Sigma

Chapter 1:

Introduction

1. Introduction

1.1 Introduction to *Streptomyces*

Prokaryotic cell life styles diverge from that of eukaryotes cells in some fundamental ways in that development of prokaryotic cells is often a reaction to nitrogen, carbon and/or phosphorus limitations. Although not controlled directly by nutritional signals, long-term oligotrophic growth possibly instituted the need for cellular development in bacteria. Cellular growth causes alterations in cellular structure that are different to the parent despite containing the same genetic content (Shimkets, 2014). The relationship of the organism to its environment is essential and conditional for every biological system. On the nature of cellular intelligence, however, it is not immediately clear if there is a fundamental approach to sensing the surroundings in prokaryotic cells. The molecular approaches established in bacterial signalling are very different, ranging from simple transcriptional activators (single proteins containing two domains) to the many component and pathway signalling cascades that activate important steps of the cell cycle, for instance in biofilm formation, dormancy, sporulation, pathogenesis or flagellar biosynthesis (Marijuán et al., 2010). The prokaryotic life cycles are divided based on the function of cell development into three types of growth: dormancy, nutrient acquisition, and dispersal. An example of dormancy growth is aerial spore formation in *Streptomyces* (Shimkets, 2014).

Actinomycetes are significant in clinical situations; some human pathogenic agents belong to the taxonomic order of the actinomycetes such as *Mycobacterium tuberculosis* (tuberculosis), *Mycobacterium leprae* (leprosy) and *Corynebaterium diphtheriae* (diphtheria). Exploring the developmental biology of *Streptomyces* could inform on significant features of the biology of these pathogens. Moreover, streptomycetes are of great industrial importance because of their ability to produce antibiotics (Bignell et al., 2005, Kato et al., 2007, Dyson, 2009).

This thesis explores the role of PG in the growth and development of streptomycetes. *Streptomyces* is one of 120 genera in the order *Actinomycetales.* From the 1870s when the first actinomycetes were discovered up to the late 1950s, they were thought

to fall between bacteria and fungi. However, in fact they are the largest genus of Gram positive bacteria in the phylum of *Actinobacteria*. They are also characterised by a high G+C content in their DNA, frequently over 70%. This is in comparison with other Gram positive bacteria such as *Staphylococcus*, *Streptococcus*, and *Bacillus* with a G+C content of less than 50%. There are a number of reasons why *Streptomyces* are fascinating and significant to explore, but perhaps most importantly they differ from most bacteria in that they possess a complex life cycle of development involving some morphological differences of cell types such as rounded spores, branching hyphae that produce a mycelium and aerial filaments that become spore chains (Hopwood, 2006, Dyson, 2009).

From the perspective of basic research, *Streptomyces* has a developmentally complex life cycle that provides a multi-cellular prokaryotic model that contains programed cell death phenomena that perhaps provides the evolutionary basis of some genes that contribute to eukaryotic apoptosis. In the context of applications, streptomycetes form a wide range of secondary metabolites for agricultural and medical purposes, various anticancer drugs, as well as several eukaryotic cell differentiation effectors of large cells including apoptosis inducers and inhibitors (Yague et al., 2012). These natural products include clinically-important antibiotics (tetracyclines, streptomycins, & β-lactams), immunosuppressants (FK506/520 & rapamycin) and anti-cancer drugs (doxorubicin). The association between development and antibiotic formation in lab-scale bioreactors has also been defined. Morphological development in liquid culture is similar to that taking place during pre-sporulation periods in solid media. This development was one of the keys to understand biophysical fermentation parameters and to improve metabolite formation by *Streptomyces coelicolor* via optimization of the development of the antibiotic forming mycelium (Rioseras et al., 2014).

S. coelicolor, the model organism upon which this thesis is focused, is the species of *Streptomyces* that has been best characterised (Bentley et al., 2002). It is the most genetically investigated species of the streptomycetes and since the 1960s, it has been the focus of research in the field of prokaryotic developmental biology (Chater,

2001, Chater and Chandra, 2006, Elliot et al., 2008, Hopwood, 2006). The genome of *S. coelicolor* was sequenced in 2002 and has a large chromosome of 8 Mb (Bentley et al., 2002). The genome of streptomycetes differs from that of many other actinomycetes as the chromosomes of members of this genus have acquired the capability to replicate as a linear structure (Paradkar et al., 2003). The chromosome of this organism has a centrally placed origin of replication (*oriC*) that is close to *dnaA* and *gyrB* that encode respectively the replication initiation protein and DNA gyrase (Jakimowicz et al., 1998, Zakrzewska-Czerwinska et al., 1995). The *oriC* region has a somewhat higher content of A-T sequences than the rest of the chromosome, is characterised by bacterial replication origins and contains 19 conserved DnaA boxes (Jakimowicz et al., 1998). The ends of chromosomes are comprised of inverted terminal repeats (TIRs) ranging in size from 20-500bp (Lin et al., 1993, Lezhava et al., 1995, Pandza et al., 1997). However, in general, these sequences are not conserved between streptomycetes, with the exception of the first 200bp, which are rich in palindromic sequences (Yang et al., 2002, Huang et al., 1998). The expansion of the chromosome has supported *S. coelicolor* with a vast selection of genes which allow the bacteria a more complex life cycle and also the capacity to adjust to various surrounding conditions (Bentley et al., 2002). While both *S. coelicolor* and *M. tuberculosis* are classified under the order of actinomycetes even with differences in their lifestyles, their genomes have revealed great similarity in the synteny of many genes, operons and gene clusters (Bentley et al., 2002).

1.2 Life cycle of *S. coelicolor*

The selection of spore production when nutrients become available in the adjacent environment is a survival approach and leaves bacteria belonging to the genus *Streptomyces* with the capability to proliferate. Streptomycetes exist abundantly in nature and are mainly soil bacteria, while their spores remain dormant for long time until the surrounding environment becomes suitable for growth (Flärdh and Buttner, 2009, Hopwood, 2006). The lifecycle of *Streptomyces* is shown in (Figure1-1). When a spore encounters an environment suitable for growth, it germinates. This is the first stage of morphological differentiation in the life cycle (Elliot et al., 2008, Flärdh and Buttner, 2009). A germ tube develops from the spore and extends into long,

branching filamentous cells in vegetative growth, producing hyphae with a mesh appearance and are named the substrate or vegetative mycelium that grow into solid media. Hyphal elongation is achieved by the insertion of new cell wall material at the hyphal tip (Chater, 1998, Kelemen and Buttner, 1998). At the tips of vegetatively growing *S. coelicolor* hyphae, DivIVA is the earliest known protein to be specifically located (Flärdh, 2010, Flärdh, 2003). This DivIVA protein, which is activated by AfsK, plays an important part in controlling tip growth and commencement of new branches of hyphae in order to produce the vegetative mycelium. Therefore, DivIVA performs as a landmark protein that recruits the cell wall biosynthetic machinery directly or indirectly to new the hyphal tip (Hempel et al., 2012, Hempel et al., 2008, Flärdh and Buttner, 2009, Flärdh, 2003), and its partial deletion leads to poor extension and abnormal vegetative hyphal morphology (Flärdh, 2003). Occasional cross walls divide the hyphae into cellular compartments. Every compartment has many copies of the chromosome and DNA is extended in the entire compartment with little partitioning of individual nucleoids (Hopwood, 2006). Septation commonly requires the assembly of the cell division protein, FtsZ at multiple intervals in the hyphae that dictate the places to which other division proteins will be recruited (McCormick, 2009). Once the vegetative mycelium growth has developed into a colony, nutrient restriction and, most likely, cell density signals, participate in activating aerial mycelium formation on the colony surface (Figure1-1) (Chater, 1998, Kelemen and Buttner, 1998). The aerial hyphae appear as reproductive structures and are converted into pigmented spore chains that mature and, ultimately, free separated spores (Figure 1-1).

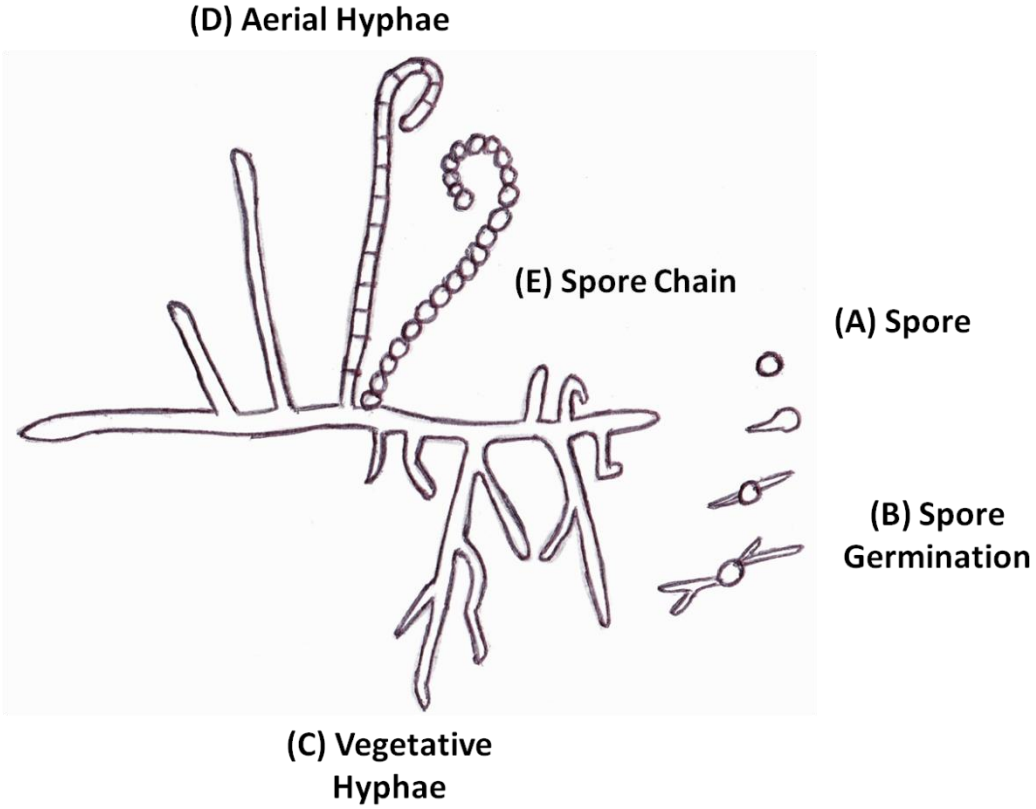

Figure 1-1: The *S. coelicolor* life cycle.

The figure was modified from (Ruban-Osmialowska et al., 2006): *Streptomyces* colonies are comprised of several differentiated cell types. A spore (A) typically produces more than one germ tube (B) that extends by tip growth and generates new hyphae by branching (C). Due to nutrient limitation, the vegetative hyphae make branches that elongate into the air (D). Then these aerial hyphae divide by sporulation septa into compartments to form spore chains (E) (Hopwood, 2006).

Sporulation of the aerial hyphae is limited to the apical compartment known as the sporogenic cell (Figure 1.2) in which a large number of DNA replications occur, producing up to 50 copies of uncondensed DNA, evenly dispersed along the entire sporogenic cell (Ruban-Osmialowska et al., 2006). A developmentally regulated production of cell division proteins results in sporulation septation and compartmentalises the sporogenic cell into prespores (Figure 1.2C). In coordination with this spore formation, the chromosomes are spaced and partitioned, so that every prespore compartment obtains one copy of the genome (Figure 1.2C) (Flardh, 2003).

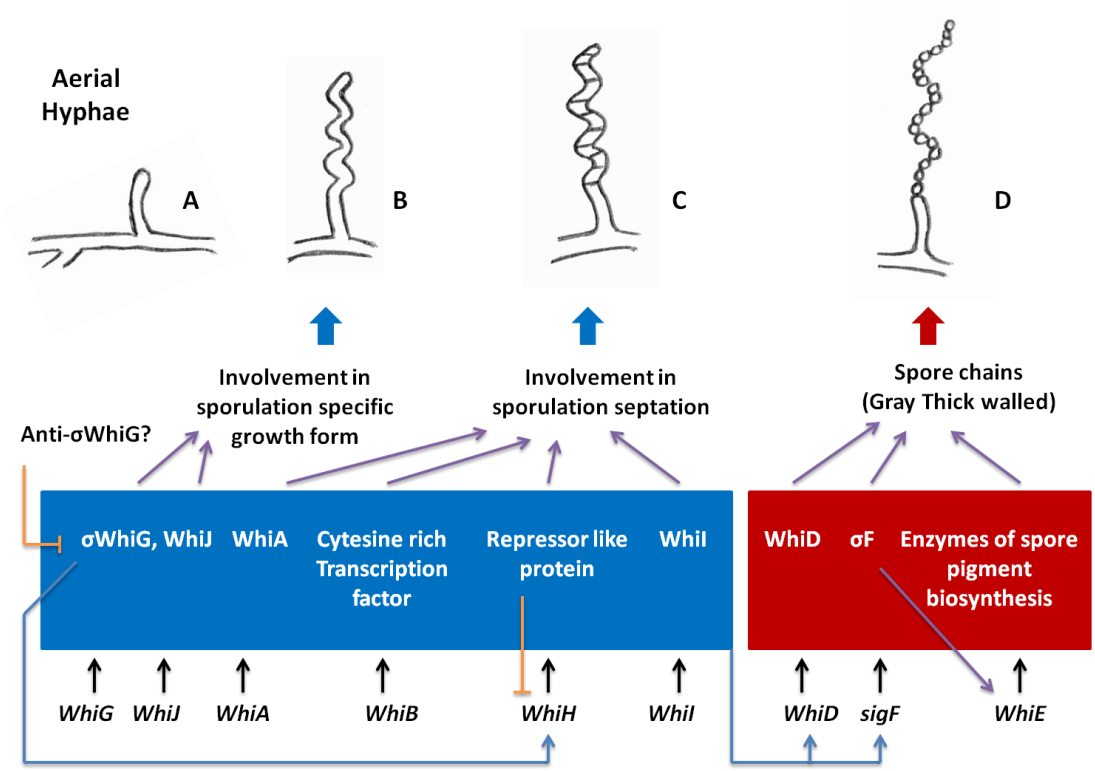

Figure 1-2: An overview of the function and the nature of aerial hyphal phenotypes in early *whi* mutants, during sporulation in *S. coelicolor*.

Modified from (Chater, 1998).

1.3 Morphological development in *S. coelicolor*

1.3.1 Aerial hyphae formation

Streptomycetes are mycelial organisms that are different from most other bacteria. The complete mechanism of aerial mycelium erection remains unclear, whereas the mechanisms of mycelial growth in fungi have been intensively studied. These bacteria develop by apical extension to generate a mycelium of branched hyphae. Most apical development at hyphal tips takes place through *de novo* integration of peptidoglycan precursors at the growing cell wall (Prosser and Tough, 1991, Gray et al., 1990, Brana et al., 1982, Flardh, 2003). Vegetative hyphae form new sites of growth through the creation of branches from the lateral wall, frequently in sub-apical cells that are divided from the tip by a cross wall.

Streptomyces hyphae grow by tip extension and this polarised growth is controlled by a cluster of proteins named the polarisome, also named the tip organising centre (TIPOC). The three identified polarisome proteins are DivIVA, which is vital for the organism growth, and two dispensable cytoskeletal proteins that also have important functions in tip extension, Scy and FilP (Hempel et al., 2012, Holmes et al., 2013). All three members of the polarisome interact together directly and Scy has been proposed to work as a molecular scaffold for the other constituents (Holmes et al., 2013). The intermediate filament forming protein, FilP is controlled by DivIVA and localises at the hyphal tip just after DivIVA (Fuchino et al., 2013).

Another protein associated with the polarisome is CslA, which encodes a putative cellulose synthase that is located at hyphal tips (De Jong et al., 2009, Xu et al., 2008). CslA is thought to support developing tips by cellulose formation and deletion of *cslA* results in an extreme delay in the production of aerial hyphae (Xu et al., 2008, De Jong et al., 2009). Although *cslA* expression is mostly not changed in a *whiA* mutant, there is a 2-fold enhancement of expression at a late period in growth (20 h) and it is proposed that WhiA represses *cslA.* This gene emerges as the initial gene of a bicistronic operon as well as *glxA*, which encodes a galactose oxidase involved in normal aerial growth during osmotic stress. Despite this, the two genes are co-transcribed, although *glxA* is also regulated by an independent promoter

within the coding sequence of *clsA* (Liman et al., 2013, Bush et al., 2013). ParA has been observed to produce filaments that initiate from the tip and elongate down the sporogenic cell and it is proposed that it organises ParB binding to DNA before septation (Jakimowicz et al., 2007, Jakimowicz and van Wezel, 2012). Recently, this system of development has been revealed to be coordinated by an interaction between ParA and Scy, one of the constituents of the polarisome that controls tip elongation in vegetative and aerial hyphae (Ditkowski et al., 2013).

The control of sporulation appears primarily in studies of two important types of regulatory genes involved in morphological developmental in *S. coelicolor*. They have been recognised through genetic studies of mutants blocked in aerial mycelium formation. The first type is the *whi* (white) genes, which are involved in the production of the spores in the aerial mycelium. However, although *whi* mutants form aerial hyphae, they are not able to produce the gray spore-related pigment and for that reason have a phenotype of a white colony (Chater, 1972, Hopwood et al., 1970). The second type of genes, named *bld* (bald), is involved in the erection of aerial hyphae and the colonies of these mutants have a shiny and bald form. Many *bld* mutants have been identified, such as *bldA, bldB, bldC, bldD, bldF, bldG, bldH, bldI, bldK and bldM*. These mutants demonstrate pleiotropic effects including cell signalling and antibiotic production inhibition (Kim et al., 2004). The *bld* and *whi* genes are engaged in complex regulatory networks that control growth in *Streptomyces*. It is not completely understood how the *bld* genes perform in these networks to form aerial mycelium and to what degree the *bld* genes and *whi* genes interact to initiate further aerial hyphae growth that engages the *whi* genes and directs them to the production of spores (Chater, 1972, Hopwood et al., 1970).

As well as the peptidoglycan of the cell wall, *S. coelicolor* spores and aerial hyphae contain an additional outer layer of amphipathic proteins, termed chaplins (*coelicolor* hydrophobic aerial proteins), and rodlins, associated with the hydrophobicity of the aerial hyphal surface (Claessen et al., 2002, Elliot et al., 2003). Streptomycete aerial hyphae and spores have a surface layer, termed the rodlet layer, with a characteristic ultra-structure and form an 8–10-nm wide parallel mosaic of rods. Two homologous

proteins, the rodlins RdlA and RdlB, are necessary for the production of this layer. RdlA and RdlB are secreted in the growing aerial hyphal cell wall, where they produce a homogenous insoluble surface layer. There is a depletion of expression of both *rdl* genes in the absence of the rodlet layer with no effect on the surface hydrophobicity (Claessen et al., 2003).

In addition, the activity of the rodlins in the formation of aerial hyphae is based on both the secreted proteins, chaplins (Claessen et al., 2004, Capstick et al., 2007) and the lantibiotic SapB, which is an amphiliphilic 'antibiotic-like' small secreted peptide. These molecules also accumulate on the surface of the developing substrate hyphae and connect to the aerial hyphae (Kodani et al., 2004, Willey et al., 1993, Guijarro et al., 1988, Willey et al., 1991). Their capability of lowering the water surface tension is most likely needed for aerial hyphae to emerge from an aqueous environment into the air (Willey et al., 1993, Willey et al., 1991). SapB is a morphogenetic peptide that is encoded by *ramS* and undergoes extensive post-translational modifications, probably mediated by the putative lantibiotic synthetase RamC (Willey et al., 2006, Kodani et al., 2004). The chaplins are eight secreted proteins that are important for forming aerial hyphae in *S. coelicolor*. These eight chaplins are divided into two types: long chaplins (ChpA to C) and short chaplins (ChpD to H). The short chaplins are further sub-divided according to their ability to produce intramolecular disulfide bonds: ChpD, F, G and H have two Cys residues whilst ChpE has none. The eight chaplin proteins contain Sec secretion signal sequences and share the chaplin domain. Five of the chaplins (ChpD –H, short chaplins) contain a single chaplin domain, and the residual three long chaplins (ChpA to C) contain two chaplin domains. The chaplin domain is hydrophobic and comprises two conserved Cys residues that are found in all chaplins except ChpE (Di Berardo et al., 2008). The mechanism for the development of the streptomycete rodlet layer is through the self-assembly of chaplins into amyloid-like fibrils. It is based on the interplay between rodlins and chaplins. Chaplin monomers accumulate into small fibrils that are distributed randomly in the absence of rodlins. In the presence of RdlA and RdlB rodlins, the fibrils are placed in rodlets. These rodlets comprise two rods, each of which consists of two fibrils. The expression of *chp*

genes is initiated in a nutrient or limited environment before aerial hyphae formation. Nevertheless, when *chp* genes are deleted, *S. coelicolor* does not form aerial hyphae on a minimal medium and is strongly affected in a rich environment (Claessen et al., 2004). SapB is believed to be transported to the cell surface by RamA and RamB and consists of an ATP-binding cassette transporter (Willey et al., 2006). The gene cluster responsible for SapB biosynthesis (*ramS*, *ramA*, *ramB* and *ramC)* forms an operon and expression is controlled by a response regulator, RamR. There is no evidence of phosphorylation and no cognate sensor kinase is recognised for RamR (O'Connor and Nodwell, 2005, Keijser et al., 2002, Nguyen et al., 2002). On rich media, both the chaplins and SapB are formed in a *bld* dependent way and are involved in normal aerial hyphae production. On the other hand, on minimal media SapB is not formed and development is dependent on the chaplins. This suggests that there are two regulatory pathways directing the formation of aerial hyphae; one of them growing on rich media and engaging the *bld* genes and the formation of both SapB and the chaplins and secondly a *bld* independent pathway that growth of aerial hyphae on poor media through the chaplins and independently of SapB formation (Capstick et al., 2007).

1.3.2 *Bld* gene regulation

The erection of aerial hyphal is initiated on rich media by an extracellular signalling cascade based on the *bld* genes. Some *bld* mutants are separated into different types of extracellular complementation, which are placed higher in the hierarchy, dependent on the ability of one type of *bld* mutant to initiate aerial hyphal development of another *bld* mutant class. This is the phenomenon that occurs when mutants from two different types of complementation are grown adjacently on rich media. For instance, for the relief of a *bld* mutation by another *bld* mutant, the former has to develop close to one that is placed higher in the hierarchy. A logical explanation of this complementation is that extracellular molecules, formed and transferred by *bld* mutants blocked in the signalling cascade in later stage, are recognised by the *bld* mutants that are blocked the cascade in the early step; hence maintaining the development of aerial hyphae (Willey et al., 1991, Willey et al., 1993, Elliot et al., 2008). However, a large number of known *bld* genes are

transcriptional regulators, so rather than being involved in the generation of signals, their function is more likely to be the transduction and/or perception of signal production (Chater and Horinouchi, 2003). Six different complementation types are found in *S. coelicolor*. Development of aerial hyphae is initiated by an extracellular signalling cascade, which engages five extracellular signals. The only signal discovered so far is an extracellular oligopeptide, which is possibly the first signal in the signalling cascade and is moved outside the cells by an ATP-dependent transporter synthesised by *bldK* (Nodwell and Losick, 1998, Nodwell et al., 1996). A *bldJ* mutant fits in the cascade and is complemented by all *bld* mutants and it is suggested that the generation of the first signal is produced through the action of BldJ, (Nodwell and Losick, 1998, Willey et al., 2006). The next phase engages *bldA* and *bldH*, which belong to a similar complementation type. The *bldA* gene has an unusual way of regulation, which is by synthesising a tRNA for leucine that translates UUA codons. TTA codons are not often present in *S. coelicolor*; only 2% of the genes in the genome contain this codon (Li et al., 2007, Chater and Chandra, 2008). The inability of the *bldA* mutant to create aerial hyphae has mostly been based on the existence of the *bldH* (*adpA*) gene that encodes the AdpA regulator and contains a TTA codon. In *S. griseus*, AdpA directs genes engaged both in antibiotic formation and morphological differentiation, but in *S. coelicolor* no control targets of the AdpA orthologue, BldH are found in sporulation genes (Chater and Horinouchi, 2003, Ohnishi et al., 1999), even though several genes have been found to be *bldH*-dependent, such as *SCO0762* that encodes a serine protease inhibitor (Kim et al., 2005).

An anti-anti-sigma factor BldG is involved in the morphological development and antibiotic formation of *S. coelicolor*. Both the anti-sigma factors UshX and PrsH are required for "partner-switching"- like regulation of the sigma factor σ^H that has a function in the osmotic stress response (Sevcikova et al., 2010). This activation appears to be complex since BldG interacts with an anti-sigma factor, ApgA, although no interaction has yet been identified with other the anti-sigma factors and ApgA (Sevcikova et al., 2010, Parashar et al., 2009). The *bldG* gene has a pleiotropic role, directing together antibiotic formation and *S. coelicolor* development

(Champness, 1988, Bignell et al., 2000). BldG has a highly conserved serine motif (Ser57) which is most probably phosphorylated by the serine kinase activity of BldG related anti-anti sigma factors. This serine is found to be phosphorylated reversibly in *S. coelicolor* and this phosphorylation is vital for the activation of antibiotic formation and morphological development (Bignell et al., 2000). It has been demonstrated that BldG and the anti-sigma factor RsfA interact directly, which was previously revealed to regulate antibiotic formation and *S. coelicolor* development and to particularly interact with the sporulation specific sigma factor σ^F. The phosphorylation of BldG showed that RsfA is a protein kinase for BldG and regulates its activity in a negative way (Mingyar et al., 2014). The *bldC* gene encodes a putative MerR family transcriptional regulator. Deletion of the *bldC* gene causes an inability to secret undecylprodigiosin and actinorhodin due to the required activation by BldC of the *actIIORF4* and *redZ* genes (Hunt et al., 2005, Brown et al., 2003). BldB is a small protein with no known role in developmental regulation whose function remains unknown (Chater and Chandra, 2006, Eccleston et al., 2002, Pope et al., 1998). *bldN*, synthesising an ECF sigma factor that controls *bldM* regulation from one of its two promoters. BldM is a response regulator that, together with σ^{BldN}, is significant for the normal expression of chaplin and rodlin genes (Elliot et al., 2003, Bibb et al., 2000). BldD, having a predicted helix-turn-helix motif similar to the DNA binding domain of the lambda cI repressor, regulates development in *bldN* expression via repression. Repression through BldD was also observed for *whiG*, synthesising an extra sigma component that is the first factor in the regulatory pathway directing sporulation. This is the only known direct association between *bld* genes and *whi* genes to date. It was shown recently that *bldD* is the master regulator that governs streptomycete development through control of a large regulon hat consists of many *bld* genes and other genes previously known to control development; for instance, *ssgA*, *ssgB*, *smeA*, *sffA* and *ftsZ*, which are engaged in sporulation (Kim et al., 2006, Elliot et al., 2001, Den Hengst et al., 2010).

Recent finding has indicated that tetrameric cyclic-di-GMP performs as a dimerization molecule that directs the transcription factor BldD to bind DNA. This results in the repression of the BldD regulon of sporulation genes in vegetative

growth, thus controlling the sporulation in a manner of cyclic-di-GMP-mediated dimerization (Tschowri et al., 2014).

1.3.3 Development of aerial hyphae to spores

a) Early genes are required for sporulation

The early common characteristic of *whi* mutants is that they are defective in chromosome segregation and sporulation septation, but every mutant is arrested at a precise point in regular growth and possesses its own feature of aerial hyphal phenotype. *whiA*, *whiB*, *whiG*, *whiH*, *whiI* and *whiJ* mutants are all influenced in the processes of sporulation and are unable to establish the otherwise produced sporulation septum correctly (Figure 1.2). Moreover, they are incapable of dividing and condensing chromosomes in the aerial hyphae accurately (Aínsa et al., 2010, Flärdh et al., 1999, Aínsa et al., 1999). Light and scanning electron microscopy analysis of the hyphal morphology of *whi* null mutants illustrates that the *whiG* mutant produces long, straight aerial hyphae with occasional deep constriction of the walls (Figure 1.2B). Cell wall staining with Fluo-WGA (fluorescein-conjugated wheat germ agglutinin), which binds oligomers of peptidoglycan showed that septa were produced, but they were similar to vegetative cross walls and thinner than the sporulation septa. In addition there was no direction to the division of sporogenic cells. An RNA polymerase sigma factor is encoded by *whiG* with a high sequence similarity to σ^{D} of *Bacillus subtilis* and σ^{FliA} of *Salmonella typhimurium*; these sigma factors direct transcription of genes engaged in motility and chemotaxis (Chater et al., 1989, Flärdh et al., 1999, Helmann, 1991). The *whiH* mutant aerial hyphae are loosely coiled with occasional deep constrictions observed, showing that this mutant in fact produces a few sporulation septa (Figure 1.2C) (Flärdh et al., 1999, Ryding et al., 1998). The disruption of the *whiI* hyphal phenotype mutant is similar to the *whiH* mutant, but fewer constrictions are observed (Figure 1.2C). The function of WhiH is that of a transcriptional regulator that displays similarity to the GntR family of regulatory proteins (Ryding et al., 1998). The extended similarity is in a region where a DNA-binding helix-turn-helix motif was predicted. WhiI is similar to response regulators of two-component systems (Aínsa et al., 1999). The function of these regulators is that of transcription factors that transfer a signal from a sensor

kinase that, through phosphorylation/dephosphorylation, regulate the activity of the regulator (Hutchings et al., 2004). Response regulators normally contain a phosphorylation pocket, having a conserved aspartate in their N-terminal domains. The putative phosphorylation pocket of whiI protects two out of three conserved aspartate residues, including the one that is normally phosphorylated. Usually, for these family members, the gene encoding the linked sensor protein kinase is placed close to the gene encoding the response regulator, but there is no kinase gene has been found for *whiI*. This suggests that WhiI is regulated in another manner than through aspartate phosphorylation (Tian et al., 2007). The C-terminal regions of responsive regulators commonly contain a helix-turn-helix motif; this is also found between two members of the FixJ subfamily to which WhiI belongs, and the similarity of the amino acid sequence in this region suggests that this is the DNA-binding part of WhiI (Aínsa et al., 1999).

whiA, whiB, whiI and *whiG* disruption mutants show no signs of nucleoid separation in aerial hyphae. DNA stained with 4',6-diamidino-2-phenylindole (DAPI) demonstrate that the chromosomes are in an uncondensed condition and DNA is evenly distributed all along the hyphae (Aínsa et al., 1999, Flärdh et al., 1999). The *whiH* mutant is also defective in chromosome partitioning, but the distribution mode of the nucleoids is distinct compared to *whiA, whiB, whiI* and *whiG* mutants. *whiH* mutants develop into aerial hyphal fragments with spore-like characteristics. These fragments are poorly separated and the nucleoids are condensed and partially distributed from each other, producing irregularly-shaped bodies that are distributed unevenly (Figure 1.2C). Cell type-specific expression of the sporulation gene *hupS* shows that these fragments can initiate at least part of the usual developmental process in a *whiH* mutant (Flärdh et al., 1999, Salerno et al., 2009).

The *whiJ* mutant in aerial hyphae is straight and un-branched and spore chains are seldom observed. *whiJ* is expected to encode a transcription regulator with an N-terminal DNA-binding helix-turn-helix. *whiJ* alleles result in mutants incapable of sporulation and are highly efficient in sporulation as the disruption of the whole *whiJ* gene displayed a gray wild-type phenotype with strong sporulation. This suggests

that WhiJ performs as a negative regulator of sporulation in certain environments. Inactivation of *whiH* does not entirely block sporulation; several cross wall are produced in the aerial hyphae and nucleoids are condensed. Furthermore, a *whiH* mutant is somewhat gray because of the low spore pigment production; this is also the case for a *whiJ* mutant. *whiI, whiA, whiB* and *whiG* mutants are entirely white and show no signs of nucleoid positioned or sporulation septation. The execution of illegitimate cell cycle processes can at least partly be explained by the failure of these mutants to upregulate the expression of genes synthesising components of the cell division mechanism and chromosome segregation apparatus (Kelemen et al., 1998, Aínsa et al., 2010).

b) Late genes lead to spore formation

As the spores mature they become gray in colour because of the formation of a spore-related polyketide pigment (Yu and Hopwood, 1995). This gray pigment formation is characteristic of *S. coelicolor* morphological differentiation since many developmental mutants incapable of differentiating into spores were recognised due to their inability to generate the pigment and therefore were white or less gray than the wild type strain. Mutations in some loci allow sporulation septa production, but still influence later phases of sporulation though loss of pigmentation (Kelemen et al., 1998). For instance, the *whiE* locus that encodes enzymes engaged in the pigment biosynthesis comprises an operon of seven genes (ORFI-VII) and one gene (ORFVIII) that is transcribed in the reverse direction (Kelemen et al., 1998, Davis and Chater, 1990). To date, the pigment has not been chemically characterised and purified; possibly because it is cross-linked to the spore wall (Yu and Hopwood, 1995); however the homology of *whiE* s to genes that encode type II polyketide biosynthetic enzymes implies that the pigment is an aromatic polyketide (Davis and Chater, 1990).

The late stage sporulation gene *sigF* encodes a second sporulation sigma factor, σ^F, that has great similarity to σ^B of *B. subtilis,* which is involved in the general stress response and directs gene expression during stationary phase (Kelemen et al., 1996, Potúčková et al., 1995). The phenotype of a light green colony of a *sigF* null mutant

suggests that the spore pigment is not formed accurately and indicates that the transcription of *whiE* ORFVIII is *sigF* dependent. Spores are synthesised in the *sigF* mutant, but they are frequently deformed, contain thinner spore walls, have less condensed chromosomes and are more sensitive to detergent than the spores of the wild type (Kelemen et al., 1998, Potúčková et al., 1995, Kelemen et al., 1996).
WhiD belongs to the family of Wbl proteins, as does WhiB, and is essential for the later events of sporulation (Molle et al., 2000). While the production of the sporulation septum in the early *whi* mutants, such as the whiB mutant, is eliminated, a *whiD* mutant is capable of generating spores. However, these vary in size and show irregularity in septal placement. Septa are frequently laid down adjacent to the spore poles and in several planes leading to mini-compartments missing chromosomal DNA in the *whiD* mutant. Furthermore, many spores show extreme variation in wall deposition and lysis and spores are more sensitive to heat than in the wild type (Molle et al., 2000).

Other genes that influence late sporulation systems have also been described. One example is *mreB*, which impacts the deposition of peptidoglycan morphology around the spores (Mazza et al., 2006). In addition, the *S. coelicolor* genome encodes seven paralogues of SsgA (SALPs), of which all (SsgA-SsgF), have been indicated to direct different phases in the conversion of aerial hyphae into spores (Noens et al., 2005). Previously, the SALPs, small acidic proteins, with no similarity to any recognised proteins, had been found only in actinomycetes in both morphologically complex genera and non sporulating species (Traag and van Wezel, 2008). Various SALPs influence many different sporulation systems and affect sporulation septum formation, chromosome segregation and maturation of spore processes such as spore wall synthesis and spore separation. For instance, in many of the *ssgD* mutant spores, a thick peptidoglycan layer close to normal spores is absent, whilst *ssgE* and *ssgF* mutants influence the efficiency of separation of surrounding spores (Noens et al., 2005).

The operon of *smeA-sffA*, is upregulated late in growth in a *whiH*, *whiI*, *whiG* and *whiA* dependent fashion and pleiotropically impacts spore formation. Mutants

missing *smeA*, encoding a small putative membrane protein, display decreased spore pigment levels, inaccurately positioned sporulation septa, thinner spore walls and chromosomes that are less condensed, with a somewhat higher incidence of anucleate spores. The *sffA* mutant phenotype indicates specific expression in sporogenic compartments and placement of SffA in sporulation septa, which is *smeA*-dependent. The minor defect in chromosome segregation of a *smeA-sffA* mutant suggested the role of SffA in clearing of the genome from closing septa (Ausmees et al., 2007).

c) Pathway regulation of morphological differentiation and secondary metabolism in aerial hyphae

σ^{WhiG} is essential for the earliest known phase of sporulation and is likely to play a part in the involvement of septation in sporulation in *S. coelicolor*. Molecular investigations have revealed that *whiG* is an epistatic gene to *whiI, whiA, whiB,* and *whiH* (Chater, 1975, Flärdh et al., 1999) and that expression of *whiG* is not based on any of these early sporulation genes, even *whiG* itself (Chater, 1975, Kelemen et al., 1996). The fact that ectopic overproduction of *whiG* leads to sporulation in the vegetative mycelium, where most *Streptomyces* species do not sporulate, supports the understanding of σ^{WhiG} as a master regulator of aerial hyphae sporulation (Chater et al., 1989). The *whiG* transcripts even exist before aerial hyphae formation, which suggests that uncharacterized expression of σ^{WhiG} is probably activated during the sporulation of aerial hyphae (Kelemen et al., 1996). Despite this, no anti-sigma factor or other machinery for σ^{WhiG} activity direction has been recognised. Although transcripts exist during vegetative development, *whiG* expression is directed negatively by BldD in vegetative hyphae (Elliot et al., 2001). For many years it was not known how BldD activity is expressed, however the recent research by (Tschowri et al., 2014) has showed the connection between cyclic-di-GMP signalling and BldD during the multicellular development of streptomycetes.

It has been shown that σ^{WhiG} directs the two early sporulation genes promoters, *whiH* and *whiI,* while *whiA* and *whiB* expression is not based on *whiG,* suggesting that there are two convergences of pathway regulation directing *S. coelicolor*

development (Aínsa et al., 1999, Ainsa et al., 2000, Ryding et al., 1998, Soliveri et al., 1992). *whiH* and *whiI* transcripts are first reported in the initiation of aerial mycelium formation and the transcript level reaches its highest point when spores are formed (Aínsa et al., 1999, Ryding et al., 1998). StrepDB states that both WhiH and WhiI specify repressors of their own transcription, suggesting that this indirect or direct auto repression is released at this time of sporulation (Ryding et al., 1998, Aínsa et al., 1999). WhiH and WhiI belong to different families of regulators that contain a DNA-binding motif and a domain that usually senses signals. This has led to speculation that the DNA-binding capability of WhiH, with similarity to some other members of the GntR (regulatory protein) family, is possibly influenced by binding of a ligand. In addition, the WhiI DNA binding activity, which is homologous to response regulators, may be altered in response to other signals or phosphorylation (Chater, 2001). The expression of *whiH* is not only influenced by WhiH itself, but WhiI also appeared to have a negative action on *whiH* transcription (Aínsa et al., 1999). It is unknown how *whiG* expression independent of *whiA* and *whiB* is accomplished. All *whiA* and *whiB* genes so far discovered have a common constitutive promoter and another that is active in aerial mycelium production (Ainsa et al., 2000, Davis and Chater, 1992). The strongly up-regulation of *whiA* expression in sporulation is eliminated in *whiA* and *whiB* deletion mutants, while the expression of *whiB* increases. This suggests that in addition to potential auto regulation, these genes also influence each others' expression (Jakimowicz et al., 2006).

The *whi* genes have long been known to affect the expression of a number of genes, although few promoters under their direct control have been recognised, except *whiH* and *whiI* that are WhiG-dependent. In sporulation, the FtsZ cell division protein and chromosome positioning proteins ParA and ParB are expressed in large quantities (Flärdh et al., 2000, Jakimowicz et al., 2006). This involves the increased expression of sporulation-specific promoters for the *ftsZ* and the *parA parB* operons, whose expression is based on *whiA*, *whiB*, and *whiI*. BldD binds to the *smeA-sffA* upstream region and to the most upstream promoter of the *ftsZ* gene, although the consequence of this binding on the expression is still unknown (Den Hengst et al., 2010). The early *whi* genes also influence the expression of sporulation genes. The *whiE* locus

that controls the pathway of the gray polyketide spore pigment is directed from two divergently oriented promoters, both being regulators of development. One promoter directing *whiE* ORFI-ORFVII activity is based on the early *whi* genes for its expression, whilst the divergently transcribed *whiE* ORFVIII gene depends on the late sigma factor σ^F for its up regulation. *whiH* and *whiJ* mutants have a somewhat gray colour, consistent with the transcription of *sigF* and *whiE* which is present at a low level (Kelemen et al., 1998). The transcription of *smeA-sffA*, initiated through sporulation, is also based on the early *whi* genes (Ausmees et al., 2007). *hupS* requires *whiA, whiG*, and *whiI* for its aerial hyphae up regulation but is not totally reliant on *whiH*. *sigF* expression is dependent on *whiG*, although a direct response has not been observed, suggesting that a third, unknown, sigma factor is also engaged in regulating morphological differentiation (Kelemen et al., 1996).

bldD is the first instance of a gene that is engaged both in the choice of aerial hyphae formation and directly in gene control that is engaged in the development of aerial hyphae to spores via its negative impact on the expression of *whiG (Den Hengst et al., 2010, Elliot et al., 2001)*. The regulatory cascade of the *whi* gene affects genes engaged in cell division and chromosome positioning in the aerial hyphae. Later events of sporulation also are based on the early *whi* genes and links to the formation of the spore pigment and up regulation of σ^F have also been demonstrated. However, there is an incomplete understanding of the gene regulation required for spore maturation, such as how the developmental control of *mreB* expression is accomplished (Kleinschnitz et al., 2011, Heichlinger et al., 2011).

1.4 Growth control in sporulation

1.4.1 Hyphal growth, cell wall formation, and morphogenesis

Streptomycetes are mycelial bacteria that develop by intercalation of a new cell wall substance (peptidoglycan) at the tips of the hyphae (Flärdh, 2010, Flärdh, 2003). Vegetative hyphae produce new sites of growth by production of branches from the side wall, frequently in sub-apical cells that are split from the tip by a cross wall. However, it is also likely that incorporation of peptidoglycan into the side wall may also give rise to the rapid growth of aerial hyphae, although there is as yet little direct confirmation of this (Jakimowicz et al., 2005, Chater, 2011).

When *S. coelicolor* aerial hyphae separate into spores, some changes in their development and morphogenesis occur. The morphology of the sporulating aerial hyphae differs from the vegetative mycelium hyphae in that it frequently contains a coiled shape in the apical parts (Figure 1.2D). The straight form of the aerial hyphae of a *whiG* mutant, (Figure 1.2B) shows that the alteration in morphology is based on the WhiG sporulation sigma factor, which is likely to be one factor causing sporulation of the aerial hyphae (Chater et al., 1989). The *whiG*-dependent exchange from straight to coiled hyphae might be explained by a change in the peptidoglycan composition of the cell wall. One prospect would be a change in how the production of new cell wall substances occurs or there could be a re-modelling of the previously existing cell wall peptidoglycan (Flärdh et al., 1999).

Eventually the aerial hyphae stop developing (Figure 1.2A and B). *whiA* and *whiB* mutants contain longer and more tightly coiled aerial hyphae than the parent strain, suggesting that they are incapable of fully arresting the extension of the aerial hyphae (Figure 1.2C). The coiling indicates that the *whiG*-dependent modification in the cell form begins in these two mutants and the coiling is *whiG*-dependent as *whiA whiG* or *whiB whiG* double mutants contain straight aerial hyphae similar to a *whiG* single mutant (Chater, 1975, Flärdh et al., 1999). However, it is possible that *whiA* and *whiB* mutants become excessively coiled due to their incapability to arrest development and continue to the next phase when the sporulation septa are laid down (Flärdh et al., 1999).

The MreB proteins are prokaryotic homologues of actin. They form actin-like cytoskeletal proteins and define the cell form in many rod-shaped bacteria in which MreB has become necessary for development and for controlling the insertion of new peptidoglycan into the side walls of the cells (Margolin, 2009, Carballido-Lopez, 2006, Thanbichler and Shapiro, 2008). On other hand, MreB is not engaged in *Streptomyces* polar growth or other actinobacteria and is not even present in rod-shaped corynebacterial and mycobacterial species, which also develop by cell wall synthesis at the cell poles. *mreB* transcription is controlled by three promoters, with two of these constitutively activated and the other developmentally regulated with an increase of transcription during sporulation (Burger et al., 2000). MreB has an impact on sporulation and influences the integrity of the spore walls. An *mreB* mutant produces deformed and swollen spores that are sensitive to heat and detergent. The changes in spore shape suggest that the synthesis of peptidoglycan layers is mediated by MreB. Consistent with a function in spore wall assembly, MreB is located in sporulation septa and afterwards it appears to extend along the walls all around the matured spores and ultimately vanishes (Mazza et al., 2006).

1.4.2 Bacterial cell division

Cell division in most bacteria takes place through the production of a divisome and a multiprotein complex at the division location. This causes cell membrane invagination of new peptidoglycan synthesis, which is the main structural determinant of the bacterial cell wall and ultimately the separation of the daughter cells (Scheffers and Pinho, 2005). The first protein to dictate the future division location is FtsZ, which is a structural homologue to the cytoskeletal tubulins in eukaryotes. FtsZ polymerises into tubulin-like protofilaments, and protofilaments bundled to assemble into a ring-like formation named the Z-ring, which is anchored to the cell membrane inside through interaction with other proteins (Figure 1.3). The Z-ring begins the divisome formation and its constriction directs cell membrane invagination (Adams and Errington, 2009, Margolin, 2005). FtsZ is utilised in most bacteria in cell division, with only a few bacteria groups as exceptions, such as planctomycetes and chlamydia (Margolin, 2005, Errington et al., 2003). In all *ftsZ*-containing bacteria that have been reported, except *S. coelicolor*, *ftsZ* is essential.

Strikingly, *ftsZ S. coelicolor* deletion mutants are viable. They do not produce any septa of cell division, although they can still propagate and develop (McCormick et al., 1994). However, they grow weakly, produce only vegetative mycelium and some aerial hyphae and are incapable of sporulation.

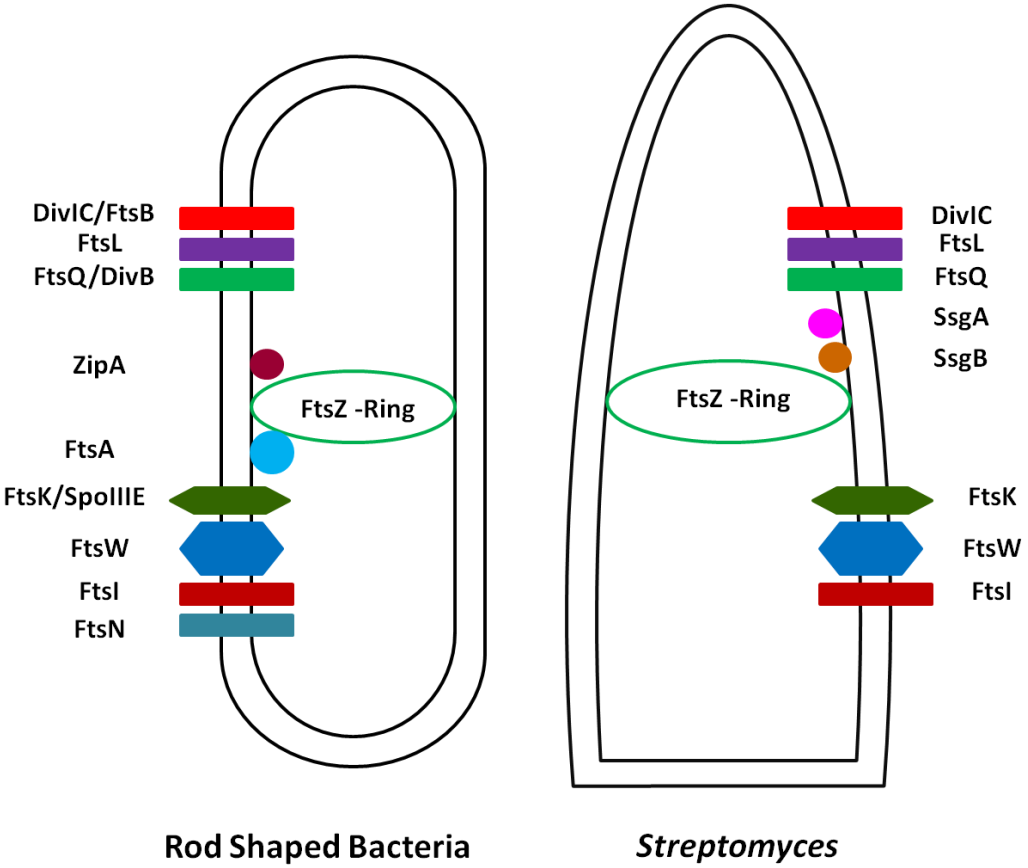

Figure 1-3: A comparison of the cell division mechanism in rod shaped bacteria model (*E. coli*, *Bacillus* and *Streptomyces*.

In rod shaped bacteria, cell division is initiated by polymerization of the conserved protein FtsZ into a ring structure at mid cell. This Z ring works as a scaffold for a group of proteins that carry out the synthesis of the division septum. Also, this FtsZ protein is part of the "divisome" which performs the process of cell division (Hamoen et al., 2006). Then, other division proteins are engaged in the Z ring: ZipA, FtsA, FtsK, FtsQ, FtsL, FtsB (YgbQ), FtsW, FtsI and FtsN (Koppelman et al., 2004). In *S. coelicolor*, FtsA (widely conserved) and ZipA & FtsN (less widely conserved) homologues are absent and while no other proteins with the identical role have been recognized, it is a mystery how FtsZ interacts with the membrane in *S. coelicolor*. FtsK is localized at that sporulation septum and the loss of this protein influences many developmental processes. In *Streptomyces* SsgA and SsgB recruit FtsZ during sporulation, modified from (McCormick, 2009, Bush et al., 2013).

1.4.3 *S. coelicolor* cell division

In *S. coelicolor,* two types of structural cell division have evolved in sporulation division and vegetative hyphal cross walls (vegetative division) (McCormick, 2009). In vegetative development, cell division is comparatively uncommon and leads to the formation of thin cross walls of peptidoglycan that separate hyphae into separate cells. These septa do not separate completely and the cells that constitute hyphae thus remain connected to each other. During sporulation, a particular structure of cell division occurs to separate the sporogenic cell into several prespore compartments of equal sizes. These sporulation septa are formed synchronously all along the cell, and provide thick, frequently double-layered cross walls that divide after division, resulting in the separation of closed spores. Both kinds of cell division are based on FtsZ, which produces ring-like structures where the future division will occur (Wildermuth and Hopwood, 1970). Therefore, it is probable that *S. coelicolor* utilises the same core cell division mechanism in both types of division (Grantcharova et al., 2005, McCormick et al., 1994, Schwedock et al., 1997).

Through cell division in aerial hyphae, the septa must be accurately positioned between chromosomes to ensure appropriate chromosome segregation into pre-spores. The mechanism that determines the sites for the localisation of Z-rings along the aerial hyphae in *S. coelicolor* is by SsgB. One significant example of spatial control of Z-ring formation is the Min system of *E. coli* and *B. subtilis* that prevents cell division in the cell poles and enhances division in the middle of the cell (Willemse et al., 2011, Lutkenhaus, 2007, Bush et al., 2013). Nucleoid occlusion is a further mechanism preventing division over chromosomes by specific protein action (Noc in *B. subtilis* and SlmA in *E. coli*) (Adams and Errington, 2009, Rothfield et al., 2005). In *S. coelicolor,* there are no clear homologues of the Min system or any proteins engaged in nucleoid occlusion. Furthermore, there is no verification of a precise mechanism of nucleoid occlusion occurring during sporulation since the septum begins to form over apparently non-segregated chromosomes (Flardh, 2003). To date, no substitute system for division location placement has been found in *Streptomyces*.

1.4.4 Divisome Proteins

In addition to FtsZ, *S. coelicolor* activates homologues of well-characterised cell division proteins, suggesting that streptomycete cell division performs in a similar way to that of unicellular bacteria once the Z-rings are formed (Figure 1.3). In *E. coli*, FtsK is required for both cell division and the last step of chromosome segregation (Bigot et al., 2004); its final role being as a chromosome pump through the septum. The homologous protein of *B. subtilis* SpoIIIE is engaged in appropriate translocation of DNA chromosomes into prespore compartments (Bath et al., 2000). *S. coelicolor* FtsK appears to have an identical function in chromosome segregation as in *E. coli*, although it is not essential for cell division (Wang et al., 2007).

In *B. subtilis* some proteins that are homologues of *E. coli* cell division proteins are expressed. These are FtsL, DivIC (a likely relative of FtsB) and DivIB (a homologue of FtsQ). The three proteins (FtsL, FtsB and FtsQ) are membrane proteins and have an identical topology. They contain one transmembrane segment localising a smaller domain at the cytoplasmic membrane side and large part on the outer face of the membrane. Interaction studies of these cell division proteins have proposed that they exist as a multimeric complex and that FtsK-independent oligomeric interactions occur before an FtsK-dependent placement to the divisome; however, their role in cell division is still not entirely understood (Buddelmeijer and Beckwith, 2004).

FtsW consists of 10 transmembrane spans; it belongs to the SED family of proteins influencing cell elongation, division and shape (Errington et al., 2003). These proteins are usually encoded adjacent to a gene coding for a penicillin-binding protein (PBP) with transpeptidase activity that stimulates the formation of the peptide bonds among peptidoglycan strands. (Errington et al., 2003, Scheffers and Pinho, 2005). *ftsW* in *E. coli* and the vast majority of other bacteria, is engaged in cell division and is placed adjacent to *ftsI*, which encodes a PBP that is necessary for cell division. The cell division function of FtsW is unclear; however it is presumed that it acts in the translocation of the lipid-linked peptidoglycan precursors into the cytoplasmic membrane to FtsI and other PBPs on the outer cell membrane (Errington et al., 2003).

FtsQ, FtsL, FtsB, FtsW and FtsI in *S. coelicolor* all have an impact on the sporulation in septa production (McCormick, 2009). Null mutants are blocked in the alteration of the aerial hyphae into spores. A disruption of the *ftsQ* mutant is incapable of forming septa in most aerial hyphae (McCormick and Losick, 1996), whereas *ftsL* and *ftsB* mutants produce aerial hyphae containing shallow constrictions (Bennett et al., 2007). *ftsI* and *ftsW* mutants produce a combination of hyphae, one part with no septa and the other with partially constricted septa (Bennett et al., 2009). With the latter four mutants, the phenotypes are dependent on the growth environment and are not as severely affected on minimal media with low osmolarity as they are when grown on a high osmolarity rich medium. This shows that in certain circumstances cell division can occur in the absence of *ftsL*, *ftsB*, *ftsI* or *ftsW*, possibly because of the presence of proteins with overlapping roles (Bennett et al., 2007, Bennett et al., 2009).

It has been suggested that another cell division protein, FtsN, is involved in cell wall hydrolysis in many bacteria because of the weak similarity of the sequence to amidases. FtsN is required to allow the beginning of constriction. It is thought that the suppressor activity of FtsN overproduction can be achieved through damaging the wall so that somehow that division mechanism is partially not functional; for instance, through a temperature sensitive mutation influencing FtsA, FtsQ, or FtsI (Errington et al., 2003).

1.5 Chromosome partitioning and nucleoid structure in sporulation

In recent years, bacterial DNA replication and separation have mostly been explored in unicellular model organisms that divide by binary fission and contain circular chromosomes. In these, bacteria segregation and chromosome replication occur concurrently and the newly replicated *oriC* areas are actively moved towards the cell poles as replication continues in the middle of the cell (Reyes-Lamothe et al., 2008, Thanbichler and Shapiro, 2008). The mechanisms that govern bacterial DNA segregation are mostly unknown; however, a partitioning system of the ParAB group, has been shown to be involved in this system in some bacteria. This system resembles partitioning systems on some plasmids and comprises an ATPase

(characterized by the deviant Walker A motif) synthesized by *parA* and a DNA-binding protein synthesized by *parB*. In addition a DNA sequence motif (*parS*) which binds to ParB is also required. As several *parS* locations bind close to the replication origin, ParB produces a high order nucleoprotein complex, named the partition complex. ParA and ParB homologues are prevalent in most bacteria, with the notable exception of *E. coli*, suggesting a more fundamental function in the placement of DNA in the prokaryotic cells exists (Leonard et al., 2005).

S. coelicolor has various types of life cycle and has a large (8.6 Mbp) linear chromosome, with a central replication origin (Bentley et al., 2002). During vegetative development, the genome is replicated, with the result that each cell, divided by cross walls, has several copies of the chromosome. However, in this phase of the life cycle, it is unclear how DNA segregates and no obvious nucleoid division or condensation is seen by DNA microscopy and staining. Moreover, the dozens of chromosomes in the sporogenic compartment are equally distributed during the replication phase. However, in the final phase of sporulation, these become divided into regularly located bodies of DNA, one in every prespore. This suggests an association between chromosome condensation and segregation (Flardh, 2003, Flärdh, 2010).

1.5.1 Chromosome localisation and segregation in aerial hyphae

The *S. coelicolor* genome encodes ParA and ParB homologues, each having an impact on chromosome segregation into prespore compartments. *parA* and *parB* are found in an operon, the transcription of which is activated from two promoters upstream of *parA*. Consistent with their assigned function in spore formation, the transcription from the more upstream putative promoter, ($parAB_{P2}$), is upregulated in sporulation septation and its activity dependent on the early time point in sporulation genes *whiA*, *whiB*, *whiH* and *whiI* (Jakimowicz et al., 2006, Kim et al., 2000). The other downstream putative promoter ($parAB_{P1}$) has a constitutive expression during development, although the function of parA and parB in vegetative growth has not yet been determined.

A *parAB* mutant and the *parA* and *parB* single mutants display no obvious defect in chromosome positioning, but DNA staining shows reduced DNA content in the spores (Jakimowicz et al., 2007, Kim et al., 2000). In *parAB* and *parB* mutants, around 15 % of the prespore compartments are lacking in DNA, compared to 1.8 % in the parental strains of the wild type. The defect in segregation is more unusual in the *parA* deletion mutant, where 26 % of the spore chain is DNA free (Jakimowicz et al., 2007). An explanation of this is that the presence of ParB in the absence of ParA has a far stronger impact on the chromosome placement into the prespores than its complete absence. ParB is a DNA-interaction protein and recognises most (21 out of 24) *parS* sites placed around the *oriC* region of the chromosome, and forms a vast nucleoprotein complex (Jakimowicz and Chater, 2002). In sporulation, ParB foci are regularly spaced between sporulation septa in aerial hyphae, with overlapping chromosomes (Jakimowicz et al., 2005). A mutated ParB prevents ParB foci formation and interacts with chromosomal DNA, implying that the ParB complex assembly is based on a DNA-interaction (Jakimowicz et al., 2005). Further, a lack of activation of the sporulation-specific promoter ($parAB_{P2}$) has a negative influence on the formation of a large number of ParB complexes and results in a similar frequency of anucleate spores to inactivation of *parB* (Jakimowicz et al., 2006), showing the significance of an elevated level of ParB for correct chromosome partitioning during aerial growth. ParA is placed at the tips of aerial hyphae in early development and afterwards extends along the aerial hyphae in a spiral structure, in a *parB*-independent way (Jakimowicz et al., 2007).

1.5.2 Last phase of chromosome partitioning into spore septation

In *S. coelicolor*, FtsK, which is positioned at sporulation septa, influences the last chromosome separation and their transportation into spore compartments during septum closure. FtsK homologues in other bacteria belong to the family of DNA translocases; for instance, SpoIIIE transfers the chromosome into developing spores in *B. subtilis*. In *E. coli,* FtsK transfers the last part of the chromosome through the closing septa (Bigot et al., 2007). An *ftsK* null mutant of *S. coelicolor* demonstrated a high level of genetic instability that was linked with large deletions of the end regions of the linear chromosome (Wang et al., 2007). The *ftsK* mutant also seemed

defective in transferring misplaced DNA from closing septa (Ausmees et al., 2007). This suggests that FtsK has a function in moving the terminal parts of the chromosomes through the closing septum in spore formation to ensure that they are not trapped (Wang et al., 2007). SffA, another homologue of SpoIIIE/FtsK DNA translocases, is also placed at the sporulation septa, suggesting a potential role of SffA as a DNA translocase, but its specific function remains unknown. Although SffA and FtsK co-localise at the sporulation septum, the levels of redundancy or carrying out overlapping tasks in the partitioning of chromosomes is unknown (Ausmees et al., 2007).

1.5.3 Genes influencing condensation of chromosomes through stress responses

The Dps protein (DNA-binding protein from starved cells) in *E.coli*, organises the chromosome into a nucleoprotein complex that protects DNA from environmental damage in the stationary phase. It has also has been implicated in stress responses to high temperature, oxidative damage and low pH (Almiron et al., 1992, Frenkiel-Krispin et al., 2004, Nair and Finkel, 2004). The *S. coelicolor* genome encodes three Dps homologue genes (*dpsABC*). The levels of these Dps proteins increase in response to environmental stress conditions. The primary function of these proteins is chromosome protection, particularly in oxidative stress. Induction of DpsA expression is affected by osmotic stress response, while DpsB and DpsC expression remains unaffected and the induction of their expression is independent on both oxidative stress and SigB. The disruption of individual *dps* genes in *S. coelicolor* affects chromosome condensation in prespore compartments in a specific way. In a *dpsA* disruption mutant, the DNA compaction was incomplete. In contrast, deletions of *dpsB* or *dpsC* result in mutants that display a more condensed nucleoid shape compared to the wild-type strain. This shows that neither DpsB nor DpsC, in the absence of DpsA, can compact chromosomes, perhaps because of antagonistic effects on each other's role in the absence of DpsA. This suggests that these three Dps proteins are require in a critical balance for an appropriate level of nucleoid condensation within the cell (Facey et al., 2009). Recently, it has become clear that many *Streptomyces* genomes display osmotic stress induction of *dps* genes. This may

have occurred in two ways. Either by gene duplication, whereas one of the paralogs afterwards appears as part of the osmotically inducible SigB regulon, or, in the absence of such an incident, *Streptomyces* might have obtained an osmotically induced *dpsA* that is thereafter transcribed as part of the SigB regulon (Facey et al., 2009).

1.6 The bacterial cell envelope

Bacterial cell envelopes can conveniently be classified on the basis of their cellular membranes as being either "monoderm" (i.e. having one biological membrane) or "diderm" (i.e. possessing two biological membranes) (Sutcliffe, 2010). The former applies to Gram-positive bacteria, such as *S. coelicolor*, while the latter applies to Gram-negative bacteria such as *E. coli* (Silhavy et al., 2010, Sutcliffe, 2010). Gram-negative bacterial cell envelopes have a much thinner, but more complex structure than Gram-positive cell envelopes, and do not retain the crystal violet colour of the Gram stain dye which makes them appear pink when seen under a microscope. The Gram staining procedure is a simple staining technique developed in 1884 and it succeeded in differentiating the bacteria into two large groups. After heat fixation, the bacteria are stained with carbol gentian violet and iodine (Lugol's solution). Then, when the bacteria appear dark blue/violet under the microscope, they are known as Gram-positive, while if they are pink/red, they are termed Gram-negative. The difference in the staining ability of Gram-positive and Gram-negative bacteria lies in the cell envelope architecture and composition, particularly in the localisation of the peptidoglycan layer (Seltmann and Holst, 2002).

The diderm bacterial envelope in Gram-negative bacteria such as *E. coli* is composed of a single thin peptidoglycan layer placed inside a periplasmic space that is formed between two distinct membranes (hence diderm), called the inner and outer plasma membranes (Sohlenkamp and Geiger, 2015, Silhavy et al., 2010, Sutcliffe, 2010). The outer membrane is composed of a complex construction that contains porins, which allow small hydrophilic molecules to pass across the membrane, while lipoproteins, PLs and lipopolysaccharide (LPS) molecules extend into the extra-cellular space. In this way, the outer membrane appears to be a permeable barrier that

controls the movement of large molecules in and out of the cell. Therefore, glycopeptide antibiotics are not effective on a Gram-negative bacteria cell envelope, because they cannot penetrate the outer membrane (Cabeen and Jacobs-Wagner, 2005, Jordan et al., 2008).

In contrast, the monoderm bacterial cell envelope such as that of *S. coelicolor* consists of an inner cytoplasmic membrane and an outer thick (20-80 nm), multi-layered, peptidoglycan cell wall (Sutcliffe, 2010). Because of this, they retain the crystal violet dye and hence these organisms appear dark blue/purple in colour when viewed under a microscope. Typically, cell envelopes of Gram-positive bacteria have a very small amount of lipids; as an alternative, they tend to have a high level of lipoteichoic acids, teichoic acids and proteins. Teichoic acids are mostly entrenched in the peptidoglycan layer. Lipoteichoic acids extend across the peptidoglycan layer and span the cytoplasmic membrane. These anionic polysaccharides play very important functions in cell development, morphology and division. Despite this, the structure of the cell wall differs substantially among different Gram-positive bacteria (Cabeen and Jacobs-Wagner, 2005, Jordan et al., 2008).

1.6.1 The peptidoglycan cell wall

In bacteria, the peptidoglycan layer is frequently known as murein and occasionally as glycopeptide, mucopeptide or basal structure. Peptidoglycan forms a sacculus comprising of polysaccharide chains cross-linked by peptide bridges. Therefore, a highly solid structure in the form of a net is produced, resulting in the stability and retention of the mechanical shape of bacteria. Based on the type of the bacteria, the amount of peptidoglycan in the cell wall can vary from 5 to 90% of the total mass, and is higher in Gram-positive bacteria than in Gram-negative bacteria (40 and 60%) (Seltmann and Holst, 2002).

In Gram-positive bacteria, the cell wall represents the outermost limit of the barrier between the bacterial membrane and the environment. Due to its position, it has many roles including a separatory role, in that the cell wall divides the inside of the bacteria from the surrounding milieu, while protecting it from harmful environmental

influences. It addition it has a connecting role, enabling the cell wall to transport information and substances from inside to outer and *vice versa*, as well as to communicate with the environment. Furthermore, the cell wall gives the bacteria adequate solidity, such as shape stability and osmotic stress resistance, in addition to assisting the metabolism, growth and development of cells. The structures of bacterial cell walls are adaptable to these roles, but still differ in individual bacteria. Thus, the cell walls are more complex and vary in detail between different bacteria. However, when comparing the cell walls of bacteria, the structural principles are shared between the majority of them (Seltmann and Holst, 2002). Most bacterial cells are enclosed by a cell wall. However, there are bacteria that are not, and yet, display distinctive, diverse morphologies. For instance, *Spiroplasma* and *Mycoplasma* are members of the Mollicutes class that contain the smallest and simplest genomes found in self-replicating and free-living bacteria (Wolgemuth et al., 2003).

Being Gram-positive, *S. coelicolor* possesses a "monoderm" cell envelope composed of a thick outer peptidoglycan cell wall and an inner plasma membrane, and there is no outer plasma membrane (Sutcliffe, 2010). The peptidoglycan (or murein) wall is made up of alternating residues of *N*-acetylglucosamine (GlcNAc) and *N*-acetylmuramic acid (MurNAc) which produce the glycan backbone, through β-1→4 linkages and the side chains of peptides that connect the glycan bonds together (Dramsi et al., 2008, Schleifer and Kandler, 1972). The D-lactoyl group in each *N*-acetylmuramic acid moiety is substituted by a peptide stem composed mostly of L-Ala-γ-D-Glu-meso-2,6-diaminopimelic acid (or L-Lys)-D-Ala in nascent peptidoglycan, the last D-Ala being absent in mature peptidoglycan) (Dramsi et al., 2008).

The major function of this peptidoglycan cell wall is to maintain cell integrity by withstanding the turgor, thus supplementing the role of the inner plasma membrane (Silhavy et al., 2010). Inhibition of its biosynthesis through mutation or antibiotics (e.g. penicillins) results in cell lysis (Vollmer et al., 2008a). Through bacterial growth, peptidoglycan is remodelled actively to permit integration of new

peptidoglycan and to accommodate alterations in cell shape (Vollmer and Bertsche, 2008). In *S. coelicolor*, the peptidoglycan remodelling is required during the many steps in growth and development; although poorly understood, this is thought to be achieved through cell wall hydrolases (Haiser et al., 2009, Flardh, 2003).

1.6.2 Peptidoglycan synthesis

The synthesis of the peptidoglycan sacculus is a dynamic form of growth and is under tight spatiotemporal regulation with cytoplasmic and cytoskeletal proteins playing central roles in defining the shape and structure of the peptidoglycan sacculus (Schleifer and Kandler, 1972, Labischinski and Maidhof, 1994). Peptidoglycan biosynthesis occurs through a series of enzyme-catalysed reactions that take place in the cytoplasmic membrane (nucleotide-linked precursor synthesis), on the inside (lipid-linked intermediate synthesis) and on the outside of the cytoplasm (polymerisation reactions). This procedure of biosynthesis can be divided into four types of reactions that take place in various parts of the bacterial cell. (1) The soluble nucleotide precursors UDP-*N*-acetyl-glucosamine (UDP-GlcNAc) and UDP-*N*-acetyl- muramic acid (UDP-MurNAc) are formed in the cytoplasmic membrane (Egan and Vollmer, 2013, Barreteau et al., 2008, Vollmer and Bertsche, 2008). UDP-GlcNAc and UDP-MurNAc generate the fundamental strength of the peptidoglycan backbone. (2) At the inner membrane leaflet, nucleotide precursors are coupled with undecaprenyl phosphate to create the lipid anchored cell wall precursor. This has a monomeric structure that contains a disaccharide pentapeptide subunit named lipid II. Next lipid II is flipped onto the extracellular side of the membrane, which possibly occurs by FtsW-RodA (Mohammadi et al., 2011, Vollmer et al., 2008a, Bouhss et al., 2008). (3) Glycosyltransferases then polymerise lipid II and thus liberate the undecaprenyl phosphate, which rotates back to the interior of the cytoplasmic membrane. Consequently, glycan chains are integrated into the peptidoglycan cell wall. (4) The glycan chains produce cross-linkage by transpeptidases (Vollmer et al., 2008a, Vollmer and Bertsche, 2008, Vollmer et al., 2008b).

1.6.3 Teichoic and lipoteichoic acids

The bacterial cell wall incorporates long anionic polymer chains of teichoic acids which are intertwined within the peptidoglycan layer. Teichoic acids consist mainly of repeating monomers of glycerol phosphate, ribitol phosphate or glucosyl phosphate. There are two classes of teichoic acid polymers: wall teichoic acids (WTAs) are covalently attached to peptidoglycan while lipoteichoic acids (LTAs) are anchored membrane lipid head groups (Silhavy et al., 2010).

Given the polymeric nature and relative abundance of teichoic acids in the plasma membrane [60% of the total mass in Gram-positive cell walls (Silhavy et al., 2010)] and the fact that they are widely distributed in both pathogenic and non-pathogenic bacteria (Rahman et al., 2009b), they are thought to play a key role in cell envelopes. For instance, it has been suggested that polyanionic LTAs might play a significant role in the retention of divalent cations such as Mg^{2+} ions within cell envelopes, thereby influencing cell division (Rahman et al., 2009b). Prototypical lipoteichoic acids are polymers of polyglycerophosphate (PGP) containing a glycolipid anchor; although in some cases they are variably replaced by glycosyl and/or D-alaninyl units. Instead of teichoic acids, some bacterial cell envelopes predominantly contain lipoglycans which are less anionic or neutral and arabinogalactan polysaccharides as secondary components of the cell wall. For instance, in the bacterium *Micrococcus luteus* an Actinobacteria, the cell envelope contains both a succinylated lipomannan lipoglycan and teichuronic acids (Powell et al., 1974). The latter are polysaccharides of uronic acid whose production is triggered when the cell has limited supply of phosphate. In this case, the available phosphate is used solely for DNA, RNA and phospholipid synthesis, rather than in the production of teichoic acids. Both teichoic acids and teichuronic acids are functionally interchangeable (Sutcliffe, 2010).

Lipoteichoic acids (LTA) are the main lipid-linked glycopolymers that are also known as macroamphiphiles, encountered in the majority of low G+C bacteria (Firmicutes) (Sutcliffe and Shaw, 1991) . LTA consists of a lipid anchor linked to a chain of polyglycerol or poly-ribitol units separated by a phosphate group and it has been reported that such repeated units are also characteristic of teichoic acids linked

to peptidoglycan (Cot et al., 2011). A detailed structure of LTA isolated from *Streptomyces hygroscopicus subsp. hygroscopicus* was described for the first time recently (Cot et al., 2011). It was shown to consist of a polyglycerolphosphate backbone substituted with α-glucosaminyl and α-N-acetyl-glucosaminyl residues without an amino-acid substituent. The structure was found to be closely related to that of the WTA of this organism. This supported growing recognition of LTA as a component of Gram-positive cell envelopes in Actinobacteria (Rahman et al., 2009a), despite them having high G+C, and further supports the hypothesis that there is an overlap between the synthetic pathways of LTA and WTA in these bacteria (Rahman et al., 2009b). The LTA from *S. hygroscopicus* induced signalling by human innate immune receptor TLR2 which confirmed its role as a molecular pattern associated with microbes. This activity was partially dependent on TLR1, TLR6 and CD14. In addition, it stimulated release of IL-6 and TNF-α in a human macrophage cell line to levels similar to those induced by *S. aureus* LTA (Cot et al., 2011).

The synthesis of lipoteichoic acid (LTA) proceeds via linkage of glycerolphosphate units, which originate from membrane phosphatidylglycerol and glycolipid anchor units synthesised independently under the action of glycosyltransferases (Rahman et al., 2009b). It is important to note here that biosynthesis of LTA is likely independent of PG in *Streptomyces* (Rahman et al., 2009b). The polymerisation of polyglycero-phosphate (PGP), a component of LTA, occurs through the action of a glycerophosphate polymerase known as PGP-lipoteichoic acid synthase (LtaS). In Firmicutes, this polymerisation reaction takes place in the plasma membrane (outer leaflet). This process is facilitated by a membrane permease protein, LtaA, which transfers glycolipid acceptors exteriorly from the inner plasma membrane leaflet to the outer leaflet. During the transfer of glycerolphosphate units from phosphatidylglycerol to form PG-LPA polmers, diacylglycerol is released and, through the action of diacylglycerol kinase, is then recycled into phospholipid metabolism (Rahman et al., 2009b). The *S. coelicolor* genome encodes a protein (SCO7547) which is a homologue of the PGP-lipoteichoic acid synthase (LtaS). However, this homology is restricted to a very short region and, unlike the LtaS, SCO7547 is not a membrane protein. This has led to the suggestion that LtaS is not

likely to be involved in PGP synthesis in *S. coelicolor*. It has thus been suggested that there might be an overlap between the synthetic pathways of teichoic acids and LTA in LTA-producing bacteria such as *S. coelicolor* (Rahman et al., 2009b).

1.6.4 Other cell wall components

In addition to teichoic and lipoteichoic acids, bacterial cell walls contain various proteins including porins and adhesins which are attached either to peptidoglycan or teichoic acids via noncovanent ionic interactions; although they may be attached covalently to stem peptides within the peptidoglycan layers (Silhavy et al., 2010, Dramsi et al., 2008). Another component that has been identified in the outer hydrophobic layer of the aerial hyphae of *S. coelicolor* is a new class of secreted proteins named chaplins. These amyloid fibrils at the cell surface of the aerial hyphae act together to assist aerial development. These secreted proteins, have been suggested to be associated with neurodegenerative diseases such as Alzheimer's disease and Parkinson's disease and contain a conserved structural domain, the cross-β structure. In addition to chaplins, rodlets are another component that have been identified in the cell surface of the aerial hyphae (Claessen et al., 2004). The production of a rodlet layer in the aerial hyphae is due to the interplay between rodlins and chaplins (Bokhove et al., 2013, Capstick et al., 2011, Duong et al., 2012, Elliot et al., 2003, Sawyer et al., 2012, Sawyer et al., 2011, Talbot, 2003).

1.6.5 The plasma membrane of a monoderm bacterial cell envelope

The plasma membrane of a monoderm architectural cell envelope is analogous to the inner membrane of diderm-type envelopes found in Gram-negative bacteria. Thus it lacks many of the components found in the outer membrane of the latter type of bacteria such as lipopolysaccharides. The plasma membrane is a trilamellar structure composed of a phospholipid bilayer and different lipoproteins (Hutchings et al., 2009, Chatterjee and Chaudhuri, 2012). The lipoproteins play a key role in nutrient scavenging, protein folding, cell envelope assembly, environmental signalling, virulence and host cell adhesion (Widdick et al., 2011). With the help of embedded proteins, it acts primarily as a diffusion barrier and an interface for communication between the inside of the cell (cytoplasm) and its immediate surrounding

environment (Jordan et al., 2008). The commonest phospholipids present in bacterial cell membranes are: PG, PE and CL. Other less frequent ones include phosphatidylcholine, phosphatidylinositol and membrane lipids such as ornithine lipids, glycolipids and sphingolipids (Sohlenkamp and Geiger, 2015).

In monoderm plasma membranes, lipoproteins are found anchored into the outer leaflet while in diderm bacteria, they are on the outer membrane (Sutcliffe et al., 2012). Lipoproteins are a functionally diverse class of peripheral membrane proteins which are formed by lipid modification of lipoprotein signal peptides via covalent addition of a diacylglyceride to the peptide's indispensable N-terminal cysteine residue (Hutchings et al., 2009). This lipid modification helps to tether these proteins to the outer face of the plasma membrane and provides a means by which PLs turnover into lipoproteins (Sutcliffe et al., 2012). Protein lipidation occurs as a post transcriptional modification of bacterial lipoprotein precursors (pre-BaLpp) after they have been translocated to the surface of the membrane via the secretory (Sec) or twin arginine protein transport (Tat) location pathways (Hutchings et al., 2009, Widdick et al., 2011, Thompson et al., 2010); the choice of which pathway is dependent on the presence of specialised signal peptides (Sutcliffe et al., 2012).

Thus the biosynthesis of membrane lipoproteins is a three step pathway that is conserved in Gram-positive bacteria (Hutchings et al., 2009). Firstly, using membrane lipid substrates, the enzyme prolipoprotein diacylglyceryl transferase (Lgt) catalyses the formation of a thioesther linkage by transferring a diacylglyceryl moiety to the conserved 'lipobox' sequence motif containing an invariant cysteine residue (Hutchings et al., 2009). Secondly, through the action of Type II lipoprotein signal peptidase (Lsp), the signal peptide is cleaved next to the 'lipobox' conserved cleavage site leading to the formation of a mature lipoprotein containing a lipid-modified cysteine at the N-terminus. The final step, which occurs in Gram-negative bacteria and mycobacteria, involves the addition of a third fatty acid residue, through an amide linkage, to the free amino residue of the lipidated cysteine to give triacylated lipoproteins (Widdick et al., 2011). This step is catalysed by the enzyme lipoprotein N-acyl transferase (Lnt) and is essential for the release, from the plasma

membrane, of lipoproteins and their eventual transportation across the membrane via the Lol (lipoprotein localisation) pathway (Hutchings et al., 2009, Widdick et al., 2011).

It has been suggested that all *Streptomyces* species encode two homologues of Lnt, while some encode two homologues of Lgt. The essentiality of Lgt and Lsp has been studied in *Streptomyces scabies,* a plant pathogen, which revealed that *lgt* and *lsp* mutants were defective in growth and development while their virulence was only moderately affected (Widdick et al., 2011). Mutation in *lgt* led to loss of lipoproteins from the membrane, but were restored when *S. coelicolor lgt1* or *lgt2* were expressed which confirmed that both code for functional Lgt enzymes. *Streptomyces* membrane lipoproteins are N-acylated and it has been shown that efficient N-acylation is dependent on Lnt1 and Lnt2; although deletion of *lnt1* and *lnt2* neither had any effect on growth and development nor on virulence (Widdick et al., 2011). This impliesthat this step is not essential for lipoprotein function in the organism. However, in *E. coli* it has been suggested that depletion of Lnt leads to accumulation of lethal levels of outer membrane lipoproteins within the plasma membrane (Robichon et al., 2005). This further supports the idea that maturation, via N-acylation, of outer membrane lipoproteins in Gram-negative bacteria by Lnt is essential for their efficient recognition by the Lol system which transports them from the plasma membrane to the outer membrane (Fukuda et al., 2002).

1.6.6 Cell wall stress

The cell envelope of the bacterial cell wall and membrane is the first and main boundary of protection against any environmental threat, including osmotic stress of the cell envelope as well as some antibiotics. A number of clinical studies found that antibiotics target the cell wall of bacteria in particular and inhibit biosynthesis of peptidoglycan either by mimicking or binding to a substrate or direct inhibition of enzyme function. Cell envelope stress responses through signal transduction systems are coordinated by two principle regulatory systems: (1) two-component systems (TCS) or (2) extra cytoplasmic function (ECF) sigma factor (σ factor) / anti-sigma factor pairs (σ anti-factor). Usually, all systems are analogous in function in that they

contain a membrane- associated stress sensor protein and a cytoplasmic transcriptional regulator (Jordan et al., 2008). TCS consists of a cognate response and a sensor histidine kinase regulator. In the absence of the stimulus conditions the kinase is inactive and the regulator is not phosphorylated. Once the stimulus is present, the sensor kinase auto phosphorylates on a His-residue and the phosphate is moved onto the response regulator, resulting in its activation (Whitworth and Cock, 2009, Goulian, 2010).

On the other hand, in the absence of stress conditions, an anti-sigma factor tightly binds to the sigma factor to separate it from RNA polymerase core enzyme. However, upon signal perception, it frees the sigma factor, permitting the formation of holoenzyme and expression of the target regulon. In the genome of *B. subtilis* there are seven encodes ECF sigma factor and at least three of them (σ^X, σ^W, σ^M) play a role in the response of *B. subtilis* to cell envelope stress conditions (Hughes and Mathee, 1998, Eiamphungporn and Helmann, 2008, Luo et al., 2010).

In *Streptomyces,* the signal transduction system σ^E –CseABC, senses and responds to changes in cell wall integrity (Figure 1.4), where Cse stands for control of σ^E (sigma E) (Hong et al., 2002). This system unusually contains both a TCS and an ECF sigma factor; as yet, no involvement of an anti-sigma factor has been found in this *S. coelicolor* system. It comprises of four proteins encoded in an operon; σ^E (RNA polymerase σ factor), CseA (an extra-cytoplasmic novel lipoprotein), CseB (response regulator) and CseC (sensor kinase). On the perception of a signal CseC stimulates CseB through phosphorylation and then the expression of *sigE-cseABC* operon is induced. These signals might contain cell wall precursors or breakdown products since the *sigE* operon is induced in reaction to stress signals from the cell envelope (Hong et al., 2002, Hutchings et al., 2006). Somehow, the lipoprotein CseA appears to modulate the signal sensing of CseC and as a result, upregulates the *sigE* promoter (Hutchings et al., 2006).

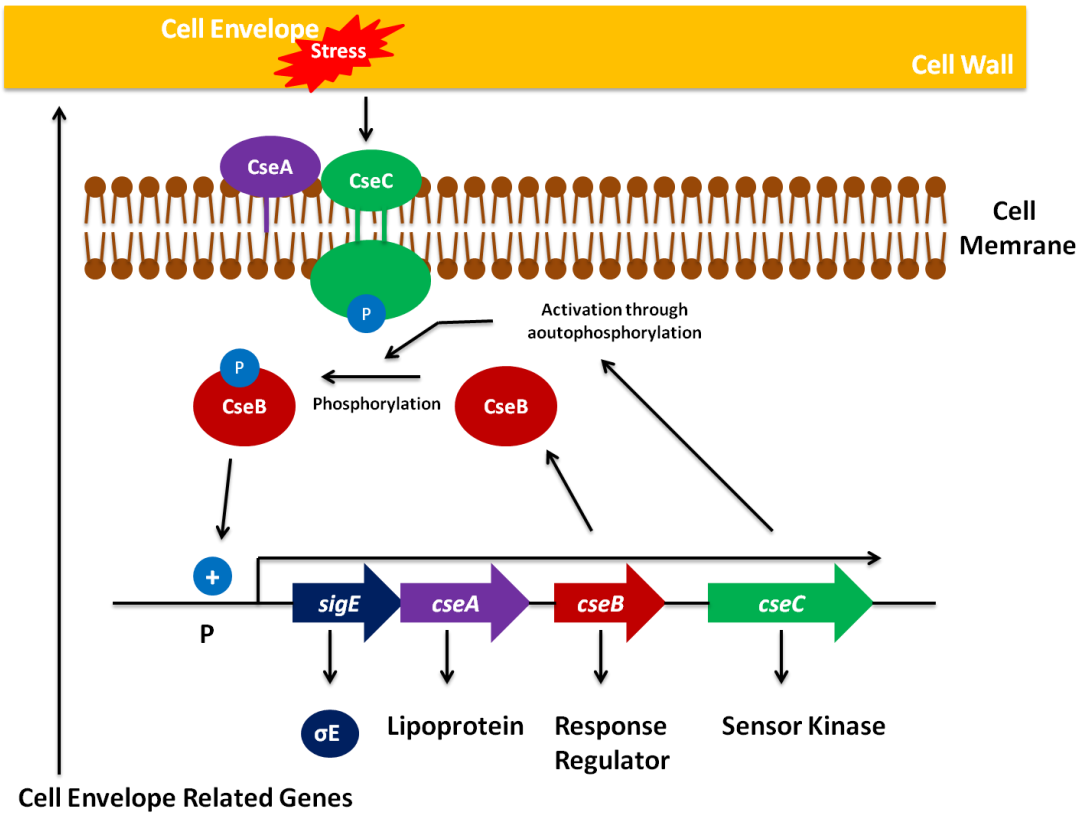

Figure 1-4: The model σ^E CseABC signal transduction system in *S. coelicolor*.

Gene expression that encodes σ^E (*sigE*) is regulated at the transcriptional level via the CseB/CseC two component signal transduction system. Signals that initiate cell envelope stress activate the sensor kinase, CseC, that is auto phosphorylated at His-271 and, consistent with the identified system for other two-component regulatory mechanisms, this phosphate is then removed to Asp-55 in the response regulator, CseB. Phospho-CseB regulates the promoter of the *sigE* operon, and σ^E is controlled by the central RNA polymerase to transcribe genes with cell envelope associated roles, including 12 genes of a putative operon (the *cwg* operon) that possibly is involved in cell wall glycan biosynthesis, modified from (Hoskisson and Hutchings, 2006, Hong et al., 2002).

1.6.7 Alternative Sigma Factors

Sigma factors proceed by interacting with and affecting the specific promoter of the RNA polymerase core enzyme, resulting in selectively directing transcription of various sets of genes, organising gene expression in response to different environmental hardships. Phylogenetic studies of streptomycete sigma factors show that they are divided into four groups. *S. coelicolor* contains (1) 1 housekeeping sigma factor (HrdB), (2) 3 sigma factors (HrdA, C, D), (3) 10 sigmas and (4) 45 extra-cytoplasmic role (ECF) sigma factors. At least two group 3 sigma factors regulate the events of development after the appearance of aerial hyphae ending in sporulation. This sporulation system initiates, before sporulation septation, through σ^{WhiG} that eventually results in late spore σ^{F} expression (Figure 1.5) (Dyson, 2009).

The sigma factor *sigF* is involved in the late phases of sporulation; a *sigF* mutant undertakes spore formation and septation, although spore chains appear irregular, thin-walled, lacking pigment, sensitive to detergent and have uncondensed DNA (Kelemen et al., 1996, Kormanec et al., 1996, Potúčková et al., 1995). *sigF* belongs to a similar subgroup of Gram- positive specific σ factors, named *sigB* for *B. subtilis* stress response. There are nine stress response sigma factors that are similar to *sigB* in *S. coelicolor;* one of them is *sigF* (Lee et al., 2004). The *sigF* gene is transcribed during late sporulation septa formation. σ^{F} is involved in the expression of the *whiE* gene cluster, specifically polyketide synthase type II which controls the gray spore pigment synthesis (Chater and Chandra, 2006, Kelemen et al., 1996). There are some indications that show that *sigF* controls the expression of the *whiE* gene cluster both directly and indirectly (Kelemen et al., 1998, Potúčková et al., 1995). Two of the other group 3 sigma factors, σ^{H} and σ^{B}, (Lee et al., Kelemen et al., 2001, Sevcikova et al., 2001, Sevcikova et al., 2010) have dual functions; they are involved in directing appropriate differentiation and, combined with another group 3 sigma factor, σ^{I} (Homerova et al., 2012, Viollier et al., 2003b), they are also implicated in responses of osmotic stress; certainly, σ^{H} is also engaged in a response to temperature stress (Dyson, 2009).

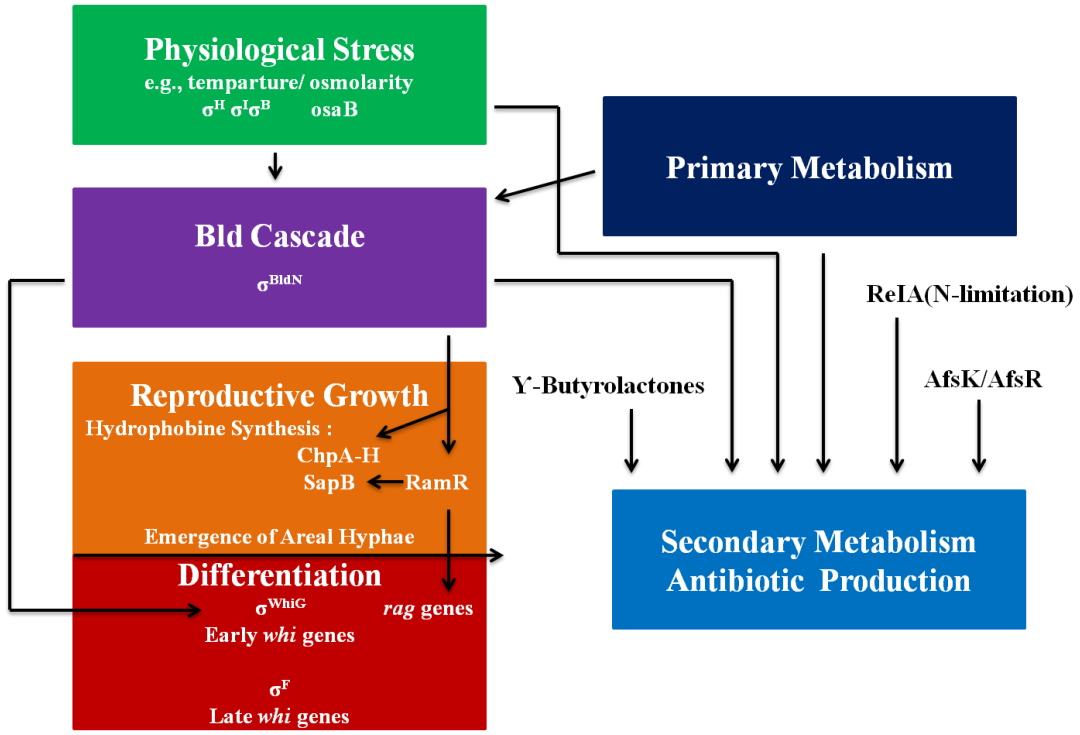

Figure 1-5: Regulation physiological and morphological development in *S. coelicolor*.

This illustration shows the difficulty of genetic regulatory networks, emphasising the function of some of the significant alternative sigma factors and other regulatory molecules required in reproductive growth controlling like sporulation and secondary metabolism like antibiotic formation, modified from (Dyson, 2009).

The other sigma factors that influence the stress response and growth are σ^B and σ^H. σ^B is a controlling regulator in *S. coelicolor* for osmotic stress response. It has been demonstrated that *sigB* is the master regulator in *S. coelicolor* for osmotic stress response and governs the induction of approximate 280 genes. Also, it is a component of an operon that preceded by *rsbA* and *rsbB* genes which encodes homologues of an anti-sigma factor (RsbW), and its antagonist (RsbV) from *B. subtilis* respectively (Fernandez-Martinez et al., 2011, Lee et al., 2005).

1.7 Relevance of PLs in bacterial development and growth

1.7.1 PLs

As an essential composition of all living cells, biological membranes have different roles in cellular processes and allow adaptation to surrounding conditions. The suggested lipid groups listed in (Table 1.1, A) contain names that are the most accepted in the literature (Fahy et al., 2005). Also in response to the demand from many experts in lipid biochemistry, the abbreviations of the glycerophospholipid classes have been updated in the LIPID MAPS database to the new universal format of two letters 'PC, PE, PS, PG' (Fahy et al., 2009) (Table 1.1, B). Prokaryotic and eukaryotic membranes comprise a selection of lipids, with PLs as the main lipid class (Moser et al., 2014).

Table 1-1: Lipid classification (A): a comprehensive classification of lipids based on LIPID MAPS classification system.

A

Group	Abbreviation	Structures in Database
Fatty acyls	FA	5869
Glycerolipids	PK	7541
Glycerophospholipids	GP	8002
Sphingolipids	SP	4338
Sterol lipids	ST	2715
Prenol lipids	PR	1259
Saccharolipids	SL	1293
Polyketides	GL	6742

B

Class	Synonym	Old	New
Glycerophosphocholines	Phosphatidylcholines	GPCho	PC[1]
Glycerophosphoethanolamines	Phosphatidylethanolamines	GPEtn	PE
Glycerophosphoserines	Phosphatidylserines	GPSer	PS
Glycerophosphoglycerols	Phosphatidylglycerols	GPGro	PG
Glycerophosphoglycerophosphates	Phosphatidylglycerol phosphates	GPGro	PPGP
Glycerophosphoinositols	Phosphatidylinositols	GPIns	PI
Glycerophosphoinositol monophosphates	Phosphatidylinositol phosphates	GPInsP	PIP
Glycerophosphoinositol bis-phosphates	Phosphatidylinositol bis-phosphates	GPInsP2	PIP2
Glycerophosphoinositol tris-phosphates	Phosphatidylinositol tris-phosphates	GPInsP3	PIP3
Glycerophosphates	Phosphatidic acids	GPA	PA
Glyceropyrophosphates		GPP	PPA
Glycerophosphoglycerophosphoglycerols	Cardiolipins	CL	CL
CDP-glycerols		GCDP	CDP-DG
Glycosylglycerophospholipids		(glycan)GP	(glycan)GP
Glycerophosphoinositolglycans		(glycan)GPIns	(glycan)PI
Glycerophosphonocholines		GPnCho	PnC
Glycerophosphonoethanolamines		GPnEtn	PnE

This database is driven from the idea of two primary 'building blocks': isoprene groups and ketoacyl groups. These lipids are chemically classified and based on the characterisation of different components that comprise the lipid as hydrophobic or amphipathic. Depending on this scheme, lipids have been separated into eight groups (Fahy et al., 2011, Fahy et al., 2005) (Date of access March 2015). Abbreviations for phospholipid modifications for the main classes 'Glycerophospholipids' (red rectangle) in the comprehensive classification system **(B)**. The green rectangle indicates our target phospholipid (PG). [1]To abbreviate monoradylglycerophospholipids or lysophospholipids, the latter 'L' may be used in the abbreviation, for instance, LPC LPC, LPE, LPA, etc (Fahy et al., 2009).

One main function of lipids in cellular development is to produce the lipid bilayer of cell membranes.. Neutral diacylglycerol glycans are key membrane producing constituents in several Gram-positive bacteria and in the membranes of plants. Despite this Gram-negative bacteria use a saccharolipid, Lipid A as a main structural part of the outside membrane. The diversity of hydrophobic domain lipids results in additional variety. These domains in eukaryotes and eubacteria can contain saturated or unsaturated fatty acids or alkyl alcohols (Vance and Vance, 2008). Bacterial membranes have been explored in depth in the model organisms of Gram-negative (*E. coli*) and Gram-positive (*B. subtilis*) bacteria. The most frequent bacterial membrane lipids are PE, PG and CL (Moser et al., 2014). *Streptomyces* produces secondary metabolites during the stationary phase, many of which have been utilised as antibacterial compounds in clinical use. Several of these compounds target the cell wall through peptidoglycan synthesis or disrupt the function of the membrane (Challis and Hopwood, 2003, Hachmann et al., 2009). In the terms of the applications, the lipopeptide antibiotic, daptomycin is a recently FDA-approved antimicrobial treatment. Daptomycin displays activity against a wide range of Gram-positive infections as well as multidrug-resistant infections, such as methicillin-resistant *Staphylococcus aureus* (MRSA) and vancomycin-resistant enterococci (VRE) (D'Costa et al., 2012, Steenbergen et al., 2005). Daptomycin is produced by the actinomycete *Streptomyces roseosporus* and consists of linear or cyclic peptide with an N-terminal end that is acylated with a fatty acid side chain. The suggested mechanism of activity is through the insertion of the lipophilic daptomycin tail into the cell membrane of bacteria, resulting in fast membrane potassium ion efflux and a depolarization (Beiras-Fernandez et al., 2010, Straus and Hancock, 2006).

1.7.2 Fatty acid biosynthesis in actinomycetes

Lipids function primarily as structural constituents of membranes and stores of metabolic fuel. They are involved in protection of the outside layer on the membrane surface and also act as species-specific markers for cell recognition and immunological detection (Fahy et al., 2005). Fatty acid production in all organisms occurs through a cycle of repeated reactions. In mammals and several animals, these synthetic reactions occur via type I fatty acid synthase (FAS I) system. On the other hand, among bacteria and plants the system utilised is type II where each synthetic reaction is controlled by a discrete FAS II protein. The biosynthetic pathway, in *E. coli*, of fatty acids (FAs) is well studied and has offered a basis of explaining other FAS II pathways in bacteria (White et al., 2005). Nevertheless, biosynthesis of FAs is different among Actinobacteria; for instance *Mycobacterium* contains both FAS systems, *Streptomyces* have only FAS II, while *Corynebacteria* exclusively have FAS I (Gago et al., 2011, Parsons and Rock, 2013).

Fatty acid biosynthesis is the initial step in membrane lipid production and is crucial to all organisms (De Rosa et al., 1986). The initial step in the synthesis involves carboxylation of acetyl-CoA to form malonyl-CoA via action of acetyl-CoA carboxylase (ACC). In order to be accessible to the enzyme, the malonyl moiety of malonyl-CoA must be transferred to ACP forming malonyl-ACP. This takes place under the action of malonyl-CoA:ACP transacylase, typically named FabD (Parsons and Rock, 2013, Parsons and Rock, 2011).

Streptomyces uses a FAS II system to synthesise fatty acids *de novo*. Most of these are produced from branched initiators such as isovaleryl, isobutyryl and anteisovaleryl, leading to production of even and odd numbered fatty acids with a methyl branch at the omega-terminus (80–90% by weight of total fatty acid); the others are synthesized from unbranched initiators such as butyryl and acetyl units (Wallace et al., 1995, Kaneda, 1991). Research in the genes for fatty acid biosynthesis has led to the revealation that some of the genes encoding the core enzymes required during biosynthesis of saturated fatty acids are located in a cluster of conserved fatty acid biosynthesis (*fab*) genes comprising of *fabD, fabH, acpP* and

fabF. This cluster was partially characterized in *S. coelicolor* and its association with the FA biosynthetic pathway was verified through biochemical and genetic studies (Revill et al., 1996, Revill et al., 1995, Revill et al., 2001). The *fabD* gene encodes malonyl-CoA:ACP transacylase which does the transfer of malonyl-ACP substrate to the core enzymes. The *E. coli* FabD protein functionality could be replaced by FabD in *S. glaucescens* (sgFabD) when the latter is activated in the bacterium (Summers et al., 1995). *In vitro* analysis also showed that sgFabD is expressed with many ACPs such as TcmM (tetracenomycin PKS ACP in *S. glaucescens*), AcpP (FAS ACP in *E. coli*) and FabC (FAS ACP in *S. glaucescens*) (Florova et al., 2002). The sgFabD protein has low specificity for various ACPs suggesting that its functional task is to offer malonyl-ACP precursors for the biosynthesis of type II PK and fatty acids (Florova et al., 2002). *S. coelicolor* contains just one copy of *fabD* in the major *fab* cluster (Revill et al., 1995), indicating that, in addition to its vital function in FA biosynthesis, it also contributes to the biosynthetic pathway of type II PK (Revill et al., 1995). The gene *fabH* in *S. coelicolor* was confirmed to be essential which was in agreement with its vital function as the FAS protein-encoding gene (Revill et al., 2001). On the other hand, the *acpP* gene is one of the FAS complex members in *S. coelicolor* and, in accordance with its function, is subject to constitutive regulation and can carry out fatty acid synthesis in *E. coli* (Revill et al., 1996). The other two ACPs are activated during development and are involved in the catalysis of the type II PKs produced by *S. coelicolor,* including the blue and gray pigments linked with the spore wall (Revill et al., 1996).

The genes *SCO2389* and *SCO4744* encoding actinorhodin ACP in *S. coelicolor* were found to be required in the synthesis of the aromatic polyketides in various steps of the life cycle (Zhou et al., 1999, Revill et al., 1996, Florova et al., 2002). The genes that encode for the two reductases: β-ketoacyl-ACP and enoyl-ACP reductases, and that of (3*R*)-hydroxyacyl-ACP dehydratase, have not yet been identified in streptomycetes. However, according to genetic and biochemical information available for these enzymes and their association with other members of actinobacteria, these roles can be assigned to putative genes. For instance, in *S.*

coelicolor, it was found to be homologous to *mabA-inhA* from *Mycobacterium tuberculosis* (Gago et al., 2011, Cole et al., 1998).

1.7.3 Phospholipid composition in *Streptomyces*

Bacterial PLs play a key role in the fluidity, stability and structural modifications of membranes. They influence morphological development and growth of different bacteria. A given class of phospholipids may consist of various molecular species and there have been various attempts to elucidate the molecular composition of phospholipid classes because of their importance in the functioning of biological membranes. However, current knowledge of the molecular phospholipid composition of many bacteria is still restricted because of difficulties with traditional techniques such as TLC (Hoischen et al., 1997b).

In *Streptomyces*, the membrane phospholipid that has received most attention in recent years is cardiolipin (CL) or diphosphatidylglycerol which consists of two phosphatidyl moieties linked together by a glycerol. As a result, CL possesses four hydrophobic acyl chains and a small hydrophilic head group. This conical structure allows CL to accumulate in membrane domains of higher curvature (Jyothikumar et al., 2012).

In addition to CL, other PLs have been putatively identified in *Streptomyces coelicolor* based on TLC to be phosphatidylglycerol (PG) and phosphatidylethanolamine (PE). In this study, the authors reported that *clsA*, the gene encoding CL synthase, was essential since it could not be deleted without providing a second functional copy elsewhere in the chromosome. It was also shown that depletion of *clsA* caused alterations in the PL profile especially in the content of PG and CL. More interestingly, the study reported that *ClsA* depletion produced new PL species detectable by negative ion electrospray ionisation (ESI) mass spectrometry (MS) analysis of PL extracts from mid-log phase liquid grown cultures. Several differences were noted in various envelopes of peaks corresponding to phosphatidic acid (PA, m/z 600–680 and 790–840), phosphatidylethanolamine (PE, m/z 650–700),

phosphatidylglycerol (PG, m/z 700–750 and 850–890), and phosphatidylinositol (PI, m/z 780–840) (Jyothikumar et al., 2012).

A study was also reported that characterised the molecular PL species in the cytoplasmic membranes of a *Streptomyces hygroscopicus* L form; a strain that had been grown without a cell wall and periplasmic compartment for 20 years. This lead to its membrane becoming more stable and resistant to environmental stress, presumably so that its membrane could take over the role of the cell wall. This study found no qualitative differences in membrane-derived PLs phosphatidylethanolamine (PE1 and PE2), lyso-cardiolipin (LCL), cardiolipin (CL), lyso-phosphatidylethanolamine (LPE), phosphatidyl-inositolmannoside (PIM), phosphatidic acid (PA) and dilyso-cardiolipin-phosphatidylinositol (DLCL-PI), which is actually two distinct lipids, PI and dilyso-CL, and in 13 main fatty acids compared to the parent vegetative cells (N-form) or its protoplasted derivative (Hoischen et al., 1997a, Hoischen et al., 1997b). Instead, clear quantitative differences were noted where membranes from the L-form contained 3-4 times more extractable lipids, 20% more PLs and altered proportions of individual PL classes. These differences included increased content of CL and PIM and a reduced content of DLCL-PI (Hoischen et al., 1997b). Further characterisation of three of the PLs above using MS techniques led to identification of molecular ion groups for PE1 (four groups), LCL (six groups) and CL (six groups) which eventually yielded 18, 43 and 59 molecular lipid species for these PLs respectively. However, the role of each of these complex and diverse assembly of molecular species in the membrane remains largely unknown in terms of the structural and functional organisation of the cytoplasmic membrane (Hoischen et al., 1997b).

1.7.4 Phosphatidylglycerol

PG was discovered in 1958 (Benson and Maruo, 1958) in the alga, *Scendesmus.* They isolated ^{32}P-labelled glycerophosphoglycerol from the *Scendesmus* lipids, and found glycerol and glycerophosphate upon acid hydrolysis. Thereafter, in 1962, Haverkate et al., (1962) isolated ^{32}P-labelled PG from *Bacillus cereus* and examined its susceptibility to phospholipases (Haverkate et al., 1962). Phospholipase A

transformed PG to lysoPG, phospholipase C provided diacylglycerol and glycerophosphate and phospholipase D provided phosphatidic acid and glycerol (Hawthorne and Ansell, 1982). PG is a lipid that provides the major constituent of some bacterial membranes and is also found in the membranes of plants and animals, where it seems to carry out specific roles (Christie, 2014, Nie et al., 2010, Tanoue et al., 2014), structure for this PG is shown in (Figure 1.6).

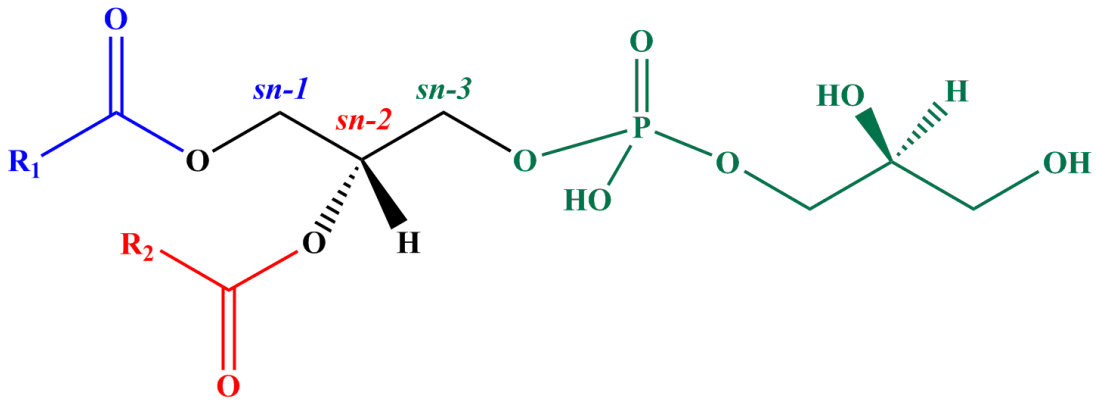

Phosphatidylglycerol (PG): 1,2-diacyl-*sn*-glycero-3-phospho-(1'-*sn*-glycerol)

Figure 1-6: PG structure.

A glycerol (core) group (black) in bacteria is *sn*-3glycerol typically esterified at locations of *sn*-1 and *sn*-2 with two acyl chains R1 (blue) &R2 (red). Also the molecules contain PG (green) headgroup (Fahy et al., 2005, Vance and Vance, 2008), modified from (Anon, 2015) via Chemdraw.

PG exists in almost all bacterial groups. For instance, in *E. coli*, PG comprises up to 20% of cell membranes, whereas the rest are made up of PE with a low amount of CL (CL). In several bacteria, diacyl hydrophobic chains are found predominately in the lipid, yet in other organisms, alkylacyl and alkenylacyl forms are present. In non-photosynthetic eukaryotes, PG is synthesised only in mitochondria, and is utilised as the precursor for CL, where is positioned in the inner membrane of mitochondria, and is required for the appropriate function of the enzymes implicated in oxidative phosphorylation (Christie, 2014, Matsumoto, 2001, Seddon et al., 2008). CL is named diphosphatidylglycerol and is the only PL with a dimeric structure and contains four acyl chains and two negative charges. It originates in specific bacterial membranes, hydrogenosomes and mitochondrial membranes where there is a requirement to produce an electrochemical potential for substrate transport and ATP synthesis (Schlame et al., 2000).

The *pgsA* gene in *E. coli* encodes phosphatidylglycerolphosphate synthase (PgsA) which catalyses the first committed step for synthesis of the anionic PLs. Null mutants of these anionic PLs (PG and CL) showed they are not indispensable for cellular development. In the mutants, the main external membrane lipoprotein precursor, which requires PG for its lipid component, accumulates on the inside of the membrane and causes the death of the cell. Cells incapable of producing this lipoprotein still grow normally but are growth sensitive for temperature at 42°C showing that PG and CL are not totally needed for basic development function and viability, just for optimal growth (Vance and Vance, 2008, Matsumoto et al., 2006, Kikuchi et al., 2000, Matsumoto, 2001). CL appears to have a unique function which involves operating either as a bilayer or non-bilayer lipid based on the absence or presence of divalent cations (Mileykovskaya and Dowhan, 2009). CL is used for energy transduction in the mitochondria and bacteria membranes (Table 1). A large number of undefined properties of CL are the constant ionization of its two phosphate diesters. Instead of exhibiting two values of pK in the range of 2–4, pK_2 of CL is greater than 8.5, showing that at physiological pH, CL is protonated. This means that CL has become a conduit for protons. Even though PG substitutes for CL in in both yeast and bacteria, in yeast the lack of CL is accompanied with a reduction

in cell growth (Vance and Vance, 2008). PG and CL are abundant in bacterial cell membranes and other PLs such as PE, phosphatidylserine (PS), and phosphatidylinositol (PI) are also found in the cell membranes; a defect of any of these PLs could influence the growth and development of bacteria (Geiger et al., 2013).

1.7.5 Biosynthesis of PG

All the main components of the PL pathway originate from the precursor phosphatidic acid in the PL biosynthetic pathway. *E. coli* contains three simple main PL species in its cell membranes, which make it a simple organism to investigate according to PL biosynthesis. PE forms the bulk of the PLs at 75%, with PG and CL making up the rest with 15–20% and 5–10%, respectively (Miyazaki et al., 1985). CDP-diacylglycerol is the key activated intermediate in synthesis of bacterial PLs.

The enzyme phosphatidate cytidylyltransferase, alternately known as CDP–diacylglycerol synthase (CDS), catalyses the transformation of phosphatidic acid to a combination of CDP–diacylglycerol (CDP-DAG) and dCDP–diacylglycerol (dCDP-DAG). CDP–DAG is the precursor to phosphatidylethanolamine synthesis and PG and CL syntheses. The CDP-diacylglycerol is combined with glycerol-3-phosphate to produce PG phosphate, an intermediate in the formation of the acidic PLs, PG and CL. Then PG is dephosphorylated in this step by the products of two independent genes, *pgpA* and *pgpB* that encode PG phosphate phosphatases.

The crystal structure of PgpB, which has been determined in *E.coli*, was found to contain identical folding topology and an almost similar binding site to ‘soluble membrane-integrated type II phosphatidic acid phosphatase (PAP2) enzymes’ (Fan et al., 2014, Touzé et al., 2008). In *E. coli*, PgpB is the sole enzyme identified as showing PAP activity (Dillon et al., 1996). The heterologous expression of *S. coelicolor* PAPs in *E. coli* was shown to increase intracellular levels of DAG by almost 6-fold and improved activity of PAP in membrane fractions by up to 5-fold when compared to the control strain (Comba et al., 2013).

Eventually, CL is formed by condensing two molecules of PG (Figure 1.7) (Clark et al., 1980, Vance and Vance, 2008). In the last step of CL synthesis, there is a unique reaction that is different between prokaryotes and eukaryotes. CL synthase of prokaryotes catalyses a transesterification in which the phosphatidyl molecule of one PG is moved to the free 3'-hydroxyl group of another PG. On the other hand, CL synthase of eukaryotes binds an activated phosphatidyl molecule (phosphatidyl-CMP) to PG. As the synthase of eukaryotic CL is a mitochondrial enzyme and mitochondria are phylogenetically derived from ancient prokaryotes, it seems that the conversion from bacteria to mitochondria also resulted in a change from the prokaryotic to the eukaryotic reaction mechanism (Schlame et al., 2000). Moreover, in eukaryotes the type II CL synthase (Cls) is related to the CDP-alcohol phosphatidyl transferases super family that produces CL by making CMP from the reaction between CDP-DAG and PG. SCO1389 in *S. coelicolor* corresponds to the class II Cls which produces CL from a eukaryotic pathway. Recent data reveals that *SCO1389*, coding for Cls, complements the *Rhizobium etli* mutant and restores CL production. Additionally, biochemical analyses indicated that SCO1389 can synthesise CL from CDP-diacylglycerol and PG as a donor which is identical to the eukaryotic pathway (Sandoval-Calderon et al., 2009). This gene was subsequently shown to be essential and necessary for development in *S. coelicolor* (Jyothikumar et al., 2012).

1.7.6 Role of *pgsA* in phospholipid synthesis

The *pgsA* gene encodes the protein phosphatidylglycerolphosphate synthase (PgsA) which is involved in the synthesis of the acidic membrane phospholipids in bacteria. PgsA condenses glycerol-3-phosphate with CDP-DAG to form phosphatidyl-glycerol-phosphate (PGP) (Miyazaki et al., 1985). The role of the *pgsA* gene mutation has been widely studied in *Escherichia coli*, whose suitability as a useful model to study *pgsA* arises from the fact that it contains only 3 phospholipids each having relatively simple fatty acids (PE, PG and CL) as previously noted above. It was demonstrated that mutation in the *pgsA* gene results in deficiency of the acidic phospholipids phosphatidylglycerol and cardiolipin but not phosphatidyl-ethanolamine (Miyazaki et al., 1985, Sohlenkamp and Geiger, 2015, Uchiyama et al.,

2010). The *pgsA* mutants grew more slowly compared to the wild type in media with low osmotic pressure but normally when media was supplemented with sucrose and MgCl2. In addition, this mutation caused a reduction of cardiolipin and phosphoglycerol derivatives of membrane derived oligosaccharides (Miyazaki et al., 1985). *pgsA* mutants are more tolerant to high temperatures of growth compared to the wild type but show less tolerance at low temperatures unless when supplemented with $MgCl_2$ and sucrose in the growth medium (Miyazaki et al., 1985).

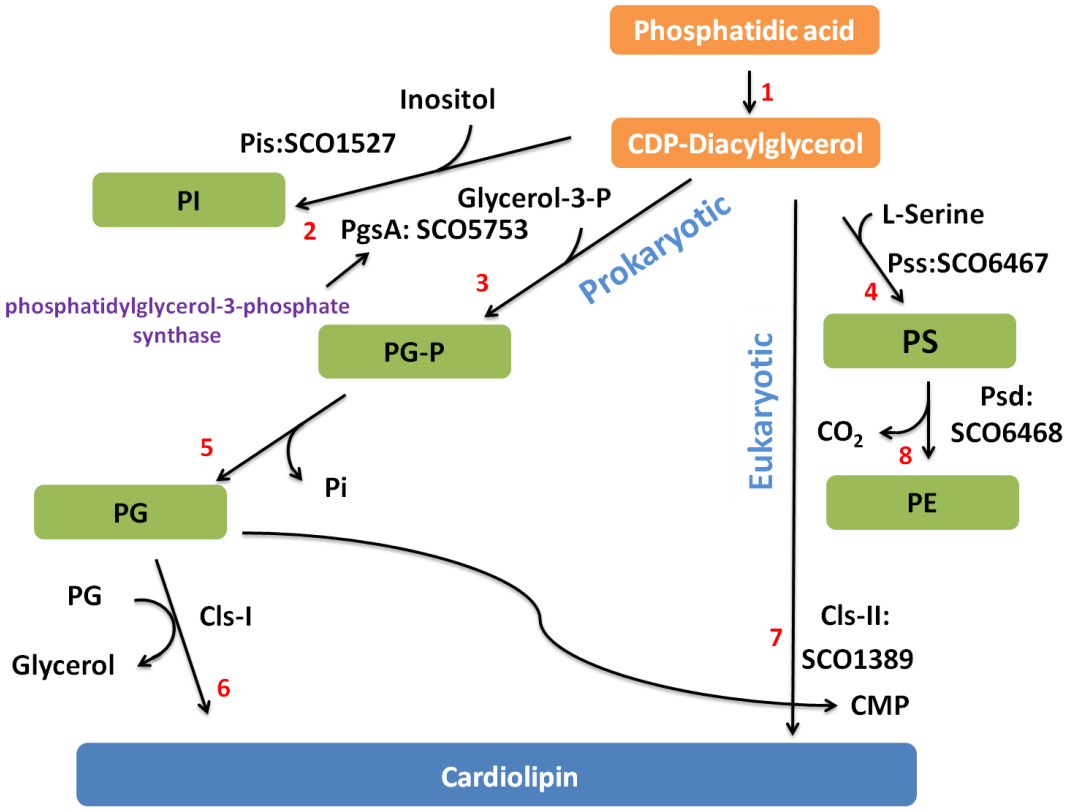

Figure 1-7: The PG biosynthesis pathway in prokaryotes and eukaryotes.

The substrates and enzymes required in this pathway are: (1) CDP-diglyceride synthetase Cds; (2) Phosphatidylinositol synthase Pis; (3) Phosphatidylglycerol-3-phosphate synthase PgsA; (4) Phosphatidylserine synthase Pss; (5) Phosphatidylglycerol phosphate phosphatase PgpA or PgpB; (6) Bacterial type cardiolipin synthase Cls-I; (7) Eukaryotic type cardiolipin synthase Cls-II; (8) Phosphatidylserine decarboxylase Psd; modified from (Sandoval-Calderon et al., 2009) . The genes *SCO1525* and *SCO1526* encode proteins that likely help turn PI over into phosphatidylinositol mannoside (Rahman et al., 2009b).

1.8 Aim of this Research

PG is an important membrane component of the filamentous antibiotic producing bacterial genus *Streptomyces*. In this study we have focused on the gene *SCO5753* (*pgsA*) from the model organism *S. coelicolor* M145, whose product is predicted to synthesize PG the precursor of CL. In order to study the gene *SCO5753*, the characterization of other members of its operon, such as *SCO5755* will also be investigated as this gene is speculated to regulate the operon. In many living organisms the *clp* gene encodes the proteolytic protein Clp. Five *clpP* genes exist in *Streptomyces lividans*, including the *clpP1 clpP2* operon, which are implicated in the *Streptomyces* life cycle as a mutation prevents differentiation during the vegetative mycelium (Bellier and Mazodier, 2004). Four *Clp* ATPase subunits have been determined in *S. coelicolor*, namely *ClpX* and three *ClpC* proteins, as well as *clpP1* and *clpP2*. The *clpC1* gene appears to be important, since no mutant so far has been achieved. *ClpP1, clP2* and *clpC1* are very significant in *Streptomyces* cell division (Bellier and Mazodier, 2004). Therefore, ClgR seems to be a regulator for expression of the ATP-dependent protease Clp in *Streptomyces*. The conserved sequence for ClgR binding site on the *clp* promoter has also been determined. Furthermore, ClgR appears to contribute to *Streptomyces* development, since *clgR* overexpression induces a delay in differentiation in *S. lividans.* Thus, we believe that *clgR* (*SCO5755)* might regulate the *pgsA* operon (Figure 1.8).

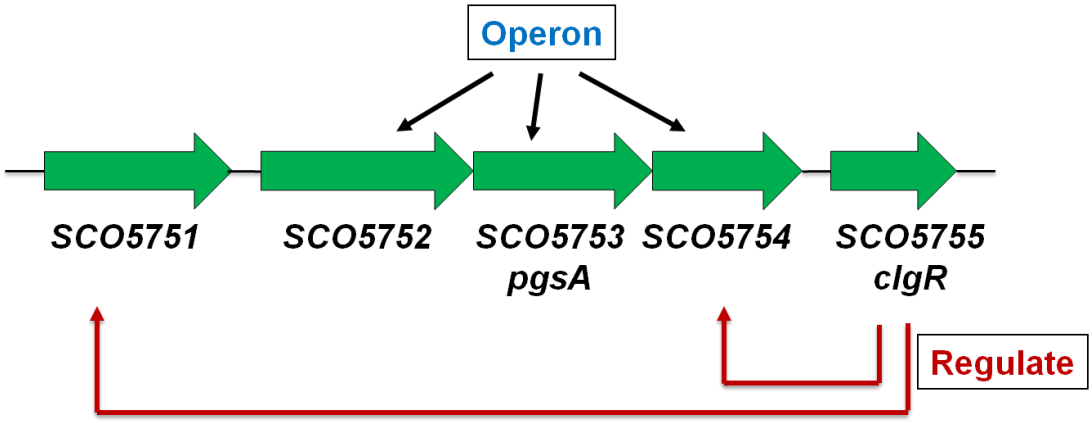

Figure 1-8: The region of *pgsA* operon obtained from StrepDB.

The diagram shows the location of genes *SCO5751*, *SCO5752*, *SCO5753* (*pgsA*) whose product is predicted to synthesize PG, the precursor of CL, and *SCO5755* (*clgR*).

The function of *SCO5752* and *SCO5753* are unknown, although earlier genetic evidence (Rajaghopal and Herron, unpublished data) suggested that at least one of these may be essential for growth and development of *S. coelicolor*. In this project we used systematic insertional mutagenesis to disrupt the *pgsA* operon. This procedure is based on *in vitro* transposon mutagenesis and is ideally suited for the new era of functional genomics analysis and was used for producing a transposon mutant library of *S. coelicolor* (Bishop et al., 2004). Along with the generation of mutations we also analysed the PL content of *S. coelicolor* membranes in response to changing expression levels of these genes in concert with measuring the effect of osmotic stress on the PL content of the *S. coelicolor* membrane. In addition to this we also analysed changes in development and the mycleial architecture of *S. coelicolor* in response to changing expression levels of the *pgsA* operon.

Chapter 2:

Materials and methods

2. Materials and Methods

2.1 General materials

All bacterial strains and vectors used in this chapter are scheduled in tables 2.1, 2.2, and 2.3.

Table 2-1: *E.coli* strains and plasmids

Strain or plasmid	Characteristics	Reference
E. coli DH5α	Host for general cloning. F^-, *endA1*, *hsdR17* ($r_{K-}m_{K+}$), *supE44*, *thi-1* λ^-, *recA1*, *gyrA96*, *relA1*, *deoR*, Δ(*lacZYA-araF*)U169, ϕ80d*lacZ* ΔM15	(Grant et al., 1990)
E. coli JM109	Host for general cloning.recA1, endA1, gyrA96, thi, hsdR17, supE44, relA1, Δ(lac-proAB)/F' [traD36, $proAB^+$, $lacI^q$, lacZΔM15	(Yanisch-Perron et al., 1985)
E. coli ET12567 (pUZ8002)	Mobilisable host of DNA to *Streptomyces* through intergeneric conjugation. Contains non-transmissible *oriT* mobilising plasmid pUZ8002; te^{tr}, chl^r, km^r	(Kieser et al., 2000)
pLR101	Insert that contains *SCO5751*,*SCO5752*,*SCO5753*,*SCO5754*,*SCO5755*,*SCO5756*; ter^r	(Herron et al., 1999)
pMA57542	*SCO5754* cloned in to pUC19; ap^r	This work
pMA53541	*SCO5753&SCO5754* cloned in to pPM927; $spec^r$ (sense orientation)	This work
pMA532	*SCO5753* cloned in to pPM927; $spec^r$ (antisense orientation)	This work
pMA101	SCO5751,SCO5752,SCO5753,SCO5754,SCO5755,SCO5756 cloned into pIJ925; ap^r	This work
pMA102	*SCO5752* cloned into pGEM-T Easy; ap^r	This work
pMA103	*SCO5753* cloned into pGEM-T Easy; ap^r	This work
pMA104	*SCO5754* cloned into pGEM-T Easy; ap^r	This work
pMA105	*SCO5755* cloned into pGEM-T Easy; ap^r	This work
pMA106	*SCO5752* cloned into pIJ6902; am^r (antisense orientation)	This work
pMA109	*SCO5755* cloned into pIJ6902; am^r (sense orientation)	This work

Table 2-2: *S. coelicolor* strains

***Streptomyces* strains**	**Characteristics**	**Reference**
S.coelicolor M145	Wild type, SCP1$^-$ SCP2$^-$ Pgl+	(Kieser et al., 2000)
S.coelicolor MA51F05	M145::SC7C7.2.F05 ; *am*^{r},*km*^{r}, (single cross over)	This work
S.coelicolor MA52B06	M145::SC7C7.2.B06; *am*^{r},*km*^{r}, (single cross over)	This work
S.coelicolor MA53B07	M145::SC7C7.2.B07; *am*^{r},*km*^{r}, (single cross over)	This work
S.coelicolor MA55A02	M145::SC7C7.2.A02; *am*^{r},*km*^{r}, (single cross over)	This work
S.coelicolor MA53541	M145::pMA53541; *spec*^{r}, *tsr*^{r} , (single cross over)	This work
S.coelicolor MA532	M145::pMA532; *spec*^{r}, *tsr*^{r} (single cross over)	This work
S.coelicolor MA52	M145::pMA106; *am*^{r}, *trs*^{r}	This work
S.coelicolor MA55	M145::pMA109; *am*^{r}, *trs*^{r}	This work
S.coelicolor MA927	M145::pMA927; *spec*^{r}, *tsr*^{r}	This work
S.coelicolor MA6902	M145::pIJ6902; *am*^{r},*tsr*^{r}	This work
S.coelicolor osaA	(*SCO5748*) *osaA*::Tn5062; *hyg*^{r}	(Herron et al., 1999)
S.coelicolor osaB	(*SCO5749*) *osaB*::Tn506;,*am*^{r}	(Herron et al., 1999)
S.coelicolor osaC	(*SCO5747*) *osaC*::Tn5062; *am*^{r}	(Herron et al., 1999)
S.coelicolor osaD	(*SCO7327*) *osaD*::Tn5062; *am*^{r}	(Herron et al., 1999)

Table 2-3: Plasmid vectors

Vector	Characteristics	Reference
pIJ925	*E. coli* cloning vector, *with lacZ* selection; ap^r	(Herron et al., 1999)
pUC19	*E. coli* cloning vector, with *lacZ* selection; ap^r	(Yanisch-Perron et al., 1985)
pPM927	Integrative *Streptomyces* vector that contains *ori* $_{TRK2}$, *int attP* $_{pSAM}$, *ptipA* promoter; $spec^r$, tsr^r	(Smokvina et al., 1990)
pGEM-T Easy	*E. coli* cloning vector; ap^r	Promega
pIJ6902	Integrative *Streptomyces* vector that integrates at *attB* $_{\phi C31}$ site that contains tsr-inducible promoter *ptipA*; am^r, tsr^r	(Huang et al., 2005)
St7C7B	Cosmid containing SCO5751, SCO5752, SCO5753 ,SCO5755; km^r, ap^r	(Redenbach et al., 1996)
SC7C7.2.F05	St7C7 containing *SCO5751*::Tn*5062* insertion; ap^r, km^r, am^r	(Bishop et al., 2004)
SC7C7.2.B06	St7C7 containing *SCO5752*:Tn*5062* insertion; ap^r, km^r, am^r	(Bishop et al., 2004)
SC7C7.2.B07	St7C7 containing *SCO5753*:Tn*5062* insertion; ap^r, km^r, am^r	(Bishop et al., 2004)
SC7C7.2.A02	St7C7 containing *SCO5755*:Tn*5062* insertion; ap^r, km^r, am^r	(Bishop et al., 2004)

2.2 General preparation of methods

2.2.1 Growth conditions for bacterial strains and preservation

Unless otherwise stated, all bacterial culture conditions, antibiotic concentrations and media preparations are based on general descriptions of (Sambrook and Russell, 2001) for *E.coli* and (Kieser et al., 2000) for *Streptomyces.*

2.2.2 Sterilization

All chemical solutions and constituents of different growth media were sterilised by autoclaving at 121°C for 30 minutes. Antibiotic stock solutions and heat labile solutions, e.g. amino acids, were sterilised by filtration via a 0.22µm pore membrane.

2.2.3 *E. coli* strains

E. coli strains were grown on solid or in liquid medium in the presence of appropriate antibiotics if needed and incubated overnight at 37°C (from 16 to18 hours). Liquid culture was incubated with shaking at 225 rpm and glycerol stocks were prepared by adding 330µl of sterile 80 % (w/v) glycerol to 670µl of fresh overnight culture mixed and stored at -80°C.

2.2.4 *S. coelicolor* strains

For solid culture, *Streptomyces* strains were cultured on SFM medium with appropriate antibiotics if necessary and incubated at 30°C for 4 to 7 days or until grayish colour spores appeared. For spore stock preparation, *Streptomyces* strains were streaked (from a single colony streak) to obtain a dense grayish confluent lawn and incubated at 30°C for about 6-9 days. *Streptomyces* spores were harvested and stored in 20% glycerol at -20°C or -80°C as explained by (Kieser et al., 2000). Further details on *Streptomyces* spore suspension preparation are described in Section 2.2.7.

For liquid culture, *Streptomyces* were pre-germinated with approximately $2x10^7$ spores for every 25 ml of final liquid culture volume. The liquid medium was incubated at 30°C, with shaking at 250 rpm in an Erlenmeyer flask containing sterile spring or in a baffled flask to allow mycelia aeration and dispersal. The culture was

usually harvested after 24- 48 hours or until the commencement of undecylprodigiosin formation, further details on pre-germination of *S. coelicolor* spores are described in Section 2.2.8. For gene expression using the tsr-inducible promoter, *ptipA*, tsr with concentrations between 0.1 and 50 μg/ml were used.

2.2.5 Antibiotics, chemicals and media

As mentioned above, antibiotic concentrations and media preparations were based on the general descriptions of (Sambrook and Russell, 2001) for *E. coli* and (Kieser et al., 2000) for *S. coelicolor*. The tables 2.4 and 2.5 below show the concentrations of antibiotics and the different types of media employed in this study.

Table 2-4: Antibiotic concentrations used in this study, all antibiotics stored at -20°C (Kieser et al., 2000, Sambrook and Russell, 2001)

Antibiotic	Solvent used	Stock concentration (mg/ml)	Working concentration (µg/ml)	
			E. coli	*S. coelicolor*
Ampicillin (Ap)	SDW	50	50	Not used
Apramycin (Am)	SDW	25	100	25
Chloramphenicol (Chl)	Ethanol (100%)	25	25	Not used
Kanamycin (Km)	SDW	25	25	25
Nalidixic acid (Nal)	0.25M NaOH	25	25	Not used
Spectinomycin (Spec)	SDW	50/200	50	400
Hygromycin (Hyg)	Ethanol (100%)	50	50	50
Thiostrepton (Tsr)	DMSO	25	Not used	25
IPTG	SDW	20	25	Not used
X-gal	DMSO	20	25	Not used

Table 2-5: Component of different media used in this study

Media	Amount per litre
Luria Bertani (LB) (Sambrook and Russell, 2001)	10 g tryptone, 5 g NaCl, 5 g yeast extract, 1 g glucose, 10 g agar (exclude for broth) add up to 1 litre with distilled water: adjust pH to 7.0 with NaOH
Mannitol soy flour (SFM) (Kieser et al., 2000)	20 g soya flour, 20 g mannitol, 20 g agar : add up to 1 litre with tap water
2x YT (Kieser et al., 2000)	16 g tryptone, 5 g NaCl, 10 g yeast extract add up to 1 litre with distilled water adjust pH to 7.0 with NaOH
Minimal medium (MM), Including minimal medium with mannitol (3MA) and minimal medium with glucose (MMG) (Kieser et al., 2000)	0.5 g L-asparagine, 0.5 g K_2HPO_4, 0.2 g $MgSO_4.7H_2O$, 0.01 g FeSO4.7H2O, 10 g agar add up to 1 litre with distilled water For minimal medium agar with glucose (MMG): 10 g glucose added after autoclaving For minimal medium agar with mannitol (3MA): 5 g mannitol added after autoclaving
Nutrient agar (Kieser et al., 2000)	13 g nutrient broth (Oxoid), 12 g agar add up to 1 litre with distilled water

Continue 2.5 Table	
SOC (Hanahan, 1983)	20 g Tryptone, 5 g yeast extract, 10 ml 1M NaCl, 2.5 ml 1M KCl add up to 1 litre with distilled water, After autoclaving, add sterilised components by filtration with a 0.22 µm filter: 1 M $MgCl_2.6H_2O$, 1 M $MgSO_4.7H_2O$, 1 M Glucose
SOB (Hanahan, 1983)	20 g Tryptone, 5 g yeast extract, 10 ml 1M NaCl, 2.5 ml 1M KCl add up to 1 litre with distilled water, After autoclaving add sterilised components by filtration with a 0.22 µm filter: 1 M $MgCl_2.6H_2O$, 1 M $MgSO_4.7H_2O$
Yeast extract malt extract (YEME) (Kieser et al., 2000)	3 g yeast extract, 5 g peptone, 3 g malt extract, 10 g glucose add up to 1 litre with distilled water, After autoclaving add 2 ml sterile 2.5 M $MgCl_2.6H_2O$
R5 medium (Kieser et al., 2000)	103 g sucrose, 0.25 g K_2SO_4, 10.12 g $MgCl_2.6H_2O$, 10 g glucose, 0.1 g casamino acids, 2 ml trace element solution[1], 5 g agar yeast extract, 5.37g TES buffer Distilled water to 1 litre, 2.2 g agar per 100 ml solution autoclave At time of use re-melt the medium and add in the order listed: 1 ml KH_2PO_4 (0.5%), 8 ml $CaCl_2.2H_2O$ (5M), 1.5 ml L-proline (20%), 0.7 ml NaOH (1N)

[1]**Trace element solution:** 40 mg ZnCl2, 200 mg FeCl3.2H2O, 10 mg CuCl2.2H2O, 10 mg MnCl2.4H2O, 10 mg NaB4O7.10H2O, 10 mg (NH4)6Mo7O24.4H20 in 1 litre deionised water.

2.2.6 *Streptomyces* spore suspension preparation

The following method was used to preserve spores of *Streptomyces*: 10 ml of sterile distilled water was added to a well-grown sporulating *Streptomyces* plate. The spores were gently scraped off the mycelium surface into water using autoclaved cotton buds, taking care not to dig hard into the agar surface. Spores were poured into a sterile tube and vortexed to break spore chains. Then, spores were poured into a 10 ml syringe barrel containing a piece of sterile cotton wool and were expelled into a suitable tube (sterile Oakridge tube or sterile 15ml Falcon tube) through the cotton wool by replacing the syringe plunger. Spore liquid was centrifuged for ten minutes at 4000 rpm, the supernatant was removed and the spore liquid was vortexed to loosen the pellet. The spore liquid was suspended by adding 1 ml sterile 20% (w/v) glycerol by a gentle vorteing, and finally the spore suspension was transferred to a sterile Eppendorf tube and stored at −80°C**.**

2.2.7 Pregermination of *S. coelicolor* spores (Kieser et al., 2000)

Two methods were used to germinate *S. coelicolor* spores. For both methods, a dense spore suspension was required for successful germination. In the first method, the spores were pelleted by centrifugation to remove all the glycerol solution from the spore suspension; otherwise it could impair spore viability during the heat shock process. The spore suspensions were re-suspended in 5ml of TES buffer and heated at 50°C for 10 minutes in a water bath and cooled under tap water. A similar amount of double strength germination medium was added and incubated at 37 °C, with shaking at 220 rpm for 2-3 hours. The germinated spores were pelleted by centrifugation, re-suspended in an appropriate volume of SDW or TES buffer, and the mixture vortexed to disperse the clumps. The second method also began with a dense spore suspension. The spores were pelleted by centrifugation, res-suspended in 5 ml of SDW, heated at 50°C for 10 minutes in a water bath and cooled under tap water. Then the mixture was added to 50 ml of 2XYT in a 250 ml baffled flask and incubated at 30 °C, with shaking at 220 rpm for 5-6 hours. Next the spore suspension was pelleted by centrifugation and re-suspended in an appropriate a volume of SDW. The optical density of the spore's growth was read at OD_{450} (0.03-0.05), and the spore suspensions were diluted based on the readings from the spectrophotometer.

Finally the measurement was used to calculate the volume of spore suspensions required to inculcate $2x10^7$ pre-germinated spores.

2.2.8 Growth of *S. coelicolor* mycelium in liquid (Kieser et al., 2000)

Baffled flasks (250 ml, 2 L, 2 L) and YEME broth were used for growing liquid cultures of *Streptomyces*. The culture was inoculated with approximately $2x10^7$ pregerminated spores of *Streptomyces* and incubated at 30°C, with agitation at 220 rpm for a designated period of time. The amount of culture was based on the final requirement of the mycelium. For TLC plates, 25 ml-50 ml of YEME broth were used, maintaining the volume of the flask at least 4 or 5 times the volume of the YEME broth to assist aeration during incubation in an orbital shaker. For the growth curve experiment, YEME broth 400 ml in a 2 L baffled flask was used.

2.3 Molecular Microbiology Methods

2.3.1 Isolation of plasmid DNA from *E. coli*

For high quality purposes, plasmids were prepared using the Wizard® *Plus* SV DNA purification system kit (Promega) according to the manufacturer's instructions. Alternatively, for screening for inserts, plasmids were extracted by alkaline lysis (Bimboim and Doly, 1979). Plasmid DNA was prepared by alkaline lysis using the SDS (minipreparation) method, Table 2.6. *E.coli* 2ml to 10 ml LB overnight cultures were harvested by centrifugation for 2 minutes at 13000 rpm. The supernatant was discarded and the bacterial pellet was then resuspended in 100 µl of ice-cold alkaline solution 1 by vigorous vortexing. 200 µl of freshly made solution II was added by mixing the tube by inversion five times and stored on ice for 5 minutes. After this, 150 µl of ice-cold alkaline solution III was added by inverting the tube 5 times, and the tube was kept on ice for 3–5 minutes. This was followed by centrifugation of the bacterial lysate at 13000 rpm at 4°C, and the supernatant was transferred into a fresh Eppendorf tube. A similar volume of phenol/chloroform was added and mixed by vortexing before centrifugation at 12000 rpm for 5 minutes at 4°C; the aqueous upper layer was transferred to a fresh Eppendorf tube. The nucleic acids were precipitated by adding two volumes of ethanol at room temperature and mixed by inversion and the mixture left to stand for two minutes at room temperature. The

precipitated nucleic acids were then concentrated by centrifugation at 13000 rpm for five minutes. After the precipitation step, the supernatant was transferred by gentle aspiration by allowing the tube to stand on a paper towel to drain the fluid and also by using a disposable pipette tip to remove any fluid drops adhering to the tube wall or used vacuum concentrator to dry DNA for 20 to 30 minutes. Finally, the nucleic acids were dissolved in 20 µl sterile distilled water and 1–2 µl RNaseA (10mg/ml); the solution was vortexed briefly and stored at −20°C.

Table 2-6: Buffers and solutions are used for plasmid isolation

Solution 1 (Resuspension)	Solution 2 (Lysis)	Solution 3 (Neutralisation)
50mM glucose 25mM Tris HCl (pH 8.0) 10mM EDTA (pH 8.0)	0.2N NaOH 1% (w/v) SDS	60ml 5M potassium acetate 11.5ml glacial acetic acid 28.5ml SDW

2.3.2 Agarose gel electrophoresis

DNA molecules were separated according to size by gel electrophoresis using an appropriate amount of agarose that was added to the correct volume of 1 x TAE buffer to make 0.5 - 1% (w/v) agarose gels. For example, to prepare a 1% (w/v) agarose gel, 1.5 g of agarose and 150 ml of lx TAE buffer were mixed into a conical flask, and the agarose was melted by heating the solution in the microwaving oven for 1–4 minutes. The agarose solution was swirled to ensure the agarose disappeared entirely in the mixture. The agarose mixture was allowed to cool slightly to 50°C before pouring the gel into a gel tray. Then the ethidium bromide (EtBr) was added to the agarose solution to give final concentration of 10mg/ml and swirled until the EtBr was dissolved completely in the solution. The agarose was poured slowly into the gel tray, removing any air bubbles. The comb was replaced on the gel tray about 1.5 cm from the edge of gel; the agarose gel was then left for 3–5 minutes to solidify. After this, the comb was removed with a careful motion back and forth so as not to tear the gel. Any tape used from the gel tray ends was taken away and the gel tray was positioned in the electrophoresis tank at the central supporting platform. The electrophoresis buffer was added to the buffer chamber until it reached the maximum

level above the gel surface. The DNA samples with loading dye were loaded, the lid was positioned on the gel box, and the electrodes attached. The power supply was turned on at 90–100V for 1−2 hours or until the dye front reached the last half of the gel. As a size marker, 1 kb & 100bp DNA ladder (Promega), λ HindIII (our lab stock) and λ PstI (our lab stock) were used. Ultimately, the gel was documented by a digital imaging system and recorded by the Syngene GelDoc system.

2.3.3 DNA extraction from agarose gels (Promega)

The desired DNA fragments were extracted from agarose gels as described above. DNA bands were visualised using the UV transilluminator on a low emission of UV radiation for ethidium bromide stained gels to reduce damage to the DNA molecules. The DNA fragments were transferred from the agarose gel with a sharp clean scalpel. The gel slice was removed to a 1.5 ml pre-weighed Eppendorf tube before adding the extracted gel slice to calculate the amount of agarose in the tube. 10 µl of membrane binding solution per 10 mg of gel slice was added, vortexed, and the mixture dissolved at 50°C- 60°C in a water bath. For processing PCR amplifications, a similar volume of membrane binding solution was added to the PCR amplification. After this, the mixture (gel mixture or prepared PCR product) was transferred to the spin column and incubated for 1 minute at room temperature followed by centrifugation at 14000 rpm for 1 minute. Then the flow-through was removed and the minicolumn re-inserted into the collection tube. 700µl of membrane wash solution (ethanol added) was added and centrifuged at 14000 rpm for 1 minute. Next the flow-through was removed and the minicolumn re-inserted into the collection tube. The previous step was repeated with 500µl of membrane wash solution (ethanol added) for 5 minutes. The collection tube was emptied and the column assembly re-centrifuged for 1 minute with the Eppendorf tube lid open to permit escape of any residual ethanol. The minicolumn carefully was removed to a clean 1.5ml Eppendorf tube. The required amount of SDW was added to the minicolumn and incubated at room temperature for 1 minute. Then the mixture was centrifuged at 14000 rpm for 1 minute. Finally the minicolumn was removed and DNA was stored at –20°C.

2.3.4 DNA digestion with restriction enzymes

Restriction enzyme digestion of plasmids was performed according to the enzyme manufacturer's instruction (Promega or NEB). The amount of enzyme required is calculated in units (1 unit of enzyme cuts 1 µg of DNA in 1 hour at 37 °C). The volume of restriction digestion reaction was set up as shown in Table 2.7, using 20 µl for analytical digests and 50-100 µl for preparative digests.

Table 2-7: Restriction enzymes digest mixture was combined as follows

Component	Amount (µl)
DNA sample (0.2-1.0 µg)[1]	1 µl
10X restriction enzyme buffer	2µl
Restriction enzyme (5-12U)[2]	1 µl
BSA (1mg/ml) (when required)	0.2 µl
SDW made up to	20
[1] Approximate DNA concentration ranging from 0.2 to 1.0 µg	
[2] The number of restriction enzyme units ranging from 5 to 12units	

The appropriate length of incubation time required depends on the amount of DNA/enzyme. Typically restriction digest reactions were carried out for 1-4 hours at the appropriate temperature. Occasionally, if digestion by two different enzymes was carried out, enzyme with compatible buffers could be used simultaneously. If there was no compatibility between the enzyme and the buffer, digestions were processed individually using the most acceptable level of the reaction buffer for each enzyme, precipitating the DNA between reactions. Finally, at the end of digestion, one fifth volume of DNA sample, loading dye (4µl) was added and the digested DNA could be used for further analysis by gel electrophoresis.

2.3.5 Dephosphorylation of 5' ends from linearized Plasmids DNA, (Promega)

To avoid self re-circularisation of linearized cloning DNA vector in the ligation process, TSAP thermosensitive alkaline phosphatase was used to remove 5′ phosphate groups from DNA.

Table 2-8: The amount of constituents in a DNA dephosphorylation reaction

Constituent	Amount (µl)
DNA	containing up to 1µg
Multicore 10 x buffer	added to a final concentration of 1x
TSAP	added 1µl for reactions containing up to 1µg
SDW to final volume of	20 µl to 50 µl

The DNA dephosphorylation reaction was set up as shown in the above table. Multicore 10 X buffer was added to final concentration (20 µl or 50 µl) of 1X before moving to the next step. 1µl of TSAP was added to the reaction containing up to 1µg of digested DNA. The reaction was incubated at 37 ˚C for 15 minutes to dephosphorylate all vector DNA overhang types (3', 5' or blunt). Then, the TSAP was heat-inactivated by incubating the reaction mix at 74 ˚C for an additional 15 minutes. Next, the mixture was briefly left on ice. The last step required the DNA purification using DNA purification kits such as PCR clean up kit. Finally, the digested DNA was stored at –20˚C.

2.3.6 Ethanol precipitation of DNA

1/10 volume of 3M of sodium acetate pH 5.2 was mixed well with the DNA mixture. Then 2.5 volumes of ice-cold absolute ethanol solution was added and also mixed well. This was placed on ice for 15–30 minutes to allow the DNA to be precipitated. The DNA was recovered by centrifugation at 4°C at 12000 for 10 minutes. The supernatant was removed. The tube was half filled with 70% (v/v) ethanol and subjected to further centrifugation at 12000 at 4°C for 2 minutes. The supernatant was removed and the tube was stored upside down on a tissue until the last fluid traces were removed. Afterwards the tube was placed in a speed vacuum until the last traces of ethanol had evaporated. The DNA pellet was dissolved in the required volume of buffer (TE or sterile distilled water). Ultimately, the mixture was mixed well and stored at −20°C.

2.3.7 Ligation (Promega)

The amount of insert DNA (typically in surplus) and vector were mixed in the ligation mixture according to the below formula. A molar ration of 1:3 or 1:5 or 1:10

of vector: insert was used and an amount of vector between 50-100ng was used in the cloning experiment.

$$\frac{ng\ of\ vector\ x\ kb\ size\ of\ insert}{kb\ size\ of\ vector}\ x\ \frac{molar\ ratio\ of\ \ insert}{vector} = ng\ of\ insert$$

The ligation reaction was assembled in a 1.5 ml tube as shown in Table 2.9, followed by the incubation at 4°C (16-18 hours) overnight before the recombinant DNA used to transform *E. coli* competent cells.

Table 2-9: The ligation reaction solution

Ingredient	Amount (µl)
Vector DNA	Re-calculated according to the formula above
Insert DNA	Re-calculated according to the formula above
T4 DNA Ligase (3 Weiss units/µl)	1 µl
10X Ligation Buffer, T4 DNA Ligase	2 µl
SDW to final volume of	10 µl

2.3.8 Preparation and transformation of electro-competent *E. coli* (Dower et al., 1988, Sambrook and Russell, 2001)

A single colony of *E.coli* strain was streaked out on LB medium agar and incubated overnight at 37°C. 10 ml of LB medium broth was inoculated from a single colony of *E.coli* strain and was incubated overnight at 37°C with shaking at 225 rpm. 50 ml of fresh LB medium broth was inoculated with 500 µl of the fresh overnight *E. coli* culture and incubated at 37°C with shaking at 225 rpm for several hours until the OD_{600} reached 0.4–0.6, as measured on a spectrophotometer. The culture was chilled on ice for 20 minutes as in this step the cells should not be warmed to room temperature. All reagents and equipment were chilled on ice and a cool centrifuge rotor and tips used prior to the start of the experiment. The culture was then transferred to a 50 ml chilled falcon tube and centrifuged at 4000 rpm 4°C for 5 minutes. The supernatant was removed carefully and thoroughly. The pellet was re-suspended gently in 25 ml ice-cold 10% (w/v) glycerol, followed by centrifugation at 4000 rpm 4°C for 5 minutes and the supernatants removed carefully. The previous

step was repeated twice. Finally, the pellet was re-suspended gently in 0.5 ml ice-cold 10% (w/v) glycerol; 50–100 µl of cell suspension was aliquoted quickly to chill (on ice) Eppendorf tubes and stored at –80ºC. The transformation efficiency of competent cells was measured in colony forming units (cfus) per input DNA. The transformation efficiencies of competent cells generally had a transformation efficiency of 10^8 - 10^9 cfu/µg. The transformation efficiencies were calculated as the number of transformants per microgram of plasmid DNA of pUC19.

0.2 cm electrocuvette and cuvette holders were pre-chilled on ice at 4ºC, and the Micropulser apparatus (Biorad) switched on. 50 µl of the competent cells were defrosted on ice. 1 µl of DNA was added to the competent cells by gentle mixing with a yellow tip, and then incubated on ice for 1 minute. Using a yellow tip, the mixture (competent cells and DNA) was transferred to the cuvette bottom of the electrocuvette to ensure that there was none left on the sides. The cuvette top was replaced and taped gently to the bench. The cuvette and cuvette holder were dried thoroughly. The cuvette was placed into the holder and inserted into the Micropulser. Then the pulse button was pressed until the instrument emitted its beeping sound. 1 ml of SOC media was immediately added to the cuvette, mixed, and transferred to a sterile universal 5 ml tube. The tube was incubated at 37°C for 60–90 minutes (*E.coli* strains: DHFα, JM109 and ET12567 (pUZ8002) with shaking at 225 rpm. Three plates of 25 ml LB medium were prepared, containing an appropriate antibiotic. Respectively, 250 µl, 100 µl, and 50µl of the culture were added to the three plates. Subsequently, the culture was spread out on the agar with a spreader and the plates air-dried for 10-15 minutes and then incubated overnight at 37°C.

2.3.9 Preparation and transformation of chemically competent *E. coli*

A single colony of *E.coli* strain was streaked out on LB agar and incubated overnight at 37°C. 10 ml of LB medium broth was inoculated from a single colony of *E.coli* strain and was incubated overnight at 37°C with shaking at 225 rpm. 50 ml of fresh LB medium broth was inoculated with 500 µl of the fresh overnight *E.coli* culture and incubated at 37°C, with shaking at 225 rpm for several hours until the OD_{600} reached 0.4–0.6 as measured on a spectrophotometer. All reagents and

equipment were chilled on ice and a cool centrifuge rotor and tips used prior to the start of the experiment. The culture was then transferred to a 50 ml chilled Falcon tube and centrifuged at 4000 rpm 4°C for 7-10 minutes. The supernatant was removed carefully and the pellet re-suspended gently on ice in 12.5 ml ice-cold 100 mM $MgCl_2$, for 3-5 minutes, followed by centrifugation at 4000 rpm 4°C for 7-10 minutes, and the supernatants removed carefully. Next the pellet was re-suspended gently in 3 ml of ice cold 100 mM $CaCl_2$, followed by the addition of 22 ml of 100 mM $CaCl_2$ with the suspension remaining on ice for at least 20 minutes. After this, the cell suspension was centrifuged at 4000 rpm 4°C for 10 minutes and re-suspended gently on ice in 1 ml of ice-cold sterile 100 mM $CaCl_2$ in 20% (w/v) glycerol. 50–100 µl of cell suspension was aliquoted quickly to chilled Eppendorf tubes and stored at –80ºC.

50 µl of the competent cells were placed in an ice bath for about 5 minutes until just defrosted. 1-5 µl of DNA was added to the competent cells by gentle mixing with a yellow tip or gentle flicking, and then incubated on ice for 20 minutes. The mixture (competent cells and DNA) was transferred to a water bath of exactly 42°C for heating shock for 45-50 seconds. Immediately, the mixture was replaced in the ice bath for 2 minutes. After this, at room temperature, 900 µl ml of SOC media was added to the mixture. Then the mixture was incubated at 37°C for 60–90 minutes, with shaking at 225 rpm. Three plates of 25 ml LB medium were prepared, containing appropriate antibiotics. Respectively, 250 µl, 100 µl, 50µl of the culture were added to the three plates. Subsequently, the culture was spread out on the agar by spreader and the plates air-dried for 10-15 minutes and then incubated overnight at 37°C.

2.3.10 Intergeneric transfer from *E. coli* to *S. coelicolor* by conjugation

A colony was inoculated (*E.coli* ET12567/pUZ8002 containing the plasmid of interest) in 10 ml of LB broth medium containing kanamycin and chloramphenicol to retain the selection of pUZ8002 and the dam mutation respectively, also appropriate antibiotics were used for the selection of the *oriT*-containing plasmid. The culture was grown overnight at 37°C, with shaking at 225 rpm. The overnight culture was

diluted 1:100 in fresh LB broth medium with the required antibiotics and incubated at 37°C with shaking at 225 rpm for several hours (usually 3–4 hours) until the OD_{600} reached 0.4–0.6 as measured by a spectrophotometer. The culture was then placed into a 50 ml Falcon tube and centrifuged at 4000 rpm for 5 minutes. Subsequently, the supernatant was removed and the pellet was re-suspended twice for cell washing with the same amount of LB broth medium. This was done to remove any traces left of antibiotics before the starting the re-suspension in 1ml of LB broth medium. The pellet was then re-suspended in 1 ml of LB broth medium and the *E.coli* cells kept on ice. The spore suspension was thawed on ice and for each conjugation, 100 µl of *Streptomyces* spore was added into 500 µl of 2xYT, in an Eppendorf tube. A 50°C heat shock was carried out by incubating the spores for 10 minutes. After cooling and mixing by gentle vortexing. 500 µl of the resuspended *E.coli* ET12567/pUZ8002 culture was added to 500 µl of the heat-shocked spore suspension in an Eppendorf tube. The mixture was mixed and briefly, centrifuged for 2 minutes and the supernatant removed. Next the pellet was re-suspended in the residual liquid and a serial dilution of the mixture was made as necessary. Negative control of a *Streptomyces* spore alone was also prepared. 100 µl of the mixture and the negative control were transferred onto MS agar plates containing 10 mM $MgCL_2$ and the mixture was spread over the plate by using a spreader in a circular movement and the plate was allowed to dry completely before being incubated at 30°C for 16–20 hours. The next day, the plates were overlaid with 1 ml of water containing Nal (20 mg nalidixic acid) and desired plasmid selection antibiotics. Next, using the spreader, the antibiotic solution was distributed over the plate and further incubated at 30°C for 3–4 days. If growth occurred, the colonies were patched on MS/Nutrient agar with nalidixic acid and the recommended antibiotic selected for the required exconjugants.

2.3.11 Polymerase Chain Reaction (PCR)

Amplification of genes *SCO5752, SCO5753, SCO5754, SCO5755* using the cosmid, St7C7B as the template DNA was carried out using My Taq^{TM} DNA Polymerase Kit (Bioline). The general reaction mixture of PCR was added according to the manufacturer's instructions (My Taq^{TM} DNA Polymerase, Bioline) and was set up as

shown in Table 2.10. The PCR reactions were cycled using thermocycler (Biorad) (Table 2.11).

Table 2-10: The volume of components in PCR reaction mixture by My Taq DNA Polymerase Kit, (Bioline)

Components	volume	Final Concentration
5x MyTaq Reaction Buffer	10 µl	1X
DMSO	2.5 µl	5%
Forward primer 100 µM (100 pmols)	1 µl	25 µM (25 pmols)
Reverse primers 100 µM (100 pmols)	1 µl	25 µM (25 pmols)
Template DNA	1 µl	10^{-1} Diluted Plasmid DNA (10ng-50ng/µl)
MyTaq DNA Polymerase (5 units/µl)	1 µl	5 units/µl
Nuclease Free Water up to	50 µl	50 µl

Table 2-11: PCR cycling conditions

Cycle	Temperature (°C)	Time	Number of Cycles
Initial denaturation	95°C	2 minutes	1
Denaturation	95°C	15 seconds	25
Annealing	55°C		
Elongation	72°C		
Final Elongation	72°C	5 minutes	1
Leaving	5°C	0	0

2.3.12 Oligonucleotides used in this study

Oligonucleotides were designed to complement the sequence of *SCO5752*, *SCO5753*, *SCO5754*, and *SCO5755* and purchased dried from Integrated DNA Technologies (IDT), with concentrations provided by the manufacturer. The oligonucleotides were reconstituted with the required amount of nuclease-free water to an overall of 100 pmol/µl stock concentrations and a 25 pmol/µl final work concentration and stored at -20°C. For an oligonucleotide, a stock concentration of 100 µM solution was achieved by using the following preparation. The number of nm of each oligonucleotide provided on the tube label or the oligo sheet was taken and multiplied by 10. The result presents the number of microliters of the nuclease free water to be added to the tube, which is equivalent to a 100 pmol/µl. For a final

concentration in a PCR reaction of 25 µM (25 pmol), a working solution was obtained by adding 25 µl of 100 µM oligo stock solutions to 75 µl of the nuclease-free water in a 1.5 ml Eppendorf tube. BamHI, XbaI and NdeI restriction sites were included in the primers to assist cloning. PCR reactions were normally carried out in PCR in a 0.5ml Eppendorf tube. MyTaq DNA Polymerase was used for various reactions setting. The oligonucleotides used in this study are described in Table 2.12.

Table 2-12: List of the oligonucleotides used in this study

Name	Sequence (5' to 3')	Site	Size (bps)
5752 Forward	CCGGATCCATGGATGCCTGAAAGCCGTACCG	BamHI	1482 bps
5752 Reverse	CCGGATCCTCATCTGCCGGCCTCCTC	BamHI	
5753 Forward	CCGGATCCATGGATGACCGGAGTCCCGGCG	BamHI	792 bps
5753 Reverse	CCGGATCCTCAAACTTCCGTCTCCTTC	BamHI	
5754 Forward	CCGGATCCATGGATGAGTTCCACGGCCGCCG	BamHI	546 bps
5754 Reverse	CCGGATCCTCAAAACCCCCCGTTCCG	BamHI	
5755 Forward	CCTCTAGACCATGGATGATTCTGCTCCGTCGC	XbaI	381 bps
5755 Reverse	CCTCTAGACCATGGATGATTCTGCTCCGTCGC	XbaI	
5752 Forward	CCCATATGCCTGAAAGCCGTACCG	NdeI	1482 bps
5753 Forward	CCCATATGACCGGAGTCCCGGCG	NdeI	792 bps
5754 Forward	CCCATATGAGTTCCACGGCCGCCG	NdeI	546 bps
5755 Forward	CCCATATGATTCTGCTCCGTCGC	NdeI	381 bps
BamHI: GGATCC	**XbaI:**TCTAGA		**NdeI:** CATATG

2.3.13 Colony PCR

Colony PCR was performed for the rapid screening of recombination plasmids from *E.coli* colonies during cloning. The colonies used for the rapid screening of insert DNA were about 1 mm in diameter at least. The PCR master mix reaction was prepared, allowing 10µl per sample (Table 2.13). Part of a colony was transferred to every tube containing PCR mix using toothpicks or pipette tips and mixed. Then the PCR reactions were cycled using a thermocycler (Biorad) Table 2.11. Afterwards, the PCR products were tested by electrophoresis on agarose gel.

Table 2-13: The master mix components of 50 µl, which could be scaled up if required

Components	volume	Final Concentration
5x MyTaq Reaction Buffer	10 µl	1X
DMSO	2.5 µl	5%
Forward primer 100 µM (100 pmols)	1 µl	25 µM (25 pmols)
Reverse primers 100 µM (100 pmols)	1 µl	25 µM (25 pmols)
MyTaq DNA Polymerase (5 units/µl)	1 µl	5 units/µl
Nuclease Free Water up to	50 µl	50 µl

2.4 Biochemical methods

2.4.1 Lipid analysis through PL extraction and identification using thin layer chromatography (TLC) (Bligh and Dyer, 1959)

PL extraction was accomplished using Bligh and Dyer's method (Bligh and Dyer, 1959) with slight modifications. The samples were grown on 50 ml of YEME media in an Erlenmeyer flask containing sterile spring or in a baffled flask and pelleted at 4000 rpm centrifugation for 10 minutes. *Streptomyces* mycelial pellets of 25 mg dry mass or 100 mg wet mass was weighed out and removed to a fresh Eppendorf tube. The mycelium was resuspended in 100 µl chloroform, 200 µl methanol and 80 µl water and vortexed vigorously for 10 minutes. Another 100 µl of chloroform was added to the sample solution and vortexed for 1 minute. Following this, 100 µl of water was added to the solution and vortexed for a further 1 minute. Then the sample was centrifuged at 13000 rpm for 1 minute, which led to the splitting of the phases (mycelial fragments were located at the interface between the two phases); the upper layer was aqueous and the lower, organic. The organic layer was transferred

carefully and dried in a vacuum centrifuge. For further analysis, the sample either immediately resuspended in 3-7 µl chloroform was stored at –80 ºC in a glass container.

Another method of PL extraction, that of (Tan et al., 2012) was also used with slight modifications. Also in this method the samples were grown on 50 ml of YEME media in an Erlenmeyer flask containing sterile spring or in a baffled flask and pelleted at 4000 rpm centrifugation for 10 minutes. 1 ml of 0.1 N HCl was added followed by 2.5 ml of methanol and 1.25 ml of chloroform to the mixture to form a single phase mixture comprising chloroform/methanol/0.1 N HCl [1:2:0.8 (vol/vol)]. Following this, the mixture was incubated for 30 minutes at room temperature with occasional mixing. Then, 1.25 ml of 0.1 N HCl and 1.25 ml of chloroform were added to change the single phase to a two phase mixture comprising of chloroform/methanol/0.1 N HCl [2:2:1.8 (vol/vol)]. After centrifugation at 4000 rpm for 20 minutes at room temperature, the lower phase was removed in a glass container and dried under a stream of nitrogen or a fume hood. The residual lipid was resuspended in 50 µl of chloroform/methanol (2:1, vol/vol), followed by sonication for 1-2 minutes. Roughly 5–15 µl of sample was loaded to TLC plate.

2.4.2 TLC Preparations

a) PL standards preparation

PL standards were provided by Avanti Polar Lipids Inc. Each standard was supplied as 25 mg of powder and dissolved in 1 methanol: 2 chloroform to make a final concentration of 5mg/ml stock (Table 2.14). Then the PL standards were transferred to a glass container and stored at -20 ºC. All lipid operations were performed in glass containers.

Table 2-14: PL standards

PL Standards	Description
PG	L-α-Phosphatidyl-DL-Glycerol (egg, chicken - Sodium Salt
CL	Heart, Bovine - Sodium Salt
PE	L- α- Phosphatidic acid (egg, chicken-Monosodium Salt

d) Tank preparations

TLC rectangular tanks were used to develop TLC plates for analysis. It was important for the plates to remain in a saturated atmosphere during the separation, using filter paper soaked in sufficient solvent solutions. The filter paper was lined vertically on part of the tank wall and soaked in the solvent, not touching the silica gel plate. The tank was allowed to equilibrate for 30 minutes before running the TLC plate to yield successful results.

e) TLC plate preparations

Silica gel 60 TLC plates were purchased from Sigma-Aldrich, with a dimension of 20X20 cm as glass plates. 1.5 cm from the bottom of the plate was measured and a line drawn across the plate. This line was the origin of all samples that were spotted (by capillary tubes) along the bottom line, at least 3 cm apart from the edge of the plate. All marks and writing on the plate were made with a soft pencil in order not to disrupt the absorbents of the plate (Figure 2.1).

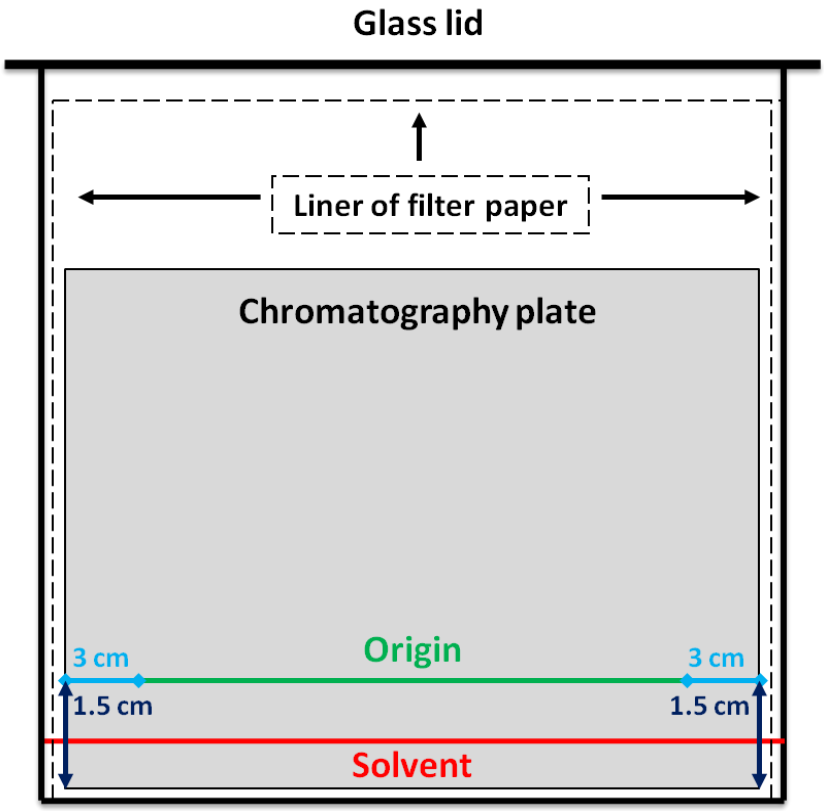

Figure 2-1: A diagram of TLC tank preparation.

It shows the chromatography plate with dimensions, TLC solvent amount, samples origin spot (origin) and a liner of filter paper, modified from (Touchstone, 1995, da Costa et al.).

2.4.3 Developing system preparation

TLC plates were developed under different solvent systems, these two solvent systems were used, solvent A: chloroform/methanol/acetic acid [(65: 25: 10 (vol/vol)] and solvent B: chloroform/methanol/acetic acid/water [(80: 12: 15: 4 (vol/vol)]. The prepared TLC plate was placed into a developing tank, covered with a glass lid and left undisturbed until the solvent had travelled to the top of the plate (1 cm from the edge). It was ensured that the solvent solutions did not cover the spot of the samples (Figure 2.1).

2.4.4 Visualizing the TLC plate

After the TLC plate was developed, the plate was removed from the tank and allowed to dry at the fume hood. The lipids were visualised with different spraying stains: Molybdenum blue (Sigma-Aldrich), 10% sulphuric acid (added slowly) in ethanol (v/v) or anisaldehyde/H_2SO_4 stain (methanol: 85 ml, glacial acetic acid: 10 ml, sulphuric acid: 5 ml added slowly and anisaldehyde: 0.5ml). The spraying process of the stains was conducted by using a Preval spray unit or chromatography sprayer from Sigma-Aldrich. Afterwards, 10% sulphuric acid in ethanol and anisaldehyde stains required heating using a hot oven or hot gun.

2.5 Microscopy Methods

2.5.1 Fluorescence microscopy

Microscopy was performed with a Nikon TE2000S inverted fluorescence microscope at 100x magnification, using various filters (FITC and TRITC). Images were captured using a Hamamatsu Orca-285 firewire digital CCD camera and further image analysis using IPLAB scientific imaging software version 3.7 (BD Biosciences Bioimaging, Rockville).

2.5.2 Image Analysis

Measurement of morphological parameters of the mycelial architecture was carried out on apical tip distance, branch angle, and inter-branch distance for the first and second days. On the third day, hyphal diameter was measured and on the fourth day spore width spore width was measured. Manual measurements of hyphal growth in

SFM were taken from the bright field images. Apical tip distance of hyphae was calculated from the apical tip to the initial branch (the longest part of free hyphae). Inter-branch distance was calculated of hyphal distance between two closest branches. Branching angle was calculated between the apical tip hyphae and its branches from an angle produced at the apical tip hyphal direction (an angle adjacent to the nearest apical tip). The manual measurement of cross wall distances was the length between adjacent cross walls and performed from the FITC field images. The spores' width was calculated from the width of spore and performed with the Bright field images with zoom. Finally, the multiple data sets were analysed using Microsoft Excel, 2007.

2.5.3 Preparation of the samples for microscopy

a) Cultures growth on cover slips

Cover slips was sterilised with ethanol and placed at a 45° angle on agar plates using sterile forceps. A 10 µl of 10^{-2} dilution of *Streptomyces* spore suspension was inoculated to the 45° angle of cover slips between the cover slips and the agar plate. Then the agar plates were incubated at 30°C for 1-4 days.

b) Fluorescein –WGA/Propidium iodide staining

For staining nucleic acid and peptidoglycan of *Streptomyces* cultures, fluorescein wheat germ agglutinin (WGA, Life Technologies)/propidium iodide (Sigma) staining was performed. The cells were fixed on a cover slip using the 500µl of fixative solution for 15 minutes at room temperature. The cells were washed twice with PBS to remove any traces of fixative and air dried thoroughly. They were then rehydrated with PBS for 5 minutes, and incubated with 2mg/ml lysozyme in GTE for 1 minute at room temperature (Table 2.15). The cover slips were washed with PBS and incubated in 2% of BSA (w/v) in PBS for 5 minutes at room temperature. Then the cover slips were incubated in the dark with the stain (2µg/ml fluorescein-WGA, 10µg/ml propidium iodide, 2% BSA in PBS) for 1-3 hours at room temperature (Table 2.16). The cover slip was washed with 10µ/ml propidium iodide in PBS 8 times. Finally, 8µl of slow fade solution was added and the cover slip was mounted on the slide, sealed with nail varnish and stored at -20°C.

Table 2-15: Buffers and Reagents

Buffers and Reagents	Volume /Litter
Phosphate-buffer saline (PBS)	NaCl 0.8, KCl 0.2g, Na_2HPO_4 1.44, KH_2PO_4 0.24 pH to 7.4 with HCl, make up to 1000 ml in SDW
GTE solution	50mM Glucose 20mM Tris, pH8.0 20mM EDTA
	50% Glucose 180µl 1M Tris-HCL, pH8.0 200µl 0.5M EDTA, pH8.0 200µl SDW 9.42ml

Table 2-16: Fluorescent stains

Dye	Stock	Working concentration	Filters used
Fluorescein-WGA	1 mg/ml	2 µg/ml	FITC
Propidium Iodide	25 mg/ml	10 µg/ml	TRITC

2.6 Bioinformatics Analysis

2.6.1 Study of the genome sequences using Uniprot

The analysis was conducted on the amino acid sequence encoded by the genes of interest from the *S. coelicolor* genome. These amino acid sequences were obtained from the *Streptomyces* annotation server (StrepDB) (http://strepdb.*streptomyces*.org.uk/) and submitted to the blast search of universal protein resource (UniProt) database's old site (http://obsolete.uniprot.org/). Then the various amino acid sequences were saved in a FASTA file before being exported into Jalview for multiple sequence alignment.

2.6.2 Jalview multiple sequence alignment program

The protein sequences of desired genes were inputted into Jalview as FASTA files and the result was obtained as a window of a multiple sequence alignment data. Then the "wrap" format was chosen to present the whole alignment view and the colour background was adjusted according to the percentage identified. The phylogenetic trees were carried out in Jalview, using neighbour joining using PAM250. Then both results of the phylogenetic trees and the multiple sequence alignment can be saved and exported as PNG images. This program was obtained from the Jalview site (http://www.jalview.org/) (Waterhouse et al., 2009).

2.6.3 Clone Manager 6

Clone Manager Software was used to perform molecular experiments using DNA sequences for multiple activities, such as cloning studies, primer design and analysis and alignment operations. This software was supplied by Scientific & Educational Software.

2.6.4 Pfam

Pfam is a comprehensive database of protein families and domains, defined by multiple sequence alignments and profile hidden Markov models (HMMs). For every search of protein family in Pfam it is possible to observe the multiple alignments, domain architectures, species distribution and other database links. Pfam was accessed via the UK servers: (http://pfam.sanger.ac.uk/) (Finn et al., 2014).

2.6.5 FIMO

FIMO (Find Individual Motif Occurrences) is a tool which is used to find motif instances in a sequence database. FIMO searches the database for the supplied motifs, and presents a q-value for every match (Grant et al., 2011). In the FIMO database, the q-value of a motif occurrence is defined as "the false discovery rate if the occurrence is accepted as significant". This program was accessed from the FIMO site (http://meme-suite.org/tools/fimo) (Grant et al., 2011).

2.6.6 Phyre2

The protein homology/analogy recognition Engine (Phyre2) is an online tool used to predict function, mutation and structure of a novel protein. This tool gives a guide to interpret the outcome of novel protein structure predicted in an informed way. This program was accessed from the Phyre2 site (http://www.sbg.bio.ic.ac.uk/phyre2) (Kelley et al., 2015).

Chapter 3:

Phylogenetic Analysis and Disruption of the *pgsA* operon in *S. coelicolor*

3. Phylogenetic analysis and disruption of the *pgsA* operon in *S. coelicolor*

3.1 Introduction to Chapter 3

Members of the genus *Streptomyces* are filamentous soil bacteria that undertake a complex life cycle of morphological development. Most studies of morphological development have used genetic studies through the characterisation of mutants. Despite this, it is only in recent years that these mutants have routinely been described at the genomic level (Hopwood, 1999, Borodina et al., 2005, Bentley et al., 2002). The reason for this slow progress is that identification and cloning of genes created by chemical induction of mutations is difficult in this organism; although next generation sequencing offers the possibility of rapid mutant characterisation following chemical mutagenesis (Gehring et al., 2000, Shin et al., 2013, Schwientek et al., 2011). Following the completion of an annotated genome sequence, the systematic disruption of each gene is a powerful method to analyze the molecular basis of a particular process. For instance, this system has been widely used for disruption of bacterial genomes in such organisms as *Francisella novicida* (Gallagher et al., 2007), *Corynebacterium glutamicum* (Suzuki et al., 2006) and *Pseudomonas aeruginosa* (Jacobs et al., 2003).

The study of *pgsA* operon function was undertaken by employing a procedure for systematic insertional mutagenesis described by (Bishop et al., 2004), which offers the advantage of being both versatile and high throughput. Gene disruption was accomplished through *in vitro* transposon mutagenesis (Goryshin and Reznikoff, 1998), using a derivative of Tn*5* in order to introduce gene insertions in cosmid representatives obtained from a library previously used in the genome sequencing of the *S. coelicolor* (Redenbach et al., 1996). Initially, we recovered cosmid transposon insertion libraries in *E. coli*, and then determined positions of each gene insertion by DNA sequencing. We included an origin of transfer (*oriT*; RK2) in the transposon in order to allow conjugal transfer of each cosmid into *S. coelicolor*, resulting in high efficiency production of exconjugants with the required gene disruptions (Bishop et al., 2004).

This method forms the basis of this chapter which investigates the functions of the *pgsA* operon through *in vitro* transposon mutagenesis with Tn*5062;* the latter is a mini-transposon which was derived from the cut and paste transposon Tn5 carrying the RP4 *oriT* (Fernandez-Martinez et al., 2011, Bishop et al., 2004). The transposon Tn*5062* carries *egfp*, which encodes a modified version of GFP taking into account the GC-rich nature of streptomycete genes. It also contains an apramycin resistance gene (*aac(3)IV*) that maintains and selects for colonies that contain the transposon. *egfp* does not contain its own promoter but when the transposon insertion is in the sense orientation, transcription can be directed by the disrupted gene's promoter. Moreover, Tn5*062* has transcriptional terminators that stop read-through from *aac(3)IV* or the promoter of the disrupted gene. Through the use of the *Streptomyces* annotation server (StrepDB), it was possible to identify the *pgsA* operon in *S. coelicolor*. Disrupting this operon was conducted in this chapter via transposon directed mutagenesis using transposon insertion library obtained from (Bishop et al., 2004) (Figure 3.1).

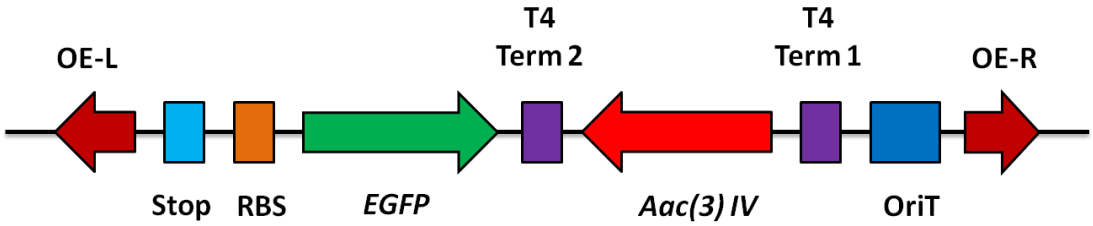

Figure 3-1: A schematic diagram of Transposon Tn*5062*.

It shows locations of inverted repeats (OE-R & OE-L), RK2 origin of transfer (*oriT*), T_4 transcriptional terminators, *aac(3)IV* (apramycin resistance gene, *egfp* (green), streptomycete consensus ribosome location site (RBS) and translational stop codon, modified from (Herron et al., 2004).

The result of gene disruption was investigated via conjugal intergenic introduction of mutated cosmids into *S. coelicolor* (Herron et al., 2004) through homologus recombination events (single or double crossovers) (Figure 3.2) (Kieser et al., 2000, Jyothikumar et al., 2012).

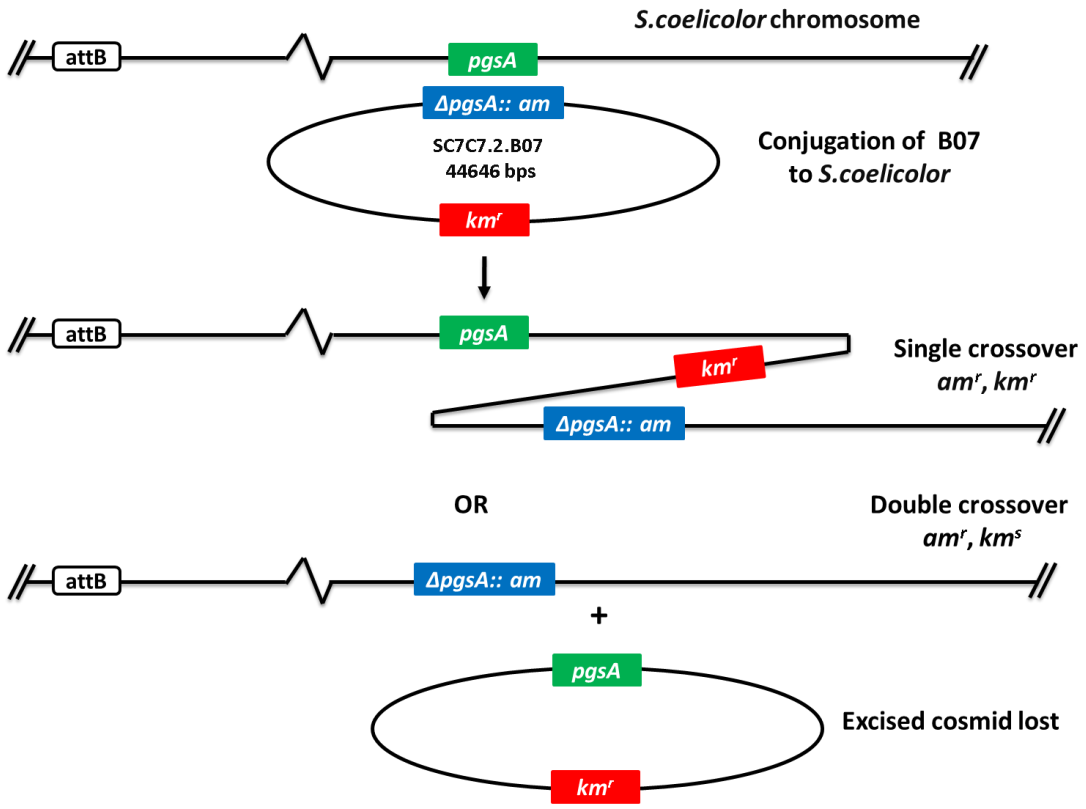

Figure 3-2: Illustration of integration and excision of the disrupted cosmid SC7C2.B07 with *S. coelicolor*.

Each of the conjugated cosmids was integrated into the *S. coelicolor* chromosome introducing an additional new copy of *pgsA*. The gene transfer into the bacterial chromosome can occur either by single crossover forming exconjugants am^r, km^r or by double crossover leading to exconjugants am^r, km^s (Jyothikumar et al., 2012).

Streptomyces are the largest developmentally complicated actinomycetes and have a large and varied selection of genes associated with their characteristic morphology. Fascinatingly, though, several of the genes linked with development in *Streptomyces* also exist in other actinomycetes. Phylogenetic analysis can then be utilised to clarify the evolution of this developmental complexity (Chater and Chandra, 2006). A phylogeny is the evolutionary history among a group of organisms; the major aim of these studies is to explain evolutionary relationships with regards to the establishment of a common ancestry. A phylogenetic analysis is a method used for estimating the relationships of protein sequences and their hypothetical common ancestors. Furthermore it allows the characterisation of the relationships between the protein sequences themselves without any regard to the host species as well as seeking to infer the roles of the proteins that have not been studied widely in the laboratory (Hall, 2013, Harrison and Langdale, 2006). A significant application of phylogenetic analysis is the comparison of genome sequences and reconstruction of metabolic networks in *Streptomyces* for biotechnology research (Alam et al., 2010).

The investigation of *pgsA* operon for systematic insertional mutagenesis was conducted on the four cosmids SC7C7.F05, SC7C7.B06, SC7C7.B07 and SC7C7.A02 obtained from Professor Paul Dyson's laboratory (Swansea University). These cosmids had transposon insertions in the genes *SCO5751*, *SCO5752*, *SCO5753* (putative *pgsA*) and *SCO5755* respectively (Bishop et al., 2004). We could not examine *SCO5754* because cosmids with transposon insertions in this gene were not available. Nevertheless, we investigated the *SCO5751* gene to obtain more observations about the mutagenesis of neighbouring genes. For the phylogenetic analysis, the *SCO5752*, *SCO5753*, *SCO5754* and *SCO5755* genes were investigated.

3.2 Aim of this chapter

The aim of this chapter was to investigate the function of *SCO5751*, *SCO5752*, *SCO5753* and *SCO5755* in *S. coelicolor* genome using systematic gene disruption through *in vitro* transposon mutagenesis using Tn*5062*. Another aim of this chapter was to study the evolutionary relationships of these genes with regards to homologous proteins encoded by other organisms.

3.3 Allelic replacement with disrupted copies of *SCO5751, SCO5752, SCO5753* and *SCO5755* in *S. coelicolor*

The arrival of genomic sequencing of bacteria has revealed large numbers of genes encoding enzymes putatively involved in bacterial lipid synthesis as well as their genetic organization. The chemical stages in fatty acid synthesis are well conserved in bacteria and there are astonishing diversities in structure and the requirements for cofactors in the enzymes that carry out these reactions in Gram-positive and Gram-negative bacteria. This understanding has lead to accelerated research to investigate the large differences in pathways and fatty acid and PL structures that take place in nature. *pgsA* has been found an essential gene in *S. aureus* and *B. subtilis*, whose membranes are mainly formed from acidic PLs (50–60%) and 20% in *E. coli* (Parsons and Rock, 2013).

A genetic approach was taken to investigate the functions of *pgsA* operon genes and the downstream gene in *S. coelicolor* M145 and we attempted to disrupt each gene individually using cosmids that contained fragments of the *S. coelicolor* genome (Redenbach et al., 1996). The disruption was done by *in vitro* transposon mutagenesis using Tn*5062* (Figure 3.1). The mutagenized cosmids F05, B06, B07 and A02 were used to do that and their insertion location is shown in (Figure 3.3B). F05, B06, B07 and A02 were introduced into *E. coli* ET12567/pUZ8002 by chemical transformation and then transferred to *S. coelicolor* M145 by intergeneric conjugation. The exconjugants were isolated on SFM agar supplemented with apramycin (Figure 3.3A).

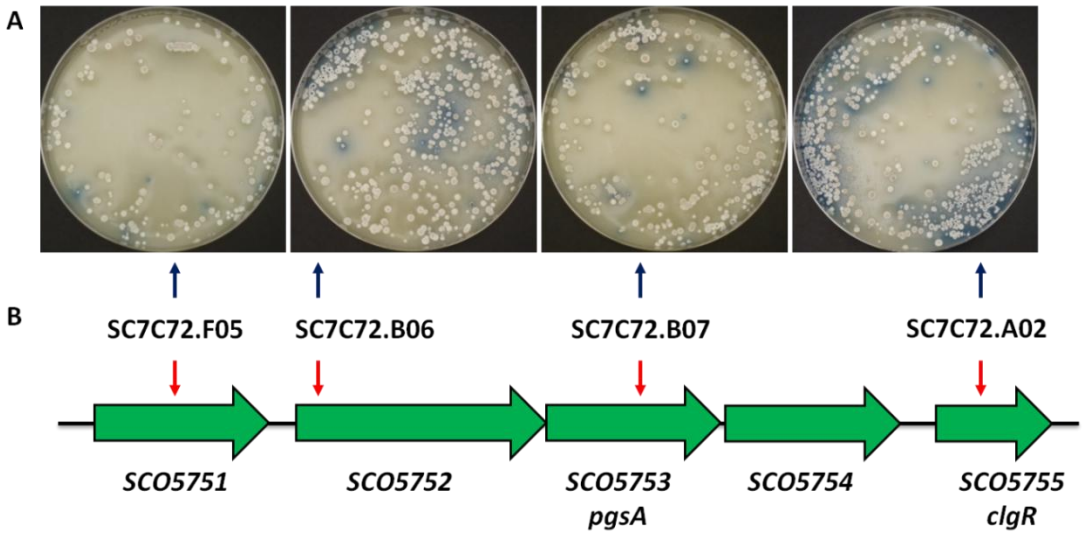

Figure 3-3: Exconjugants following gene replacement with disrupted copies of *SCO5751, SCO5752, SCO5753* and *SCO5755*.

(A) Exconjugant growth after selected by the addition of 50 µg/ml am for selecting the exconjugants and 25 µg/ml Nal to prevent growth of the *E. coli* ET12567(pUZ8002) donor strains. Also, a negative control was performed successfully (data not shown), with incubation 5-7 days at 30°C. (B) The mutagenized cosmid SC7C72.FO5, SC7C72.BO6, SC7C72.BO7 and SC7C72.A02 as well as transposon insertion location (red arrows) in the genes *SCO5751*, *SCO5752* and *SCO5753* and *SCO5755* respectively, the gene was map obtained from StrepDB.

Over 500 colonies were screened under replica plating for the am^r & km^s phenotype indicative of an allelic replacement by means of a double cross-over event. All colonies were both kanamycin and apramycin resistant and were thus derived from a single cross over event (Figure 3.4). Colonies were selected for each transposon insertion and designated MA51F05 (M145::SC7C7.2.F05), MA52B06 (M145:SC7C7.2.B06), MA53B07 (M145::SC7C7.2.B07) and MA55A02 (M145::SC7C7.2.A02). These colonies were further tested for am^r and km^s on SFM agar (Figure 3.5). The absence of double crossover exconjugants (apramycin resistant, kanamycin sensitive) suggested that these genes are essential. The Single crossover exconjugants showed that Tn*5062* was integrated into the *S. coelicolor* genome through single homologous recombination event that maintains an intact copy of the target gene; one parenteral copy originating from the chromosome and one disrupted copy from the mutagenized cosmid. Our inability to obtain double crossover exconjugants suggests that either the allelic exchange could not occur successfully or all genes contained within the operon are essential for *S. coelicolor* viability which indicates that the proteins encoded by this operon could provide new targets for drugs in pathogenic relatives of streptomycetes.

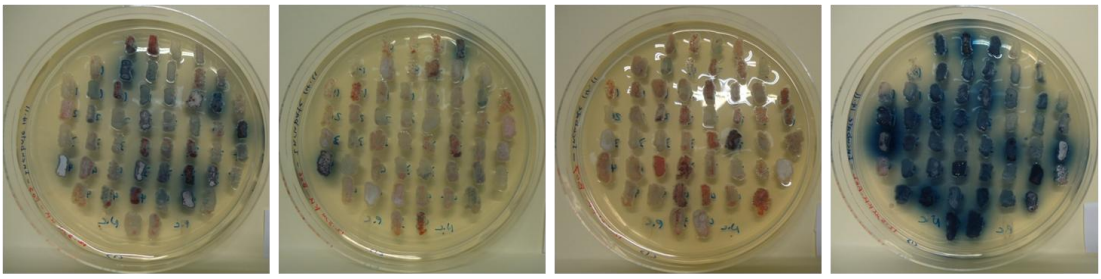

F05, *km*^{r} B06, *km*^{r} B07, *km*^{r} A02, *km*^{r}

Figure 3-4: km^r single crossover exconjugants (data not shown for amr) following replica patching.

Exconjugants (500 colonies) were patched onto replica nutrient agar plates containing apramycin (25 µg/ml) or kanamycin (25 µg/ml) with incubation 4-7 days at 30°C, to display any potential double crossover exconjugants with an am^r, km^s phenotype following integration into the *S. coelicolor* genome via a double cross-over event. As only am^r, km^r colonies were obtained this suggests that disruption of these genes is not possible in *S. coelicolor*.

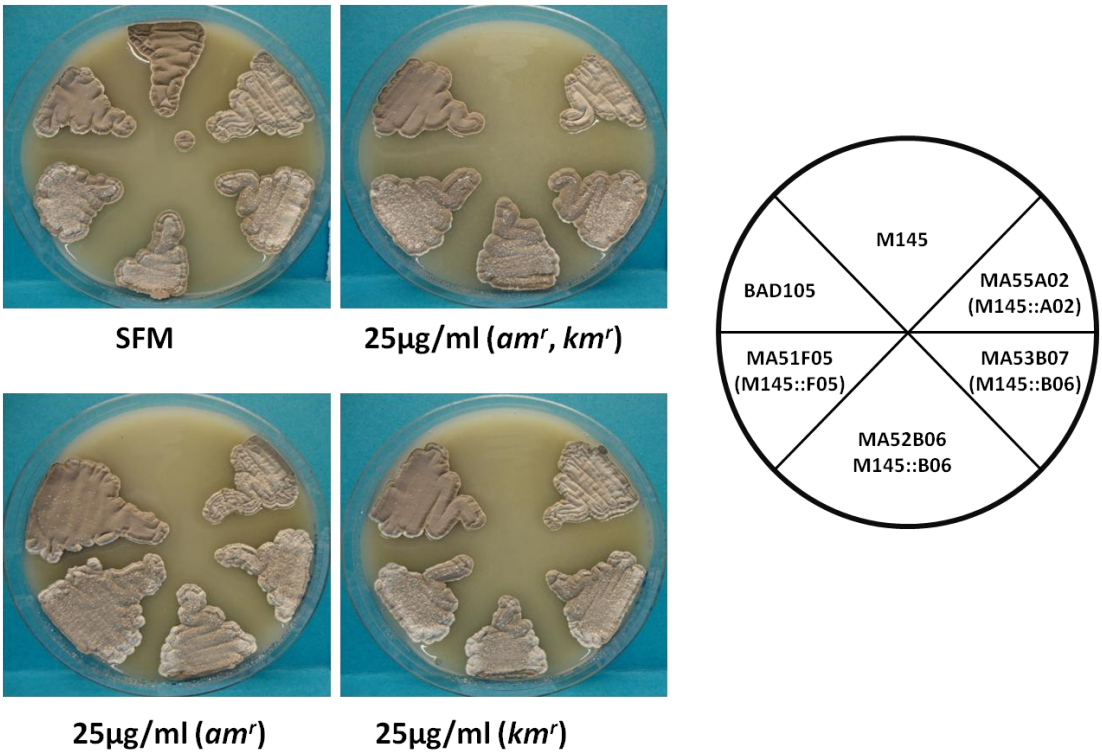

Figure 3-5: Phenotypes of single crossover exconjugants MA51F05, MA52B06, MA53B07 and MA55A02, grown on SFM with incubation for 8 days at 30°C.

These strains were obtained via single homologous recombination events and integration of the transposed cosmids SC7C7.2.F05, SC7C7.2.B06, SC7C7.2.B07 and SC7C7.2.A02.

3.4 Phylogenetic analysis and protein sequence alignment

Streptomyces are characterised by a complex life cycle of development and synthesise a large collection of significant secondary metabolites that include many antibiotics. Antibiotic formation and morphological development are strongly linked through the involvement of transcriptional factors or other activity factors (Liu et al., 2013, McCormick and Flärdh, 2012). As such, *Streptomyces* is perhaps the most well-known genus in the order *Actinomycetales* through its significance in ecology, medical science and the biotechnology industry. As a reflection of this, an understanding of the phylogeny of *Streptomyces* and constituent species is important for resolving and characterising the large biosynthetic diversity of this and related genera. For instance *Streptomyces* is related to pathogenic the pathogenic genus *Mycobacterium* (Alam et al., 2010). Therefore a phylogenetic analysis was conducted to clarify the evolutionary relationships of our target genes in this chapter. Phylogenetic analysis was performed on SCO5752, SC5753, SC5754 and SCO5755 with homologues of different prokaryotic taxa. The amino acid sequences were exported from UniProt as FASTAs file and multiple sequence alignments as well as phylogenetic trees computed in Jalview using neighbour joining using PAM250.

3.5 Protein sequence alignment and phylogenetic analysis of SCO5752 protein homologues from a variety of bacterial taxa

SCO5752 is annotated as encoding a conserved hypothetical protein SCO5752, the function of this 493AA long protein has not been determined biochemically. Genetic evidence indicates that at least one the genes found in the *pgsA* operon is essential for growth and development of *S. coelicolor*. The purpose of this analysis carried out here was to investigate any sequence similarities of SCO5752 with other proteins found in the database. The search was conducted in UniProt using the protein sequence which was obtained from StrepDB and the search of protein sequences was performed by sequence similarity (BLAST) based on the BACTERIA database. The relative abundance of SCO5752 homologues in different bacterial groups was obtained in this way (Figure 3.6). The protein SCO5752 was highly represented in two phyla of bacteria *Proteobacteria* and *Actinobacteria*; each containing 35% and 28% of hits respectively.

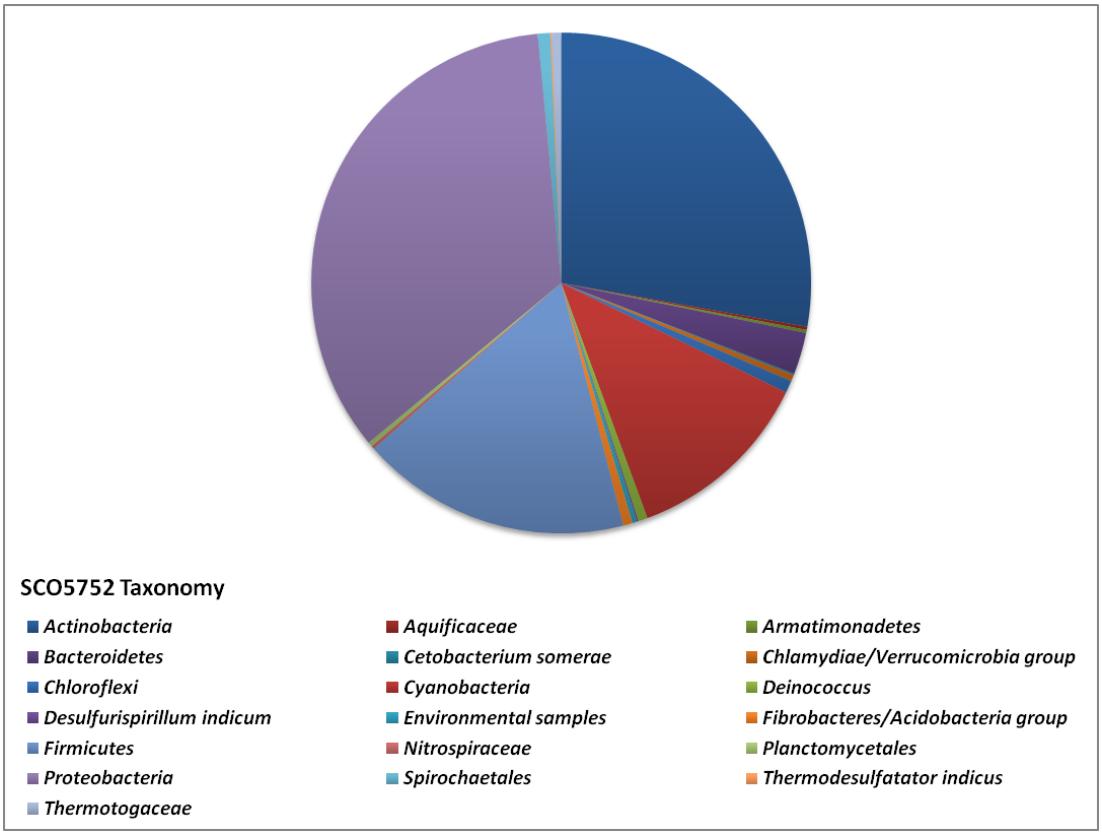

Figure 3-6: Distribution of SCO5752 proteins throughout bacterial taxa.

The SCO5752 protein taxonomy results were modified from UniProt based on the NCBI taxonomy database. The result shows the most abundant SCO5752 protein sequences in bacterial phyla. The results alos show te the class name against the number of the organisms as the following: Actinobacteria (high G+C Gram-positive bacteria) (28%), *Aquificaceae* (0%), *Armatimonadetes* (0%), *Bacteroidetes* (3%), *Cetobacterium somerae ATCC BAA-474* (0%), *Chlamydiae/Verrucomicrobia group* (0%), *Chloroflexi* (1%), *Cyanobacteria* (12%), *Deinococcus* (1%), *Desulfurispirillum indicum (strain ATCC BAA-1389 / S5)* (0%), *Environmental samples* (0%), *Fibrobacteres/Acidobacteria group* (1%), *Firmicutes* (18%), *Nitrospiraceae* (0%), *Planctomycetales* (0%), *Proteobacteria* (35%), *Spirochaetales* (1%), *Thermodesulfatator indicus (strain DSM 15286 / JCM 11887 / CIR29812)* (0%), *Thermotogaceae* (1%) (Date of access Sep 2014).

Protein sequences homologous to SCO5752 from UniProt database were identified and chosen based on the strongest BLAST protein sequences matches. The protein sequence of the SCO5752 orthologue in *Bacillus* showed a fair protein sequence homology and had similarities with the sequence of with 33-36% identity. However, it was seen that other species of *Streptomyces* and other organisms shared 61-100% homology being actinomycetes, such as *S. lividans* shared 100% of similarity to *S. coelicolor* (Table 3.1).

Table 3-1: Summary of homologues to *S. coelicolor* SCO5752 following interrogation of the UniProt database using BLAST.

Protein names	Organism	Length	Identity	Score	E-value	Gene names
Ribosomal protein S12 Methylthiotransferase (RimO)	*S. lividans*	493	100%	2,501	0	*rimO SLI_6013*
	S. coelicolor	493	100%	2,501	0	*RimOSCO5752 SC7C7.07*
	S. afghaniensis	493	93%	2,297	0	*rimO STAFG_7480*
	S. viridochromogenes	493	92%	2,290	0	*rimO SSQG_05787*
	S. griseoflavus	491	92%	2,284	0	*rimO SSRG_01559*
	S. avermitilis	495	90%	2,236	0	*rimO SAV_2508*
	Streptomyces sp.	495	85%	2.085	0	*rimO SSAG_01796*
	S. griseus	493	85%	2,067	0	*rimO SGR_1769*
	Kitasatospora cheerisanensis	484	79%	1,920	0	*KCH_53450*
	Micromonospora sp.	499	61%	1,439	0	*rimO MCBG_02456*
	Paenibacillus sabinae	442	36%	724	$5.0X10^{-86}$	*rimO PSAB_14415*
Uncharacterized protein	*Bacillus subtilis*	443	33%	639	$2.0X10^{-73}$	*BEST7613_4918*

This is unsurprising as these organisms are very closely related (Anderson and Wellington, 2001). The data from these matches was aligned using into Jalview to recognise conserved protein sequences. The sequence alignment is showed in (Figures 3.7) and the most highly conserved regions recognised in the consensus sequence were determined by percentage identity. The percentage identity selection colours the residues depending on the percentage of the residues in every column with respect to the consensus sequence. Selected motifs that agree with consensus residue of every column were turned into a group and coloured. The consensus sequences were coloured in blue to show the percentage identity in every column; the darker the blue the higher the percentage identity of conservation amino acid (Waterhouse et al., 2009). In the analysis of the alignment in (Figure 3.7A) there is a consensus amongst a number of *Streptomyces* species and other organisms. Mostly, the sequence alignment showed two highly conserved regions contained hydrophobic residues (Valine) for both motifs. The first highly conserved motif had the consensus identity of I-V-G-F-P-G-E and; the second; V-N-T-C. The data in (Figure 3.7A) also reveals several consensuses for the motif between amino acid residues 21 to 465 of the hydrophobic amino acids (Glycine).

Additional assessments of the sequence for SCO5752 show Pfam expectation value of $1.7e^{-33}$ for an uncharacterized protein family (UPF0004) and $2.2e^{-20}$ for radical SAM superfamily domain. Searches using Pfam also found two matches; the first is the uncharacterized protein family (UPF0004) which is matched between 7 and 105 (AAs) of the sequence (Figure 3.7B). Also the sequence alignment indicated several conserved motifs that are matched to the uncharacterized protein family (UPF0004) and radical SAM superfamily domain according to the Pfam database. The uncharacterized protein family was found at the N terminal region of the proteins whilst, the C-terminal half is related to MiaB proteins. This domain is known to be always in conjunction with a Radical SAM superfamily (PF04055) and a TRAM domain (PF01938) although its role is not certain (Anantharaman et al., 2001, Pierrel et al., 2002). RimO is a radical-*S*-adenosylmethionine protein that shows high sequence similarity to the MiaB protein. Both proteins belong to a subclass of radical SAM enzymes known as methylthiotransferases which catalyse the methylthiolation

of tRNA. Specifically, RimO catalyses the addition of a methylthiol group at the C-3 position of aspartate 89 in the protein S12 which is a component of the 30S ribosomal subunit of bacteria. On the other hand, MiaB catalyses the attachment of the methylthiol residue at the C-2 position of N^6-(isopentenyl)adenosine on nucleotide 37 in several prokaryotic tRNAs (Landgraf et al., 2013, Arragain et al., 2010, Atta et al., 2010, Anton et al., 2010). Ribosomal RimO protein undergoes a distinctive post-translational alteration through methylthiolation of residue S12D88 in *E. coli* and many other bacteria (Anton et al., 2008, Pierrel et al., 2002). The enzyme that causes this modification in *E. coli* is known to be encoded by the *yliG* gene product that has been recently revealed to be required for the production of the 3-methylthio derivative of residue Asp-89 in the ribosomal protein S12 *in vivo* (Lee et al., 2009, Arragain et al., 2010). In two other subgroups of bacteria, *B. subtilis* and *Methanococcus jannaschii*, YqeV and Mj0867 respectively are representatives of the methylthiotransferases family in addition to RimO and MiaB (Anton et al., 2008).

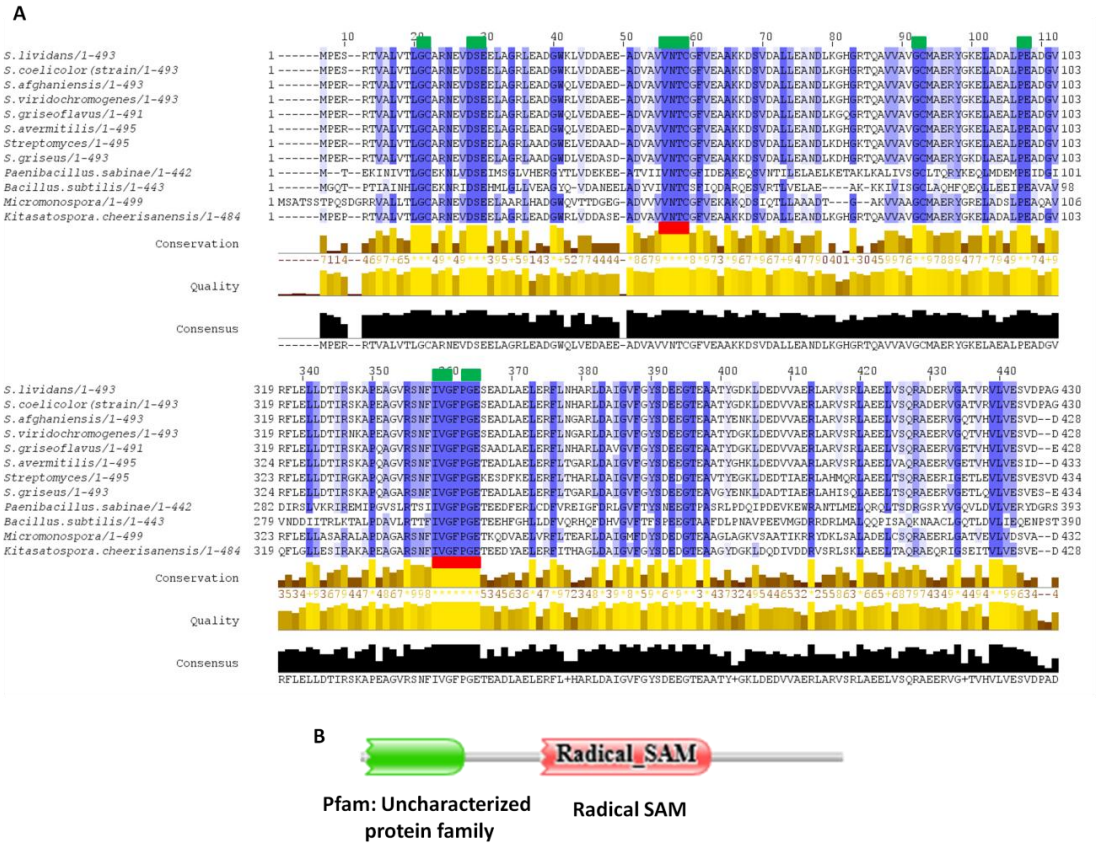

Figure 3-7: Alignment of SCO5752 protein sequence homologues.

(A) The sequences were taken from Uniprot and the alignment configured using Jalview. The Residues are coloured according to the percentage identity selections from 100% (dark blue) to 0% (no colour), the darker the blue reflects the higher the percentage identity (Clamp et al., 2004, Waterhouse et al., 2009). The two highly conserved regions that contain hydrophobic residues (Valine) are highlighted in red. Also, several conserved motifs that contain are matched to the uncharacterized protein family (UPF0004) and radical SAM superfamily domain according to the Pfam database (highlighted in green). (B) Schematic illustration of SCO5752 protein structure assessed using Pfam (the protein database). It shows the uncharacterized protein family UPF0004 at the position 6-105 and the Radical SAM superfamily domain at the position 187-359 (Date of access Jan 2015) (Finn et al., 2014).

The second domain is the radical SAM superfamily, which is matched between and 189-359 AA (Figure 3.7B), catalyses many reactions such as unusual methylations, sulphur insertion, isomerisation, protein radical formation, anaerobic oxidation, and ring formation (Sofia et al., 2001, Benjdia et al., 2010, Berteau et al., 2006). Evidence showed that these proteins with various roles have been linked to an unusual 4Fe-4S cluster associated with the production of a free radical substrate and/or protein to cleave *S*-adenosylmethionine (SAM). This group contains MoaA which belongs to the family of *S*-adenosylmethionine (SAM) proteins. Both protein MoaA and MoaC catalyze the first stage in molybdenum cofactor biosynthesis, the exchange of a guanosine to precursor Z, an oxygen sensitive tetrahydropyranopterin that contains a cyclic phosphate. This process, in where every carbon and nitrogen atoms of guanosine are utilized and requires a rearrangement of the guanine C8 atom reaction and according to the association of MoaA to *S*-adenosylmethionine (SAM) family, this transformation has been suggested to implicate radical chemistry resulting in human molybdenum cofactor deficiency (Hanzelmann and Schindelin, 2006, Hänzelmann and Schindelin, 2004). This alignment was then utilized to produce a phylogenetic tree to achieve a further graphical illustration of the relationship between SCO5752 and some of the proteins in the alignment. The evolutionary relationships history inferred was revealed using the Neighbour-Joining method using Jalview (Figure 3.8). The tree is performed to scale with branch distances in the identical units whose evolutionary lengths are utilised to construct the phylogenetic tree. The tree indicates that in measuring the SCO5752 protein sequences, *S. coelicolor* and *S. lividans* are very strongly correlated. The next branch of strongly correlated species contains the species *S. afghaniensis*, *S. viridochromogenes* and *S. griseoflavus*. The tree showed some degree of relationship between the genera *Micromonospora* and *Streptomyces*. The most different species to *S. coelicolor* belonged in the order *Bacillales*. In terms of branch distances and correlation, the *Streptomyces* species are clearly all highly conserved. The results of this phylogenetic analysis showed that the protein sequences of SCO5752 are more closely related within the Actinobacteria. A more comprehensive analysis of protein sequences would be useful in elucidating the revolutionary relationship of SCO5752 from *S. coelicolor* with other organisms.

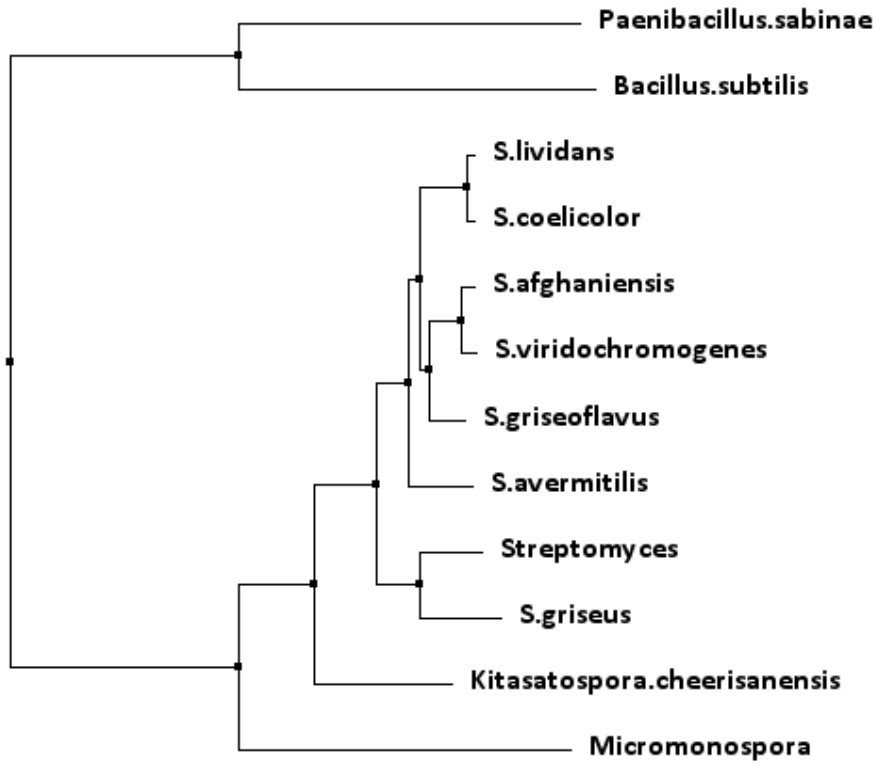

Figure 3-8: Phylogenetic tree of SCO5752 protein based on Jalview.

The evolutionary relationships were inferred for SCO5752 in 12 taxa using the Neighbour Joining (PAM 250) method (Saitou and Nei, 1987). The overview of the phylogenetic tree indicated a strong correlation in *Streptomyces* species as well as the genera *Micromonospora* and *Kitasatospora* showed some similarity to *Streptomyces* species.

3.6 Protein sequence alignment and phylogenetic analysis of SCO5753 protein homologues from a variety of bacterial taxa

SCO5753 (pgsA) encodes a probable phosphatidyl glycerophosphate synthase, although the function of the protein encoded by this gene has not been determined experimentally, the length of this protein is 263 AAs. Given the likely role of PgsA in synthesis of the PL, PG, it seems plausible that this gene might be essential; possible manifested through the essential nature of CL (Jyothikumar et al., 2012). In order to investigate the evolutionary relationship between this protein and its actinobacterial relatives, phylogenetic analysis was conducted in a similar process with that performed in the previous section.

The classification and identification of SCO5753 with respect to other bacteria was carried out (Figure 3.9). The protein SCO5753 was highly represented in two phyla of actinobacteria *Corynebacterineae* and *Streptomycetaceae* with 92% and 7% respectively. Homologues of SCO5753 from the UniProt database were selected based on the strongest BLAST protein sequences matches. The protein sequence of SCO5753 in *Streptomyces* species and *Kitasatospora setae* shared 71-100% homology, for instance (at the top of the identity); *S. lividans* shared 100% similarity to *S. coelicolor*. Also, noteworthy is that the *Corynebacterineae* genera (*Mycobacterium tuberculosis, Nocardia farcinica, Gordonia araii, Rhodococcus sp*.) showed a reasonable protein sequence homology and similarities to the SCO5753 protein sequence of *S. coelicolor* with *59*-62% identity (Table 3.2).

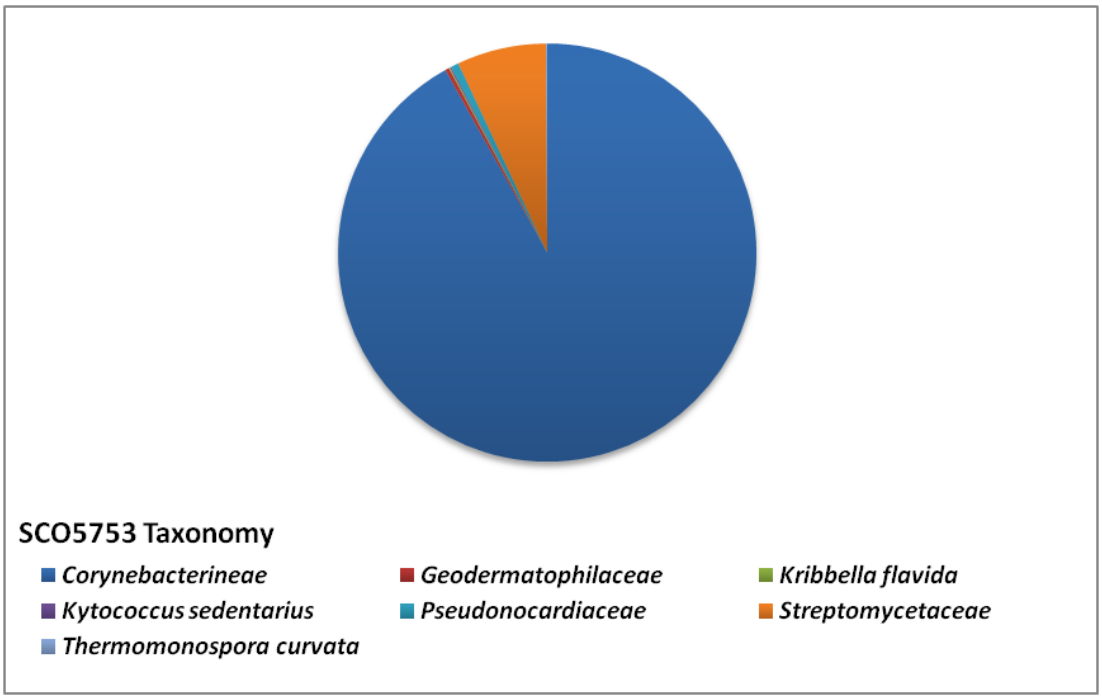

Figure 3-9: Distribution of SCO5753 proteins throughout bacterial taxa.

SCO5753 protein taxonomy result was modified from Uniprot based on the NCBI taxonomy database. The result shows the most abundant SCO5753 protein sequences in bacterial phyla. The results indicate the class name against the number of the organisms as the following: *Corynebacterineae* (92%), *Geodermatophilaceae* (0%), *Kribbella flavida* (strain DSM 17836 / JCM 10339 / NBRC 14399) (0%), *Kytococcus sedentarius* (strain ATCC 14392 / DSM 20547 / CCM 314 / 541) (*Micrococcus sedentarius*) (0%), *Pseudonocardiaceae* (1%), *Streptomycetaceae* (7%), *Thermomonospora curvata* (strain ATCC 19995 / DSM 43183 / JCM 3096 / NCIMB 10081) (0%) (Date of access Sep 2014).

Table 3-2: Summary of homologues to *S. coelicolor* SCO5753 following interrogation of the UniProt database using BLAST.

Protein names	Organism	Length	Identity	Score	E-value	Gene names
CDP-diacylglycerol--glycerol-3-phosphate	*S. lividans*	263	100%	1,317	0	*SLI_6014*
Phosphatidylglycerophosphate synthase	*S. coelicolor*	263	100%	1,317	0	*SCO5753*
Phosphatidylglycerophosphate synthase	*S. coelicoflavus*	261	90%	1,167	1.0×10^{158}	*SMCF_609*
Putative phosphatidylglycerophosphate synthas	*S. avermitilis*	282	75%	1,016	2.0×10^{135}	*pgsA1*
CDP-diacylglycerol--glycerol-3-phosphate 3	*S. turgidiscabies*	279	74%	994	3.0×10^{132}	*pgsA*
CDP-diacylglycerol--glycerol-3-phosphate 3	*S. ipomoeae*	264	72%	957	8.0×10^{127}	*pgsA*
Putative CDP-diacylglycerol--glycerol-3	*Kitasatospora setae*	210	71%	712	2.0×10^{90}	*pgsA*
CDP-diacylglycerol--glycerol-3-phosphate	*Rhodococcus sp.*	200	62%	545	2.0×10^{65}	*pgsA*
Phosphatidylglycerophosphate synthase	*Gordonia araii*	217	60%	602	7.0×10^{74}	*pgsA*
Putative phosphatidylglycerophosphate synthase	*Nocardia farcinica*	222	60%	561	1.0×10^{67}	*pgsA2*
CDP-diacylglycerol-glycerol-3-phosphate	*Mycobacterium tuberculosis*	199	59%	532	1.0×10^{63}	*pgsA3*

In analysing the alignment in (Figure 3.10A), there seems to be consensus amongst a number of *Streptomyces* species and other organisms. Mostly, the sequence alignment showed three highly conserved regions containing hydrophobic residues (Proline) for both motifs. The first highly conserved motif had the consensus identity of A-D-G-P-I-A-D-K, the second; L-P-W-W and the third region V-I-P-A. The data in (Figure 3.11A) also reveals several consensuses for the motif between amino acid residues 117 to 255 of hydrophobic amino acids. A further assessment for SCO5753 reveals Pfam expectation values of $2.5e^{-14}$ for the CDP-alcohol phosphatidyltransferase (CDP-OH P transfer). Search using Pfam found one Pfam match for this domain, which is CDP-alcohol phosphatidyltransferase matched between 73and 183 (AAs) of the sequence. Also, the sequence alignment indicated other conserved motifs which are matched to the CDP-alcohol phosphatidyltransferase protein family according to Pfam (Figure 3.10A).

The CDP-alcohol phosphotransferase (CDP-AP) enzymes catalyse the transfer, from a CDP-linked donor to an acceptor alcohol, of a substituted phosphate moeity (Sciara et al., 2014). This reaction, which is solely catalysed by CDP-APs, is an essential step in the biosynthesis of phospholipids among all life kingdoms (Nogly et al., 2014), and is the best studied function of this family of enzymes. During the biosynthetic process, the lipid reactant can participate either as donor or acceptor alcohol, or any two lipid substrates can behave as donor and acceptor respectively. The enzymes PI and PGP synthases which are found in eukaryotic and prokaryotic organisms respectively possess CDP-DAG, which is a lipophilic donor, and myo-inositol and glycerol-3-phosphate, which are polar acceptors, respectively (Rahman et al., 2009a, Widdick et al., 2011). In *E. coli*, phosphatidylglycerophosphate (PGP) synthase, the enzyme encoded by the gene *pgsA*, catalyses the crucial step in the biosynthesis of acidic phospholipids and is thus essential for cell growth (Usui et al., 1994, Suzuki et al., 2002). Just like most of the enzymes involved in phospholipid metabolism, PGP is an integral membrane protein which is found tightly associated the *E. coli* cytoplasmic membrane (Gopalakrishnan et al., 1986).

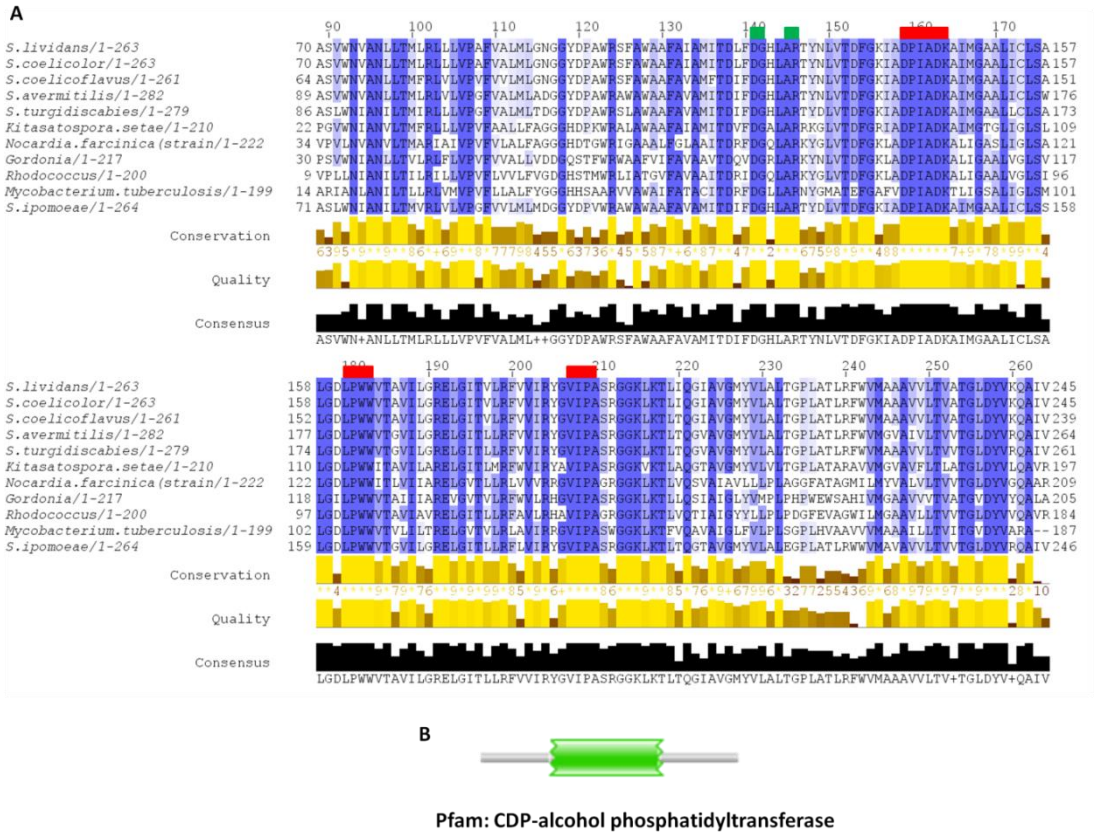

Figure 3-10: Alignment of SCO5753 homologues.

(A) The sequences were taken from Uniprot and the alignment configured using Jalview. The Residues are coloured according to the percentage identity selections from 100% (dark blue) to 0% (no colour), the darker the blue the higher the percentage identity (Clamp et al., 2004, Waterhouse et al., 2009). The three highly conserved regions contain hydrophobic residues (Proline) and are highlighted in red. Also, two conserved motifs were found that matched to the CDP-alcohol phosphatidyltransferase protein family according to Pfam (highlighted by green rectangles). (B) Schematic illustration of SCO5753 protein structure assessed using Pfam (the protein database). It shows the CDP-alcohol phosphatidyltransferase family (CDP-OH P transf) at positions 72-186 (Date of access Jan 2015) (Finn et al., 2014).

The use of software such as Phyre2 allowed us to predict the probable three dimensional structures and function of the protein SCO5753. The Phyre2 web server found two templates predicted with a confidence of 99.9% (Figure 3.11-A). Then the results obtained through Phyre2 were submitted to 'Phyre Investigator' to analyse the predicted function in more detail based on pocket detection. The result indicates that there are large pockets present (presented in red colour and wireframe mode (Figure 3.11-B&C). These large pockets are commonly found to be the location of active sites (Kelley et al., 2015, Schmidtke et al., 2010).

A

#	Template	Alignment Coverage	3D Model	Confidence	% I.d.	Template Information
1	c4mndA_	Alignment		99.9	14	**PDB header:**transferase **Chain:** A: **PDB Molecule:**ctp l-myo-inositol-1-phosphate cytidylyltransferase/cdp-l- **PDBTitle:** crystal structure of archaeoglobus fulgidus ipct-dipps bifunctional2 membrane protein
2	c4o6mA_	Alignment		99.9	16	**PDB header:**transferase **Chain:** A: **PDB Molecule:**af2299, a cdp-alcohol phosphotransferase; **PDBTitle:** structure of af2299, a cdp-alcohol phosphotransferase (cmp-bound)

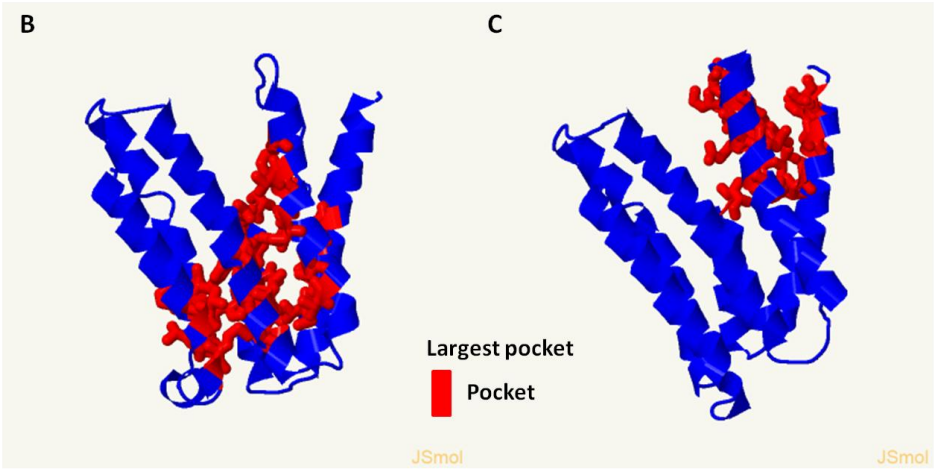

Figure 3-11: Prediction the three dimensional structure of SCO5753 protein sequence and the function of the predicted model based on pocket detection.

A: the main result of top two models that match SCO5753 with confidence degree of 99.9%. A1&A2: the given models from A1&A2 were analysed in more depth via 'Phyre Investigator' to predict the function of SCO5753 based on pocket detection analysis.

A phylogenetic tree was used again to generate a further graphical illustration of the relationship between SCO5753 and related proteins in the alignment via the method of neighbour joining in Jalview. The tree shows that the clade is divided into two main branches, the first one indicates that genera from the Corynebacterineae (*Mycobacterium tuberculosis, Nocardia farcinica, Gordonia araii, Rhodococcus sp*); phylogenetically these are the most divergent genera to *Streptomyces*. The next clade is mostly represented by *Streptomyces* species and again it is clear from the tree that SCO5753 of *S. coelicolor* and its orthologue from *S. lividans* are strongly correlated. Also, other *Streptomyces* species in the same clade display some level of similarities to *S. coelicolor* (Figure 3.12).

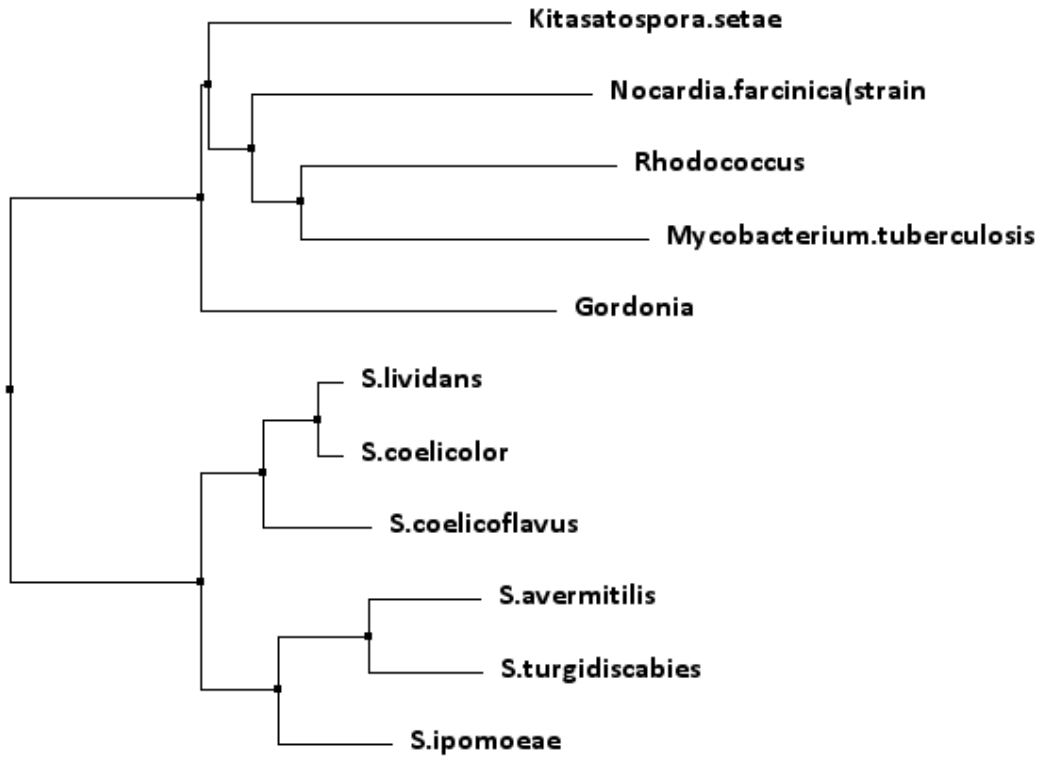

Figure 3-12: Phylogenetic tree of SCO5753 based on Jalview.

The evolutionary relationships were inferred for SCO5753 in 11 taxa using the Neighbour Joining (PAM 250) method (Saitou and Nei, 1987). Overall, it shows from the tree that *Streptomyces* species SCO5753 are closely related in the context of SCO5753 protein present.

As it can be observed in Figure 3.10A**,** the similarity in PgsA within Actinobacteria is significant. Further analysis was conducted on PgsA sequences across other organisms such as *E. coli*, *B. subtilis*, *M. tuberculosis* and *R. sphaeroides*. This multiple sequence analysis has shown two conserved regions [DG] and [AR] as being homologous among *S. coelicolor* and *E. coli*, *B. subtilis*, *M. tuberculosis* and *R. sphaeroides* (Figure 3.13). Also these two conserved regions were found to be present in Actinobacteria (Figure 3.10A). Furthermore, the phylogenetic tree sequence of these organisms has shown close phylogenetic relationships of *S. coelicolor* to *B. subtilis*, *E. coli* and *M. tuberculosis* whereas *R. sphaeroides* has branched into a separate clade that is distantly related to the PgsA sequence of *S. coelicolor* (Figure 3.14).

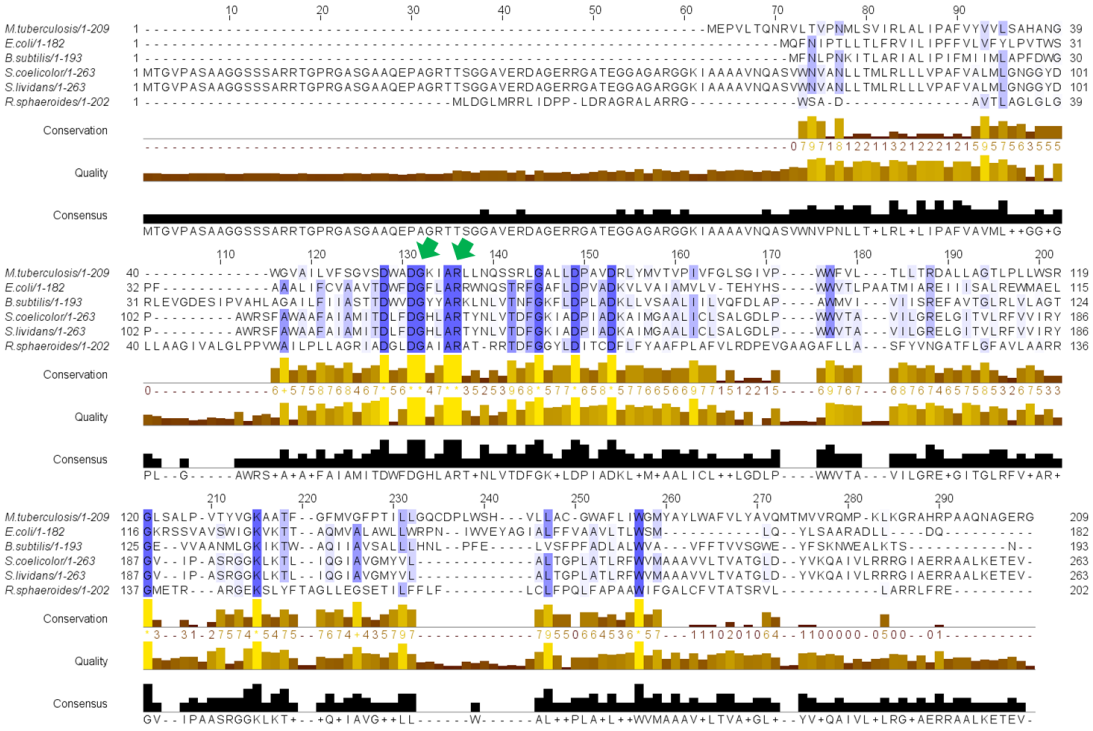

Figure 3-13: Alignment of SCO5753 (PgsA) homologues across other PgsA from *E.coli, B.subtilis, M. tuberculosis* and *R. sphaeroides*.

The sequences were taken from NCBI, and then the alignment was performed at Clustal omega and formatted with Jalview. The Residues are coloured according to the percentage identity selections from 100% (dark blue) to 0% (no colour), the darker the blue the higher the percentage identity (Clamp et al. 2004; Waterhouse et al. 2009). The two highly conserved regions are indicated by green arrows.

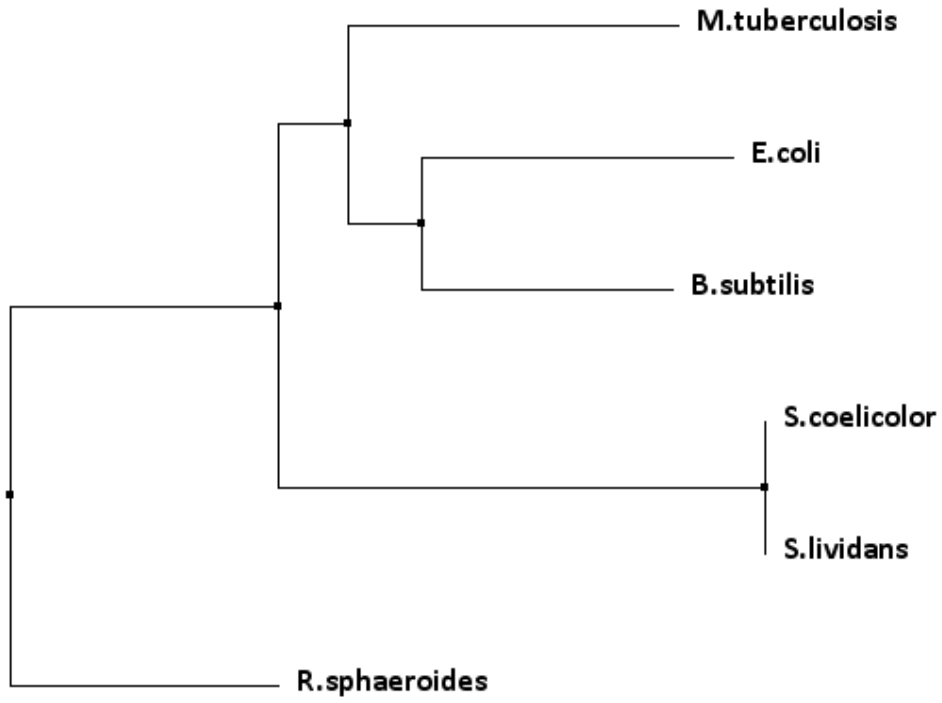

Figure 3-14: Phylogenetic tree of SCO5753 (PgsA) based on Jalview.

The evolutionary relationships were inferred for SCO5753 in 6 taxa using the Neighbour Joining (PAM 250) method (Saitou & Nei 1987). In general, it shows from the tree that *Streptomyces* species PgsA are closely related to PgsA of *B. subtilis*, *E. coli* and *M. tuberculosis*.

3.7 Protein sequence alignment and phylogenetic analysis of SCO5754 protein homologues from a variety of bacterial taxa

SCO5754 encodes a conserved hypothetical protein, the function of which is not known and the length of this gene is 188AAs. It is another gene of *pgsA* operon, which is speculated to be essential gene for growth and development in *S. coelicolor*. This gene was found to be similar to competence damage inducible proteins of *B. subtilis* and *Streptococcus pneumoniae*. A recent publication has shown that the cinnamycin biosynthetic gene cluster (*cin*) from *Streptomyces cinnamoneus* DSM 40005 synthesises the peptide antibiotic cinnamycin. It is believed to be derived by post-translational modification of a larger ribosomally synthesized peptide (Okesli et al., 2011). In order to investigate any sequence similarities of this protein with other proteins present in the sequence databases, the same process was used with the other proteins encoded by this operon to obtain alignments and construct a phylogenetic tree. The protein SCO5754 was found to be highly represented in two phyla of bacteria, the actinobacteria and the firmicutes with containing 58% and 21% respectively (Figure 3.15).

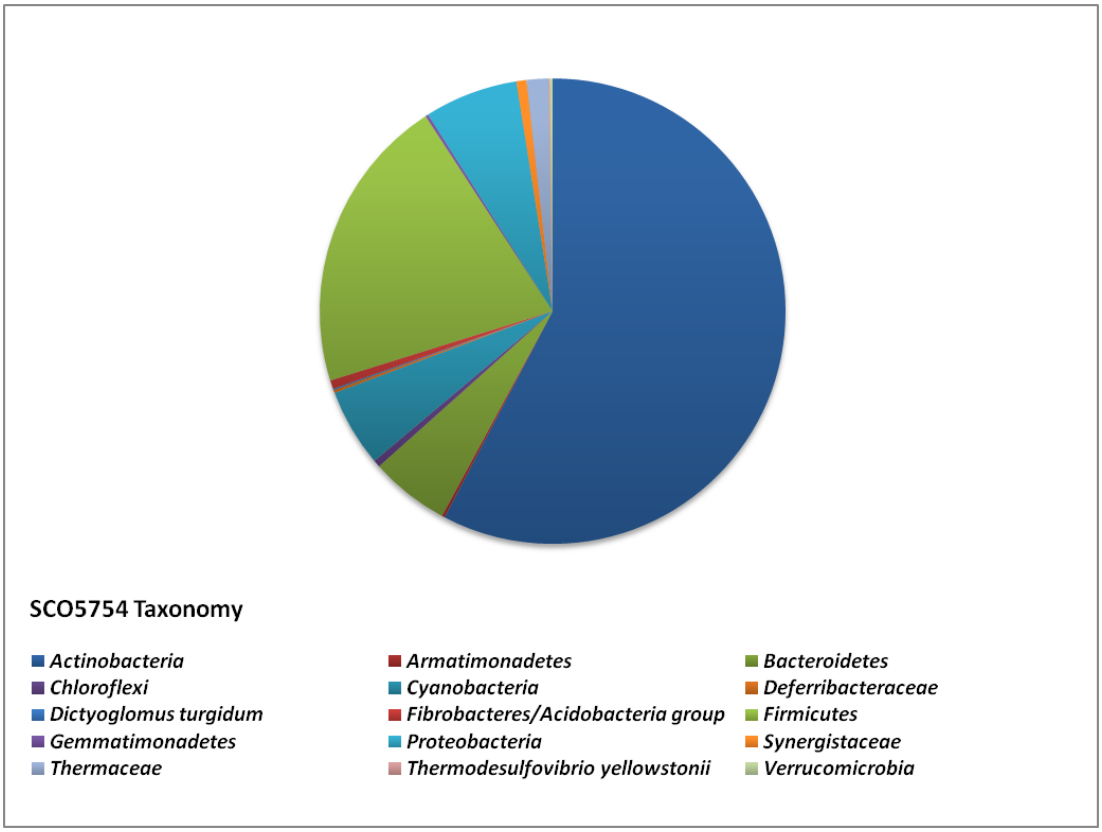

Figure 3-15: Distribution of SCO5754 proteins throughout bacterial taxa.

The SCO5754 protein taxonomy result was modified from Uniprot based on the NCBI taxonomy database. The results presented here show the most representative SCO5754 protein sequences in bacterial phyla. The results indicate the class name against the number of the organisms as follows: *Actinobacteria* (high G+C Gram-positive bacteria) (58%), *Armatimonadetes* (0%), *Bacteroidetes* (6%), Chloroflexi (1%), *Cyanobacteria* (5%), *Deferribacteraceae* (0%), *Dictyoglomus turgidum* (strain Z-1310 / DSM 6724) (0%), *Fibrobacteres/Acidobacteria* group (1%), *Firmicutes* (21%), *Gemmatimonadetes* (0%), *Proteobacteria* (7%), *Synergistaceae* (1%), *Thermaceae* (2%), *Thermodesulfovibrio yellowstonii* (strain ATCC 51303 / DSM 11347 / YP87) (0%), *Verrucomicrobia* (0%) (Date of access Sep 2014).

The protein sequence of SCO5754 from the UniProt database were chosen based on the strongest BLAST matches. The strongest matches (Match Hits) to the SCO5754 protein sequence was used to produce the summary showed in Table 3.3. The strongest hit was observed with *Streptomyces* genera 85-99%. Another protein (putative competence-damage inducible protein) of *Bacillus subtilis* showed slightly weaker identity with 52% identity, but was also similar to *Corynebacterium matruchotii* and *Mycobacterium hassiacum* with 51%, and 49% identity respectively. The competence/damage-inducible protein CinA protein of *Selenomonas sp* and competence damage-inducible protein A of *Mycobacterium tuberculosis* displayed the lowest similarity to SCO5754 protein sequence with 43-44%.

Table 3-3: Summary of homologues to *S. coelicolor* SCO5754 following interrogation of the UniProt database using BLAST.

Protein names	Organism	Length	Identity	Score	E-value	Gene names
Uncharacterized protein	*S. coelicolor*	181	99%	886	1.0×10^{118}	*SCO5754*
Competence-damage inducible protein	*S. lividans*	181	99%	882	4.0×10^{118}	*SSPG_01978*
Uncharacterized protein	*S. coelicoflavus*	181	94%	824	3.0×10^{109}	*SMCF_610*
Damage-inducible protein CinA	*S. olindensis*	181	86%	767	1.0×10^{100}	*DF19_11210*
Competence/damage-inducible protein CinA domain	*Streptomyces sp.*	181	85%	750	5.0×10^{98}	*HMPREF1211_02317*
Putative competence-damage inducible protein	*Bacillus subtilis*	416	52%	265	5.0×10^{24}	*cinA BEST7613_5069*
Competence/damage-inducible domain protein CinA	*Corynebacterium matruchotii*	170	51%	354	2.0×10^{38}	*CORMATOL_01202*
Competence/damage-inducible CinA C-terminal domain protein	*Mycobacterium hassiacum*	174	49%	329	1.0×10^{34}	*C731_1847*
CinA-like protein	*Mycobacterium paratuberculosis*	434	45%	258	5.0×10^{23}	*cinA MAP_1625*
Competence/damage-inducible protein CinA	*Selenomonas sp.*	163	44%	274	1.0×10^{26}	*cinA HMPREF1147_1358*
Competence damage-inducible protein A	*Mycobacterium tuberculosis*	193	43%	251	4.0×10^{23}	*CCDC5079_1757*

The analysis of SCO5754 protein sequence alignment displayed in (Figure 3.16) showed little sequence homology between the SCO5754 protein sequence of *S. coelicolor* amongst a number of *Streptomyces* species and other organisms. The sequence alignment showed that only one highly conserved region was present containing hydrophobic residues (Alanine, Glycine, and Proline) and contained the consensus identity of A-G-P. Furthermore, the data in (Figure 3.16A) indicated several other consensus sequences for the motif between amino acid residues 294 to 391 of the hydrophobic amino acids. Further assessments of the SCO5754 protein sequence showed that Pfam expectation value was $1.4e^{-49}$ for the competence-damaged protein (CinA) (Figure 3.16B). Searching using Pfam found one Pfam domain match between 3 and 162 (AAs) of the sequence at the C-terminal motif of the putative competence damaged proteins from the cin operon. Also, the sequence alignment indicated several conserved motifs contained residue sites which are identical to the competence damaged protein family according to Pfam (Figure 3.16A).

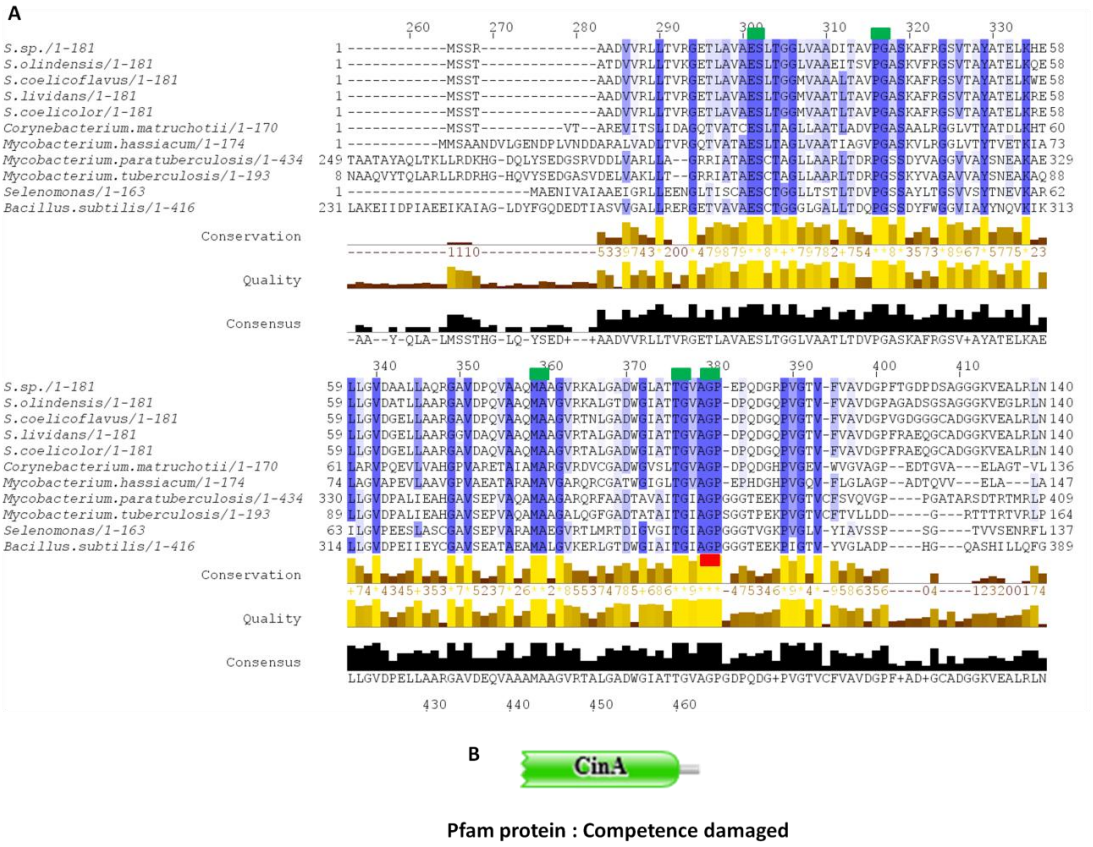

Figure 3-16: Alignment of SCO5754 homologues.

(A) The sequences were taken from Uniprot and the alignment configured using Jalview. The Residues are coloured according to the percentage identity selections from 100% (dark blue) to 0% (no colour), the darker the blue the higher the percentage identity (Clamp et al., 2004, Waterhouse et al., 2009). One highly conserved region was present containing hydrophobic residues is highlighted by red rectangles. Also, several conserved motifs which are matched to the competence damaged protein family according to Pfam (highlighted by green rectangles). (B) Schematic illustration of SCO5754 protein structure assessed using Pfam (the protein database). It shows the CinA competence damaged protein family at position 1-162 (Date of access Jan 2015) (Finn et al., 2014).

cinA is the first gene in the competence-induced operon and is believed to be necessary at some point in transformation process (Martin et al., 1995). The transcriptional regulator of the *recA* gene in the human pathogen *Streptococcus pneumoniae* was found to be akey determinant of competency for genetic transformation. This specific *recA* transcript comprised of two genes at least, *cinA* and *dinF* and also was identified to be the second gene in a competence-induced operon of *S. pneumoniae* (Mortier-Barriere et al., 1998). In *B. subtilis* and *S. pneumoniae*, *cinA* and *recA* are nearby in the genome which could suggest that they have an identical function.

The synthesis of the homologous CinA in *B. subtilis* has been suggested to undergo upregulation during the cell's stationary phase. It is recognised that loss of CinA in cells has a slight effect in competence although it does not have any impact on the localisation of RecA. In addition, CinA is linked with the nucleoid in the cell, and not with the cell membrane, as in *S. pneumoniae* (Kaimer and Graumann, 2010). The σ^R is a system for sensing and responding to disulphide stress in S. *coelicolor* (Paget et al., 2001). *cinA* is a part of the σ^R system, which is induced during periods of oxidative stress and is enoced on an operon that comprises of 27 genes (Paget et al., 2001), although several of its target functions have not yet been identified. *cinA* has been identified as the σ^R dependent system which plays a more important function in the regulation of protein quantity than previous anticipated (Sutcliffe, 2015).

Neighbour joining using Jalview in (Figure 3.17) of SCO5754 alignments shows that *S. lividans* is closely related to the SCO5754 protein sequence of all organisms in the tree. The tree also indicates that *S. coelicoflavus* is the mostly closely related to *S. coelicolor*. The genome of *Selenomonas sp.*, *Mycobacterium tuberculosis*, *Mycobacterium paratuberculosis* and *Bacillus subtilis* contain a protein sequence of SCO5754, which is most likely functionally related to CinA in *S. coelicolor*.

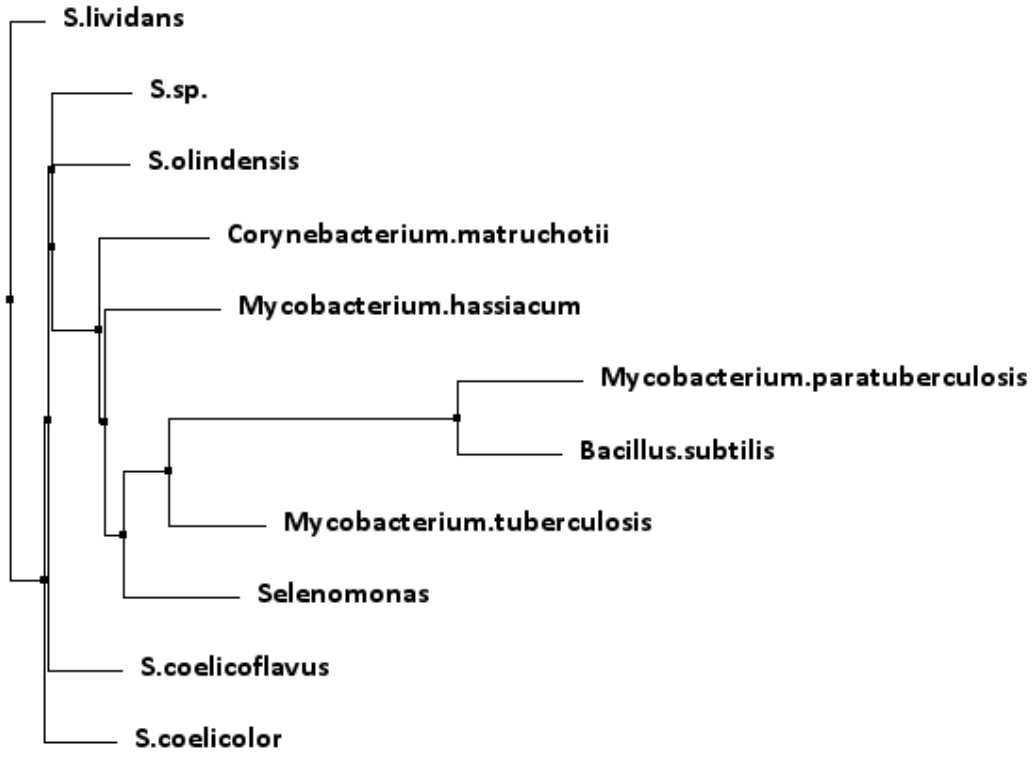

Figure 3-17: Phylogenetic tree of SCO5754 based on Jalview.

The evolutionary relationships was inferred for SCO5754 in 11 taxa using the Neighbour Joining (PAM 250) method (Saitou and Nei, 1987).

3.8 Protein sequence alignment and phylogenetic analysis of SCO5755 protein homologues from a variety of bacterial taxa

SCO5755 (*clgR*) gene is a hypothetical protein whose function was not known at the time of the annotation of the *S. coelicolor* genome sequence. The length of this protein is 156 AAs. Recently, it was shown that the *clgR* gene contributes to *Streptomyces* development since its overexpression induces a delay of differentiation in *S. lividans* (Bellier and Mazodier, 2004). *In vivo*, ClgR acts as an activator of *clpC1* gene and *clpP1* operon expression.

The *clp* genes, which code for the proteolytic complex Clp, are widely distributed among living organisms. In *Streptomyces* there are five *clpP* genes among which is the *clpP1 clpP2* operon which is important in the growth and development of this organism since mutation in this operon inhibits differentiation. The inhibition occurs at the mycelium step of the substrate. In *S. coelicolor*, there are four Clp ATPases which have been identified, including ClpX and three other proteins called ClpC which potentially work alongside ClpP1 ClpP2. It is likely that, since no mutant of the *clpC1* has been obtained so far, this gene is essential in the organism. Using *S. lividans*, it was demonstrated that the *clpP3 clpP4* operon could be induced in mutant strains with defects in *clpP1* gene, and that its expression was regulated through mediation of PopR, a transcriptional regulator. The gene *clgR* is a paralogue of *popR*. Studies on the former gene in *S. lividans* have indicated that ClgR binds to *clpP1* and *clpC1* promoters, as well to the promoters of Lon ATP-dependent protease and *clgR* genes. It was reported that this binding is made possible through recognition of the motif GTTCGC-5N-GCG by ClpP. It has further been reported that, just as is the case with PopR, the degradation of ClgR could be dependent on ClpP through recognition of the two alanine moieties at the carboxyl terminal (Bellier et al., 2006, Bellier and Mazodier, 2004, Guyet et al., 2013).

FIMO was used to find any sequences of SCO5752 that contribute to the motifs which are recognised by *S. lividans* ClgR. This has revealed 5 motif instances with a p-value less than 0.0001 (Table 3-4). The locations of these 5 motifs have also been identified (Figure 3-18).

Table 3-4: The high scoring motif instances of SCO5752 sequence to ClgR motif which has been identified in *S. lividans* by using FIMO analysis

Motif	Sequence Name	Strand	Start	End	p-value	q-value	Matched Sequence
1	SCO5752	+	1303	1315	2.67e-06	0.00301	GTCCGCGGCCGCG
1	SCO5752	−	132	144	1.11e-05	0.00625	GTTCACGACGGCG
1	SCO5752	−	1242	1254	7.33e-05	0.0183	GGTCGCCCCGACG
1	SCO5752	+	515	527	7.65e-05	0.0183	GCGCGCCGCTGCG
1	SCO5752	−	1134	1146	8.11e-05	0.0183	GGTCGCCGCCTCG

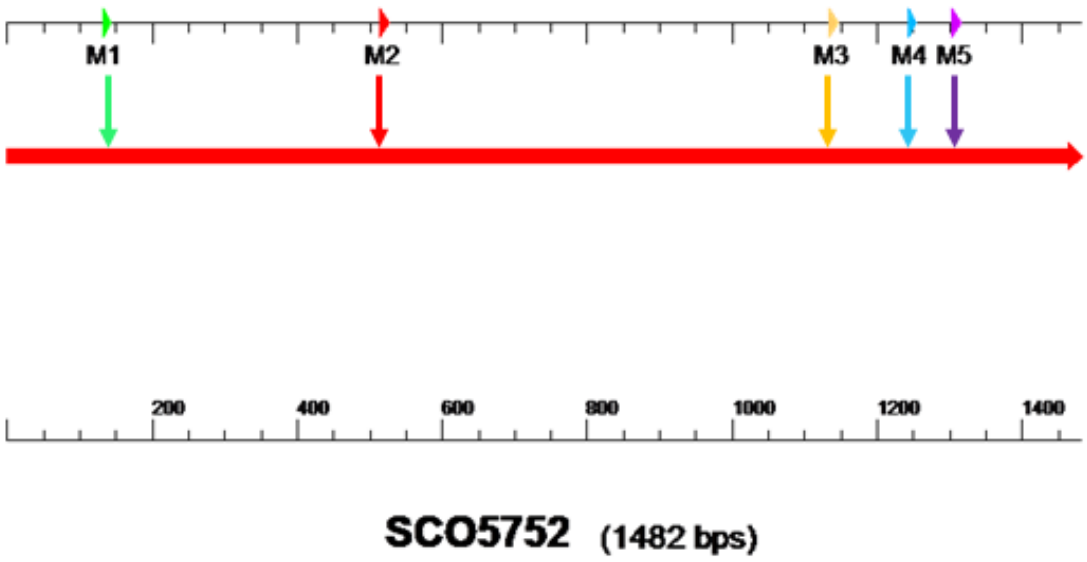

Figure 3-18: The location of 5 motif instances of the *SCO5752* gene revealed by FIMO analysis in table 3-4.

StrepDB was used to obtain the *SCO5752* gene sequence which was then mapped using Clone Manager software to identify the positions of the 5 motifs. The positions of these motifs are represented as follows: the M1 motif (GTTCACGACGGCG) starts from 132 and ends at 144; M2 (GCGCGCCGCTGCG) is from 515 to 527; M3 (GGTCGCCGCCTCG) from 1134 to 1146; M4 (GGTCGCCCCGACG) from 1242 to 1254; and finally M5 (GTCCGCGGCCGCG) sequence occupies the position from 1303 to 1315 on the *SCO5752* gene.

Further investigation is required to characterize the upstream genes *SCO5755* as this protein is speculated to regulate the *pgsA* operon. The phylogenetic analysis for this protein was conducted in the same manner as the previous proteins. SCO5755 was analysed using the UniProt database and the strongest BLAST matches selected. The summary of strongest hits to the SCO5755 sequence from BLAST searches against the UniProt database is displayed in Table 3.5. The highest level of identity was observed with the protein transcriptional regulator XRE family of *S. lividans* at 100%, whilst the transcriptional regulator ClgR, of *Mycobacterium tuberculosis* showed the lowest identity with 60% in the table.

Table 3-5: Summary of homologues to *S. coelicolor* SCO5755 following interrogation of the UniProt database using BLAST.

Protein names	Organism	Length	Identity	Score	E-value	Gene name
Transcriptional regulator, XRE family	*S. lividans*	126	100%	597	1.0×10^{76}	*SLI_6016*
Uncharacterized protein	*S. coelicolor*	126	100%	597	1.0×10-76	*SCO5755*
Uncharacterized protein	*S. coelicoflavus*	126	99%	593	5.0×10-76	*SMCF_611*
Helix-turn-helix domain-containing protein	*S. griseoflavus*	126	98%	583	2.0×10^{74}	*SSRG_01556*
DNA-binding protein	*S. sviceus*	126	97%	578	1.0×10^{73}	*SSEG_04500*
XRE family transcriptional regulator	*Streptomyces. sp.*	125	95%	550	2.0×10^{69}	*CF54_06855*
Putative transcriptional regulator	*Kitasatospora setae*	122	71%	395	4.0×10^{46}	*KSE_53500*
Transcriptional regulator ClgR	*Mycobacterium tuberculosis*	112	60%	235	3.0×10^{22}	*clgR Rv2745c*

The analysis of SCO5755 protein sequence alignment in (Figure 3.19) shows good sequence homology between the SCO5755 sequence of *S. coelicolor* amongst a number of *Streptomyces* species and other organism. The sequence alignment reveals that four highly conserved regions containing the hydrophobic residues (Alanine, Glycine, Isoleucine, Leucine, Valine) (Figure 3.19A). Further analysis of the SCO5755 protein sequence showed a Pfam expectation value of $2.8e^{-11}$ for the Helix-turn-helix domain (HTH 31). Searches using Pfam was found one Pfam domain also identified a Helix-turn-helix domain (HTH 31) that matched between AAs 8 and 65 of the sequence (Figure 3.19B). The cro/C1- type helix-turn-helix (HTH) domain is the main structural region for binding DNA, this domain approximately 20 amino acid long and is found in several proteins that regulate gene expression (Brennan and Matthews, Sauer et al., 1982, Ohlendorf et al., 1982, Takeda et al.). This protein is named after the transcriptional repressors cro and C1 of temperate bacteriophages such as 434 and lambda, respectively. The HTH DNA-binding region comprises two α helices that is located between the N-terminal part & C-terminal parts of the protein, to which they are attached by a short strand of amino acids (Pabo and Sauer, 1984, Aggarwal et al., 1988, Matthews et al., 1982). Also, the sequence alignment indicated several conserved motifs which are matched with HTH domains according to the Pfam database (Figure 3.19B).

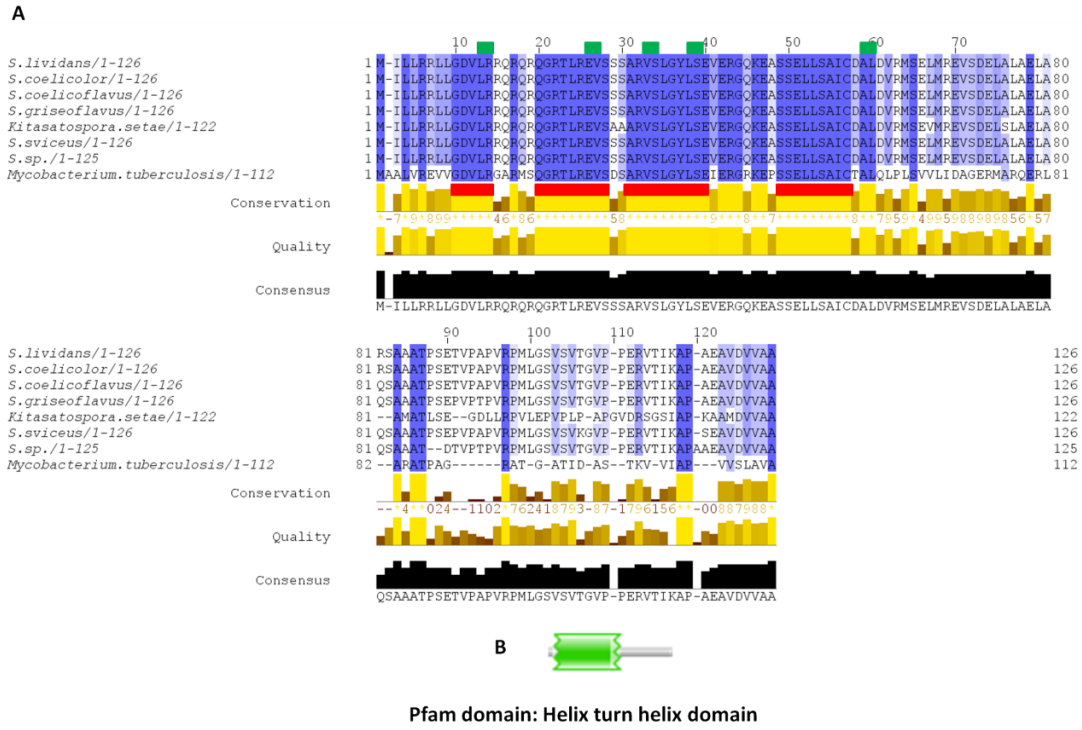

Figure 3-19: Alignment of SCO5755 homologues.

(A) The sequences were taken from Uniprot and the alignment carried out using Jalview. The residues are coloured according to the percentage identity selections from 100% (dark blue) to 0% (no colour), the darker the blue the higher the percentage identity (Clamp et al., 2004, Waterhouse et al., 2009). Four highly conserved regions contained hydrophobic residues are highlighted by red rectangles. Also, several conserved motifs which are matched to the Helix-turn-helix domain according to Pfam (highlighted by green rectangles). (B) Schematic illustration of the SCO5755 protein structure assessed using Pfam (the protein database). It shows the Helix-turn-helix domain at position 7-74 (Date of access Jan 2015) (Finn et al., 2014).

In (Figure 3.20), Neighbour-joining using Jalview of SCO5755 sequence shows that *Mycobacterium tuberculosis* is the most distant in the tree to SCO5755 protein sequence of *S. coelicolor*. The tree also indicates that *Kitasatospora setae* is distant to *S. coelicolor*. However, all the *Streptomyces* species have showed high degree of similarities in phylogenetic relationships with respect to this protein.

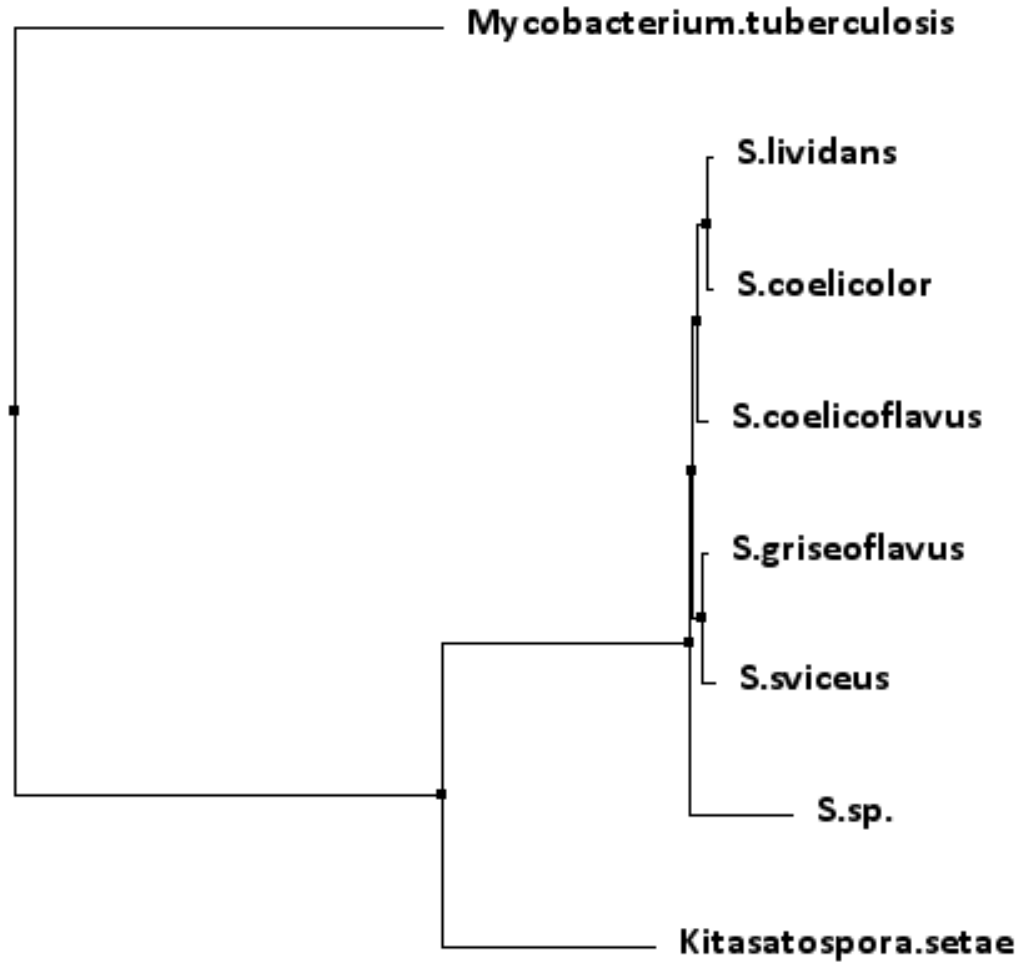

Figure 3-20: Phylogenetic tree of SCO5755 based on Jalview.

The evolutionary relationships are inferred for SCO5755 in 8 taxa using the Neighbour Joining (PAM 250) method (Saitou and Nei, 1987). In general, it shows from the tree that SCO5755 homologues sequences are highly conserved between *Streptomyces* species.

The structural origin for the DNA binding domain by transcriptional regulators that contains the HTH motif was originally revealed in the 1980s. The phage lambda repressors Cro and cI and the lactose operon repressor, LacI were the first proteins where DNA binding domains of were recognized as HTH motifs (Menon and Lawrence, 2013). HTH domains are the main structural motif for DNA binding proteins across the three kingdoms of life. It is comprised of two α helices attached by a short amino acids strand and is found in several proteins that activate gene expression (Aravind et al., 2005, Brennan and Matthews). It is frequently found in transcription factors from prokaryotes, although there are several transcription factors from eukaryotes that also have the HTH motif. The regulation of the transcription factors, positively regulated or negatively regulated, is reliant on the HTH domain in the genes or operons that are regulated by specific transcriptional regulators (Menon and Lawrence, 2013). One of the most ubiquitous types of HTH transcription factors is the GntR family of activators. These proteins have a DNA binding HTH domain at the N terminal end of the domain protein and an effector binding or/and oligomerisation domain at the C terminal (Rigali et al., 2002). These multi-domain transcription factors are found all over the bacteria where they carry out essential functions in alteration of gene expression to react to environmental changes. It has been suggested that organisms grown in complex and extremely unstable environments such as soil like *Streptomyces*, *Burkholderia*, *Rhizobium* have a larger incidence of GntR regulators than intracellular parasites and endosymbionts like *Chlamydia* and *Buchnera* (Hoskisson and Rigali, 2009). GabR from *Bacillus thuringiensis* is identify as a Sigma 54-dependent transcriptional regulator which contains of three distinctive domains, an N-terminal activator domain Per-ARNT-Sim (PAS), a central AAA+ (ATPases linked with various cellular regularities) domain and a C-terminal HTH DNA binding domain (Peng et al., 2014).

3.9 Discussion of Chapter 3

PLs have a significant function in the dynamic structure of bacterial DNA and mitochondrial membranes. PLs such as PG and CL are abundant in bacteria (Mileykovskaya and Dowhan, 2009). According to (Sandoval-Calderon et al., 2009), the gene *SCO5753* exists as a homologue of *pgsA*, which has been suggested to encode phosphatidylglycerol-3-phosphate synthase (PgsA) in *Streptomyces.* This study has explored the significance of *pgsA* in *S. coelicolor.* In addition, the genomic database of *Streptomyces* indicates that the genes *SCO5752*, *SCO5753* and *SCO5754* appear as an operon that is regulated by a single promoter. Our investigation was expanded to characterize the downstream gene, *SCO5755*, as the protein encoded by this gene is speculated to regulate *SCO5753* (Bellier and Mazodier, 2004).

Mutations in essential genes are significant in genomics as they can assist in drug discovery for target prioritization and validation and can be utilized for screening compound libraries and determining the mode of action of potential lead compounds (Herring and Blattner, 2004). At the start of this work, a preliminary investigation via mutational analysis was done on these genes *SCO5751*, *SCO5752, SCO5753* and *SCO5755* to decipher their significance in *Streptomyces.* By means of disrupted genes in the transposed cosmids SC7C7.2.F05, SC7C7.2.B06, SC7C7.2.B07 and SC7C7.A02, we showed that it was not possible to achieve any gene disruption of these genes in the bacteria. This unsuccessful attempt to disrupt these genes suggested that allelic transfer could not take place or each gene is essential for *Streptomyces* growth.

The use of *S. coelicolor* annotation server (StrepDB) indicated that *SCO5752*, *SCO5753* and *SCO5754* appear as a single operon and they could be controlled by a common promoter and also might suggest that they are transcriptionally fused. Further work would be required to investigate this; potentially involving the use of transcript analysis through S1 mapping (Sutcliffe et al., 2012) or 5’ RACE (Schauner et al., 1999). In *Streptomyces griseus*, *ftsZ* expression is governed from 4 promoters, despite its presence in the large division and cell wall synthesis operon (Kwak et al., 2001); consequently it is perhaps more

likely that the *SCO5752*, *SCO5753* and *SCO5754* expression is driven from independent promoters. The *Streptomyces lividans clpP1P2* operon, which is activated by ClgR, and as a result, incorporation of an apramycin resistance cassette in *clpP1* had a polar effect on *clpP2* expression (Billier et al 2006). This could support our hypothesis that there might a polar effect generated by the transposon insertion due to their location as an operon and this is perhaps an explanation for our inability to obtain a full homologus recombination (double crossover) in the chromosome of *S. coelicolor* and it may be at least one of these gene are essential. Also, it was revealed that the ClgR is involved in *Streptomyces* development, since *clgR* overexpression induces a delay of differentiation in *S. lividans* (Bellier & Mazodier 2004). Furthermore, in order to study the gene *SCO5753* (*pgsA*), the characterization of downstream genes such as *SCO5755* was also investigated as the protein encoded by this gene is speculated to regulate *SCO5753*. Double crossovers were also not obtained for the gene *SCO5751* suggesting it could be essential. Moreover, from StrepDB, SCO5751 is predicted to be a putative membrane protein, contains probable hydrophobic membrane spanning domain and match helix turn helix domain (Pfam 13413). Therefore, this gene could play dual role with *SCO5755* to regulate the *pgsA* operon.

In order to understand the evolutionary importance of the *pgsA* operon, phylogenetic analysis was applied to give us an overview of these genes based on homology and similarity to other genes. Overall, a protein sequence alignment and phylogenetic tree analysis showed that the *pgsA* operon and *clgR* gene of both *S. coelicolor* and *S. lividans* are mostly homologous. Other *Streptomyces* species such as *S. viridochromogenes S. afghaniensis, S. viridochromogenes, S. griseoflavus, S. avermitilis, S. griseus, S. turgidiscabies, S. ipomoeae, S. olindensis, S. coelicoflavus* and *S. sviceus* showed high degree of genetic relationships in the proteins encoded by the *pgsA* operon.

From StrepDB, we see that the gene *SCO5752* is annotated as encoding a conserved hypothetical protein, similar to an uncharacterized protein family (Pfam: UPF0004) and the radical SAM superfamily. The alignment of SCO5752 showed two highly

conserved regions [I-V-G-F-P-G-E] and [V-N-T-C] containing the hydrophobic residues.

Furthermore protein alignment revealed several consensuses for the motif between amino acid residues 21 to 465 of hydrophobic amino acids. Similarity searches using the Pfam database matched several conserved motifs that are identical to the uncharacterized protein family (UPF0004). *SCO5753* is annotated as encoding a phosphatidyl glycerophosphate synthase (PgsA) from StrepDB and is similar to a CDP-alcohol phosphatidyltransferase in the Pfam database. The alignment of SCO5753 showed three highly conserved regions [A-D-G-P-I-A-D-K], [G-V-I-P-A] and [L-P-W-W] containing the hydrophobic amino acid residues. Additional consensuses for the motif were observed between hydrophobic amino acid residues 117 to 255. Similarity searches using the Pfam database indicated several conserved motifs which are identical to the CDP-alcohol phosphatidyltransferase family. *SCO5754* is annotated as encoding a conserved hypothetical protein with similarities to the competence-damaged protein (CinA) in the Pfam database. The alignment of SCO5754 showed one highly conserved region [A-G-P], also containing hydrophobic amino acid residues.

Moreover, consensuses sequences were observed in the amino acid residues 294 to 391 of hydrophobic amino acids. Similarity search indicated conserved motifs which were identical to those of the competence-damaged protein in the Pfam database. The *SCO5755* gene is annotated as encoding a hypothetical protein (ClgR) in the StrepDB and contains domains similar to HTH domain (HTH 31) (Pfam: PF13560). The alignment of SCO5755 protein showed four highly conserved regions [G-D-V-L-R], [Q-G-R-T-L-R-E-V-S] and [A-R-V-S-L-G-Y-L-S-E] and [S-S-E-L-L-S-A-I] containing the hydrophobic residues amino acid (Alanine, Glycine, Isoleucine, Leucine and Valine). Pfam similarity indicated conserved motifs (like Leucine and Arginine) that are identical to the HTH domain family at Pfam database. The abundances of hydrophobic amino acids in each protein could suggest that these proteins contain unidentified membrane spanning domains or could show higher affinity for interaction with the membrane.

Due to the limited timeframe of this project we could not employ additional techniques to disrupt the genes of the *pgsA* operon. For instance PCR-directed mutagenesis is an efficient method in molecular microbiology which could have been employed for the introduction of gene deletions in the strains. This method has advantages over other recombinant DNA technology such as transposon-directed mutagenesis, including its ability to avoid the polar effects on genes downstream in the operon to the deleted gene (Gust et al., 2002, Gust et al., 2003). Thus it is recommeded that further investigations using these alternative approaches be considered in future.

Chapter 4:

Cloning and expression of the genes of the *pgsA* operon

4. Cloning and expression of the genes of the *pgsA* operon

4.1 Introduction to Chapter 4

The role of these genes *SCO5752*, *SCO5753*, *SCO5754* and *SCO5755* were investigated in the previous chapter through mutation and phylogenetic analysis. However, to obtain a complete picture of their activity it was also important to observe the effect of over expression of these genes. As it was impossible to disrupt expression of these four genes we decided to use another genetic approach to investigate their expression. This approach is to introduce a second copy of each gene into the chromosome of *S. coelicolor* under the control of an inducible promoter; it is one of the methods used to study essential genes (Ali et al., 2002, Enguita et al., 1996, Takano et al., 1995, Yu and Hopwood, 1995). This turns gene expression on and off with a large dynamic range, whilst the level of natural expression and regulation of the gene are exceeded by the inducible promoter (Herring and Blattner, 2004). This approach also gives a reliable and independent estimation of essential genes for bacteria. In *B. subtilis*, for example, this approach was used to estimate minimal genes by insertion of non-replicating plasmids into the desired gene through a single crossover recombination. The expression of downstream genes in the same operon was directed by an isopropyl β-D-thiogalactoside (IPTG) regulated promoter carried on the inserted plasmid. Therefore, among 4100 genes of this organism, 79 genes were expected to be essential whilst 192 genes were actually found to be indispensable (Kobayashi et al., 2003, Arigoni et al., 1998).

A main theme in the polar localization of dynamic proteins is the presence of signals. For instance lipids, geometry, or landmark proteins can recruit proteins to the poles (Treuner-Lange and Sogaard-Andersen, 2014). Lipids have long been found to be implicated in the initiation of chromosome replication in *E. coli* (Norris and Amar, 2012) and one suggestion is that anionic PLs endorse change from ADP-DnaA to ATP-DnaA *in vivo* as well as *in vitro* (Castuma et al., 1993). Recent research showed that special binding of the expressed MGS (monoglucosyldiacylglycerol synthase) to anionic lipids (particularly PG) activates a response supporting the whole lipid population in the cell. This mechanism results from an interdependent cycle of

protein formation and PL synthesis and demonstrates that MGS stimulates *E. coli* to synthesise additional lipids in a "feed-forward" way (Ariöz et al., 2014, Ariöz et al., 2013). Previous studies showed that an enlarged anionic lipid content of PG and CL in lipid bilayers *in vitro* supported enzyme activation of MGS through membrane binding. However, no lab based results have been conducted so far which revealed anionic lipid binding to MGS *in vivo* (Li et al., 2003, Lind et al., 2007).

Early studies showed that a null mutant of *pgsA* in *E. coli* is not viable and is deficient in PG and CL biosynthesis (Heacock and Dowhan, 1987). Significant evidence showed that the membrane-bound phosphoglycerol transferase catalysed a vital stage in the membrane-derived oligosaccharides (MDO) biosynthesis (Jackson and Kennedy, 1983). In contrast, mutations in *pgpA* and *pgpB* showed that they are not essential for either growth or PG synthesis, and lacked any significant alteration in phenotype. This could indicate the existence of at least one other gene that is responsible for anionic PL biosynthesis in these mutant *pgpA* and *pgpB* strains (Funk et al., 1992).

In spite of the essentiality of the anionic precursors to PG for chromosome replication and cell growth (Mileykovskaya and Dowhan, 2005), CL is not required for viability in deficient strains of *E. coli* and it is not essential in *E. coli*, since no significant impact was found of a mutation in *cls*, although small effects on growth rate in standard media and entry into stationary phase were found (Pluschke et al., 1978).

Following the observation that the *pgsA* operon is indispensable in *S. coelicolor* (Chapter 3), we decided to construct a strain containing the *pgsA* operon under the control of an inducible promoter in order for us to examine the growth and development in the presence of changing levels of PgsA and PG. Thus, to understand the effect of over production of PG, we used the *tipA* promoter, which is one of the most common promoters utilized to derived inducible overexpression of cloned genes in streptomycetes. The *tipA* promoter responded to alterations in the osmotic stress environment and has been used experimentally to control expression of cloned

genes in many streptomycetes, initially in *S. lividans*. It was found that basal level expression from *ptipA* is elevated in the presence of elevated sucrose levels (Ali et al., 2002).

Tsr regulates the expression of four proteins (17, 19, 30, and 56 KDa) which have unidentified role in *S. lividans*. While tsr is best known as an antibiotic, it is also utilised as an inducer of heterologous proteins mediated through TipAL (Takano et al., 1995, Holmes et al., 1993). The tetracycline-inducible repressor/operator regulatory system from transposon Tn*10* in *E. coli* has also been effectively used as a regulatory tool for gene expression in streptomycetes (Rodríguez-García et al., 2005). Furthermore, the P_{nitA}-NitR system was developed for regulating gene expression in streptomycetes and relies on the expression method of *Rhodococcus rhodochrous* J1 nitrilase, which is highly induced by ε-caprolactam that is both highly effective and economical (Herai et al., 2004). An efficient T7 expression vector pFX583, *S. lividans* permitted the expression of T7 RNA polymerase to control overproduction of the gene that encodes a truncated version of the *S. lividans* xylanase and this system lacks any obvious expression resulting from leakage in the absence of inducer. However, various problems limit the usefulness of all these systems primarily through leaky regulation of these promoters (Lussier et al., 2010). Common to all these tools is the need for precise regulation of expression as well as optimization of codon usage (Rudolph et al., 2013). Gene expression using synthetic riboswitches have avoided these problems because they are not based on protein activities. Riboswitches are natural RNA-reliant genetic switches, sensing metabolic small-molecules and are expressed in response to the expression of the equivalent metabolic genes (Wittmann and Suess, 2012). Many natural riboswitches are placed in the UTR of an mRNA and are comprised of a binding domain (aptamer) and an expression platform controlling gene regulation (Breaker, 2012).

The gene that encodes the 19 KDa protein (TipA) was previously cloned and sequenced by Murakami et al. in 1989. Transcription of the *tipA* promoter was regulated at least 200-fold by tsr, which suggested that the *tipA* promoter could be a valuable tool for gene expression studies in *Streptomyces* research (Murakami et al.,

1989). Moreover in *S. lividans*, this promoter regulates the synthesis of its own mRNA transcript that encodes two proteins: the 31 kDa TipAL and the 17 kDa TipAS (Murakami et al., 1989, Holmes et al., 1993). In *S. lividans* the transcriptional activation of the tsr-inducible promoter, *ptipA*, is mediated by TipAL. It binds particularly tsr, a cyclic peptide formed as a secondary metabolite by different streptomycetes (Ali et al., 2002). At extremely low, sub-inhibitory levels of tsr it can regulate expression of the *tipA* gene in *S. lividans*. It can bind covalently to TipAL, thus elevating the affinity of the transcriptional activator binding to regions of dyad symmetry within *ptipA* (Chiu et al., 1996, Chiu et al., 1999).

Through placement of our target genes under the tsr controllable promoter, morphological and biochemical analyses could be carried out on our strains. A variety of growth conditions were used to ensure that the phenotypic changes related to the various levels of gene expression. Alterations in phenotype that could be revealed by changes in gene expression might suggest functions of that gene in the absence of mutations. The results obtained from these experiments would be mostly useful in the context of essential genes, since these genes in microorganisms encode many biological functions necessary for bacterial survival and can act as useful targets for antibacterial compounds (Kobayashi et al., 2003, Arigoni et al., 1998, Gerdes et al., 2003).

4.2 Aims of Chapter 4

The aims of this chapter were to combine two types of complementary analysis and are listed below:

1. To construct strains carrying *SCO5753*, *SCO5752*, *SCO5754*, and *SCO5755* under the control of the inducible *tipA* promoter.

Since the unsuccessful attempt to disrupt our target genes, it is important to construct transcriptional fusions of each these genes *SCO5753*, *SCO5752*, *SCO5754*, and *SCO5755* under the tsr inducible promoter *ptipA* carried on a *Streptomyces* expression vector.

2. To analyse the phenotype of the constructed strains on solid and in liquid media.

The phenotypic approach was used to observe the characteristics of *S. coelicolor* strains under growth in different media where the four genes of the *pgsA* operon were placed under the control of the tsr inducible promoter, *ptipA*.

4.3 Construction of *S. coelicolor* strains carrying *SCO5753, SCO5752, SCO5754,* and *SCO5755* under the control of an inducible promoter

PG is the most abundant PL in the membranes of many microorganisms such as *E. coli* and *Streptococcus.* PG in these organisms is considered to provide different cellular properties which are thought to be essential for cell development and growth (Miyazaki et al., 1985, MacGilvray et al., 2012, Kikuchi et al., 2000). On the basis of protein analysis of SCO5753, SCO5752, SCO5754 and SCO5755, it was determined that SCO5752 belongs to the radical SAM superfamily, which is known for its diversity of catalytic reactions in a broad range of biological methylations (Frey et al., 2008, Zhang et al., 2012). SCO5753 belongs to the CDP-alcohol phosphatidyltransferase family which catalyses essential reactions for PL biosynthesis in prokaryotes (Sciara et al., 2014, Nogly et al., 2014). SCO5754 is similar to competence-damaged proteins (CinA); this protein is encoded by the first gene in the competence-induced operon and is believed to be essential at some point in transformation by DNA (Mortier-Barriere et al., 1998, Martin et al., 1995). It is proposed that there may be a polar effect due to the appearance of these genes in an operon (Paget et al., 1999); since the function of *SCO5752, SCO5753* and *SCO5754* genes are unknown, based on the above analysis of their proteins, it may be that at least one of them is essential. In addition, following our experiments carried out in chapter 3, we were not able to obtain double crossovers within the genome of *S. coelicolor* whilst attempting to disrupt these genes. Furthermore, in order to study the gene *SCO5753* (*pgsA*), the characterization of downstream genes such as *SCO5755* was also investigated as the protein encoded by this gene is speculated to regulate *SCO5753*. Also, it was revealed that the ClgR is involved in *Streptomyces* development, since *clgR* overexpression induces a delay of differentiation in *S. lividans* (Bellier and Mazodier, 2004). Analysis of SCO5755 shows that it is similar to the Helix-turn-helix domain (HTH) which is involved in binding to DNA and

further genetic evidence indicated that this protein is a regulator for gene expression. For instance, the HTH motif is found within the GntR family of transcription factors and is distributed in all bacteria where they regulate many different biological properties. This family of transcription factors are essential in changing gene expression related to the surrounding environment (Hoskisson and Rigali, 2009).

4.4 Sub cloning *SCO5752, SCO5753, SCO5754,* and *SCO5755* onto pIJ925

The general cloning strategy of *SCO5752*, *SCO5753*, *SCO5754*, and *SCO5755* into shuttle or expression vectors that was used is shown in Figures 4.1 and 4.7. At the start of this work we sub cloned our target genes as a large DNA fragment of size around 4.5 kb. pLR101 (Rajagopal, unpublished data), was used as a source for *pgsA* along with the genes *SCO5752*, *SCO5754* and *SCO5755*. This plasmid was first digested by HindIII and XbaI. The 4.5 kb fragment obtained was ligated with the cloning vector pIJ925 at the HindIII and XbaI sites. The resulting plasmid pMA101 was confirmed following plasmid isolation from putative clones followed by digestion with appropriate restriction enzymes (Figure 4.2).

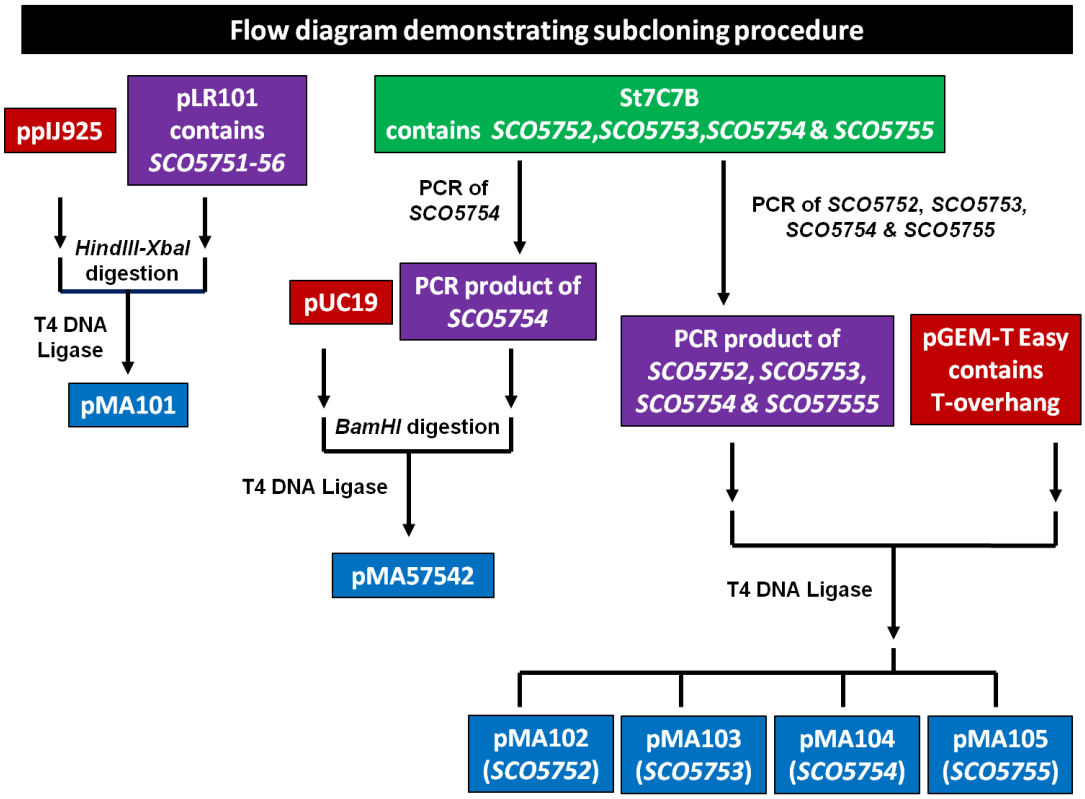

Figure 4-1: An overview of the sub cloning strategy used for transfer of the *pgsA* operon genes. Two strategies were used for sub cloning: the first was classic sub-cloning using the restriction enzyme, pLR102, and a plasmid vector containing *SCO5752, SCO5753, SCO5754* & *SCO5755* genes. This strategy was used for rapid sub-cloning in order to clone these genes into the vector as a single fragment under *tipA* control. However this attempt was not successful. Therefore we moved to the second strategy which was PCR sub-cloning using the St7C7B cosmids containing *SCO5752*, *SCO5753*, *SCO5754* and *SCO5755* genes. We amplified each gene individually for easy PCR sub-cloning. pIJ925, pUC19&pGEM-T Easy were used as cloning vectors.

4.5 Attempted cloning of the *pgsA* operon into pPM927

Once the 4.5 kb fragment was cloned into the cloning vector pIJ925 giving pMA101, the next step in the sub cloning process was to transfer it into the vector pPM927 (Smokvina et al., 1990). pPM927 was developed to integrate cloned DNA at a single location in the DNA of *S. lividans* 66 (Smokvina et al., 1990). This vector carries an *E.coli* replicon. In addition, this vector also carries a 3.5 Kb region of the *Streptomyces* integrative plasmid pSAM2 consisting of *xis, int* genes and a site for the integration of the plasmid into the streptomycete chromosome. The origin of transfer from the IncP wide host range plasmid RK2 permits the mobilisation of this the vector from *E. coil* to *S. lividans* by intergeneric conjugation. pPM927 also contains the tsr inducible *tipA* promoter that allows genes cloned downstream of this promoter to be subject to regulation by this promoter. Finally the plasmid contains the tsr and streptomycin/spectinomycin resistance gene for selection in *E. coli* and *Streptomyces* respectively.

pMA101 (Figure 4.2A), was digested by BamHI and Bg1II and the 4.5 kb fragment obtained was ligated with the cloning vector pPM927 at the BamHI site (Figure 4.3A). The presence of the insert was analysed following plasmid DNA isolation, SphI restriction digestion and agarose gel electrophoresis. A single digestion with SphI was used to determine the presence of the insert in the right orientation. Unfortunately we were unable to clone the 4.5kb fragment into pPM927 even after several attempts (Figure 4.3B and C), after which we concluded that the size of the insert was too large to clone. Therefore the cloning experiment was carried out using alternative strategies and cloning vectors.

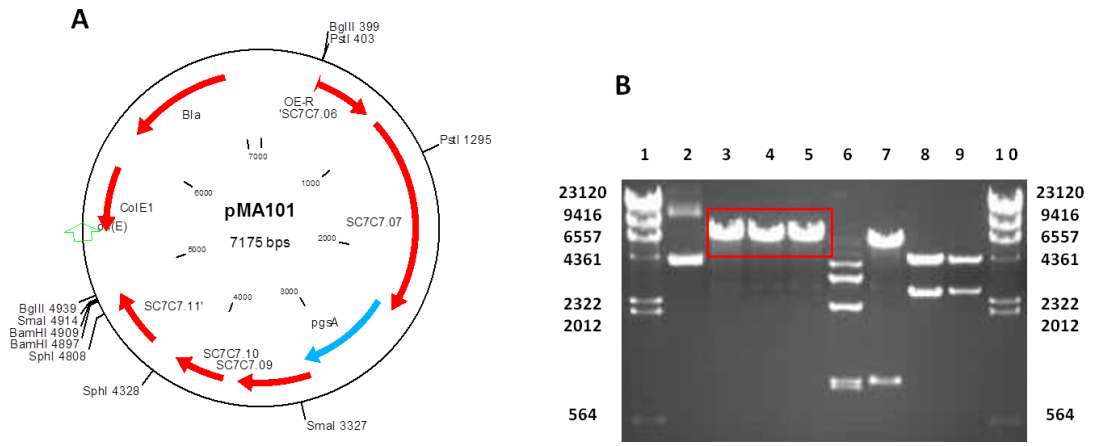

C

pMA101 (7175bps) circular		
Enzyme	**Expected fragment No.**	**Expected fragments size in (bps)**
EcoRI	1	7175
Hind III	1	7175
XbaI	1	7175
SacI	5	3267,2150,897,837,24
PstI	2	6283,892
EcoRI & Hind III	2	4519,2656
XbaI & Hind III	2	4480,2695

Figure 4-2: Confirmation of pMA101.

(A) pMA101 map was constructed by ligating a 4.5kb fragment obtained from pLR101 using the restriction enzymes HindIII and XbaI. The clone contains a functional copy of *SCO5752*, *SCO5753*, *SCO5754*, and *SCO5755* with native promoter. (B) Confirmation of agarose gel electrophoresis image of pMA101digested with: Lane 1: λ HindIII Marker, lane 2: uncut pMA101, lane 3: EcoRI, lane 4: HindIII, lane 5: XbaI, lane 6: SacI, lane 7: PstI, lane 8: HindIII & EcoRI: lane 9: HindIII & XbaI, lane 10: λ HindIII Marker. (C) The different enzymes used to confirm the strain pMA101 and the expected fragment sizes.

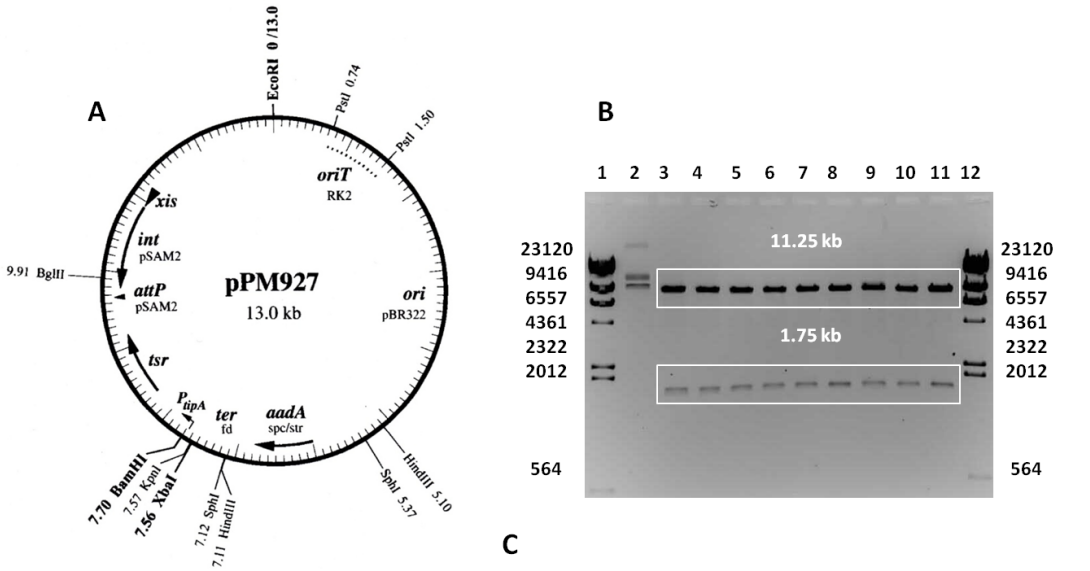

C

Fragment size expected by *SphI* cut		
Sense orientation	**Antisense orientation**	**No insert**
1.75 kb 0.480 kb 4.50 kb 10.67 kb	1.75 kb 0.681kb 0.480 kb 14.49 kb	1.75 kb 11.25 kb

Figure 4-3: Confirmation the absence of 4.5 kb fragment in pPM927.

(A) Map of pPM927 [reproduced from (Kieser et al., 2000)]. (B) The agarose gel electrophoresis image showing the expected size of restriction digest SphI; lanes 1&12: λ HindIII marker; lane 2: Undigested plasmid pPM927; lanes 3-11: Putative clones. (B) Fragments produced by SphI, indicates the expected size of band with three possibilities of cloning result.

4.6 Synthesis of *SCO5752, SCO5753, SCO5754,* and *SCO5755* by PCR prior to sub cloning into pUC19

As we were unable to place the full operon under the control of *ptipA* in pPM927, we reasoned that at least one of these genes may have been toxic if expressed in *E. coli.* As a result, we set out to apply a new strategy for cloning these genes. To do this, the target genes were cloned individually (Figure 4.4) into the BamHI site of the multiple cloning site (MCS) of pUC19 (Yanisch-Perron et al., 1985). The MCS is designed so that introduction of an insert into the MCS disrupts the *lacZα* gene, the open reading frame (ORF) coding for β-galactosidase. This allowed the identification of recombinant colonies by blue-white colony selection. *SCO5752*, *SCO5753*, *SCO5754,* and *SCO5755* were synthesised by PCR using MyTaq polymerase, as mentioned in chapter 2. Primers were designed to integrate the restriction site BamHI into the PCR product for cloning purposes (Figure 4.4). The genes were amplified effectively at a size corresponding with the StrepDB database. Parental cosmid St7C7 (Redenbach et al., 1996, Bentley et al., 2002) was used as template for PCR amplification of our genes with no native promoters (Figure 4.5). The PCR product was purified using columns according to Chapter 2 and eluted with sterile SDW. However, the only gene that could be cloned into pUC19, *SCO5754*, resulting in the plasmid pMA57542. This plasmid was confirmed as by restriction digestion and gel electrophoresis (Figure 4.6). However it proved impossible to sub clone this gene into a *Streptomyces* shuttle vector (data not shown).

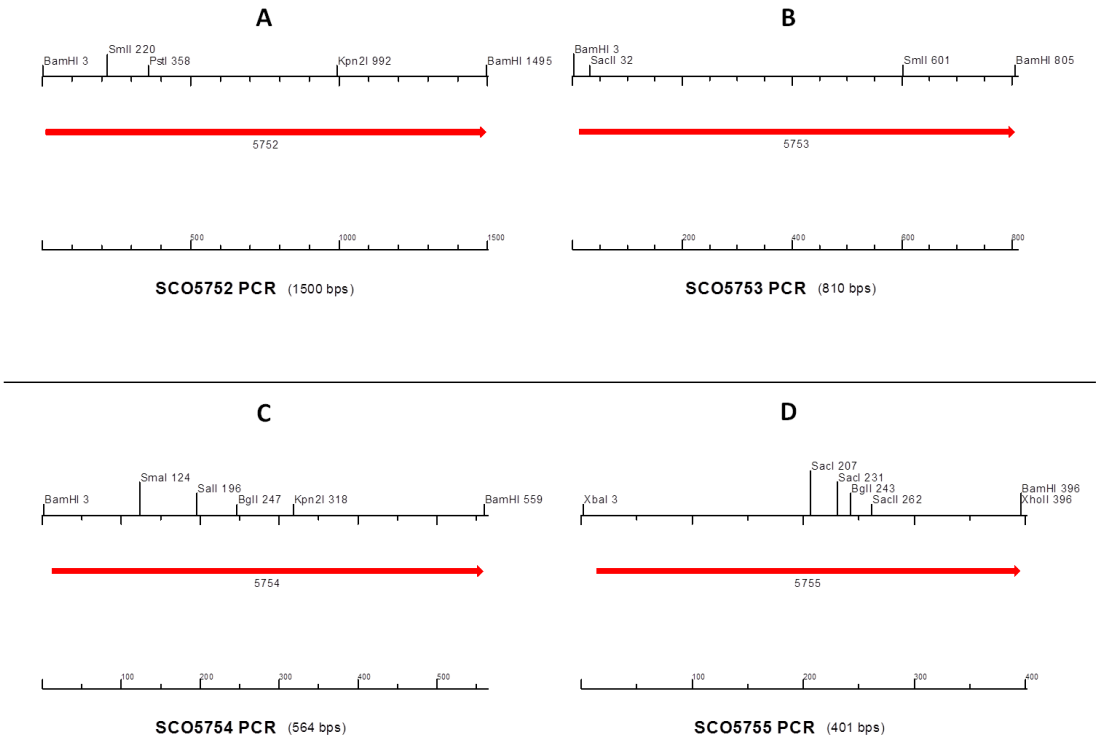

Figure 4-4: PCR amplicons from the for *pgsA* genes for sub cloning into pUC19.

(A) (B) (C) (D): *SCO5752*, *SCO5753*, *SCO5754*, *SCO5755* (respectively) maps indicating the BamHI site in the PCR product. The sequences of the primers are shown in Table 2.12, Chapter 2.

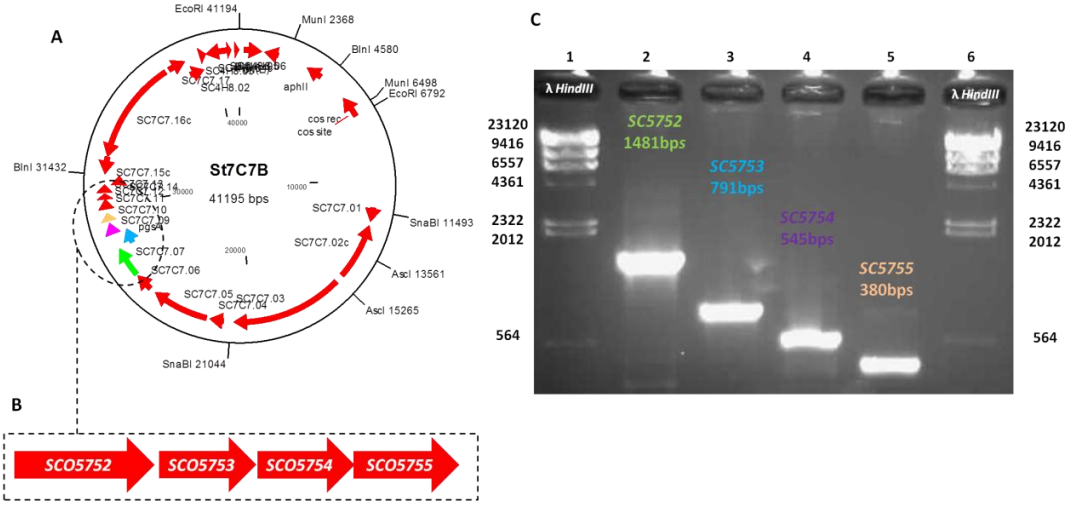

Figure 4-5: Synthesis of *pgsA* operon genes by PCR.

(A) Parental cosmid used for synthesising the genes. (B) The map of genes used was synthesised from St7C7B. (C) Agarose gel electrophoresis of genes amplification by MyTaq Polymerase.

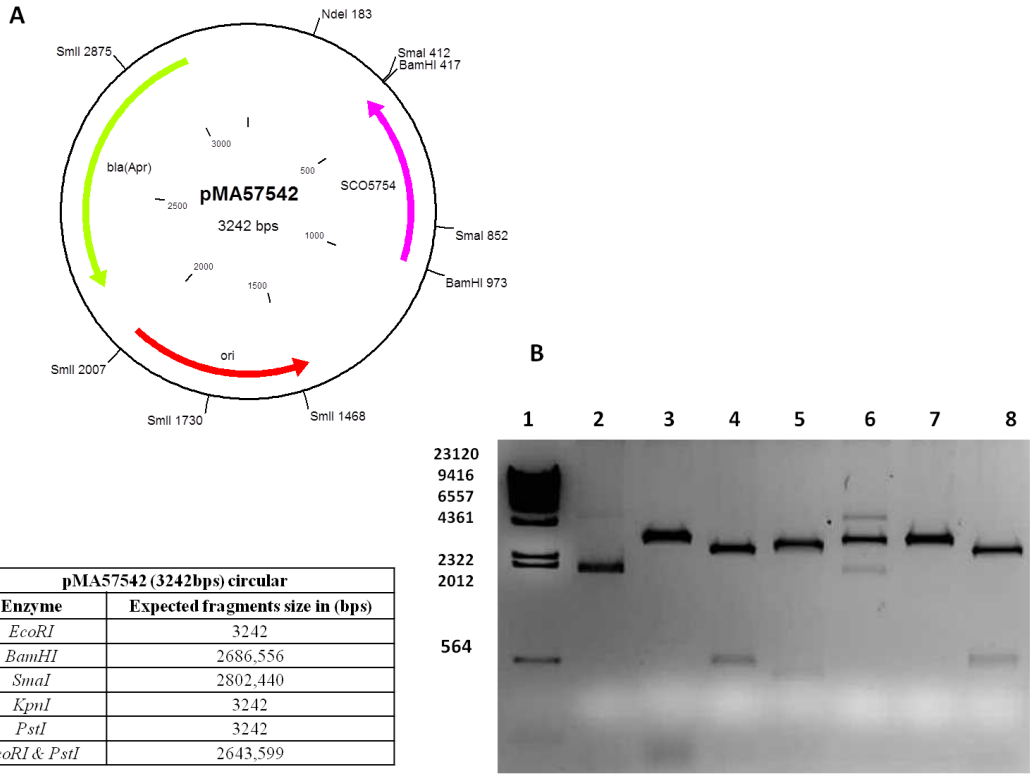

C

pMA57542 (3242bps) circular	
Enzyme	**Expected fragments size in (bps)**
EcoRI	3242
BamHI	2686,556
SmaI	2802,440
KpnI	3242
PstI	3242
EcoRI & PstI	2643,599

Figure 4-6: Confirmation of pMA57542.

(A) pMA57542 was constructed by ligating a 545 bps BamHI fragment obtained by PCR into pUC19. (B) Agarose gel electrophoresis demonstrated construction of pMA57542 after restriction digestion; lane 1: λ HindIII Marker, lane 2: Uncut pMA57542, lane 3: EcoRI, lane 4: BamHI, Lane 5: SmaI, lane 6: KpnI, Lane 7: PstI, lane 8: EcoRI & PstI. (C) Different enzymes that were used to confirm the strain pMA57542 and their expected fragment sizes.

4.7 Direct cloning of *SCO5752, SCO5753, SCO5754* and *SCO5755* PCR products into pPM927

As we were unable to successfully sub clone all our target genes, we decided to develop a different sub cloning strategy. Our first strategy was to clone the full operon in pPM927 (section 4.3A) and subsequently delete each gene in the operon in turn in order to determine which gene was essential for *S. coelicolor* growth. However since we were unable to clone the *pgsA* operon into pPM927 from pMA101, we turned to an alternative approach. This strategy was based on the amplification of more than one gene from the operon (Figure 4.8). Combinations of each gene were amplified by PCR using My Taq polymerase as described in Chapter 2. Target genes were amplified effectively at sizes that corresponded to the StrepDB database. Parental cosmid St7C7B was used as template for the PCR amplification of our genes with no native promoters. The PCR products of the new strategies (Figure 4.9) were cloned directly into pPM927. The only resulting strain obtained from this cloning strategy was pMA53541 which was confirmed via restriction digestion (Figure 4.10). The 'sense' direction of new constructed strain, pPM53541 was confirmed by sequencing (data not shown). This plasmid contained both *SCO5753* and *SCO5754* under the control of the *tipA* promoter.

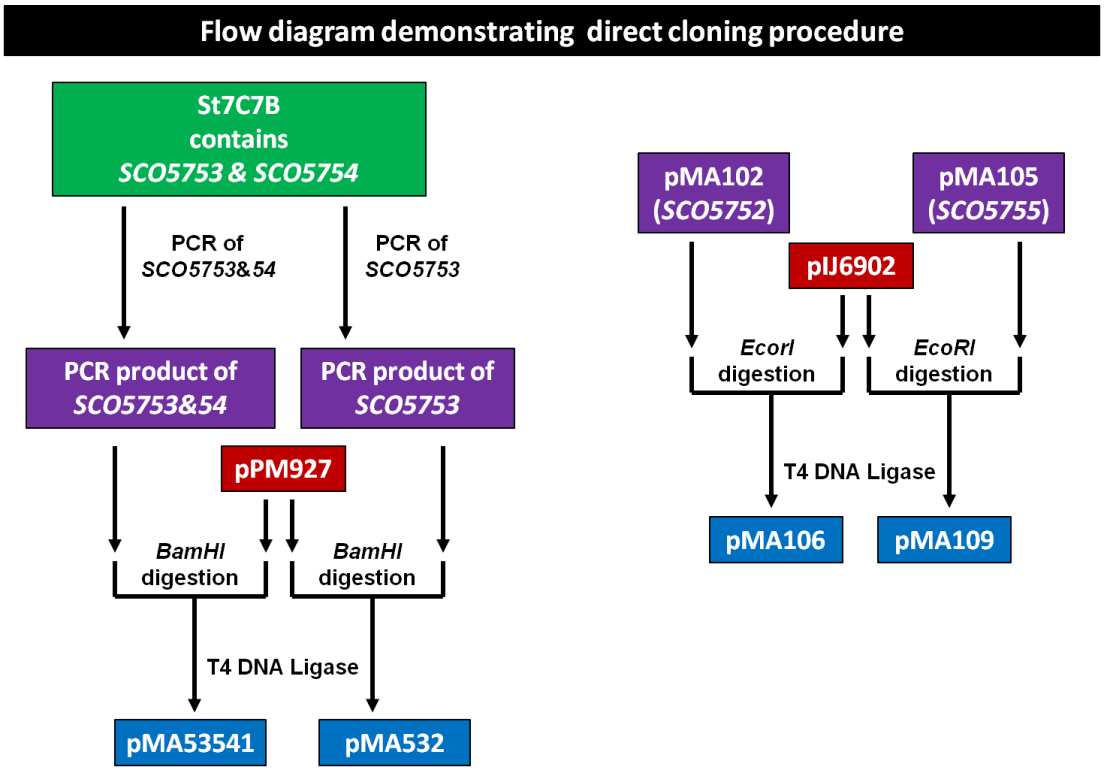

Figure 4-7: An overview of directional cloning strategy into vectors that placed the *pgsA* operon genes under the control of *ptipA*.

On the left of the diagram we used St7C7B cosmid again to clone *SCO5753* with *SCO5754* (together as different strategy) and *SCO5753* by PCR into a destination vector (pPM927). On the right of the diagram, we used pMA102 and pMA105 as parent vectors from previous sub cloning experiments to clone *SCO5752* and *SCO5755* by restriction enzymes into expression vector pIJ6902.

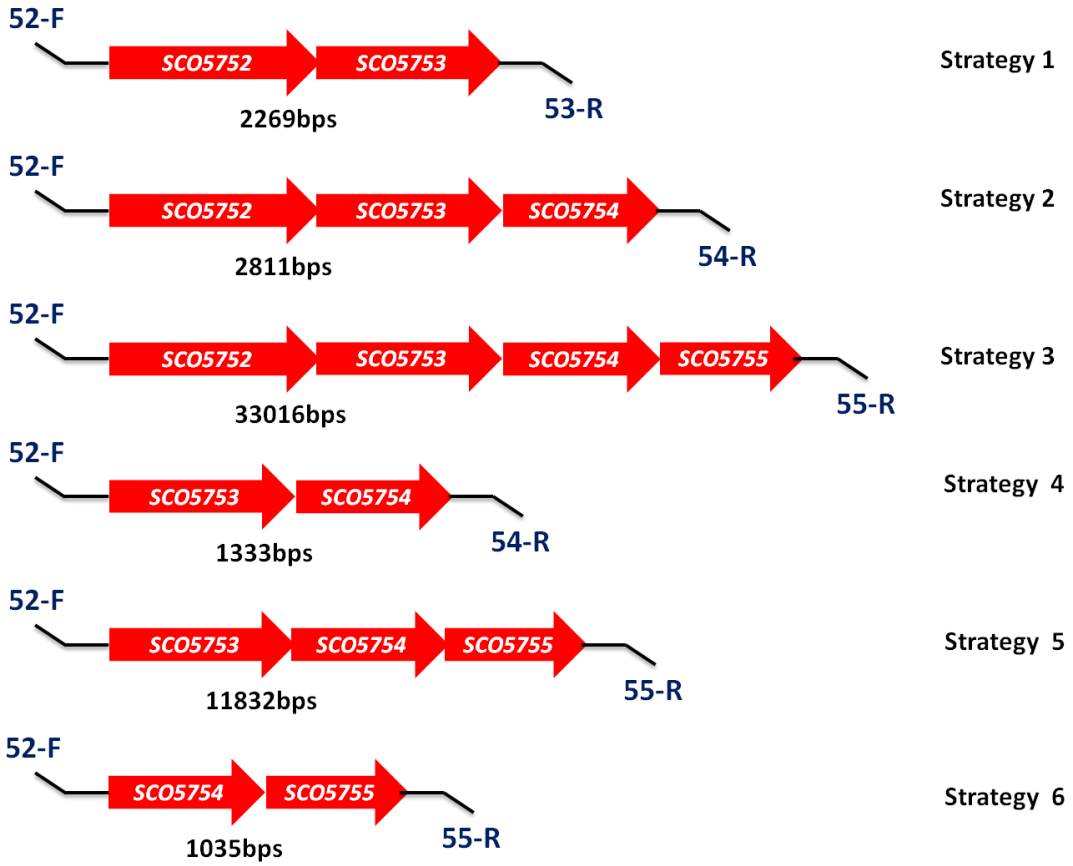

Figure 4-8: Outline map of sub cloning strategies.

There are 6 different strategies which were used; F & R letters indicate the forward and reverse primer containing a BamHI site.

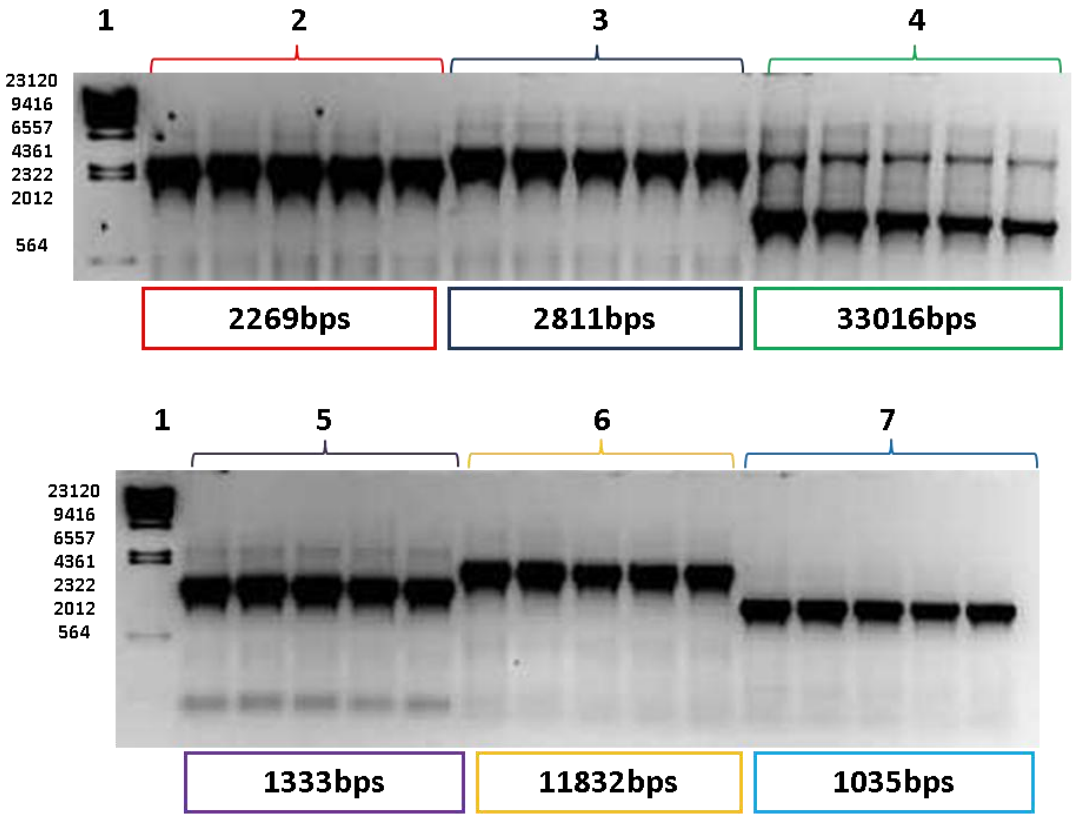

Figure 4-9: Amplification *pgsA* operon genes by MyTaq polymerase.

St7C7B cosmid used was used as template for synthesising the target genes. Lane 1: λ HindIII Marker block 2: strategy 1, block 3: strategy 2, block 7: strategy 5, block 4: strategy 3, block 5: λ HindIII Marker, block 6: strategy 4, block 7: strategy 5.

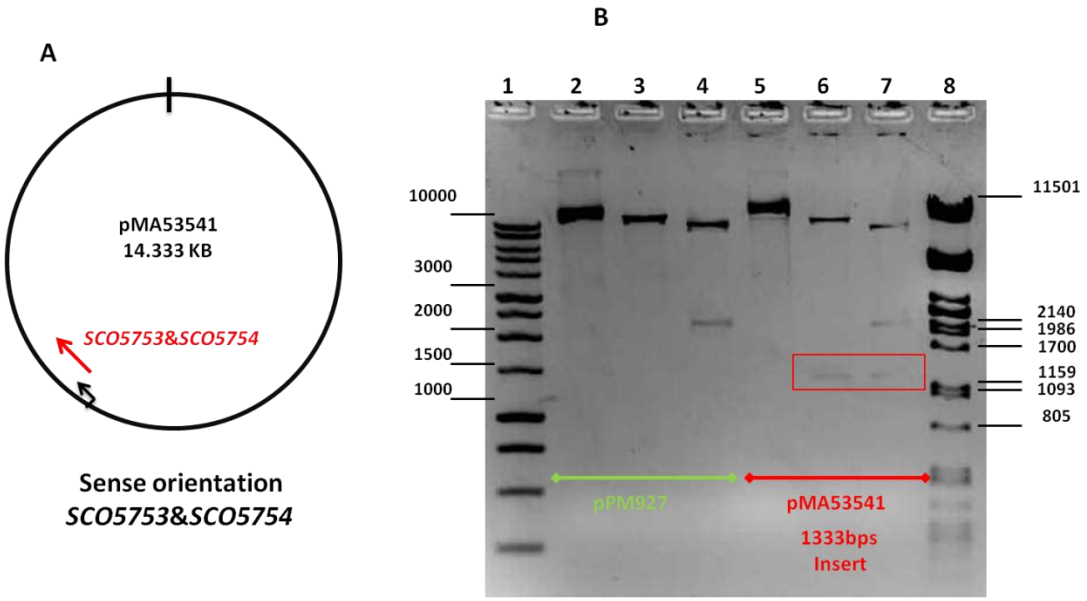

Figure 4-10: Confirmation of pMA53541.

(A) pMA53541 constructed by ligating 1333bps (strategy 4, Figure. 4.8), the BamHI fragment was obtained by PCR from cosmid St7C7B using MyTaq polymerase. (B) Agarose gel electrophoresis of new recombinant plasmid pPM53541. Lane 1: 1KB marker (Promega), lane 2 – uncut DNA, lane 3:BamHI digest, lane 4: BglII & BamHI digest, lane 5: uncut, lane 6: BamHI digest, lane 4: BglII & BamHI digest, lane 8: Lambda PstI marker.

4.8 Direct cloning of *SCO5753* into pPM927

Although cloning of *SCO5753* along with *SCO5754* was achieved via the construction of pMA53541, we wished to obtain *pgsA* (*SCO5753*) by itself inside pPM927. Thus we tried to place the *SCO5753* gene alone under the control of tsr inducible promoter in pPM927. A protocol was followed in which we synthesised the *pgsA* gene by PCR from the parental cosmid St7C7B (Figure 4.5) and cloned it directly into pPM927; unfortunately we were only able to locate a single clone containing the insert. The resulting recombinant plasmid was pMA532 that contained *SCO5753* in the 'antisense' direction with respect to the *tipA* promoter (Figure 4.11). This was confirmed by sequencing (data not shown).

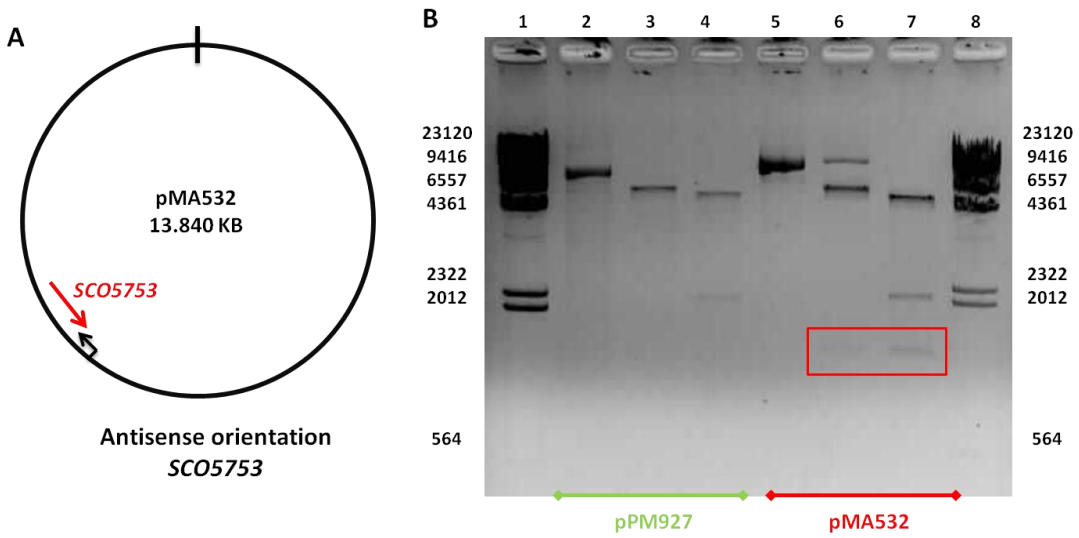

Figure 4-11: Confirmation of pMA532.

(A) pMA532 was constructed by ligating the 791bps BamHI fragment obtained by PCR from parental cosmid St7C7B using my Taq polymerase. (B) Agarose gel electrophoresis of new recombinant plasmid pPM532: Lane 1: λ HindIII Marker, Lane 2: Uncut DNA Lane 3: pPM927 cut with BamHI, Lane 4: pPM927 cut with BamHI &BglII, Lane 5: Un Lane 6: pMA532 cut with BamHI, Lane7: pMA532 cut with BamHI and BglII, Lane 8: λ HindIII marker.

4.9 A new strategy of Sub cloning *SCO5752, SCO5753, SCO5754,* and *SCO5755* PCR product into pGEM-T Easy vector provided by (Promega)

As we were unable to clone *SCO5752* and *SCO5755* in previous experiments, we decided to use another strategy of cloning. Cloning of target genes into another vector was carried out. pGEM-T Easy vector (Promega) was used for cloning PCR products; the vector has several features which increase the likelihood of cloning of PCR products. One of these features is that the ligation of PCR products into the plasmid is improved by avoiding the recircularisation of the vector as the vector provides a compatible overhang for PCR products that are generated by thermostable polymerases. A similar protocol was followed (Section: 4.5) to synthesise *SCO5752-55* from the parental cosmid St7C7B (Figure 4.6) before being cloned into pGEM-T Easy. The resulting recombinant plasmids were pMA102 (*SCO5752*), pMA103 (*SCO5753*), pMA104 (*SCO5754*) and pMA105 (*SCO5755*) and were confirmed by restriction digestion and sequencing (Figure 4.12) and the disruption of the β-galactosidase gene in the plasmid.

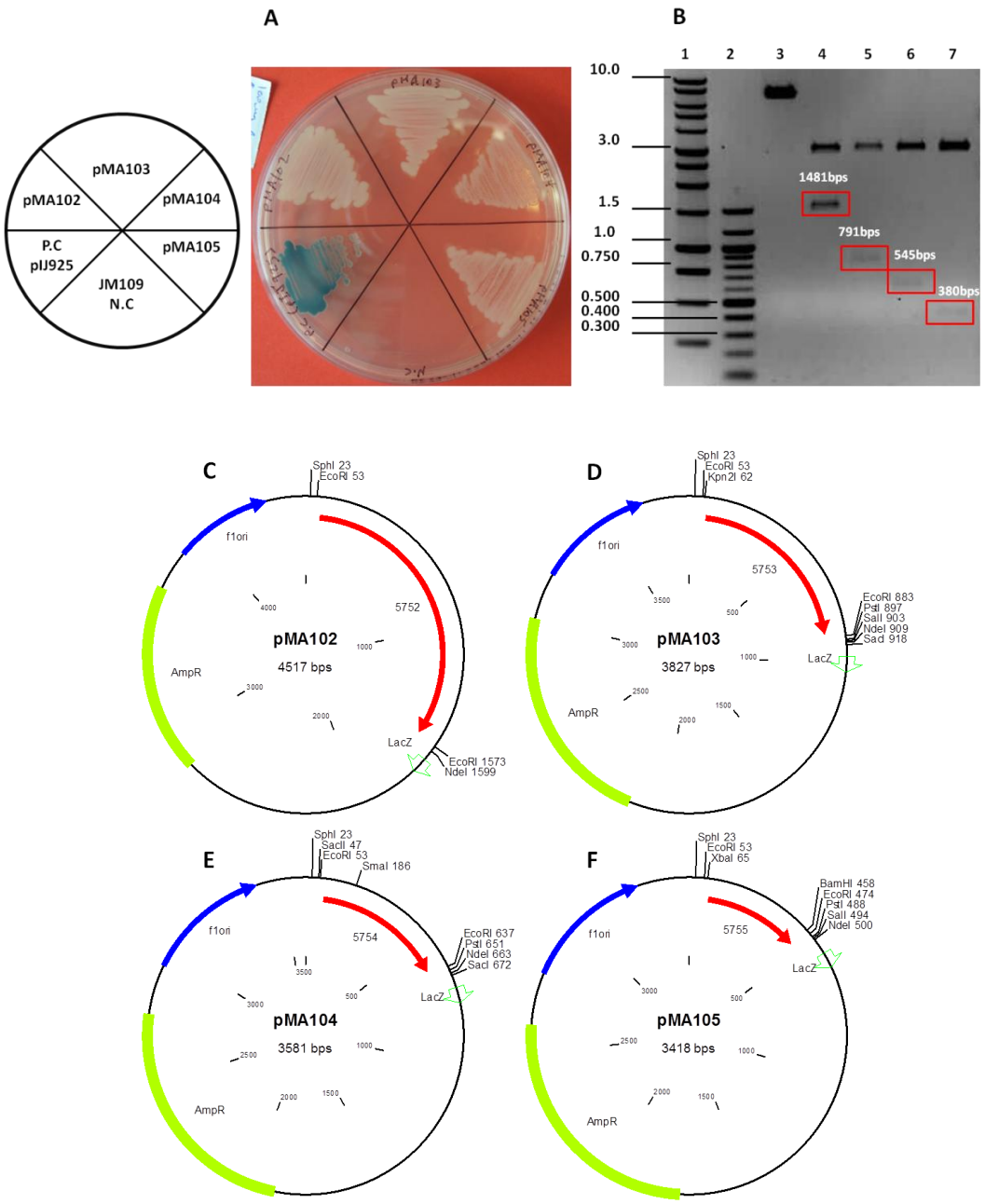

Figure 4-12: Confirmation of pMA102, pMA103, pMA104 and pMA105 sub clones.

(A) Growth of constructed strains with negative control (JM109) and positive control (pIJ925) on LB agar medium containing these selection 100µg/ml am^r, 80µg/ml Xgal, 0.5mM IPTG and incubated overnight at 37°C. (B) Agarose gel electrophoresis of recombinant plasmid digested with EcoRI: Lane 1: 1kb DNA & lane 2: 100 bps DNA marker (Biolab), Lane 3: undigested pIJ6902, lane 4: pMA102 (*SCO5752*), 1481bps, lane 5: pPM103 (*SCO5753*), 791bps, lane 6: pPM104 (*SCO5754*), 545bps, lane 7: pPM105 (*SCO5755*), 380bps. pMA102, pMA103, pMA104 and pMA105 maps were obtained by clone manager (C, D, E and F**.**

4.10 Cloning of *SCO5752* and *SCO5755* into pIJ6902

Eventually, our target genes were cloned into the pGEM-T Easy cloning vector. Subsequent cloning involved using pIJ6902 (Huang et al., 2005) as a final destination vector. pIJ6902 is integrating *ptipA* expression vector. It contains some genetic features like the important transcription terminator of phage fd, *ptipA*, tsr resistance gene and apramycin-resistance gene. This plasmid also contains the replication origin from pUC18, transfer origin from plasmid RK2 and the integrase gene and attachment location from the temperate phage ϕC31 respectively. The plasmids constructed in Section 4.9 (pMA102 (*SCO5752*), pMA103 (*SCO5753*), pMA104 (*SCO5754*) and pMA105 (*SCO5755*) were to act as the precursor plasmids for the next cloning step. Each plasmid was digested with EcoRI to yield ends for cloning into pIJ6902. However, only two recombinant plasmids were achieved from this cloning experiment resulting in pMA106 (*SCO5752* in the 'antisense' direction) and pMA109 (*SCO5755* in the 'sense' direction). These plasmids were confirmed by restriction digestion (Figure 4.13 & 4.14) and sequencing (data not shown).

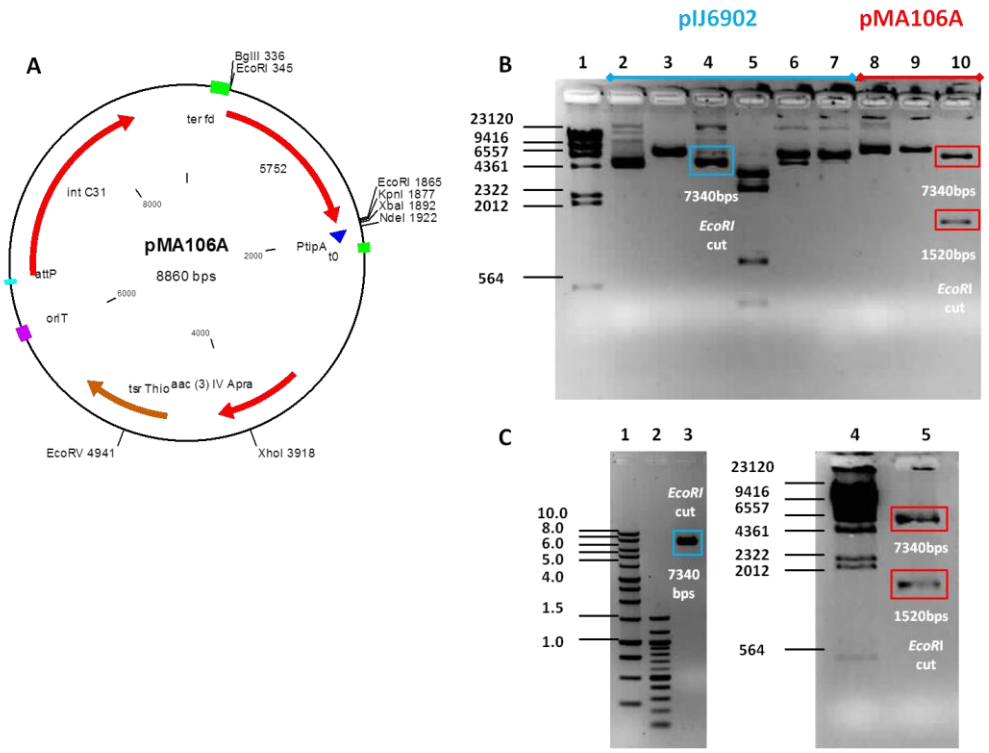

Figure 4-13: Confirmation of pMA106A.

(A) pMA106A was constructed by ligating 1481bps obtained from pMA102 by using these restriction enzyme EcoRI, the clone contains a functional copy of *SCO5752* under the inducible promoter *tipA*. (B) Confirmation agarose gel electrophoresis of pMA106A: Lane 1: λ HindIII marker, lane 2: Undigested DNA of pIJ6902, lane 3: BglII (7340bps), lane 4: EcoRI (7340bps), lane 5: PstI (3566, 2572, 802,400bps), lane 6: NcoI (7340bps), lane 7: XbaI (7340bps), lane 8: Undigested of pMA106A, lane 9: BglII (8860), lane 10: EcoRI (7340, 1520bps). (C) Another agarose gel electrophoresis **c**onfirmed digestion of pMA106A by EcoRI: Lane 1: 1kb DNA & lane 2: 100 bps DNA marker (Biolab), lane 3: pIJ6902 cut with EcoRI (7340bps), lane 4: λ HindIII marker, lane 5: pMA106A cut with EcorI (7340, 1520bps).

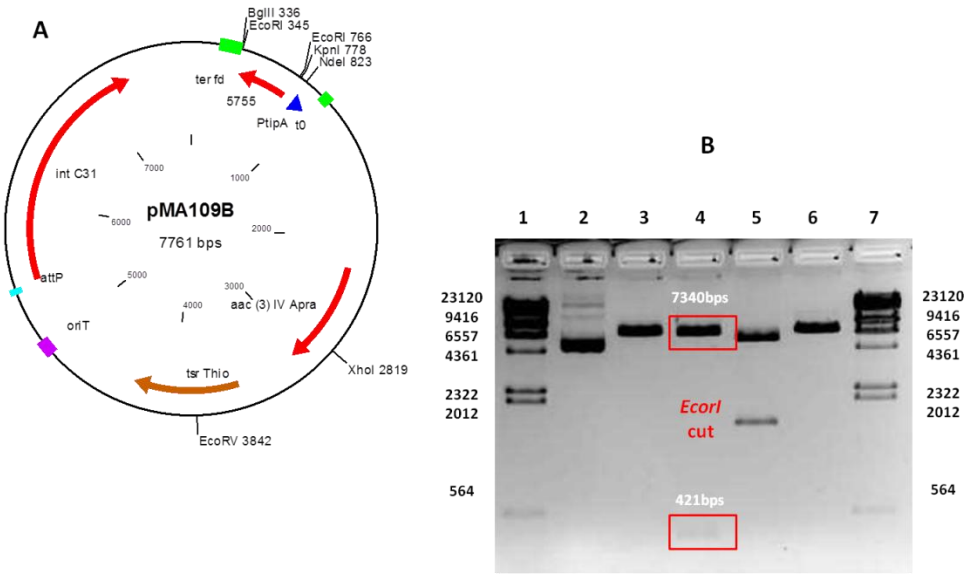

Figure 4-14: Confirmation of pMA109B.

(A) pMA109B was constructed by ligating 380bps was obtained from pMA105 by using these restriction enzyme EcoRI; the clone contains a functional copy of SCO5755 under the inducible promoter tipA of pIJ6902. (B) Confirmation agarose gel electrophoresis of pMA109B: Lane 1: λ HindIII marker, lane 2: Undigested DNA of pMA109B, lane 3: BglII (7761bps), lane 4: EcoRI (7340bps, 421bps), lane 5: NcoI (5786, 1975bps), lane 6: XbaI (7762, 39bps), lane 7: λ HindIII marker.

4.11 Final plasmids constructed for inducible expression of the *pgsA* operon in *S. coelicolor*

In conclusion of the previous sections above, the plasmids pMA53541 (*SCO5753* and *SCO5754*), pMA532 (*SCO5753*, antisense orientation), pMA106A (*SCO5752*) and pMA109B (*SCO5755*) were successfully constructed under the control of the inducible promoter *ptipA*.

4.12 Introduction of pMA53541, pMA532, pMA106A and pMA106B to *S. coelicolor* by conjugation

In order to analyse the phenotypic characteristics of regulated expression of the *pgsA* operon genes, introduction of these genes into *S .coelicolor* was conducted. Through conjugation from *E. coli* strain ET12567 containing the mobilising plasmid pUZ8002, pMA53541 and pMA532 were transferred into *S. coelicolor* M145 where they integrated into the attachment site of pPM927. The conjugation was performed in the presence of tsr (12.5µg/ml); since we used pPM927 it was useful to ensure integration of these plasmids through use of this powerful selectable marker. The resulting strains were MA53541 and MA532; containing functional copies of *SCO5753* and *SCO5754* and *SCO5753* (antisense) respectively. This plasmid, pMA53541, was introduced into *S. coelicolor* M145 by conjugation generating MA53541 and, despite the second copy of SCO5753 being present in this strain it was still impossible to disrupt *SCO5753* with Tn*5062* following introduction of the transposed cosmid SC7C.B07 into MA53541 (data not shown). Our failure to generate a mutation in this gene despite a second, complementing copy of *SCO5753* suggests that as well as its essentiality for *S. coelicolor* growth and development it is likely that regulation of SCO5753 expression is a complex process.

A similar method was used to construct a control strain by conjugating pPM927 into *S .coelicolor* via ET12567/pUZ8002, the result strain was named MA927. This strain would act as a negative control in subsequent experiments. pMA106A and pMA109B were transferred into *S. coelicolor* where they integrated into the ϕC31*attB* site attachment site through the presence of ϕC31*attP* on pIJ6902. The conjugation was also performed in the presence of tsr. The resulting strains were

MA52A and MA55B; containing copies of *SCO5752* and *SCO5755* respectively; the former being in the anti-sense orientation and the latter in the sense orientation. A similar method was used to construct an empty vector by conjugating pIJ6902 into *S .coelicolor* via ET12567/pUZ8002, the resulting strain was termed MA6902.

4.13 Phenotypic analysis of new constructed strains MA53541, MA532, MA52A and MA55B

Phenotypic analysis of growth of these strains was carried out on a selection of standard media with the presence and absence of the appropriate antibiotic marker. The reason to select a wide range of standard media was to highlight any differences in morphological or physiological differentiation during growth. SFM medium was used to analyse any changes in morphology because on this agar, *S. coelicolor* displays good morphological differentiation. R5 medium was used to reveal any changes secondary metabolism because on this agar, *S. coelicolor* undergoes high levels of antibiotic production. It was anticipated that the constructed strains might demonstrate either lack production or early overproduction of antibiotics. Minimal medium (MM) with glucose was also used as this medium promotes morphological and physiological differentiation in *S. coelicolor*. Minimal media with mannitol (3MA) which is a more suitable carbon source for morphological development was also used (Kieser et al., 2000).

S. coelicolor does not sporulate in rich liquid media, but it does form secondary metabolites, usually in the stationary phase of growth (Manteca et al., 2010). Undecylprodigiosin and actinorhodin are the most distinctly pigmented substances produced by *S. coelicolor*. Undecylprodigiosin (known as red) is composed of a combination of three prodigionines produced by *S. coelicolor*. This is a nonpolar tripyrrole substance which is chemically the same as the antibiotic prodigiosin made by *Serratia marcescens* and is produced by the same convergent biosynthetic pathway. Red formation typically takes place in transition and stationary phases in growth liquid cultures and coincides with the start of morphological development in surface grown cultures (White and Bibb, 1997). Actinorhodin is a quinone antibiotic which is also as an indicator of pH; below 8.5 it is blue, but at higher pH is often red

to purple. The associated substance γ-actinorhodin is produced into the medium (actinorhodin in a lactone form) (Bystrykh et al., 1996, Kieser et al., 2000). All actinorhodin forms are secreted in stationary phase and are subject to nutrient limited growth (nitrogen/phosphate) and are subject to glucose repression (Kim et al., 2001, Melzoch et al., 1997). *S. coelicolor* was also grown in liquid culture because we wished to remove any variability from morphological differentiation in solid media which does not take place in liquid media. The medium YEME was chosen to promote mycelium growth and reproducible antibiotic production.

4.14 Phenotypes screening of MA52A and MA55B on agar media

After growth on sporulation medium, SFM, in the presence of 25µg/ml apramycin, by day 4 phenotypic differences between MA52A and MA55B could be distinguished. MA55B produced white growth while MA52A formed gray growth which was similar to MA6902. By day 7 the phenotypes clearly showed differences in growth; the appearance of MA55B was white and the phenotype of MA52A was a darker gray than MA6902 (Figure 4.15A). In the presence of tsr that should induce expression of *SCO5755* and *SCO5752*, there were no great differences in response to the inducer. Growth of MA55B was retarded in terms of development and appearded noticeably whiter that the other strains after four days incubation. This suggests that the induced activity of *ptipA* was sufficient to induce expression of *SCO5755* and mediate an inhibitory effect on growth. Interestingly increased concentrations of tsr appeared to generate a dose dependent response to this antibiotic in terms of growth retardation. This gene encodes a known regulator and it may well be that the regulatory targets of SCO5755 are genes responsible for development; as such it is plausible that overexpression of this protein would inhibit expression of such developmental genes. It is important to remember that, even in the absence of inducer, *ptipA* still represents a strong promoter in streptomycetes and highlights the need for better gene induction systems in streptomycetes. MA52A displayed a similar phenotype to MA6902 and, in comparison between different concentrations of tsr, growth of MA52A gave a slightly less gray appearance. As *SCO5752* is expressed in the antisense orientation in M52A, an increased concentration of tsr are likely to decrease sense SCO5752 transcripts available for translation and, as such, is

equivalent to reducing expression of this gene. M145 was grown as a negative control and was inhibited at 12.5-25 μg/ml tsr (Murakami et al., 1989) (Figure 4.15B).

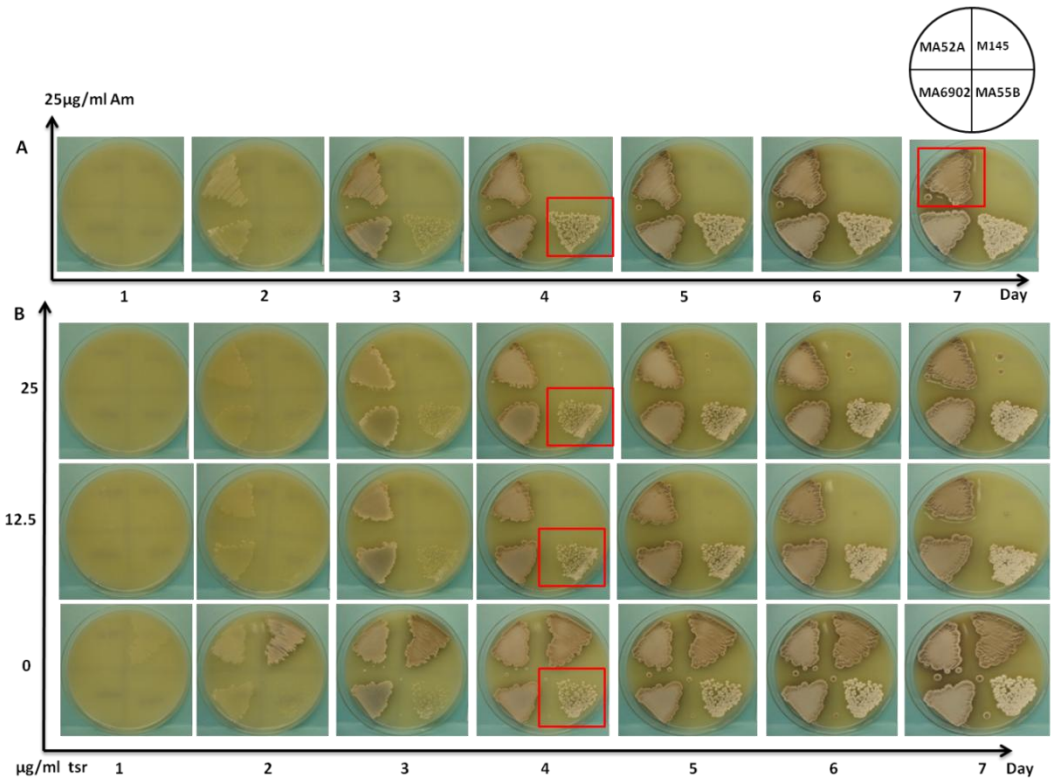

Figure 4-15: Development of MA52A (*SCO5752)*, MA55B (*SCO5755*) on sporulation medium SFM.

(A) Growth and development after 7 days in the presence of apramycin and no tsr. (B) The effect of different tsr concentrations on morphological development by MA52A, MA55B, MA6902 (empty vector) and M145 over 7 days. Both experiments were performed at n=1.

The Growth of MA52A, MA55B and MA6902 on 3MA was also investigated. In the presence of 25μg/ml apramycin, the phenotypic appearance of these strains was different. The pigmentation of MA52A on day 7 was darker red compared to the control strain, MA6902 and suggests that the former strain synthesised higher levels of undecylprodigiosin. The phenotypic appearance of MA55B displayed slower growth (Figure 4.16A) and produced noticeably less red pigmentation. In the presence of tsr, there were obvious changes in phenotypic appearance with increasing concentrations of the inducer to *ptipA*. Aerial hyphae production was impacted by tsr and the erection of aerial hyphae was slowed with increasing tsr concentration from 0 to 25 μg/ml. This strain exhibited reduced production of both undecylprodigiosin and actinorhodin in comparison to the other strains after 6-7 days incubation. MA52A and MA6902 displayed a shift in production from undecylprodigiosin to actinorhodin in response to increasing tsr concentration (Figure 4.16B).

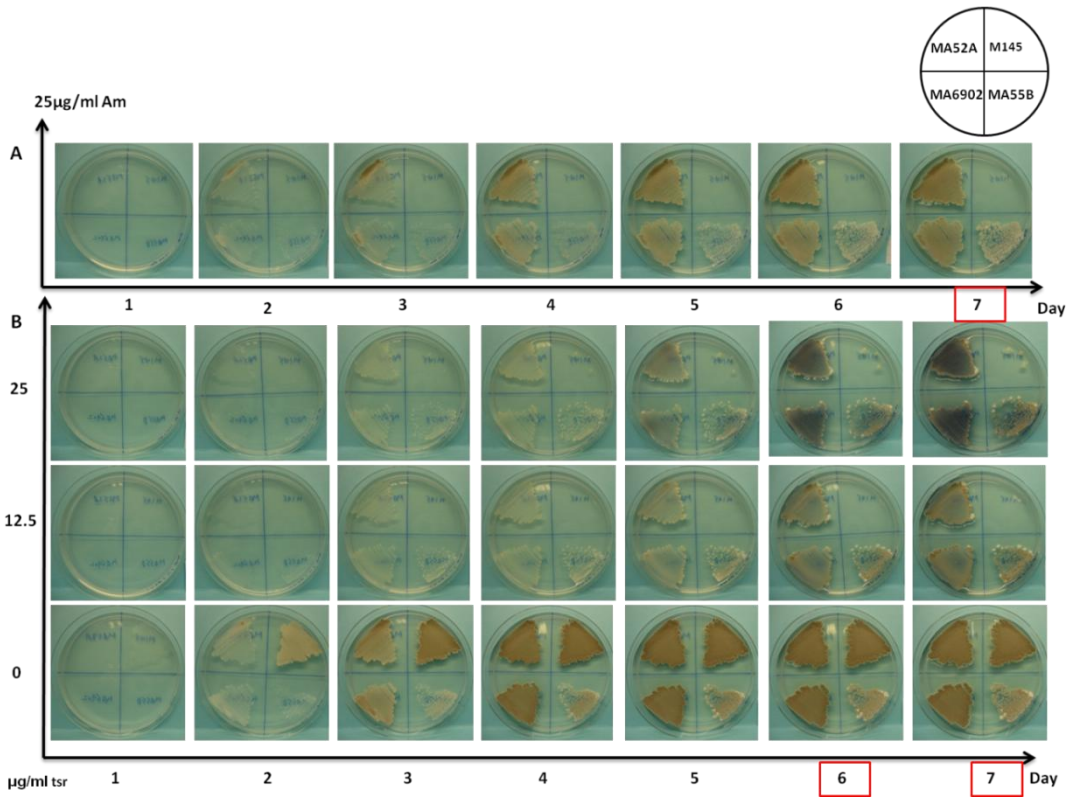

Figure 4-16: Growth of MA52A (*SCO5752)*, MA55B (*SCO5755*) on minimal media with mannitol (3MA).

(A) Growth in the presence of the antibiotic selectable marker (25µg/ml apramycin) for 7 days. (B) The effect of different tsr concentrations on development of MA52A, MA55B, MA6902 (empty vector) and M145 for 7 days. Both experiments were performed at n=1.

Growth of MA52A, MA55B and MA6902 on MMG medium was also investigated. In the presence of 25µg/ml apramycin, overall growth was slow and showed undecylprodigiosin production except for strain MA55B. On day 7, MA52A and MA6902 were reddish and pigmented patches were visible and had just begun to develop. In contrast, the strain MA55B was still unpigmented (Figure 4.17A). In the presence of tsr it was clear that all strains other than, MA55B displayed tsr dependent reduction in undecylprodigiosin production. In contrast, MA55B showed little production of this red pigmented antibiotic, but showed more rapid erection of aerial hyphae (Figure 4.17B).

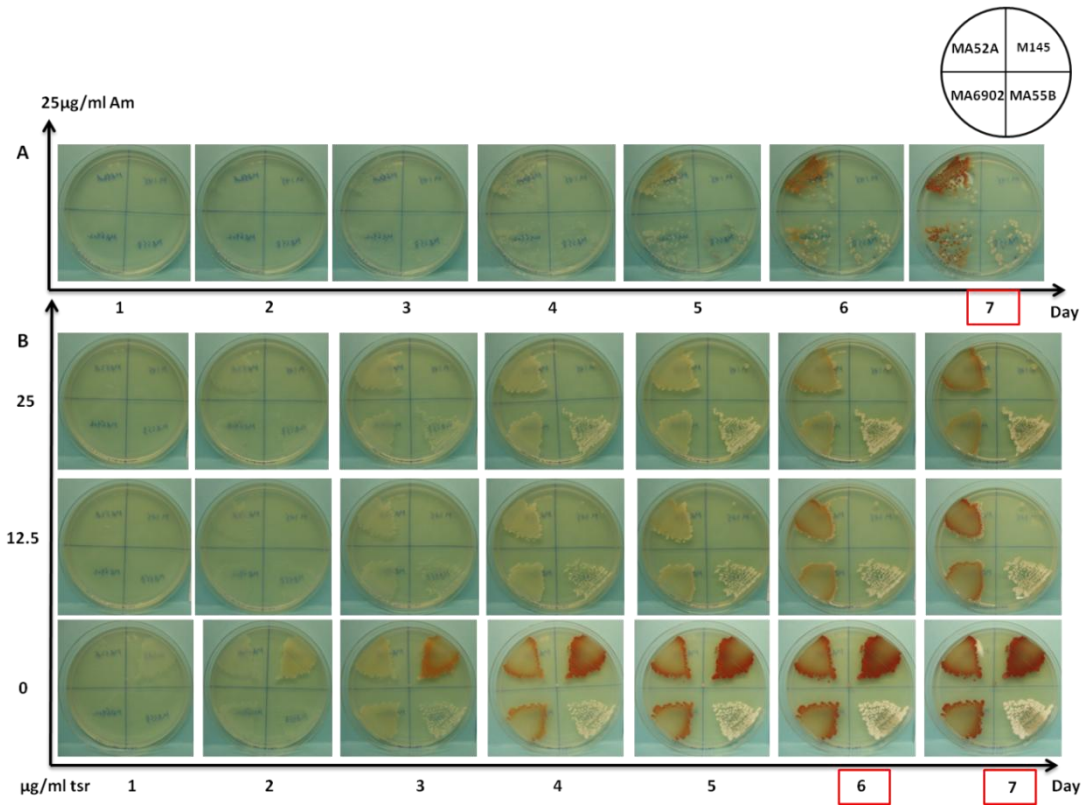

Figure 4-17: Growth of MA52A (*SCO5752)*, MA55B (*SCO5755*) on minimal media with glucose (MMG).

(A) Growth in the presence of the antibiotic selectable marker (25µg/ml apramycin) for 7 days. (B) The effect of different tsr concentrations on development of MA52A, MA55B, MA6902 (empty vector) and M145 for 7 days. Both experiments were performed at n=1.

R5 growth medium was used to further investigate the effects of changing expression of *SCO5755* and *SCO5752* in terms of antibiotic production. In the presence of 25µg/ml apramycin, on day 3 strain MA52A had already turned dark blue through actinorhodin production into the medium while the empty vector strain, MA6902 showed a delay in physiological development by one day. The strain MA55B showed a clear delay in physiological development in comparison to other strains with little production of actinorhodin (Figure 4.18A). In the presence of tsr, the strain MA52A produced more actinorhodin in response to increasing tsr concentrations from 0 to 25 µg/ml, this observation was similar to the strain MA6902. The strain MA55B showed more morphological differentiation, with the appearance of white aerial hyphae being noticeable across the patch surface on day 5-7 with increasing tsr concentration. This strain secreted less actinorhodin at all tsr concentrations (Figure 4.18B).

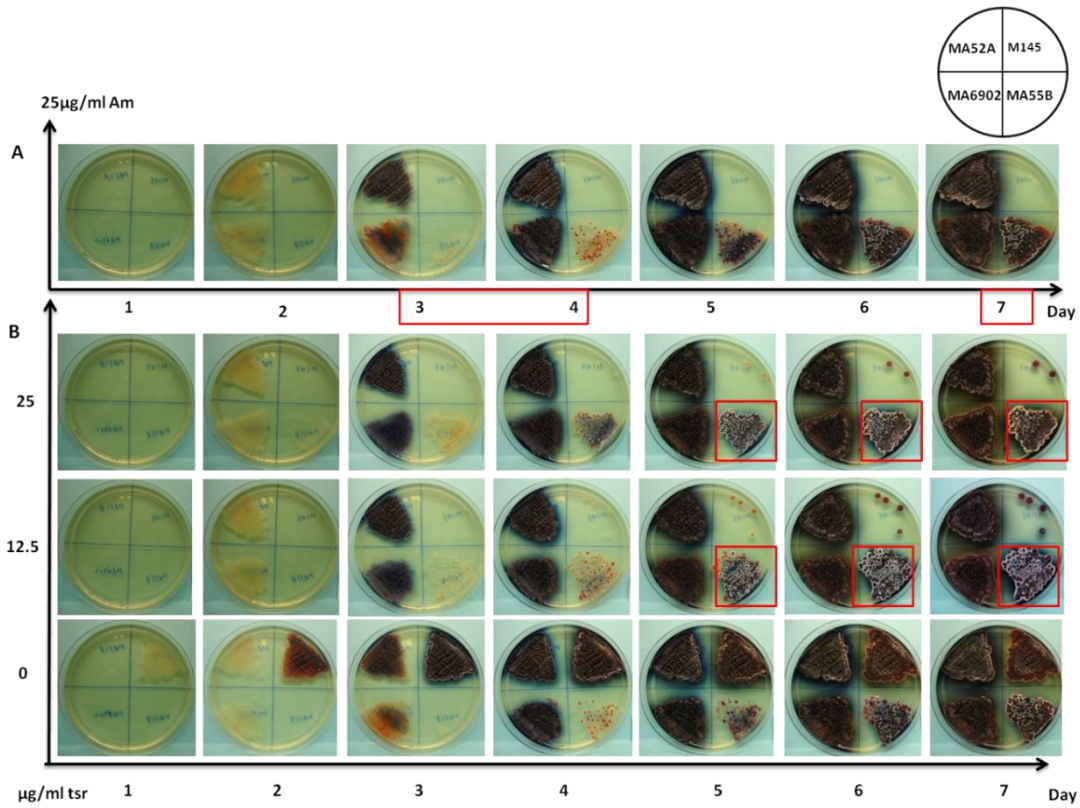

Figure 4-18: Growth of MA52A (*SCO5752)*, MA55B (*SCO5755*) on R5 agar.

(A) Growth in the presence of the antibiotic selectable marker (25µg/ml apramycin) for 7 days. (B) The effect of different tsr concentrations on development of MA52A, MA55B, MA6902 (empty vector) and M145 for 7 days. Both experiments were performed at n=1.

4.15 Phenotypes of MA53541 and MA532 on agar media

Growth on SFM medium was used to analyse any changes of gene overexpression of *SCO5753/SCO5754* and antisense *SCO5753* in terms of sporulation. In the presence of 400µg/ml spectinomycin, there was little difference observed between the growth and the morphological development of MA53541, MA532 and MA927 on day 3. After growth at day 7, MA532 showed darker gay spores (Figure 4.19A). In the presence of tsr, by day 4, the strains MA53541 and MA927 appeared pale in comparison to MA532 and M145. Increasing tsr concentration from 0 to 25 µg/ml the strain MA532 changed the appearance of this strain to a darker gray at day 7 (Figure 4.19B).

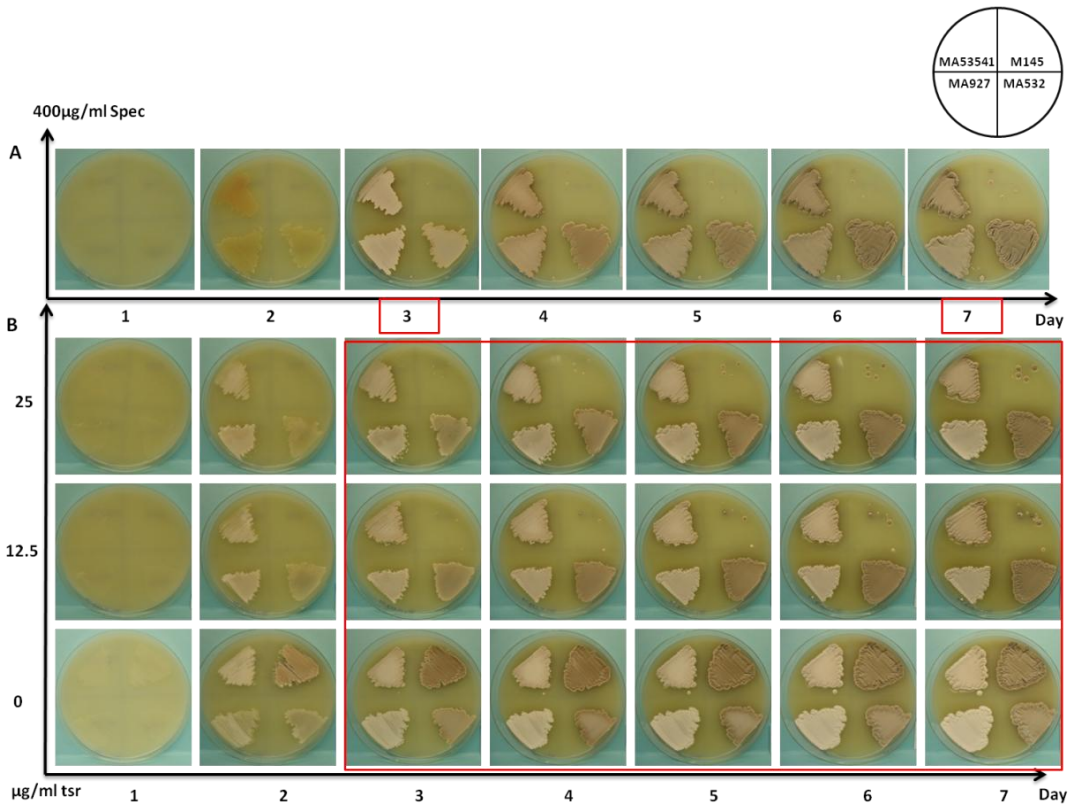

Figure 4-19: Growth of MA53541 (*SCO5753+SCO5754)* and MA532 (*SCO5753*) on SFM agar.
(A) Growth in the presence of the antibiotic selectable marker (400µg/ml spectinomycin) for 7 days. (B) The effect of different tsr concentrations in early and late growth by MA53541, MA532, MA927 (empty vector) and M145 during 7 days. Both experiments were performed at n=2.

Growth on 3MA medium was used to analyse any changes of gene overexpression in terms both morphological and physiological differentiation. In the presence of 400µg/ml spectinomycin, the overall morphological appearance of the strains MA53541 and MA927 was pale gray. The antisense strain MA532 showed a clear reddish appearance from day 4-7, presumably through stimulation of undecylprodigiosin production (Figure 4.20A). In presence of tsr, on day 4 the strains MA53541 and MA927 developed strongly with gray spores being visible with 25 µg/ml tsr added, while at the same time the strain MA532 had developed aerial mycelium but there was less sporulation. However this strain on day 5 had turned strongly dark red at 0 and 12.5 µg/ml tsr. All strains showed induction of actinorhodin production at the highest concentration of tsr (Figure 4.20B).

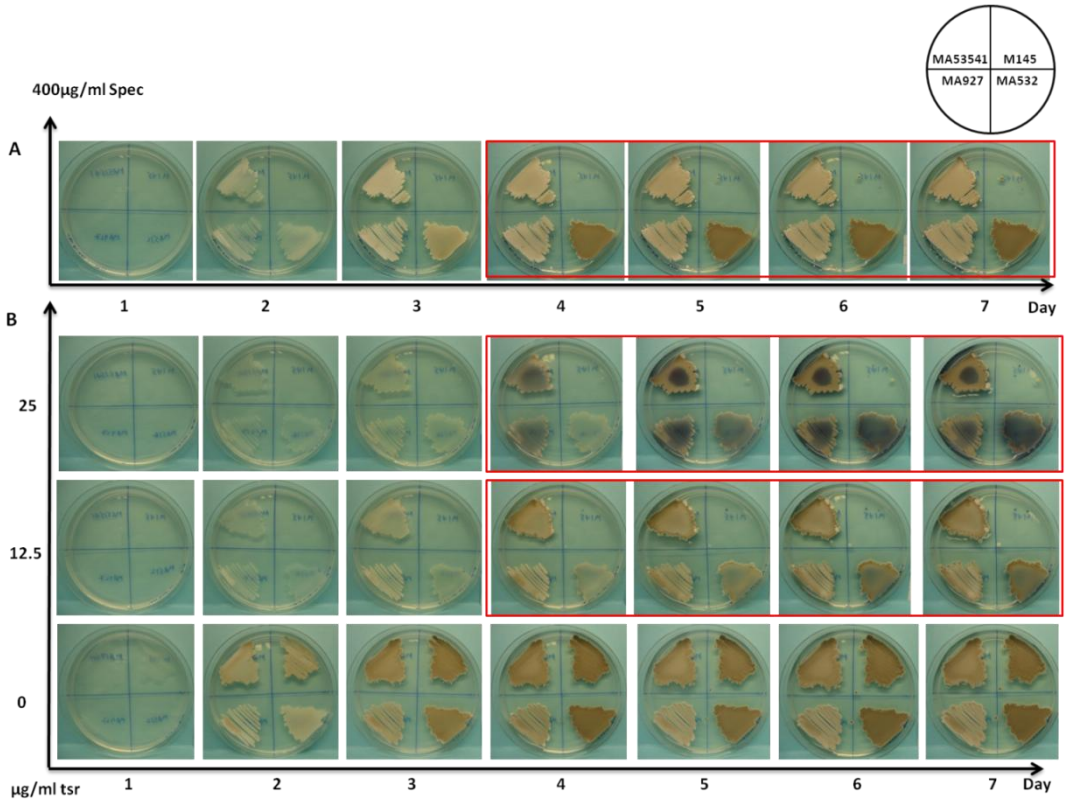

Figure 4-20: Growth of MA53541 (*SCO5753+SCO5754)* and MA532 (*SCO5753*) on 3MA.

(A) Growth in the presence of the antibiotic selectable marker (400µg/ml spectinomycin) for 7 days. (B) The effect of different tsr concentrations in early and late growth by MA53541, MA532, MA927 (empty vector) and M145 during 7 days. Both experiments were performed at n=2.

The Growth on MMG agar was used to analyse any changes of gene overexpression in terms of aerial hyphae erection and sporulation. In the presence of 400µg/ml spectinomycin, the phenotypic appearance of the strain MA53541 was dark with a ragged white border on day 7. MA532 and MA927 had a translucent phenotype in the middle of the patch surface with a slight white border for MA927 and dark red border for MA532 (Figure 4.21A). In the presence of tsr, MA53541 showed a different developmental pattern in comparison to MA532 showing induction of development in comparison to the control strain (MA927). In contrast MA532 showed lees induction of morphological differentiation but showed a greater stimulation of undecylprodigiosin production in response to the inducer (Figure 4.21B).

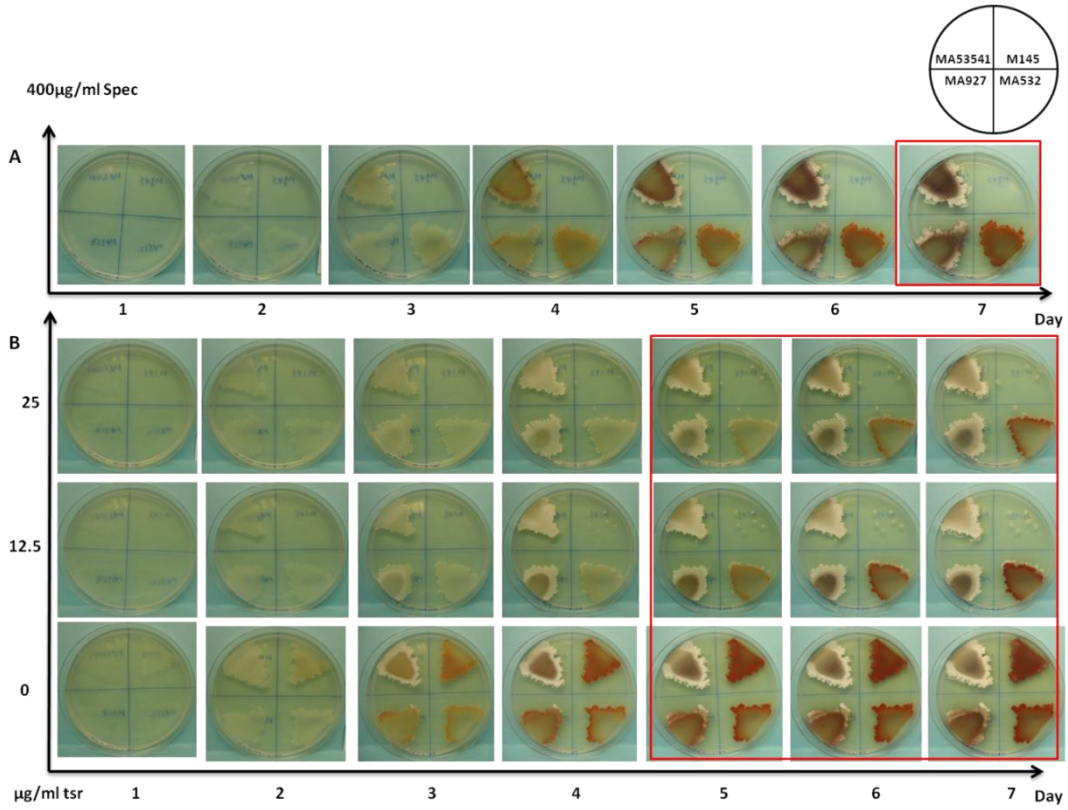

Figure 4-21: Growth of MA53541 (*SCO5753+SCO5754)* and MA532 (*SCO5753*) on MMG agar. (A) Growth in the presence of the antibiotic selectable marker (400µg/ml spectinomycin) for 7 days. (B) The effect of different tsr concentrations in early and late growth by MA53541, MA532, MA927 (empty vector) and M145 during 7 days. Both experiments were performed at n=2.

R5 medium was used to study any changes of gene overexpression of *SCO5753/SCO5754* and antisense *SCO5753* in terms of antibiotic production. In the presence of 400 spectinomycin, overall the strains were similar except that, on day 3, MA53541 and MA927 showed a delay in actinorhodin production. By day 7 all the strains had secreted large amount of actinorhodin into the medium (Figure 4.22A). It is interesting to note that, despite the addition of 400µg/ml spectinomycin, M145 was able to grow after prolonged incubation (from around 4 days onwards). This is in contrast to previous experiments in Figures 4.19a-4.21a where no growth of M145 was observed. This seems to be due to the use of R5, which is a rich media unlike the other media such as SFM, MMG and 3MA which are less enriched. In the presence of tsr, MA532 produced more actinorhodin into the medium than MA53541 and MA927 at day 3. By day 4-7, patches of gray spores were observed across the surfaces of MA53541. This is in contrast to MA927 where no spores were seen across patch and the erection of aerial hyphae was restricted to the edges (Figure 4.22B).

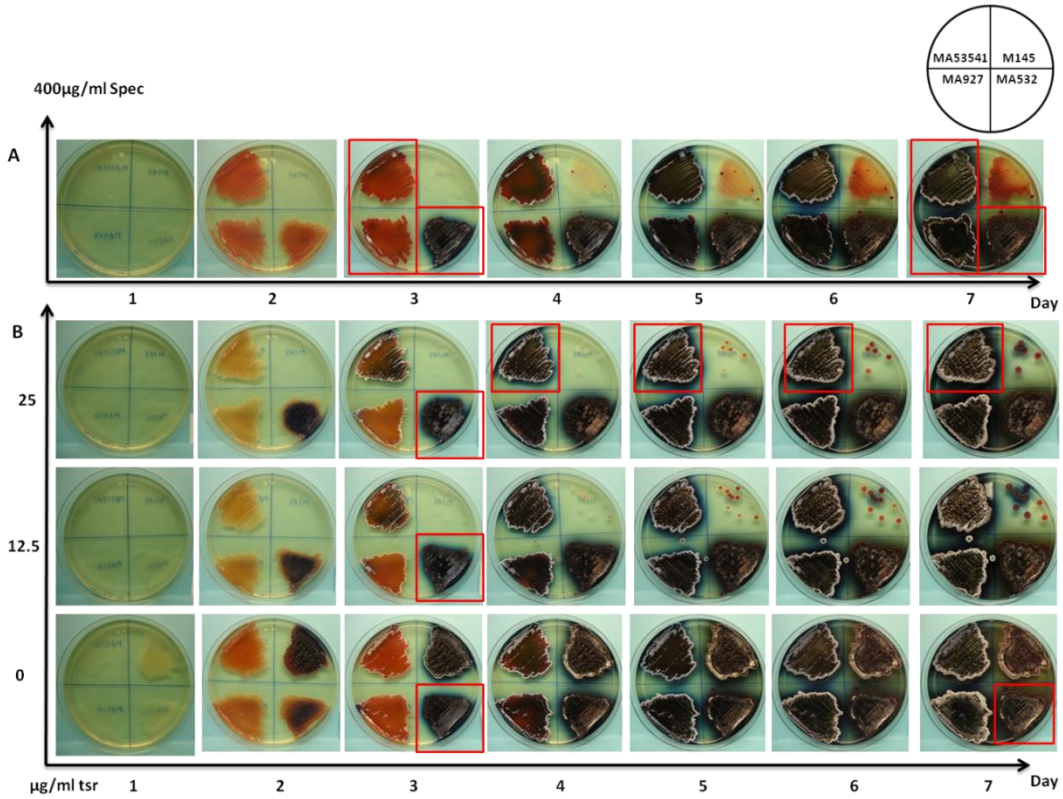

Figure 4-22: Growth of MA53541 (*SCO5753+SCO5754)* and MA532 (*SCO5753*) on R5 agar.

(A) Growth in the presence of the antibiotic selectable marker (400µg/ml spectinomycin) for 7 days. (B) The effect of different tsr concentrations in early and late growth by MA53541, MA532, MA927 (empty vector) and M145 during 7 days. Both experiments were performed at n=2.

4.16 Discussion of Chapter 4

PG is a significant membrane component of the filamentous antibiotic producing bacterial genus *Streptomyces*. In this project we have focused on the gene *SCO5753* (*pgsA*) from the model organism *Streptomyces coelicolor* (M145), whose product is predicted to synthesize PG, the precursor of CL. As mentioned before, in order to study the *SCO5753*, the characterization of downstream genes such as *SCO5755* should also be investigated as the protein encoded by this gene is speculated to regulate *SCO5753*. In this chapter we have combined two approaches of analysis; molecular and phenotypic approaches. Cloning of the genes of the *pgsA* cluster was initially difficult and it was only after repeated attempts of cloning the *pgsA* operon and *clgR* (*SCO5755*) into the vectors pPM927 and pIJ6902 (both under the tsr-inducible promoter *ptipA*) that it was later successful. pMA53541 (*SCO5753* and *SCO5754*), pMA532 (*SCO5753*, antisense orientation), pMA106A (*SCO5752*) and pMA109B (*SCO5755*) were successfully constructed under the control of the inducible promoter *ptipA*. These plasmids were introduced into *S. coelicolor* by conjugation; the resulting strains were MA53541, MA532, MA52A and MA55B. Unfortunately we could not construct a plasmid containing *SCO5753* by itself under the control of an inducible promoter in the sense orientation. It was only possible to construct a plasmid containing this *SCO5753* when coupled with *SCO5754* even after several attempts of cloning. This plasmid, pMA53541, was introduced into *S. coelicolor* M145 by conjugation generating MA53541 and, despite the second copy of *SCO5753* being present in this strain, it was still impossible to disrupt *SCO5753* with Tn*5062* following introduction of the transposed cosmid SC7C.B07 into MA53541. Our failure to generate a mutation in this gene despite a second, complementing, copy of *SCO5753* suggests that as well as its essentiality for *S. coelicolor* growth and development, it is likely that regulation of *SCO5753* expression is a complex process. It has been found that PG is essential for viability of *Synechocystis* sp. PCC6803 since it plays an important function in photosystem II of photosynthesis (Rahman et al., 2009a, Sakurai et al., 2003). In addition deletion of *pgsA* was not unsuccessful, revealing that *pgsA* might be essential in *Streptococcus* mutans (MacGilvray et al., 2012).

Despite this, it is possible to make observations about the possible role of the proteins encoded by the *pgsA* operon on growth and development of *S. coelicolor* on the basis of examining the effect of induction of gene expression through use of the *tipA* promoter in concert with its inducer, tsr. MA55B produced white growth while MA52A formed gray growth which was similar to the control strain MA6902 on all agars. This suggests that the induced activity of *ptipA* was sufficient to induce expression of *SCO5755* and mediate an inhibitory effect on growth. Interestingly increased concentrations of tsr appeared to generate a dose-dependent response to this antibiotic in terms of growth retardation. This gene encodes a known regulator and it may well be that the regulatory targets of SCO5755 are genes responsible for development; as such it is plausible that overexpression of this protein would inhibit expression of such developmental genes. The master regulator of streptomycete development, BldD (Tschowri et al., 2014), is a candidate for regulation by SCO5755. The reason for this is that deletion of *bldD* causes hyper sporulation and as such BldD is a negative regulator of development. Consequently over expression of a protein (SCO5755) that induces expression of *bldD* might be expected to repress development. It is important to remember that, even in the absence of inducer, *ptipA* still represents a strong promoter in streptomycetes and highlights the need for better gene induction systems in this group of organisms. MA52A displayed a similar phenotype to MA6902 but, when both were compared at varying concentrations of tsr, growth of MA52A gave a slightly less gray appearance. As *SCO5752* is expressed in the antisense orientation in M52A, increased concentrations of tsr are likely to decrease sense *SCO5752* transcripts available for translation and, as such, is equivalent to reducing expression of this gene (Murakami et al., 1989). Interestingly, MA55 also displayed reduced production of the pigmented antibiotics than control strains and suggests that SCO5755 is a pleiotropic regulator of both morphological and physiological differentiation (Chater and Horinouchi, 2003).

The effect of overexpression of *SCO5753/SCO5754* and antisense *SCO5753* in terms of morphological and physiological differentiation was less clear. MA53541 showed pale spores in comparison to control strains when *SCO5753/SCO5754* expression was induced by tsr. In solid media the growth of the strain MA532 that contains an

integrated copy of antisense *SCO5753* seems not affected by the gradient concentration of tsr (Figures 4.19b–22b). The mRNA expression interference with antisense RNA has been utilised efficiently in eukaryotic systems for gene expression inhibition (Burne et al., 1999). This system has also been employed in *Mycobacteria* and *Staphylococcus aureus* to recognise virulence factors and essential genes and to investigate the microorganisms' gene functions (Ji et al., 2001, Parish and Stoker, 1997, Zhang et al., 2000). We believe that the reason why inducing antisense in our organism does not inhuibit growth could be related to the different times of mRNA expression between the antisense *SCO5753* integrated copy and the functional copy *SCO5753* present in the chromosome.

MA55B contains *SCO5755* (*clgR*); this gene appears to contribute significantly to *Streptomyces* development since *clgR* overexpression induces a delay of differentiation in *S. lividans* (Bellier and Mazodier, 2004). As we thought this *clgR* gene (*SCO5755*) might regulate the gene (*SCO5753*), further investigation on the former gene could reveal the full function of *SCO5753* in the future.

Chapter 5:

Analysis of the effect of osmotic stress on the phospholipid content of *S. coelicolor*

5. Analysis of the effect of osmotic stress on the phospholipid content of *S. coelicolor*

5.1 Introduction to Chapter 5

Most microorganisms in their lifetime experience or suffer osmotic stress, mostly caused by fluctuating of outside osmolarities, but also as an effect of freezing or desiccation. Based on these conditions, the proportion of osmolytes to water and macromolecules in the cells is changed. To survive, cells must constantly sense these changes and accordingly adapt. Osmolarity is a physicochemical parameter that has profound implications for many physiological processes within a cell. Recent research has shown that different systems sense significant changes in osmolarity and are based on observing cellular changes that are related to the changed growth conditions (Heermann and Jung, 2004). Osmoadaptation covers all the physiological and genetic adaptations to high and low water surroundings. There are two osmoadaptation strategies that have been developed to survive high osmolarity: the 'salt in the cytoplasm' group and the 'organic osmolyte' group. On the other hand, adaptation to hypo-osmotic shock contains a mixture of specific (secondary transport) and non-specific (stretch activated channels) solute efflux responses coupled with aquaporins that mediate water efflux (Sleator and Hill, 2002). The stress signalling systems in *E. coli* acts as a 'watchdog' of the cell envelope. In addition to external molecules, microorganisms can respond and sense intracellular stimuli. For instance, pathways of intracellular signalling exist that can sense any cellular components, defects and react accordingly to repair them (Ruiz and Silhavy, 2005).

In *S. coelicolor* there is a relationship between stress and growth; the morphological changes that leads to aerial mycelium production and sporulation in this mycelial bacterium is based on establishing different patterns of gene expression in separate sections of the colony. In *Streptomyces*, the mycelial colony is comprised of localised morphological variations in the tissues, which are proposed to allow the organism to best cope with conditions of environmental adversity (Kelemen et al., 2001). The spatial patterns of gene expression in the various tissues can now be identified by transcriptional fusions to enhanced green fluorescent protein (EGFP).

By this method, *sigF* transcription, that encodes the late spore specific sigma factor σ^F transcribed from one of two promoters of *ftsZ*, was revealed to be limited to sporulation in aerial hyphae (Potúčková et al., 1995, Sun et al., 1999, Flärdh et al., 2000). On the other hand, *redD* transcription that encodes a specific activator of pathways for the biosynthetic genes for the antibiotic undecylprodigiosin, was limited to the substrate hyphae which is the location of undecylprodigiosin biosynthesis (Sun et al., 1999). The hyphae form these different tissues, possibly due to various metabolic and environmental stress conditions that impact on different areas of the streptomycete mycelium. These environmental stresses form self regulating groups of proteins that are thought to be encoded by nine of SigB paralogues (Viollier et al., 2003a); three paralogous sigma factors (σ^H, σ^I and σ^J) are related to the *S. coelicolor* stress responses (Kelemen et al., 2001). In *B. subtilis* this is closely associated with σ^B, which is induced by different environmental and physiological stresses like ethanol shock or slat and heat (Viollier et al., 2003a).

In regards to systematic insertional mutagenesis described in Chapter 3, the versatility of this system was revealed through the application of Tn*5062* to *S. coelicolor* functional genomics following the establishment of a connection between osmoadaptation and antibiotic secretion. The study showed that a pair of osmoregulatory genes, *SCO5748* and *SCO5749*, which encodes a hybrid histidine kinase and a response regulator respectively, were essential in signal transduction allowing osmoadaptation. These two genes were designated *osaA* and *osaB* respectively and it was revealed that their disruption led to increased antibiotic formation under hyperosmotic conditions of growth. Each gene is upregulated during conditions of high external osmolarity, as shown by *egfp* expression analysis from Tn*5062* insertional mutants. A study of transcriptional regulation illustrated that *osaB* is independently regulated from *osaA* (Figure 5.1) (Bishop et al., 2004).

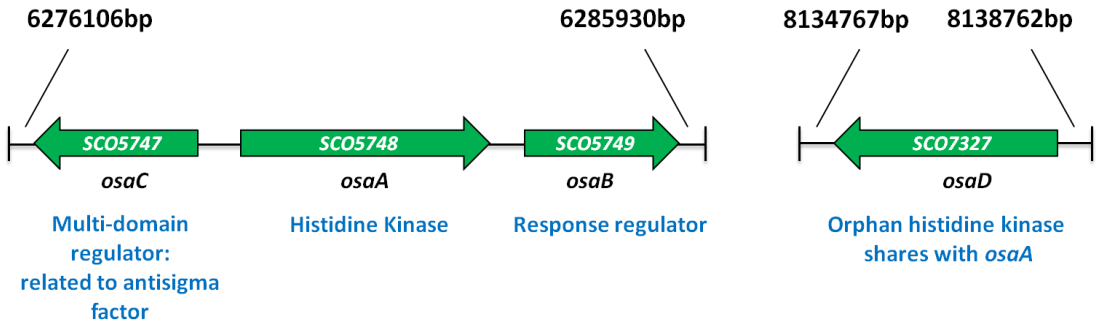

Figure 5-1: Location of *osaA, osaB, osaC* and *osaD* in *S.coelicolor*.

SCO5748 (osaA) encodes a sensory histidine kinase; *SCO5749 (osaB)* encodes a two component regulator; *SCO5747 (osaC)* encodes a regulatory protein; *SCO5747 (osaD)* encodes a possible two-component system sensory histidine kinase (The *Streptomyces* Annotation Server) (Bishop et al., 2004).

A third osmoregulation gene is *SCO5747*, which is divergently transcribed from *osaA* and encodes a new family of regulatory proteins. Members of this family have a domain structure comprising of an N-terminal kinase domain linked to an antisigma factor domain coupled with a C-terminal phosphatase domain. *SCO5747*, designated *osaC* was found to be linked to the response regulator gene *osaB* as expression studies showed that it is expressed after osmotic stress in a *sigB* dependent way. *osaC* expression is necessary to return the expression of *osaB* and *sigB* back to basal levels after osmotic stress. An orphan sensor kinase, *SCO7327*, designated *osaD*, is the fourth osmoregulation gene and is a hybrid histidine kinase gene in *S. coelicolor* which shares homology with *osaA* (Figure 5.1) (Martínez et al., 2009). However, it is not fully understood yet whether it is of any relevance that the genomic location of this regulatory system (*osaABC*), which is involved mainly in osmoregulation (Bishop et al., 2004)**,** is proximal to the *pgsA* operon in *S. coelicolor*.

Osmotic stress is required to trigger activity of the osmosensory transporter ProP and the quantity of CL among the PLs of *E. coli* increases with osmolality of growth medium. Most of the cardiolipin synthesis is attributed to the gene product of *cls*, which is subject to raised transcription under osmotic stress. The proportion of PG was high and it was elevated with medium osmotic stress in *E. coli* (Romantsov et al., 2007). Another significant function of PG was shown in in the osmotic adaptation of *B. subtilis*. The membrane of a mutant in the putative cardiolipin synthase gene, *clsA*, showed a raised PG content during exponential and stationary phases (Lopez et al., 2006). A similar effect indicated that changes in osmolality in the probiotic bacterium *Lactobacillus casei* BL23 results in structural alterations in the cell wall membrane component, lipoteichoic acid (LTA), which is comprised of glycerolphosphate chain engaged by a glycerolipid anchor to the cell membrane of bacteria. It has been shown that *L. casei* BL23 was able to increase the formation of biofilms and to attach cations in high salinity media. This behaviour is related to alterations of surface attributes that require teichoic acids, which are significant components of the bacterial cell wall. This group also showed that the reduction of LTA synthase (LtaS) activity and *ltaS* transcription is seen in conditions of high salt

growth; possibly by affecting the LTA backbone chain length resulting in the overall modification of the cell envelope during osmolality (Palomino et al., 2013).

By means of recently developed technology in gel-free proteomics, the significant human pathogen *Staphylococcus aureus* was investigated in terms of the membrane proteome and for the presence of the cationic PL lysyl-phosphatidylglycerol (Lys-PG). This phospholipid is the main membrane PL of *S. aureus*. It was shown that Lys-PG absence had no major effect on the biosynthetic enzymes for this PL, but importantly impacted on quantities in the regulatory proteins of a cell envelope stress like MsrR and SaeS, and SaeS (Sbi, Efb, and SaeP) proteins. These results show very significant interactions of membrane sensory proteins with PL compositions (Sievers et al., 2010).

Membrane PL content was previously shown be important for *Streptomyces* development and growth (Jyothikumar et al., 2012). Due to the effect of osmotic stress on the membrane content of the bacteria described above, we set out to investigate the importance of the content of anionic PLs, especially PG, during osmotic adaptation of *S. coelicolor*. As a result, our aim was to investigate the effect of osmotic stress adaptation on PLs in general and PG specifically in *osaABCD* mutants and the strains-constructed in Chapter 4 that could undergo regulated expression of the *pgsA* gene.

Even though different techniques have been used for PL extraction in previous research (Yague et al., 1997, Rementzis and Samelis, 1996), most of them employed methods for PL extraction based on chloroform, methanol and water extractions (Bligh and Dyer, 1959). Generally extraction of PL comprises different steps: enzymatic or mechanical extraction, cell disruption followed by extraction from cellular fragments. The final steps comprise of the separation, the detection and the identification of PLs. For microbiological research, even though high performance liquid chromatography (Hoischen et al., 1997a), electro-spray ionisation combined with collision expressed dissociation mass spectrometry (Hoischen et al., 1997b), rapid atom bombarded mass spectrometry, or ^{31}P NMR (Rahman et al., 2000, Rana et

al., 1991) have been previously utilized, the most commonly applied method is two dimensional thin layer chromatography (2D TLC) with separation via a mixture of chloroform, methanol and ammonia combined with appropriate staining (Hoischen et al., 1997a, Schauner et al., 1999). However, the 2D TLC method is time-consuming and generally requires a great volume of sample (Limonet et al., 2007). All these processes require an initial step such as lipid extraction, however lately, the identification of PLs has been carried out on whole cells of *E. coli* by matrix-assisted laser desorption/ionisation mass spectrometry (MALDI-MS) (Ishida et al., 2006). Having said that, PL analysis by Mass Spectrometry (MS) could not be completed within the time frame of this project. Despite this, it has been used by other members of our research group (Jyothikumar et al., 2012) who demonstrated that two different CL envelopes with varying acyl chain lengths were present in *S. coelicolor*. The spotting of the TLC plate was carried out using precisely measured volumes of the PL extract in a homogenous solution in order to minimise sample weight variations between lanes on each plate. However, since the TLC/staining approach is inherently qualitative, we recognise that our study might have benefited from additional quantitative measurements of each spot such as densitometry and phospholipid assay of spot scrapings which might have improved the precision of quantification.

In the context of a rapid, simple and sensitive method, TLC analysis is utilised for the routine separation of chemical and biochemical substances in mixtures. This separation operates on the basis of the affinity on a TLC plate for the adsorption of a stationary phase and solubility of a mobile phase in various solvents. During separation, the TLC plate edge is placed in the mobile phase solution, which is developed via capillary action. The different interactions between the spot molecules, stationary phase and mobile phase cause various compounds to travel at different rates on the TLC plate. The separation of the chemical substances on a TLC plate is calculated by the retardation factor value of R_f (distance migrated by the spot/distance migrated by mobile phase) (Cheng et al., 2011, Sandoval-Calderon et al., 2009).

5.2 Aims of Chapter 5

Work in the previous chapter has supported the involvement of PG in *Streptomyces* development. As a result, the aim of the work presented in this chapter was two-fold:

1- To investigate the effect of altering *pgsA* expression on PL content in the presence and absence of different tsr concentration using TLC plates for these strains:

- MA53541, MA532, MA52A and MA55B.

2- To determine the effect on PL content in response to increased osmolarity on *pgsA* by TLC plate for the following strains:

- *S. coelicolor*.
- Osmoadaptation mutants (*osaABCD)*.
- MA53541, MA532, MA52A and MA55B.

5.3 Investigation of the effects of altering *pgsA* expression in the presence and absence of different thiostrepton concentration using TLC plate for MA53541, MA532, MA52A and MA55B

In order to determine the effect of altering expression of the genes encoded by the *pgsA* operon on the PL content of the strains constructed during Chapter 4, PLs were extracted from cultures grown in rich liquid media (YEME) for 24 and 48 hours. PLs were developed on TLC plates and spots were analysed according to their migrated distance by association to known standards. To visualize PL spots by separation of PLs by TLC, suitable solvent systems must be applied. The plate was developed under different solvent systems; two solvent systems were used: solvent A: chloroform/methanol/acetic acid [(65: 25: 10 (vol/vol)] (Tan et al., 2012) and solvent B: chloroform/methanol/acetic acid/water [(80: 12: 15: 4 (vol/vol)] (Jyothikumar et al., 2012). PL standards were obtained from Avanti Polar Lipids Inc. Each standard was dissolved in chloroform: methanol (2:1) to make a final concentration of 5mg/ml stock. Samples of PL standards then were loaded on two separate TLC plates. The first TLC plate was placed in tank that contains solvent (A) and the second TLC plate was placed in tank that contained solvent (B). Then both tanks were left to develop

for about 45 minutes. In solvent system (A), spots of PE and CL co-travelled with a slight further migration of CL whereas PG migrated more slowly (Figure 5.2). In the image of the solvent system (B), the furthest migrated spots were PE, followed by CL then PG (Figure 5.2). Both solvent systems displayed good separation of PL standards, but was best on the TLC plate resolved in solvent system (A). Although these solvent systems both resolved PL standards, solvent A was less polar than solvent B as the addition of water increased solvent system polarity. Therefore the putative CL spots could be best resolved at the top of the plate.

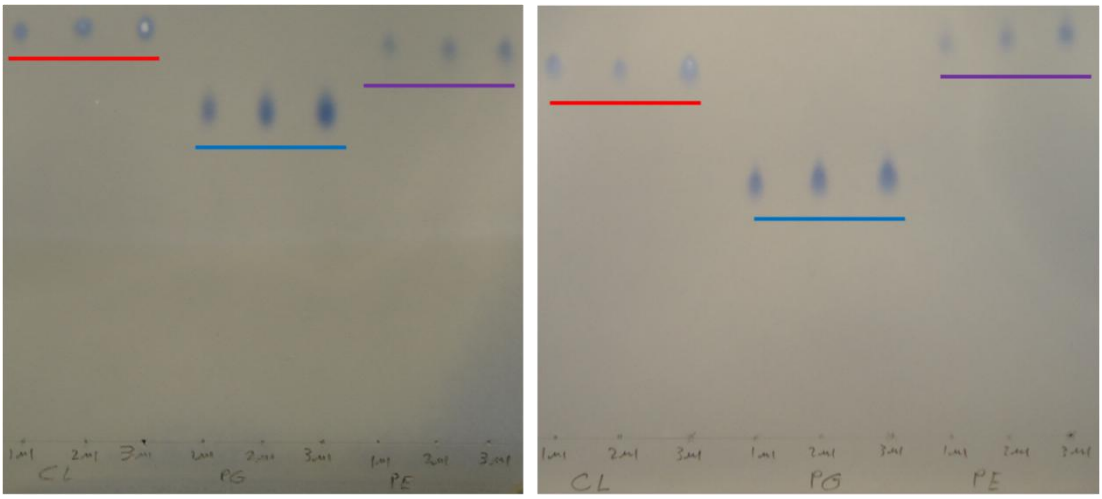

Solvent A Solvent B

Figure 5-2: Comparisons of two solvent systems were used to determine which was most appropriate for analysing *pgsA* expression.

Each PL standard was marked with lines: CL with red line, PG with blue line, PE with purple line. Solvent A: chloroform/methanol/acetic acid [(65: 25: 10 (vol/vol)] and solvent B: chloroform/methanol/acetic acid/water [(80: 12: 15: 4 (vol/vol)].

5.3.1 Study of PL profile alteration in response to regulated expression of *pgsA* during *S. coelicolor* growth

Following separation of PLs by TLC, MA53541 showed a slight reduction of PG (spot 2) at a concentration of 0.05 µg/ml tsr; this was surprising as induction of *ptipA* should increase expression of *SCO5753*. It was at this point that we decided to investigate alternatives to the use of molybdenum blue spray reagent due to the ezcessive specking produced during plate development (Figure 5.3). The empty vector MA927 also showed a slight, but less noticeable reduction in PG (spot 6) at a concentration 0.05 µg/ml tsr. The PL profiles of M145 had changed significantly over the different concentrations of tsr (spot 8) while MA532 PG remained unchanged (spot 4) (Figure 5.3). As this wild type strain does not contain a tsr resistance gene it is difficult to discount the inhibitory effects of the antibiotic on this strain. As a PG spot in MA53541 was diminished at a concentration 0.05 µg/ml tsr, we decided to grow the strain for 48 h with higher tsr concentration and visualize the plate with sulphuric acid and charring.

Further PL analysis was conducted on cultures of MA53541 (*SCO5753* & *SCO5754* sense), MA532 (*SCO5753* anti-sense), MA927 (pM927 control), MA52A (*SCO5752* anti-sense), MA55B (*SCO5755* sense) and MA6902 (pIJ6902 control) grown in YEME for 48 hours. During this experiment, given the week induction of SCO5753 by 0.05 µg/ml tsr, we decided to ensure induction by adding 25µg/ml tsr. PG produced by MA55B was used to investigate whether over expression of SCO5755, the putative regulator, influenced expression of *SCO5753* manifested in changes in abundance of PG. Using tsr to alter *SCO5753* expression, PG spots of MA53541 were not significantly affected in both spots 1 and 2 and each spot had a similar abundance, but perhaps was slightly more abundant in the presence of the inducer. MA532 (antisense *pgsA*) decreased PG slightly in the presence of tsr (spot 4) and is consistent with expression of anti-sense *SCO5753* reducing translation of sense *SCO5753*. Both treated and untreated cultures of MA55B gave very poor yield of PLs especially CL which was almost undetectable in Figure. 5.3. Clearly, as the cultures grew, they must have contained PLs in their membranes; perhaps the high levels of expression of the *SCO5755* regulator brought about chemical modifications

to the PL content that made them difficult to extract or resolve by TLC. This also might simply have been due to the limitation of the staining/detection method used which might have hindered visualisation of the CL spots especially as they were overlapped by PE.The control strains, MA927 and MA6902 both showed broadly similar TLC patterns although interestingly a purple spot about half way up the TLC plate disappeared in these strains in response to tsr treatment. This spot also disappeared in response to tsr treatment in MA52A and suggests that this strain behaves more similarly to the control strains with respect to its PL content (Figure 5.4).

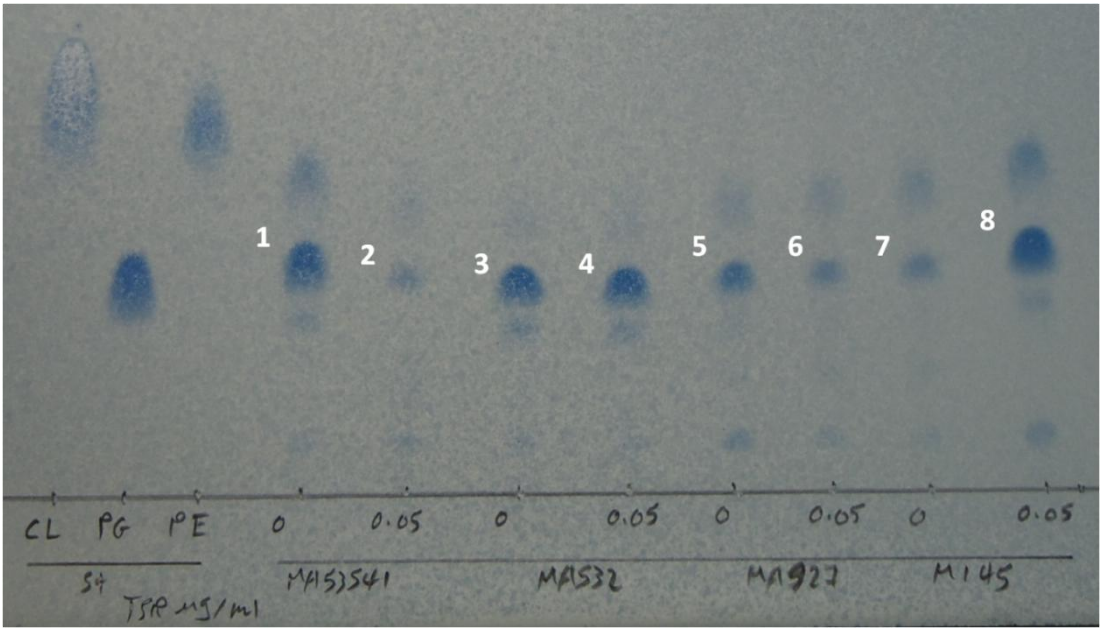

Figure 5-3: Effect of *SCO5753* overexpression, separation of PLs extracted from 100 mg wet mass of YEME grown MA53541, MA532, MA927 and M145 at two concentrations of tsr (0 and 0.05 µg/ml) at 24 h.

PLs were investigated by silica gel TLC plate and developed in chloroform/methanol/acetic acid/water (80:12:15:4) volume. Visualising was performed with by molybdenum blue spray. The numbers represent the spots that were assumed to be PG. based on their similar retardation factor (Rf) relative to the PG standard. The experiment was carried out at n=3 to ensure reproducibility of the data obtained.

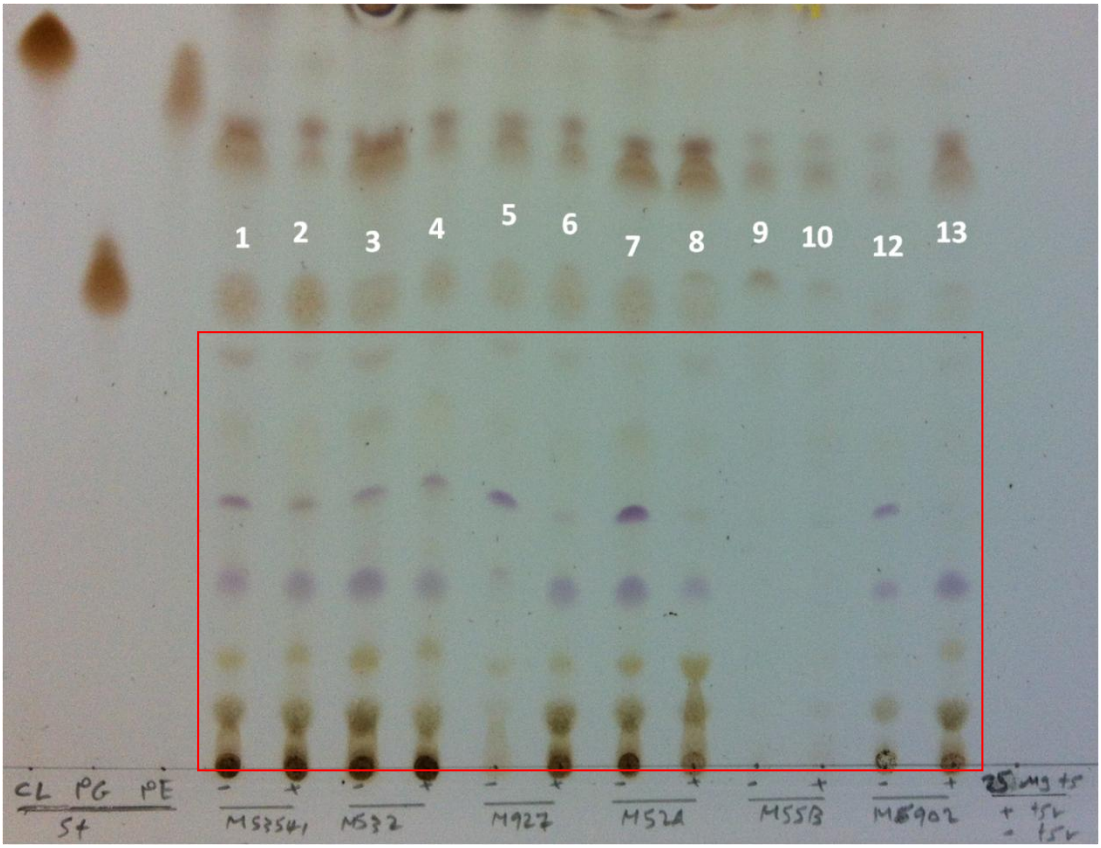

Figure 5-4: Effect of *SCO5753* overexpression, separation of PLs extracted from 100 mg wet mass of YEME grown MA53541, MA532, MA927, MA52A, MA55B and MA6902 at two concentrations of tsr (0 and 25 µg/ml) at 48 h.

PLs were investigated by silica gel TLC plate and developed in chloroform/methanol/acetic acid/water (80:12:15:4) volume. Visualisation was performed with 10% sulphuric acid in ethanol (vol/vol) followed by charring on an oven. The numbers represent the spots that were assumed to be PG based on their similarpositions relative to the PG standards. The spots within the red square are unknown. The experiment was carried out at n=2 to ensure reproducibility of the data obtained.

5.4 Analysis of PG of *S.coelicolor* M145 during growth in liquid culture, to investigate PL content in response to osmotic stress

In order to study the role of PLs in osmoadaptative mutants of *S. coelicolor*, strains carrying mutations in *osaA, osaB, osaC* and *osaD* were used to investigate the importance of the PL content in *S. coelicolor* during growth under conditions of high osmolarity. However, in the first instance we analysed the PL content of the wild-type strain, *S. coelicolor* M145. Cultures of this strain were grown in YEME media under osmotic stress conditions of KCl and PLs extracted according to Bligh & Dyer (1959). The PL analysis in Figure 5.5 performed using TLC, showed that the intensity of PG spots increased in response to KCl concentration during the growth of *S.coelicolor*. In contrast, the PE spot intensity showed a slight decrease in response to KCl concentration, also were unable to observe CL spots except at 0M & 0.15M KCl, where there are faint spots. On the basis of similarity to the standard PLs, there are unidentified spots marked with a black square. These spots are faint, implying that they represent a PL component which is present in low concentration, and they are not variant in corresponding lanes of Figure 5.6. It is not clear whether these spots represent an unidentified phospholipid in *S. coelicolor* or other components extracted during the experiment. This could be investigated further in subsequent studies. Cultures were grown for 24 hours so that the organism was in mid-exponential phase to ensure that changes in PL content were not due to nutrient limitation. This allowed us to conclude that wild type *S. coelicolor* responded to increased osmolarity through the synthesis of elevated level of PG. This may be a measure taken by an organism to protect the structural integrity of the membrane under this environmental challenge.

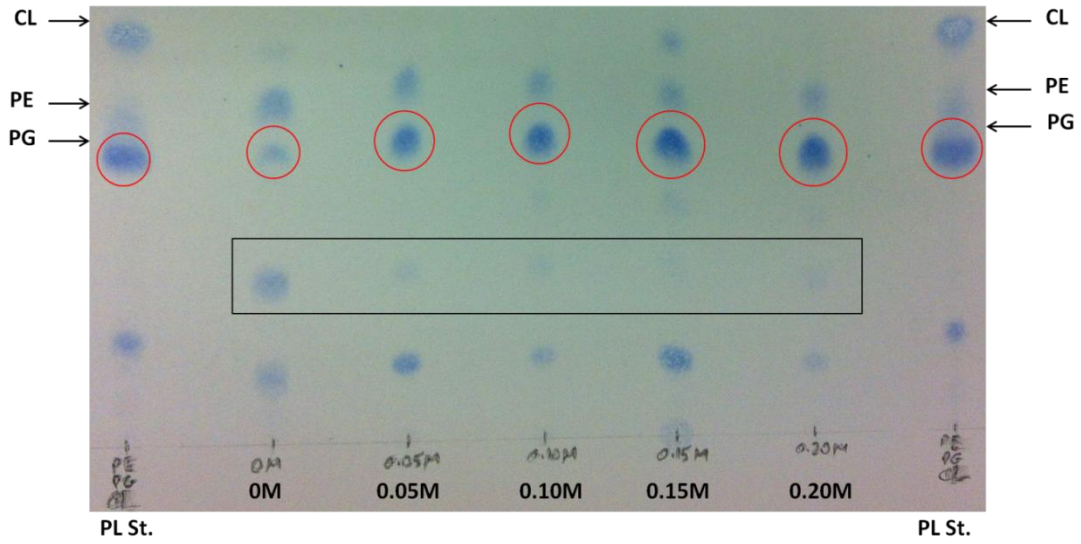

Figure 5-5: Investigation of PL content during the osmotic adaptation of *S. coelicolor* M145 in different concentrations of KCl.

PLs were extracted from 100 mg wet mass grown in YEME media incubated at 30°C, 220 RPM in 250 baffled flasks for 24 h. Cultures were supplemented with 0, 0.05M, 0.10, 0.15M and 0.20M KCl.. PLs extracted according to Bligh and Dyer (1959), analysed on silica gel TLC plates and developed in chloroform/methanol/acetic acid/water (80:12:15:4). The TLC plate was visualised by molybdenum blue spray. PG spots were marked with red circles. Markers, CL, PG, PE (Sigma). The experiment was carried out at n=4 to ensure reproducibility of the data obtained.

In addition to the previous study of *S. coelicolor* PLs, we also extracted PLs after 24h growth with a series elevated of KCl concentrations:(0M, 0.05M, 0.10M, 0.15M, 0.20M, 0.25M, 0.30M, 0.35M, 0.40M). In addition we also became aware of an alternative method for extraction and visualization of PLs (Tan et al., 2012). As a results we decided to compare this method with that of the original method (Bligh and Dyer, 1959). Both methods allowed the satisfactory visualization of PL spots by TLC (Figure 5.6); although constant clogging of the nozzle of the spray canister during visualization with molybdenum blue meant that visualization by spraying with sulphuric acid in ethanol followed by charring became our visualization method of choice. Another aim of this experiment was to display a clearer picture of the effect of KCl at higher concentrations on the *S.coelicolor* PL profile. In (Figure 5.6) we observed a decrease in PL spot intensity in response to the highest levels of KCl. It may well be that the normal systems for sensing osmotic stress may have been overcome by the high levels of KCl (0.35 and 0.4M) in these cultures.

A

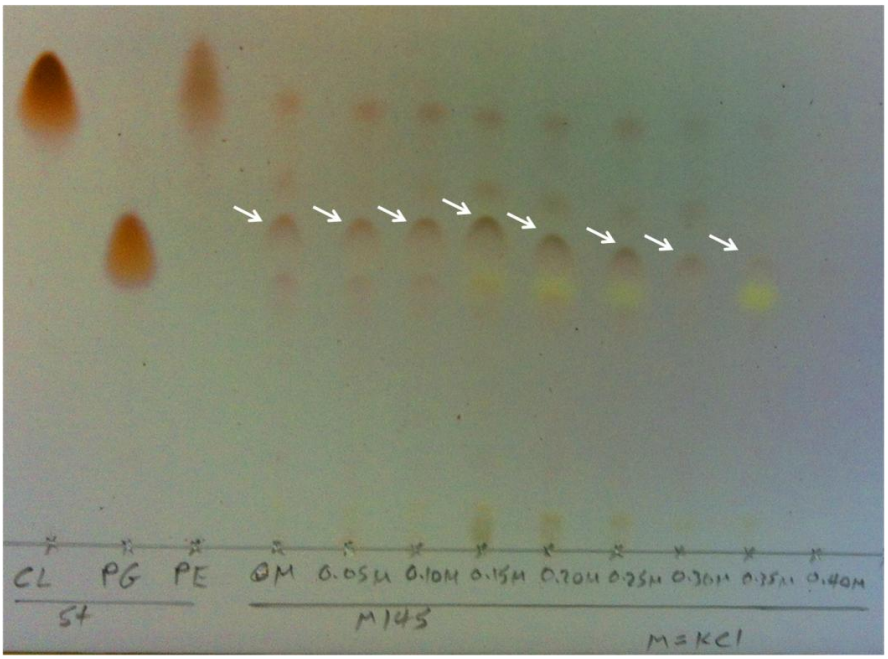

B

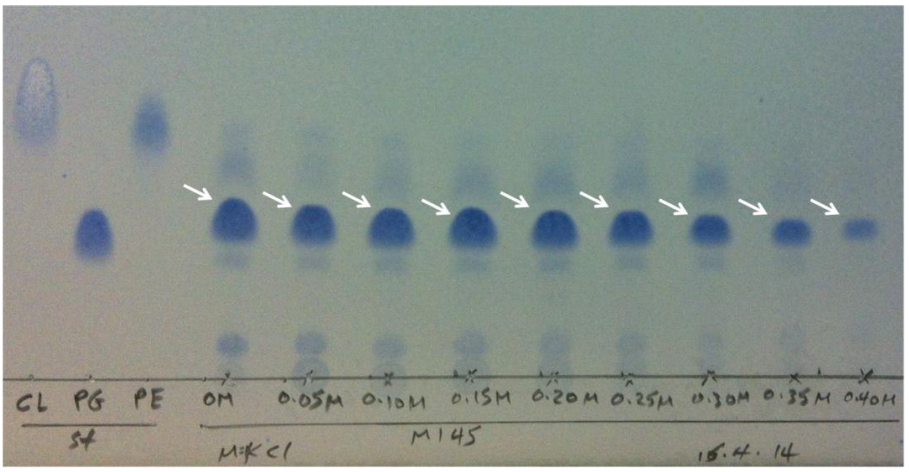

Figure 5-6: Comparison of PL content of stationary phase *S. coelicolor* during osmotic stress with a series of KCl concentrations (0M, 0.05M, 0.10M, 0.15M, 0.20M, 0.25M, 0.30M, 0.35M, 0.40M KCl).

PLs were analysed on silica gel TLC plates and developed in chloroform/methanol/acetic acid/water (80:12:15:4) (A) PLs were extracted according to (Tan et al., 2012) (with slight modifications) from 100 mg wet mass grown in YEME media incubated at 30°C, 220 RPM in 250 baffled flasks at 24 h. TLC plate visualisation was performed with 10% sulphuric acid in ethanol (vol/vol) followed by charring on an oven. (B) PLs were extracted according to (Bligh and Dyer, 1959) (with slight modifications) from 100 mg wet mass grown in YEME media incubated at 30°C, 220 RPM in 250 baffled flasks at 24 h. TLC plate visualising was performed with molybdenum blue spray. Putative PG spots are marked with white arrows. Markers CL, PG, PE (Avanti Polar Lipids). The experiment was carried out at n=4 to ensure reproducibility of the data obtained.

It was also clear that osmotic stress also had a marked effect on actinorhodin in liquid cultures that often affected the clear visualization of PL spots on TLC plates. The absence level (0M) and a higher level (0.20M) of KCl caused reduced actinorhodin production compared to concentrations of 0.5M, 0.10M, 0.15M and 0.20M KCl where they markedly increased actinorhodin productions after 48 hours (Figure 5.7). PLs were also extracted from 100 mg and TLC plate was developed and analysed in similar way with previous experiments. Spots intensities were faint, although visualization by sulphuric acid in ethanol followed by charring allowed good visualization of additional PL spots. Again the proportion of PG spot intensity increased in line with KCl concentration. The spots marked with a red square labels the unknown spots in comparison to our standards (Figure 5.8); it was clear that many of these PLs displayed changed intensity with respect to changes in KCl concentration. Currently it is not clear whether all the unidentified spots observed in the TLC experiements under different conditions (KCl stimulation and tsr) are the same or different. Further experimention to identify these spots would be required to be able to determine this.

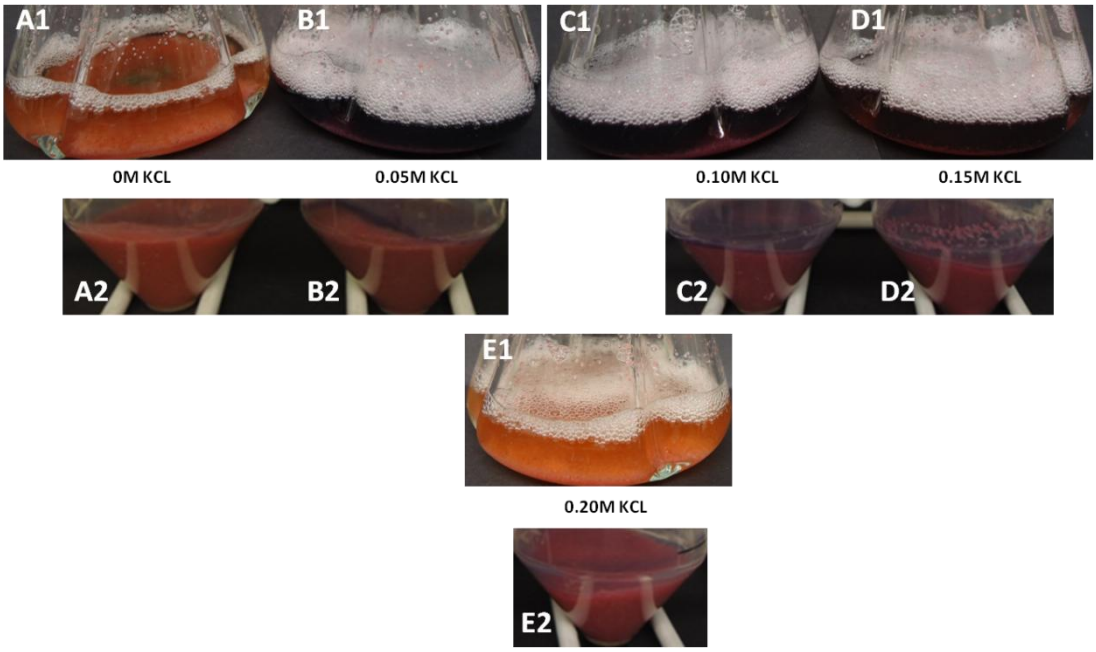

Figure 5-7: Actinorhodin production by *S. coelicolor* growth in liquid YEME after 48 hours at different concentrations of KCl (0M, A; 0.05M, B; 0.10M, C; 0.15M, D; 0.20M, E prior to TLC analysis.

Cultures (1) were pelleted (2) by centrifugation at 4000 rpm for 10 minutes in 50 ml falcon tubes.

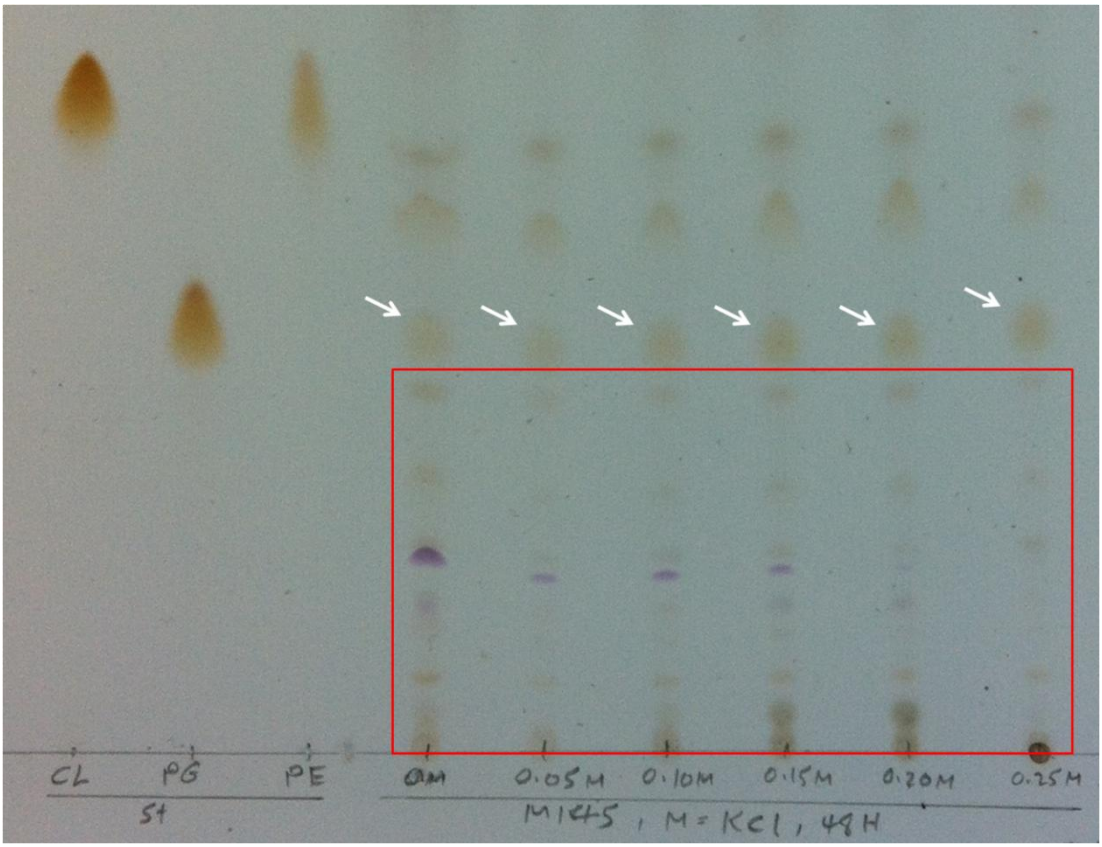

Figure 5-8: Determination of PL content during the osmotic adaptation of *S.coelicolor* at different concentrations of KCl.

PLs were extracted from 100 mg wet mass grown in YEME media incubated at 30°C, 220 RPM in 250 baffled flasks at 48 h. PLs were analysed on silica gel TLC plate and developed in chloroform/methanol/acetic acid/water (80:12:15:4) volume. TLC plate visualisation was performed with 10% sulphuric acid in ethanol (vol/vol) followed by charring on an oven. PG spots were marked with white arrows and unidentified spots were marked with red square. The experiment was carried out at n=3 to ensure reproducibility of the data obtained.

5.5 Analysis of PG of *S.coelicolor osaABCD* mutants during growth in liquid culture to investigate PL content in response to osmotic stress

5.5.1 Determination of PL content in the adaptation of *osaABCD* mutants to high salinity incubation in the absence and presence of KCl (0.20M)

osaA, B, C, and *D* mutant strains were obtained from Prof. Paul Dyson (Swansea University); these strains carry mutations in a regulatory system responsible for sensing osmotic stress in *S. coelicolor* and display normal development in the absence of osmotic stress (Figure 5.9). However, the aim of this analysis was to determine the effect of these mutations on the PL content of *S. coelicolor* in response to elevated levels of KCl. At the start of the experiment we cultured these strains on solid media (SFM) under conditions of high external osmolytes (KCl) in order to identify morphological changes (Figure 5.10). All the mutants, especially *osaC*, displayed clear differences in morphological development and actinorhodin production in response to elevated KCl concentrations when compared to *S. coelicolor* M145 The phenotypic characteristics of these strains could be distinguished; *osaA, osaB* and *osaC* mutants developed a gray appearance across the surface of the cultures while the *osaC* mutant showed a developmental delay in the production gray spores on SFM (Figure 5.9). Although the mutants could grow and form aerial hyphae on medium supplemented with KCl, they secreted large quantities of actinorhodin in agreement with previous work (Bishop et al., 2004).

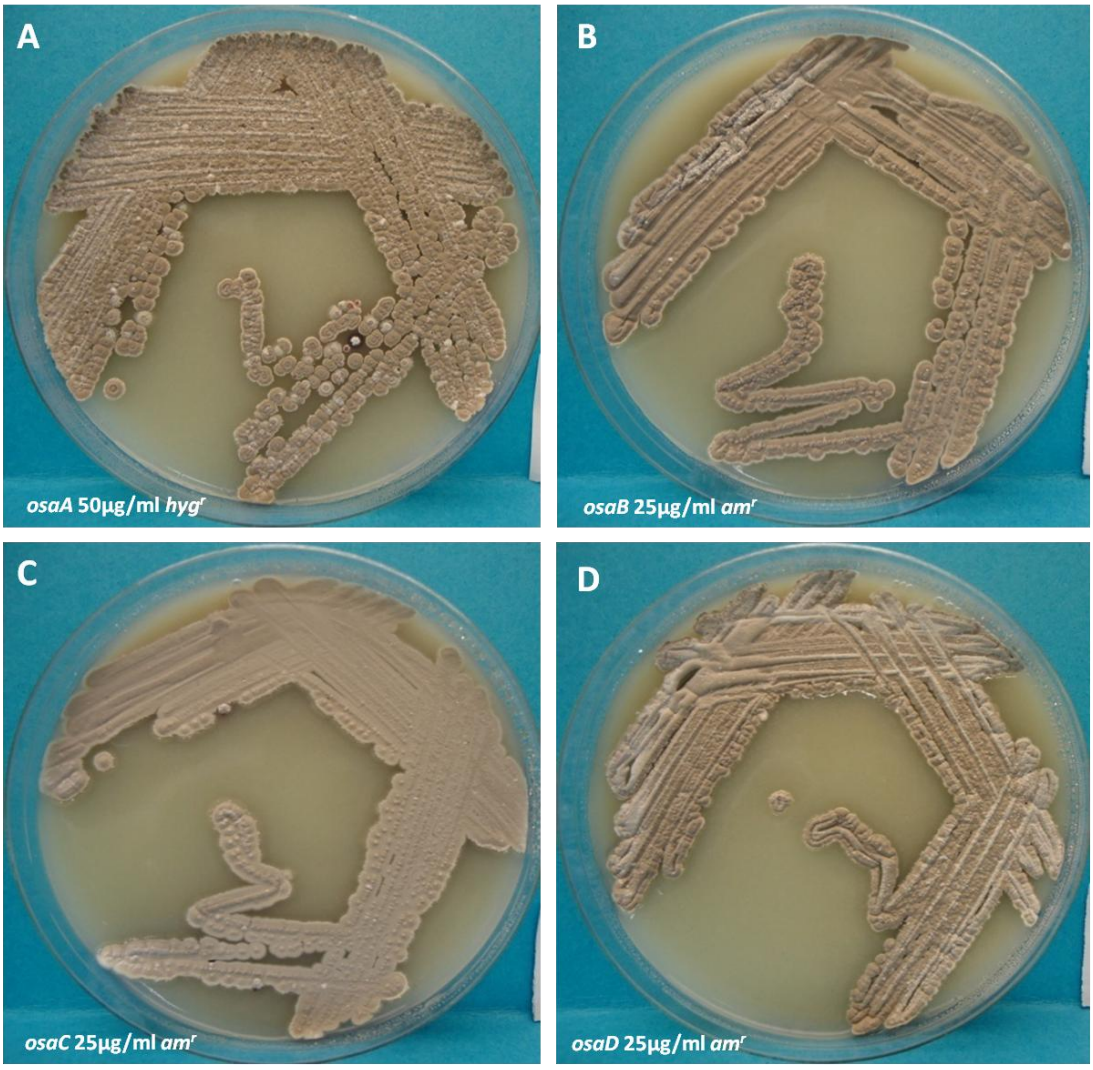

Figure 5-9: Phenotypic analysis of *osaA, B, C* and *D* mutants grown on SFM.

Growth of these mutants was visually assessed under the influence of appropriate selectable marker for antibiotic resistance. (A) *osaA* growth selected with *hyg*^{r}. (B) *osaB* growth selected with *am*^{r}. (C) *osaC* growth selected with *am*^{r}. (D) *osaD* growth selected with *am*^{r}. Cultures were incubated for 7 days at 30°C**.**

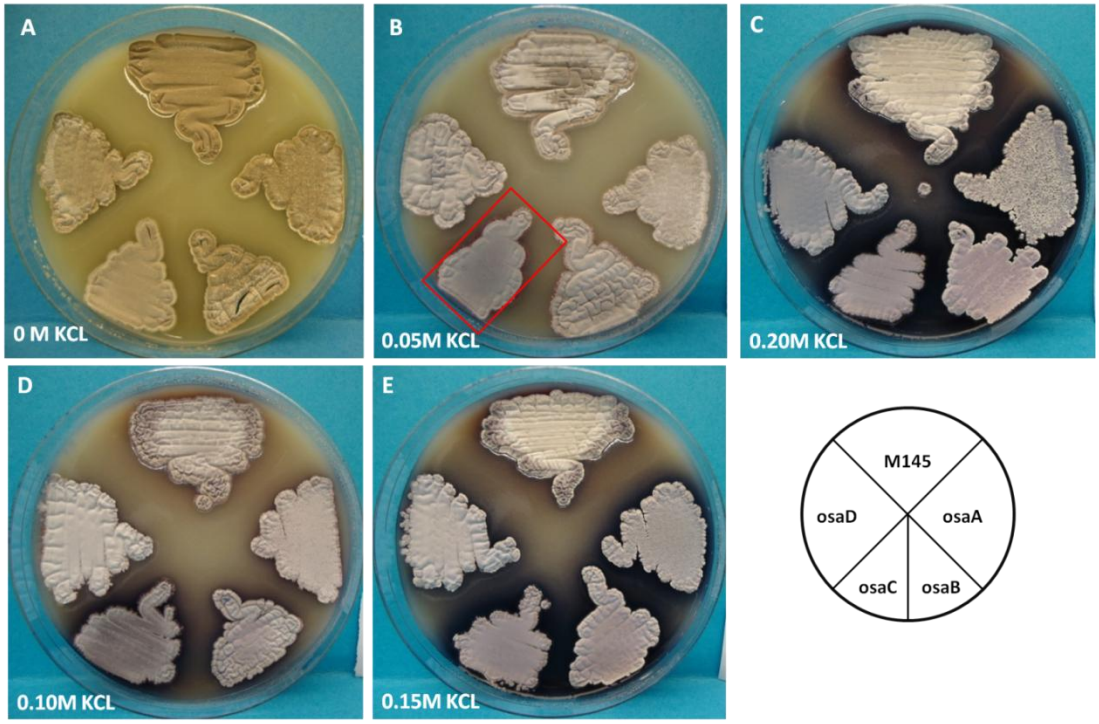

Figure 5-10: Effect of KCl on mutants of *osaA, B, C* and *D* mutant growth when cultured on SFM agar.

Concentrations of KCl were, 0.5M, 0.10M, 0.15M and 0.20M. Plates were incubated for 7 days at 30°C. All the mutants, especially *osaC*, displayed clear differences in morphological development and actinorhodin production in response to elevated KCl concentrations when compared to *S. coelicolor* M145.

After analysing changes in the development of the *osaAB* mutants on SFM agar we subsequently performed an experiment where we examined liquid grown *osaABCD* mutants cultured in YEME with elevated KCl (Figure 5.11). YEME grown cultures were examined at 24 h and 48 h to examine each strain for the production of antibiotics. The *osaA* mutant displayed a delay in growth as evidenced by the lack of growth at 24h (A1) both in the presence and absence of KCl. Despite this at 48h, this stain overproduced undecylprodigiosin in the presence of KCl; this pattern was also observed in the *osaC* mutant. On the other hand, the *osaB* and *osaD* mutants showed production of undecylprodigiosin in YEME at 24 h of growth with and without KCl (B2 and D2) and behaved similarly to the wild-type strain (Figure 5.7, A1 and E1). This allowed us to conclude that the *osaA* and *osaC* mutants are defective in their response to osmotic stress in terms of their production of undecylprodigiosin.

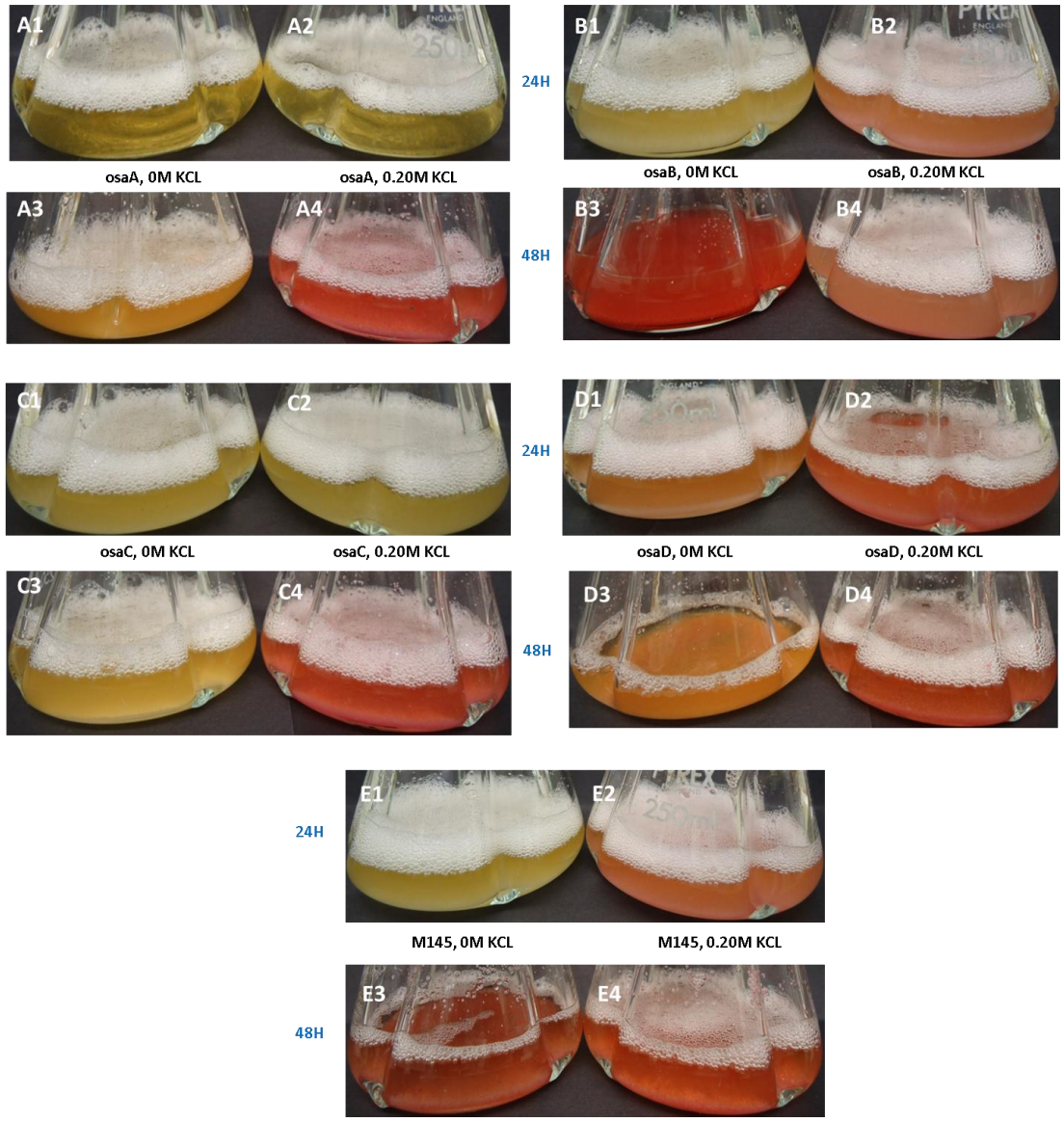

Figure 5-11: Phenotypic appearances of *osaABCD* mutants grown on YEME at 24h and 48 h, prior to TLC analysis.

Cultures were grown for 24 or 48h and examined visually for undecylprodigiosin production. Overall, undecylprodigiosin production was observed after 48h growth for the *osaA* and *osaC* mutants, while *osaB* and *osaD* increased undecylprodigiosin production after 24h growth. The experiment was carried out at n=3 to ensure reproducibility of the data obtained.

In order to investigate whether osmolarity had an effect on the PL content of the four mutant strains, we also extracted PLs from these cultures, subjected them to TLC analysis and visualised the PLs with both molybdenum blue spray (Figure 5.12A) and sulphuric acid charring (Figure 5.12B). As before, the addition of KCl to YEME media caused an increase in the amount of PG produced by *S. coelicolor* M145 (Figure 5.12, M1, M2) when visualised by both molybdenum blue and sulphuric acid charring. The delay in growth of the *osaA* mutant meant that we were unable to extract sufficient PLs for visualisation on the TLC plate (A1, A2). In a similar fashion to the wild-type strain, the *osaB* mutant showed a slight increase in PG production in response to increased KCl concentration. On the other hand, the *osaC* mutant produced similar levels of PG in both the presence and absence of KCl, whilst the *osaD* mutant produced less PG in the presence of KCl.

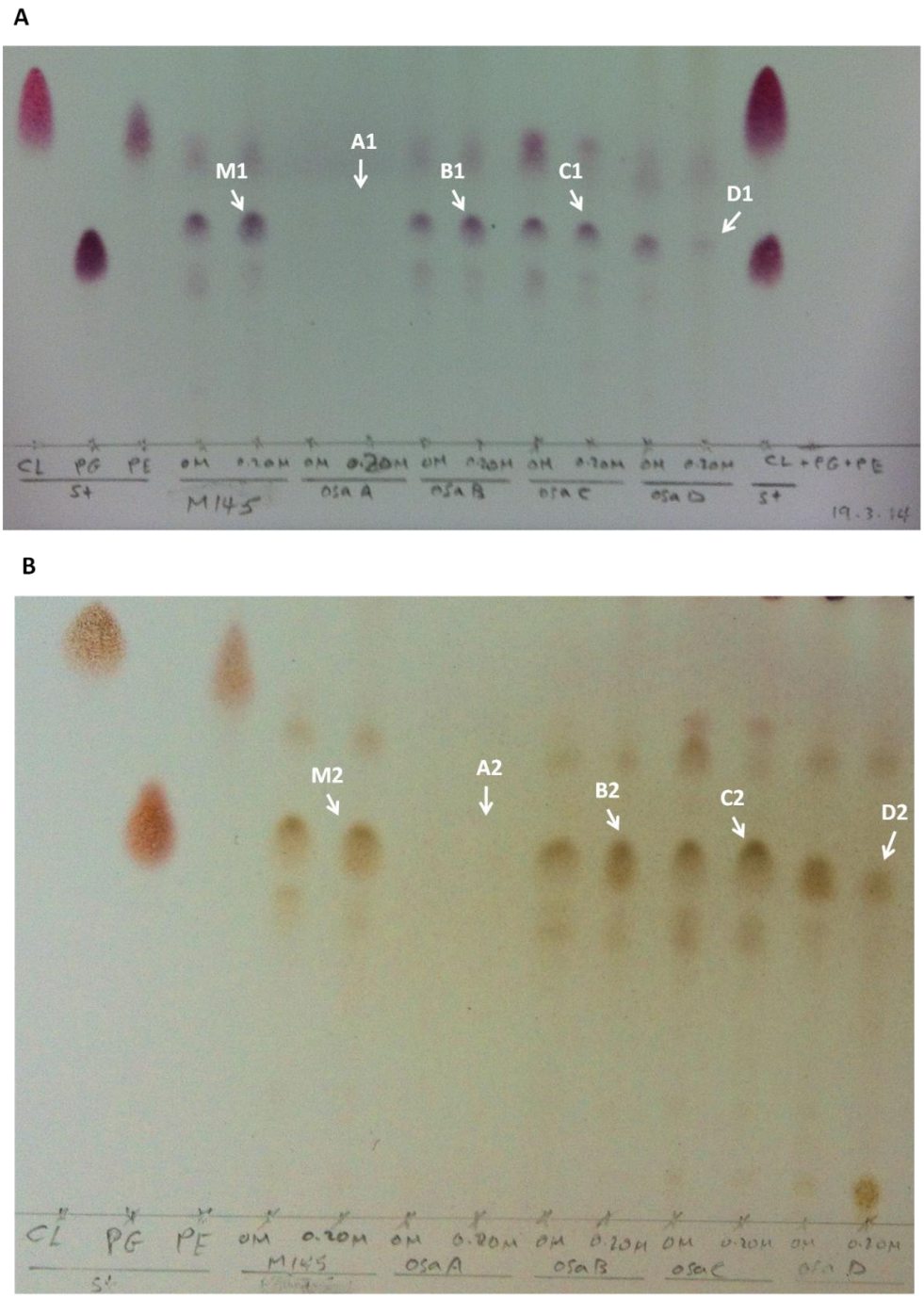

Figure 5-12: Visualisation for PL spots during the osmotic adaptation of *osaABCD* mutants in the absence and presence of KCl (0.20M) at 24h of growth.

PLs were extracted according to (Bligh and Dyer, 1959) (with slight modifications) from 100 mg wet mass grown in YEME media incubated at 30°C, 220 RPM in 250 baffled flasks. (A) TLC plate visualising was performed by anisaldehyde/H_2SO_4 spray followed by heat gun charring. (B) TLC plate visualising was performed by 10% sulphuric acid in ethanol (vol/vol) followed by charring in an oven. PG spots were marked with white arrows. The experiment was carried out at n=2 to ensure reproducibility of the data obtained.

As the PG content in *osaA* mutant under osmotic stress was undetectable after growth for 24 h, we also examined the PL content of the mutants and wild-type strain by PL extraction, TLC and visualization by sulphuric acid charring (Figure 5.13) after 48 h. As before, the addition of 0.20M KCl to *S. coelicolor* M145 led to an increase in the PG content of the mycelium (white arrow). This effect was also found in the *osaA* mutant that displayed an increase in this PL (black arrow) in addition to a number of other unidentified PLs. The *osaC* (purple arrow) and *osaD* (red arrow) mutants were unaffected by the addition of high salt (0.20M KCl) at least with respect to PG, although changes in the relative abundance of other PL spots could be seen. The PLs in *osaB* mutant at 0M KCl could not determine due to a fault of developing on the TLC plate. These results are consistent with previous results, in that the addition of osmotic stress leads to an increased content of PG of *S. coelicolor*, as is the case with the *osaA* (48h) and *osaB* mutants (24h). Both the *osaC* and *osaD* mutants differ from this, in that they both display similar levels of PG in response to osmotic stress. The exception to this is that the osaD mutant showed a reduction in PG under stress. Taken together this suggests that OsaC and OsaD may be involved in the sensing and transmission of hyperosmotic conditions to the systems that regulate PL content of the S. *coelicolor* membrane.

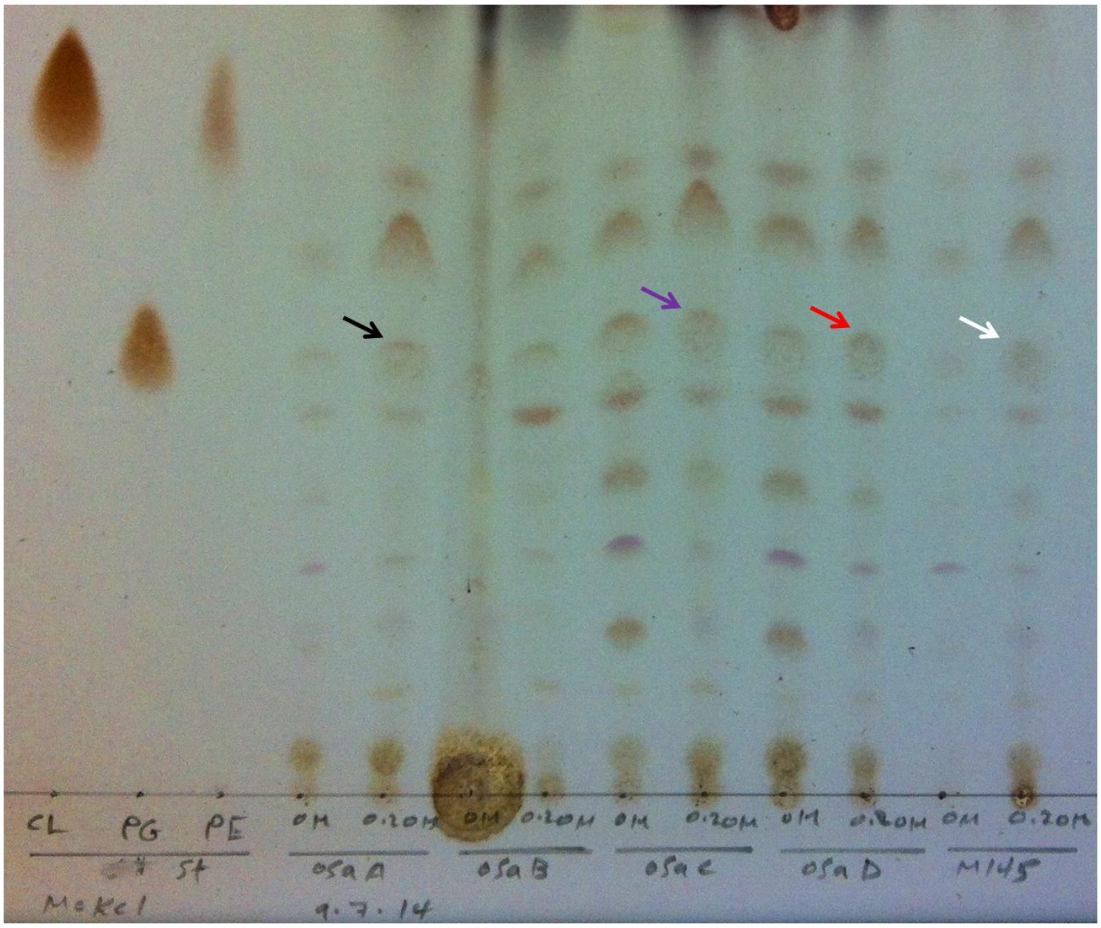

Figure 5-13: Analysis of PL content of *osaABCD* mutants in response to high salinity at 48 hours of incubation in the absence and presence of KCl (0.20M).

PG spots at 0.20M KCl concentration are marked with arrows (*osaA* with red, *osaC* with purple, *osaD* with red and M145 with white). PLs were extracted according to (Bligh and Dyer, 1959) (with slight modifications) from 100 mg wet mass grown in YEME media incubated at 30°C, 220 RPM in 250 baffled flasks. TLC plate visualised by 10% sulphuric acid in ethanol (vol/vol) followed by charring on an oven. The experiment was carried out at n=3 to ensure reproducibility of the data obtained.

5.6 Analysis of PG content of MA53541, MA532, MA52A and MA55B strains during growth in liquid culture in response to osmotic stress

Following earlier experiments that showed that the proportion of PG was increased with medium osmolarity in *S. coelicolor*, the analysis of the PL profiles MA53541, MA532, MA52A and MA55B was conducted to investigate changes in PG content in response to osmotic stress conditions. PG content of these strains was investigated under osmotic stress adaptation at 24 and 48 hours of incubation in the absence and presence of KCl (0.20M).

5.6.1 Investigation of PG content in the adaptation of MA53541, MA532, MA52A and MA55B strains to high salinity at 24 and 48 hours of incubation in the absence and presence of KCl (0.20M)

The effects of KCl concentration on the PG composition were analysed in our constructed strains containing additional copies of the *pgsA* operon genes by TLC. This experiment was carried out in order to analyse PG content at two time points, 24h and 48h. At 24 hours of growth, the most distinguishable strain that was most affected by the addition of 0.20M KCl was MA53541, the PG spot became more intense than the spot at 0M KCl. A similar observation was made with the control strain MA927 and the wild type *S. coelicolor* (Figure 5.14). No effect of adding 0.20M KCl was observed in the antisense *pgsA* strain MA532, where the PG spot retained a similar intensity to the spot at 0M KCl concentration (Figure 5.14). At 48 hours of growth, differences in PL intensity were more difficult to observe however MA53541, MA532, MA927 and MA52A showed an increase in PG spot intensity in the presence of salt (0.20M KCl) with more intensity appearance (Figure 5.15). Again, (Figure 5.15) both treated and untreated cultures of MA55B gave very poor yield of PLs. Clearly, as the cultures grew, they must have contained PLs in their membranes; perhaps the high levels of expression of the *SCO5755* regulator brought about chemical modifications to the PL content that made them difficult to extract or resolve by TLC (Figure 5.15).

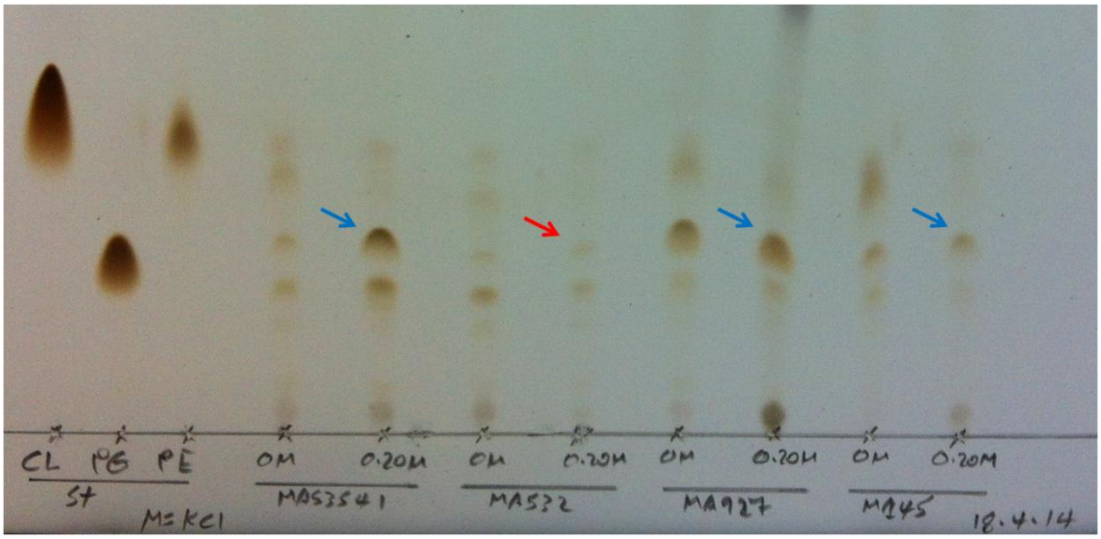

Figure 5-14: Investigation of PG content in the adaptation of constructed strains to high salinity at 24 hours of incubation in the absence and presence of KCl (0.20M).

PG spots at 0.20M KCl concentration were marked with arrows (MA53541, MA927 and M145 with blue, MA532 with red). PLs were extracted according to (Bligh and Dyer, 1959) (with slight modifications) from 100 mg wet mass grown in YEME media incubated at 30°C, 220 RPM in 250 baffled flasks. TLC plate visualised by 10% sulphuric acid in ethanol (vol/vol) followed by charring on an oven. The experiment was carried out at n=2 to ensure reproducibility of the data obtained.

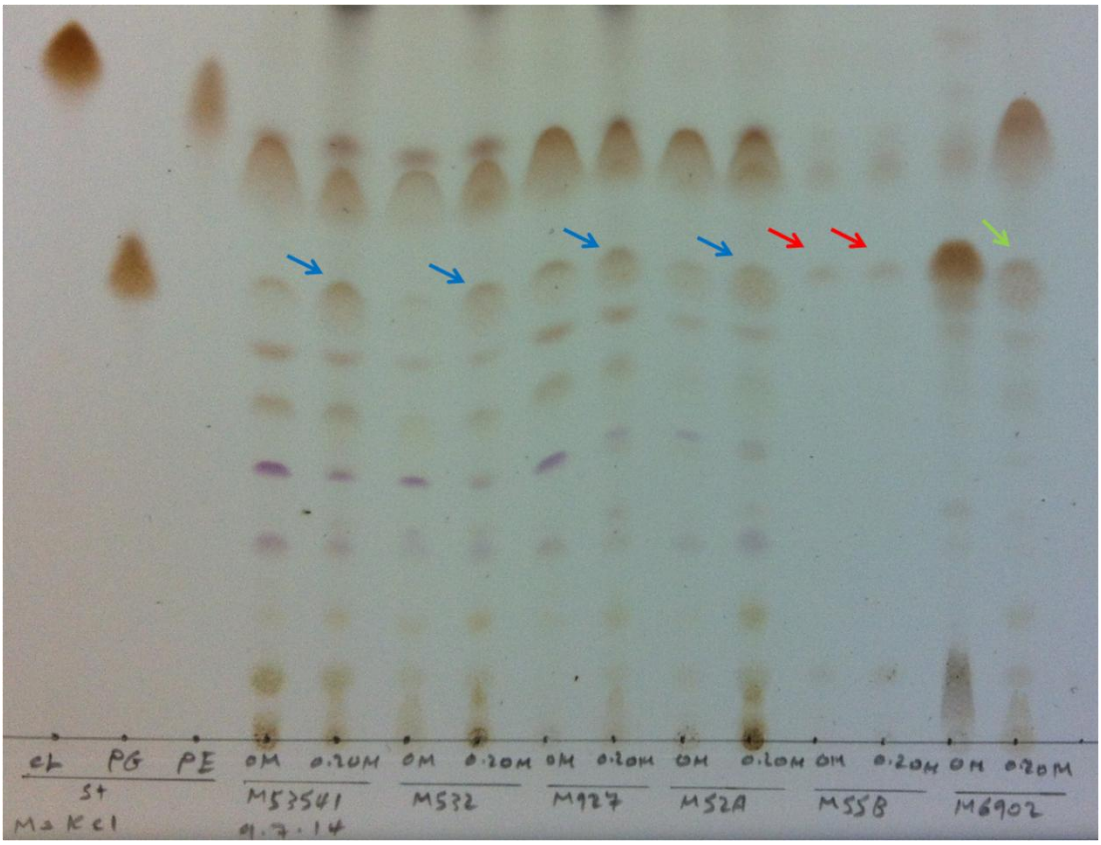

Figure 5-15: Examination of PG content in the adaptation of constructed strains to high salinity at 48 hours of incubation in the absence and presence of KCl (0.20M).

PG spots at 0.20M KCl concentration were marked with arrows (MA53541, MA532, MA927 and MA52A with blue, MA55B with red and M145 with green). PLs were extracted according to (Bligh and Dyer, 1959) (with slight modifications) from 100 mg wet mass grown in YEME media incubated at 30°C, 220 RPM in 250 baffled flasks. TLC plate visualised by 10% sulphuric acid in ethanol (vol/vol) followed by charring on an oven. The experiment was carried out at n=2 to ensure reproducibility of the data obtained.

5.7 Discussion of Chapter 5

The ability of *S. coelicolor* to grow in a range of salt concentrations was observed in this chapter; we aimed to elucidate the role of PG in the adaptation of *osaABCD* mutants as well as the constructed strains that contained genes of the *pgsA* operon cloned under the control of the tsr inducible promote. By means of an improved visualisation method, the analysis of the PL component from *S. coelicolor* suggested that PG levels increased in parallel to an increase in concentration of KCl. It was found that induction of *SCO5753* in MA53541 could not be achieved with 0.05µg/ml tsr and, as a result we decided to induce with 25 µg/ml tsr for 48 h. Although PG spots of MA53541 were not significantly affected by 25 µg/ml tsr, the small increase in spot intensity suggests that there was some induction of gene expression in the presence of the inducer. This is corroborated to some degree by the fact that MA532 (antisense *pgsA*) decreased PG slightly in the presence of tsr and is consistent with expression of anti-sense *SCO5753* reducing translation of sense *SCO5753*. Interestingly, we were unable to isolate good quality PLs from cultures of MA55, where *SCO5755* was cloned under the control of *ptipA*. Both treated and untreated cultures of MA55B gave very poor yield of PLs. Clearly, as the cultures grew, they must have contained PLs in their membranes; perhaps the high levels of expression of the *SCO5755* regulator brought about chemical modifications to the PL content that made them difficult to extract or resolve by TLC.

In order to investigate the effect of osmotic stress on the PL content of *S. coelicolor*, we first analysed the wild-type strain, *S. coelicolor* M145 where it was clear that the intensity of PG spots increased in response to KCl concentration during the growth of *S. coelicolor* and allowed us to conclude that wild type *S. coelicolor* responded to increased osmolarity through the synthesis of elevated level of PG. This may be a measure taken by an organism to protect the structural integrity of the membrane under this environmental challenge. Interestingly, this effect was reversed at very high levels of KCl and may have been as a result of the organism's osmoregulatory systems becoming overwhelmed under extreme hyper-osmotic conditions.

In *S. coelicolor*, the osmoregulatory genes (*osaA*, *osaB*, *osaC* and *osaD*) are known to be involved in evoking response to external hyperosomolarity (Bishop et al., 2004). As such, we investigated how PLs in general and PG in particular changed in this collection of mutants in response to external osmotic shock. The *osaA* mutant displayed an increase in PG in addition to a number of other unidentified PLs under elevated KCl and behaved in a similar fashion to the control strains. The *osaC* and *osaD* mutants were unaffected by the addition of high salt (at least with respect to PG; this suggests that the proteins encoded by these genes are responsible for communicating hyperosmotic conditions to the regulatory systems that govern induction of PG synthesis. Recent studies have showed that the sigma factor σ^B controls the osmotic and the oxidative response in *S. coelicolor*. Microarray studies revealed that more than 280 genes were induced by 0.2M KCl in a σ^B dependent manner. In this regulon are a number of genes that encode sigma factors whose induction is thought to direct the synthesis and uptake of osmolytes. Six genes encoding sigma factors have been clustered hierarchically and are induced by KCl (*sigB, sigL, sigM, sigH, sigI* and *hrdD*) (Lee et al., 2005). Fluorescence microscopy revealed that CL is involved in the placement of proteins (ProP) at the cell poles in *E. coli* (Romantsov et al., 2007). This protein is subject to the osmotic stress response via the subcellular localisation of ProP at the bacterial cell poles (Romantsov et al., 2008). In *B. subtilis*, PG, the direct precursor of CL, is increased in parallel to osmolarity conditions (Lopez et al., 2000). Moreover, PG in *B. subtilis*, is involved in the localisation of the cell division protein MinD to the bacterial cell membrane (Barák et al., 2008).

We also examined the effects of KCl concentration on the PG composition in our strains that contained components of the *pgsA* operon under the control of *ptipA*. The most obvious strain that was most affected by the addition of KCl was MA53541, where the PG spot became more intense than the spot at 0M KCl. This is likely due to osmotic induction of *ptipA* (Ali et al., 2002); if so it further supports the role of *SCO5753* in PG synthesis, although a similar observation was made with the control strain MA927 and the wild type *S. coelicolor*. Again, both treated and untreated cultures of MA55B gave very poor yield of PLs. Clearly, as the cultures grew, they

must have contained PLs in their membranes; perhaps the high levels of expression of the *SCO5755* regulator brought about chemical modifications to the PL content that made them difficult to extract or resolve by TLC. Alternatively, the low yields obtained in the TLC plates might have been due to low extraction yields, lack of resolution or a limitation of the staining and visualization method. It is known that CL, synthesized from PG, is required for *S. coelicolor* development (Jyothikumar et al., 2012) and the inability of this strain to synthesize a normal PL profile may explain the failure of this strain to develop normally, as described in the previous Chapter.

Future studies on *S. coelicolor* should study the growth curves of constructed strains in order to obtain a better understanding of how the strains behave in liquid media (Kieser et al., 2000). At the same time, in order to determine *pgsA* operon expression in different growth conditions and other associated metabolic functions of PL genes in *S.coelicolor* development, RT-PCR could be carried out. This approach is especially important since we have constructed *pgsA* in an antisense direction in the strain MA532; RNA isolation at various time points coupled with RT-PCR could provide a full understanding of *pgsA* expression levels during the *Streptomyces* life cycle. We provisionally identified PL spots on the basis of their similarity with known standards on TLC plates. Clearly this does not allow us to conclusively identify these spots given the many different PL that are made by bacteria. As a result the key analysis necessary to confirm many of our findings would be to purify PL spots from TLC plates, extract the PL from the plate silica and subject it to lipidomic analysis by mass spectrometry and NMR. If MS/MS were employed, not only would it be possible to identify the molecular weight of the PL it would also be possible to identify the head group and length of each individual acyl chains. Although it was used not for the purpose of identifying spots on TLC plates, this approach was used in *S. coelicolor* to carry out a provisional characterisation of the lipidome of this organism (Jyothikumar et al., 2012). This research demonstrated that the PLs predicted in earlier studies (Borodina et al., 2005, Sandoval-Calderon et al., 2009) were found *in S. coelicolor*. These PLs included CL, PG, PE, PS and PI.

Chapter 6:

Effect of induction of the *pgsA* operon genes on mycelial architecture of *S. coelicolor*

6. Effect of induction of the *pgsA* operon genes on mycelial architecture of *S. coelicolor*

6.1 Introduction to Chapter 6

Bacterial cell wall synthesis has gained new insights from localisation analysis; the cell wall is the major stress-bearing and shape-maintaining component of the bacterial cell and its integrity is of essential importance for cell integrity (Höltje, 1998, Scheffers and Pinho, 2005). The ability of bacteria to survive is dependent on membrane lipid homeostasis and on a capability to change lipid components during adaptation of the bacterial cell to various environments (Zhang and Rock, 2008). For example, with regard to chapter 5, the proportion of anionic PLs such as PG of *S. coelicolor* increased during osmotic stress treatment. The participation of lipids in bacterial cell division has recently received increasing attention, for example, PG has been suggested to act as a principal constituent of the lipid spiral developing along the cell membrane in *B. Subtilis* (Muchova et al., 2011, Muchova et al., 2010, Mileykovskaya and Dowhan, 2005) and these recent developments have provoked renewed attempts to understand cell wall development and the maintenance of cell shape. Fluorescence imaging methods are nowadays being used on single bacterial cells for locating protein position, protein-protein responses, protein localisation and protein mobility *in vivo* (Meyer and Dworkin, 2007).

The application of fluorescence microscopy has changed our understanding of bacterial morphogenesis within the last few years. This revolution in the use of fluorescence microscopy has allowed scientists to investigate the localisation of enzymes implicated in bacterial cell wall synthesis in growing cells, plus to look at localisation of recently integrated cell wall components in live cells (Scheffers and Pinho, 2005). Furthermore, developments in fluorescence microscopy have revolutionised our understanding of the structure of bacterial cells, mainly through cell division proteins and lipid localisation. For example, it has shown that the CL and FlAsH-labeled transporters ProP and LacY are localised more at the poles of *E. coli* cells (Romantsov et al., 2010). Similar inroads were promoted by fluorescence microscopy in growth polarity and cell division in *S. coelicolor* where DivIVA is localised at the tips and is engaged in tip elongation (Flärdh, 2003).

The latest biochemical and physiological analysis has showed that bacterial membrane lipids are required for the main cell cycle events. For instance, acidic PLs such as PG in the fluid phase, are involved in activating DnaA, the initiator protein of *E. coli* DNA replication by assisting a replacement of tightly bound ADP with ATP (Fishov and Woldringh, 1999). It has been suggested that the incorporation of external membrane proteins possibly contributes to chromosome segregation by interacting with specific lipid domains (Woldringh et al., 1995). The involvement of these lipid domains' was studied indirectly using a range of techniques; for example the distribution of PLs in *E. coli* was revealed by fluorescence imaging microscopy (Fishov and Woldringh, 1999). Another association was anticipated, in that PL defects might influence the accurate response of FtsZ to the cell membrane and change the ring structure (Mileykovskaya et al., 1998).

Membrane constituents with the ability to induce a high extent of curvature include the anionic PL, CL, which is established in bacterial and mitochondrial membranes. CL is visualized in living cells by staining with 10-*N*-nonyl-acridine orange, (NAO), a fluorescent dye that interacts with PLs of cell membranes and has higher affinity for CL than other anionic PLs (Mileykovskaya and Dowhan, 2000). In *B. subtilis*, staining cells with NAO revealed green fluorescence domains which were observable in the septal areas and poles. These fluorescent domains were hardly visible in a *clsA* disrupted mutant that was deficient in CL (Kawai et al., 2004). Despite these examples of *E. coli* PLs, heterogeneity of PLs in *S. coelicolor* was not fully studied until recently (Jyothikumar et al., 2008). In this chapter we used fluorescein–WGA/propidium iodide staining to detect any morphological changes of nucleic acid and peptidoglycan of *S.coelicolor* cultures in response to changing expression of the *pgsA* operon genes. By means of imaging with immunofluorescence microscopy such as this, it was revealed that following accumulation of the cell division protein FtsZ into ladder shapes in the aerial filaments of *S. coelicolor*, cross wall are laid down that divide the aerial hypha into prespore compartments (Schwedock et al., 1997). Also, fluorescein–WGA/propidium iodide wall staining method was able to visualise apical tip development in vegetative hyphae (Schwedock et al., 1997). The cell walls were visualized after lysoyme treatment and staining them with fluorescent

conjugates of letin wheatgerm agglutinin (WGA). WGA binds to oligomers of N-acetylglucosamine and N-acetylmuramic acid and, as such, binds to lysozyme treated cell walls. Nucleoids were stained with the fluorescent intercalating agent propidium iodide (PI) (Schwedock et al., 1997). In this chapter we used this staining technique to stain DNA and cell walls in *Streptomyces* in order to determine the effect of modulation of expression of the *pgsA* operon on the architecture of the *S. coelicolor* vegetative mycelium, aerial mycelium and spores. The strains constructed during this project MA53541 (*pgsA/ptipA*, sense orientation) and MA927 (*pgsA/ptipA*, empty vector control) samples were analysed using a Nikon TE200S inverted microscope with a 100X objective lens. In order to examine any morphological alterations that could be observed in response to changes in expression levels of genes of the *pgsA* operon before and after tsr addition, captured images were processed using IPlabs 3.7 image processing software. All strains were visualised by phase contrast (bright field) and fluorescence microscopy (FITC and TRITC filters).

6.2 Aim of Chapter 6

In conjunction with the analysis presented in the previous chapter, microscopic analysis of apical growth, branching, and morphogenetic development of *S .coelicolor* were carried out. Through the use of fluorescence microscopy, we attempted to study the changes of *pgsA* overexpression in *S. coelicolor* and the morphological consequences of this on substrate, aerial hyphae and spores. In order to study this, we grew MA53541 and MA927 on SFM agar in the presence and absence of tsr. We were not able to include MA532 in our study because we did not have this strain available at the time of this investigation; when it later became available, we were fully focused on other investigations. Thus our findings should be interpreted in the context of this limitation. The measurements of morphological parameters that quantitatively illustrated mycelial architecture were made from still images. This measuring scheme was carried out on apical tip distance, branch angle, and inter-branch distance for the first and second days (Figure. 6.1). On the third day, measurement was carried out on cross wall distance in aerial hyphae and on the fourth day measurement was made on spore width. Eventually, statistical analysis of these multiple data sets was carried out using Microsoft Excel 2007 and Minitab

(Version 17) to obtain mean±SD and bar charts. Statistical differences between the data sets obtained for the two strains under normal and stressful conditions were measured using the Student t-test. Where data was found to significantly deviate from normality following a Kolmogorov-Smirnov normality check, analysis was proceeded using the Mann-Whitney test which is non parametric. In either case, significance was tested at p = 0.05 level and the 95% confidence intervals were determined.

6.3 Morphological analysis of MA53541 and MA927 using fluorescence microscopy

The effect of changing expression *pgsA* on growth and morphology were investigated by growing MA53541 and MA927 on SFM in the presence and absence of tsr. *Streptomyces* spore suspensions of MA53541 and MA927 strains were inoculated on coverslips placed at 45° angles into SFM agar. The plates were incubated at 30ºC for 1 to 4 days and coverslips were removed daily for fixation and staining with FITC-WGA/PI for analysis by fluorescence microscopy. Samples were analysed using a Nikon TE200S inverted microscope at 1000X magnification in two ways. Firstly using a bright field filter for measurements of apical tip distance, interbranch distance, branching angle and spore width measurements (Figure. 6.1) and secondly with a FITC filter for cross wall distance measurements. The measurement of several parameters was carried out which quantitatively illustrated mycelial architecture of fixed cells. These parameters used in this chapter are as follows: on the first and second day of development, measurements were performed on apical tip distance, branch angle and inter-branch distance. On the third day of incubation, measurement was on cross wall distance while on the fourth day of growth spore widths were measured. Quantitative analysis was carried out between treated (with tsr) and untreated (without tsr) strains with the use of Microsoft Excel (Histogram). Both strains MA53541 and MA927 was visualised using FITC (green) and TRITC (red) filters. Staining was done using the fluorescent dyes FITC-WGA and PI (TRITC) that allowed the visualization of peptidoglycan and nucleoids respectively.

6.4 Morphological analysis of altering *pgsA* expression on the apical tip distance of *S. coelicolor*

In this experiment we investigated the effect of altering *pgsA* expression on apical tip distance from MA53541 in comparison to the control strain MA927 in the presence and absence of tsr. Measurements were based on the schematic diagram of hyphal measurements in (Figure 6.1). The staining pattern with PI and WGA are shown in panel 1, 2, 3 and 4 of the (Figure 6.2A, B, Figure 6.3 D, and E). For Examples, panel 1 illustrates hyphae with DNA stained with PI (red), panel 2 is cell walls stained with WGA (green), panel 3 is phase contrast image and panel 4 is multiprobe image where all channels are merged. After one day of growth, the majority of apical tip distances fell within the range of 1-17 µm for all strains. MA53541 (+tsr) displayed more apical tip distances that fell in the range 1-17µm in comparison with MA927 (+tsr) (Figure 6.2C). Interestingly, the largest distance measured was 61 µm for MA927 (+tsr) whilst for MA53541 (+tsr) the largest distance measured was 41 µm (Figure 6.2C). Although not as marked, this effect was also seen in the absence of tsr, as the largest tip distances were seen in MA927 (-tsr) at 57µm compared to 33µm for MA53541 (-tsr) (Figure 6.3). Although tsr strongly induces *ptipA* expression, even in the absence of the inducer expression from this promoter is still significant. A maximum of 36% of apical tip distances fell within the 1-5µm range for MA53541 (+tsr) compared to 56% for MA53541 (-tsr) (Figure 6.3F).

Further statistical analysis was done using t-test to compare the data obtained for the two strains with and without treatment. The mean±SD of the apical tip distances for MA927 (+tsr) and MA53541 (+tsr) were 15.6±14.8 µm and 8.11±6.80 µm respectively, while for MA927 (-tsr) and MA53541 (-tsr) were 9.4±10.8 µm and 7.69±8.75 µm respectively. There was a statistically significant difference between apical distances for MA927 (+tsr) and MA53541 (+tsr) ($p = 0.003$, 95% CI = 2.65, 12.42 µm) but the apical tip distances for MA927 (-tsr) and MA53541 (-tsr) were not significantly different statistically ($p = 0.509$, 95% CI = -3.56, 7.01 µm).

Therefore, we observed that in the presence of tsr, MA927 (+tsr) seems to grow in long apical tip distance, whereas MA53541 (+tsr) forms many apical tips rather than

growing over a long distance (Figure 6.2A, B white arrows). This difference is statistically significant with a p-value < 0.05. Likewise we observed a related effect in the absence of tsr on MA927 (-tsr) and MA53541 (-tsr) (Figure 6.3D, E white arrows), but this was found not to be statistically significant ($p > 0.05$).

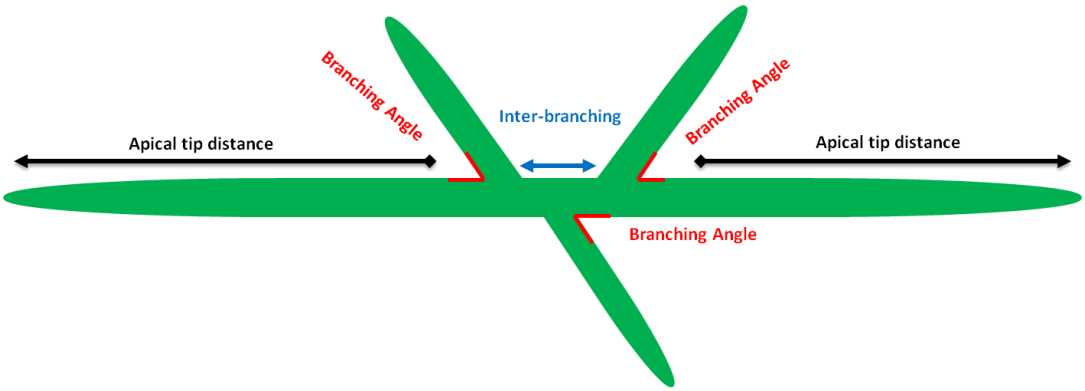

Figure 6-1: Schematic diagram for measurements of the mycelial architecture.

Measurements were the apical tip distance of hyphae that was determined from the apical tip to the initial branch, branching angle was calculated between the apical tip hyphae and its branches from an angle produced at the apical tip hyphal direction (an angle adjacent to the nearest apical tip). Finally, inter-branch distance was calculated of hyphal distance between the two closest branches.

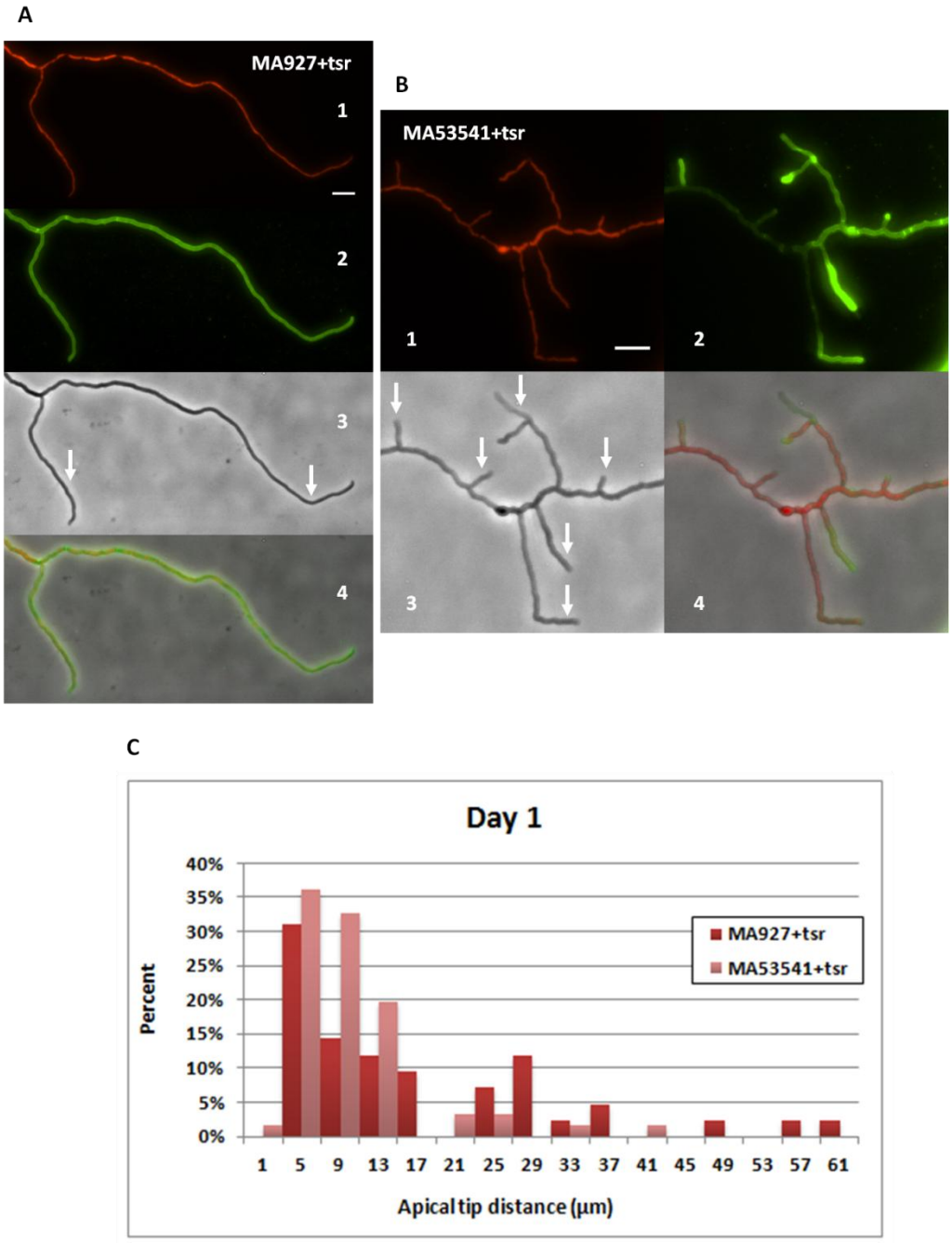

Figure 6-2: Morphological investigation of changing *pgsA* expression on the apical tip distance in the presence of thiostrepton after one day of growth.

Representative images of MA927 +tsr (A) and MA53541+tsr (B) showing DNA stained with PI-TRITC (1); cell walls stained with WGA-FITC (2); bright field image examined by phase contrast microscopy (3); composite image where all filters were merged (4). White arrows illustrate long hyphae without branching in MA927 and increased branching in MA53541. Quantitative analysis of apical tip distances in the strains (C). The data was divided into bins of 4µm and is displayed as a percentage of the total number of measurements (n=42, MA927; n=61, MA53541. White scale bar is 5µm.

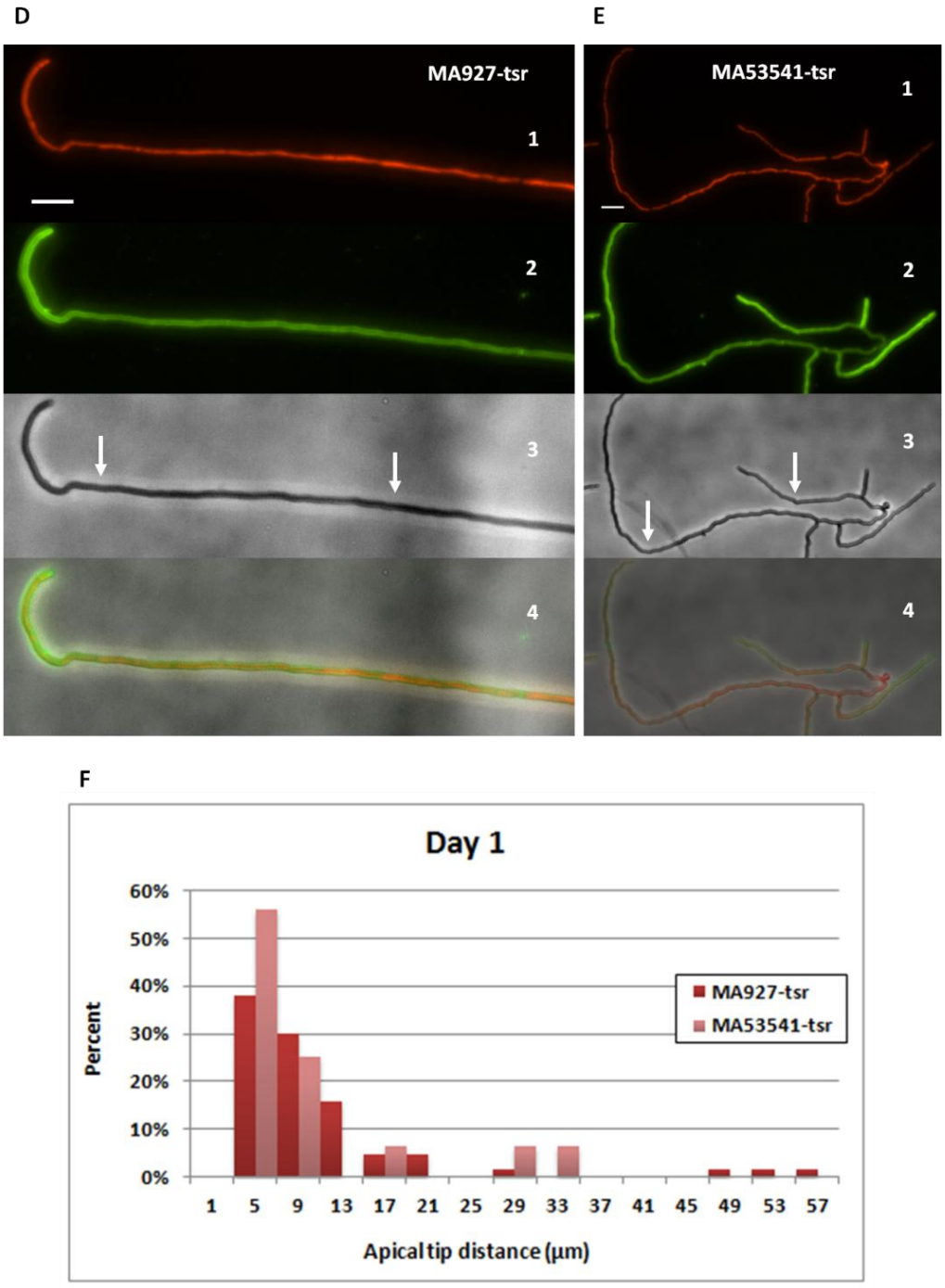

Figure 6-3: Morphological investigation of changing *pgsA* expression on the apical tip distance in the absence of thiostrepton after one day of growth.

Representative images of MA927 (D) and MA53541 (E) showing DNA stained with PI-TRITC (1); cell walls stained with WGA-FITC (2); bright field image examined by phase contrast microscopy (3); composite image where all filters were merged (4). White arrows illustrate long hyphae without branching in MA927 and increased branching in MA53541. Quantitative analysis of apical tip distances in the strains (F). The data was divided into bins of 4µm and is displayed as a percentage of the total number of measurements (n=63, MA927; n=61, MA53541. White scale bar is 5µm.

After two days of growth, we could observe that the general view after one day of development was similar. Examples of phase contrast and fluorescence microscopy images showed a similar effect with growth after one day (data not shown). MA53541 (+tsr) showed again a greater percentage of apical tip distances that were smaller than the treated control MA927 (+tsr), with the former having 40%, 36% and 19% of apical tip distances in the range of 0 µm to 15 µm. Again MA927 (+tsr) showed longer apical tip distances (over 20 µm) than MA53541 (+tsr) (Figure 6.4A). Under normal conditions of growth, MA927 (-tsr) had a slightly higher percentage of apical tip distances at the ranges 5 µm to 10 µm than MA53541 (-tsr) (Figure 6.4B). The mean±SD of the apical tip distances for MA927 (+tsr) and MA53541 (+tsr) were 20.6±23.1 µm and 7.21±6.75 µm respectively, while for MA927 (-tsr) and MA53541 (-tsr) were 8.07±7.94 µm and 8.28±7.01 µm respectively. There was a statistically significant difference between apical distances for MA927 (+tsr) and MA53541 (+tsr) ($p = 0.001$, 95% CI = 5.84, 20.86 µm) but the apical tip distances for the controls MA927 (-tsr) and MA53541 (-tsr) were not significantly different ($p = 0.819$, 95% CI = -2.056, 1.628 µm).

Therefore, in consistence with the results obtained in day 1, we observed that in the presence of tsr, MA927 (+tsr) grows in long apical tip distance whereas MA53541 (+tsr) forms many apical tips. Taken together this suggests that increased expression of the *pgsA* operon genes in MA53541 (*SCO5753* and *SCO5754*) leads to branching closer to the hyphal tip which significantly shortens its apical tip distance. This is consistent with the role of PG as a precursor to CL (Sandoval-Calderon et al., 2009), as increased production of CL leads to increased branching in *S. coelicolor* (Jyothikumar et al., 2012).

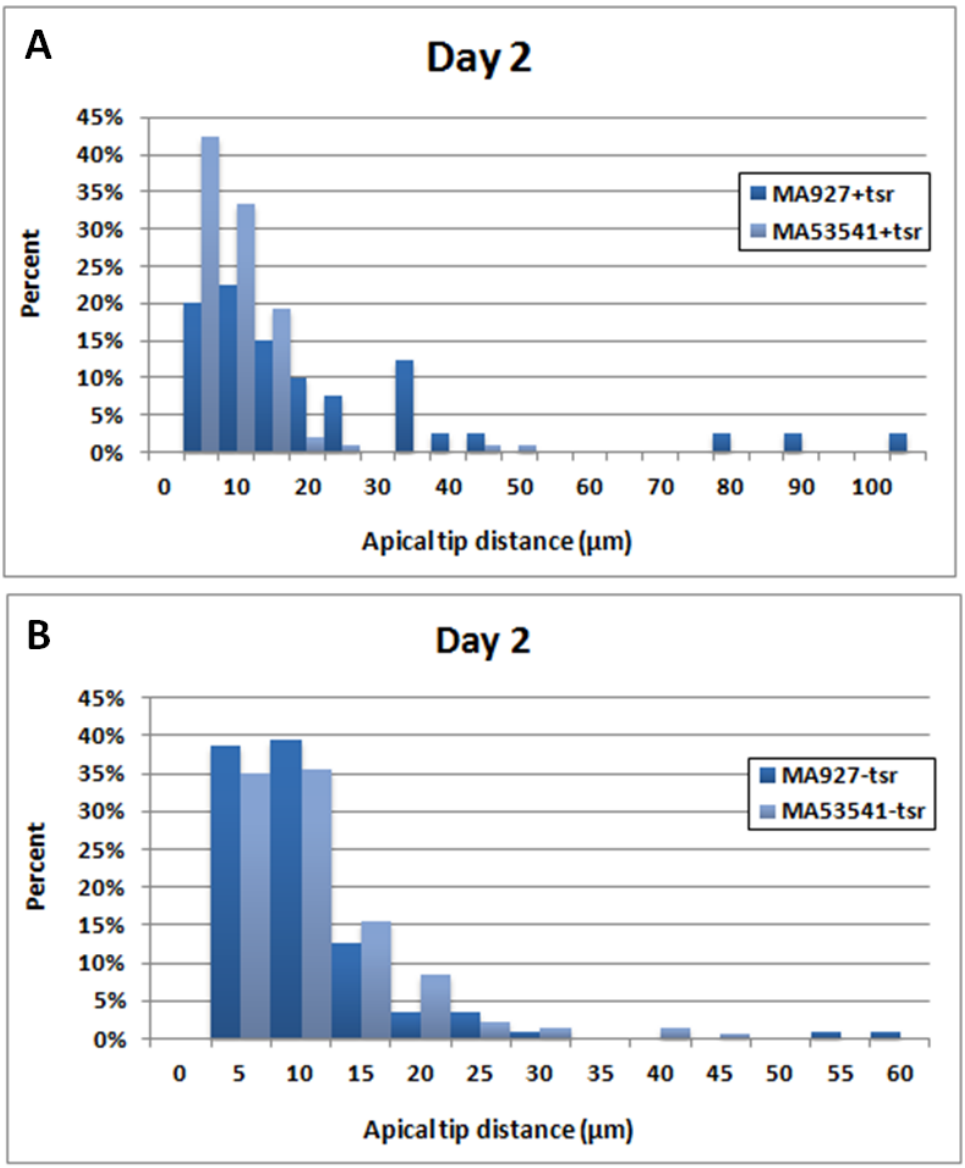

Figure 6-4: Quantitative analysis of apical tip distances in the strains MA53541 (+ tsr) and MA927 (+ tsr) (A) and MA53541 (-tsr) and MA927 (-tsr) (B) after two days of growth.

The data was divided into bins of 4µm as a percentage of the total number of measure and is displayed as a histogram. n= 40 for MA927 (+tsr), 99 for MA53541 (+tsr), 119 for MA927 (-tsr) and 143 for MA53541 (-tsr).

6.5 Morphological analysis of altering *pgsA* expression on the branch angle of *S. coelicolor*

Further image analysis was carried out on branching angles to investigate the effect of changing *pgsA* operon gene expression during the first and second day of growth. A similar schematic diagram was followed in (Figure 6.1) for microscopy and statistical analysis. The staining pattern with PI and WGA is shown in the panels 1, 2, 3 and 4 (Figure 6.5A, B, Figure 6.6 D, and E). For Example, panel 1 illustrates hyphae with DNA stained with PI (red), panel 2 is cell walls stained with WGA (green), panel 3 is phase contrast image and panel 4 is a merged image where all channels are merged. After one day of growth both treated strains showed a variety of angles with majority in the range 50-122° for MA927 (+tsr). MA53541 (+tsr) showed a higher percentage than MA927 (+tsr) of branch angles in the range of 98-110°. Also, MA927 (+tsr) revealed a higher percentage than MA53541 (+tsr) of branch angles in the range of 56-74°. Interestingly, MA927 (+tsr) was observed with the largest angle of 158° (Figure 6.5C). With no addition of tsr, the pattern of growth changed slightly, we observed that the MA53541 (-tsr) branch angle mostly lay in the ranges 86-110° whereas those of MA927 (-tsr) were more widely distributed (Figure 6.6F). Therefore, we observed that in the presence of tsr the mean±SD of the branching angles were 84.1±26.4º for MA927 (+tsr) and 82.5±35.3º for MA53541 (+tsr) respectively. The latter strain had visibly more cells which developed so that branches emerged in a more perpendicular fashion, in the range of angles 98-110° (Figure 6.5A3, B3 inset), which probably explains the slightly higher standard deviation (SD) value around the mean. Comparison of the data using a t-test, however, showed no statistically significant difference between branching angles of the two strains ($p = 0.818$, 95% CI = -12.49°, 15.77°). In the absence of tsr, growth for MA927 (-tsr) still develop in wide range of distributed angles (mean = 87.9º, SD = 30.6°) whereas MA53541 (-tsr) formed many branches more close to right angles in terms of branch emergence (mean = 93.2º, SD = 13.7°) (Figure 6.6D, E white arrows). However, this observed effect was not statistically significant after comparison of the branching angles using the t-test ($p = 0.291$, 95% CI = -15.04°, 4.57°).

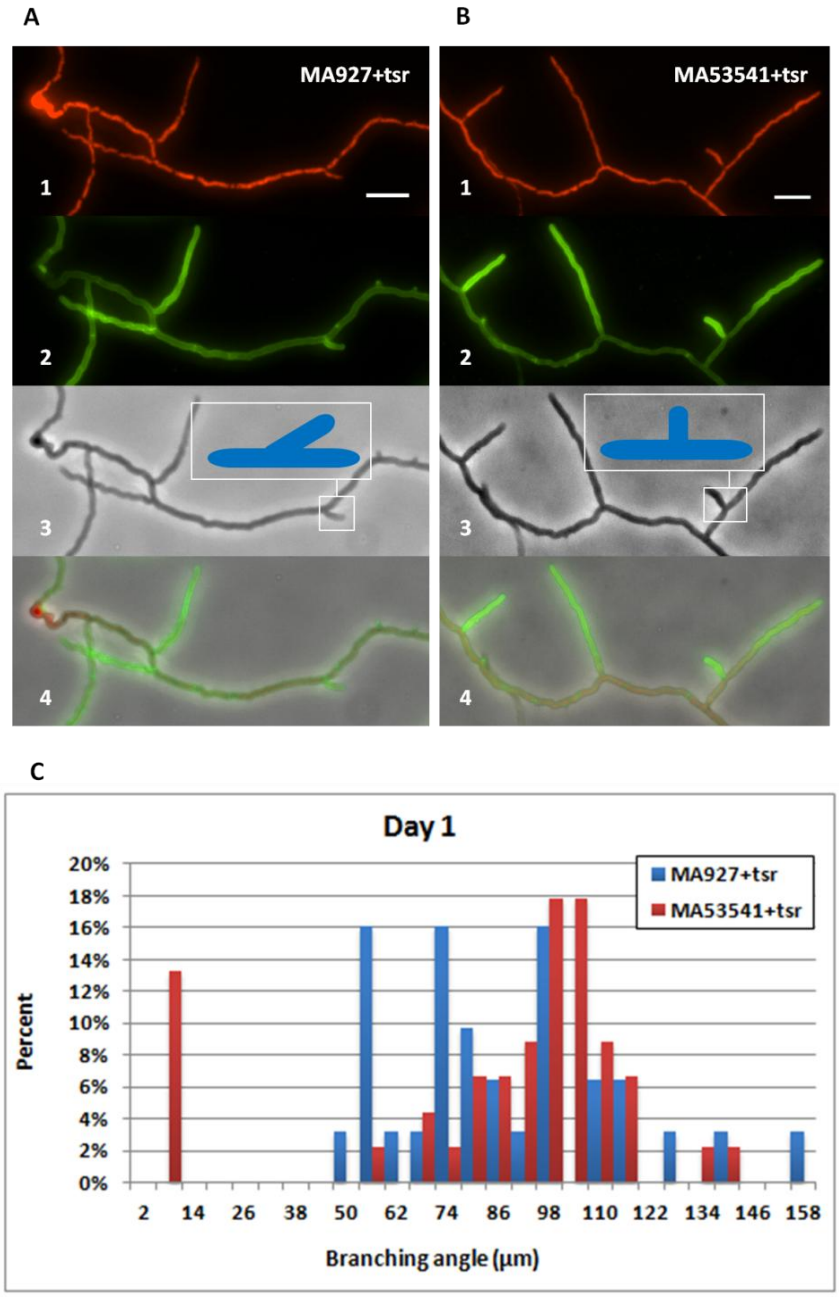

Figure 6-5: Morphological investigation of changing *pgsA* expression on the branch angle in the presence of thiostrepton after one day of growth.

Representative images of MA927 +tsr (A) and MA53541+tsr (B) showing DNA stained with PI-TRITC (1); cell walls stained with WGA-FITC (2); bright field image examined by phase contrast microscopy (3); composite image where all channels were merged (4). Strains grown on coverslips inserted at 45° angles into SFM agar. Quantitative analysis of branching angle was carried out on the two treatments (C); the inset in A3 and B3 images demonstrates the difference between branch angle growths in these strains. The data was divided into bins of 6° as a percentage of the total number of measurements and is displayed as a histogram (n=31, MA927; n=45, MA53541). White scale bar is 5µm.

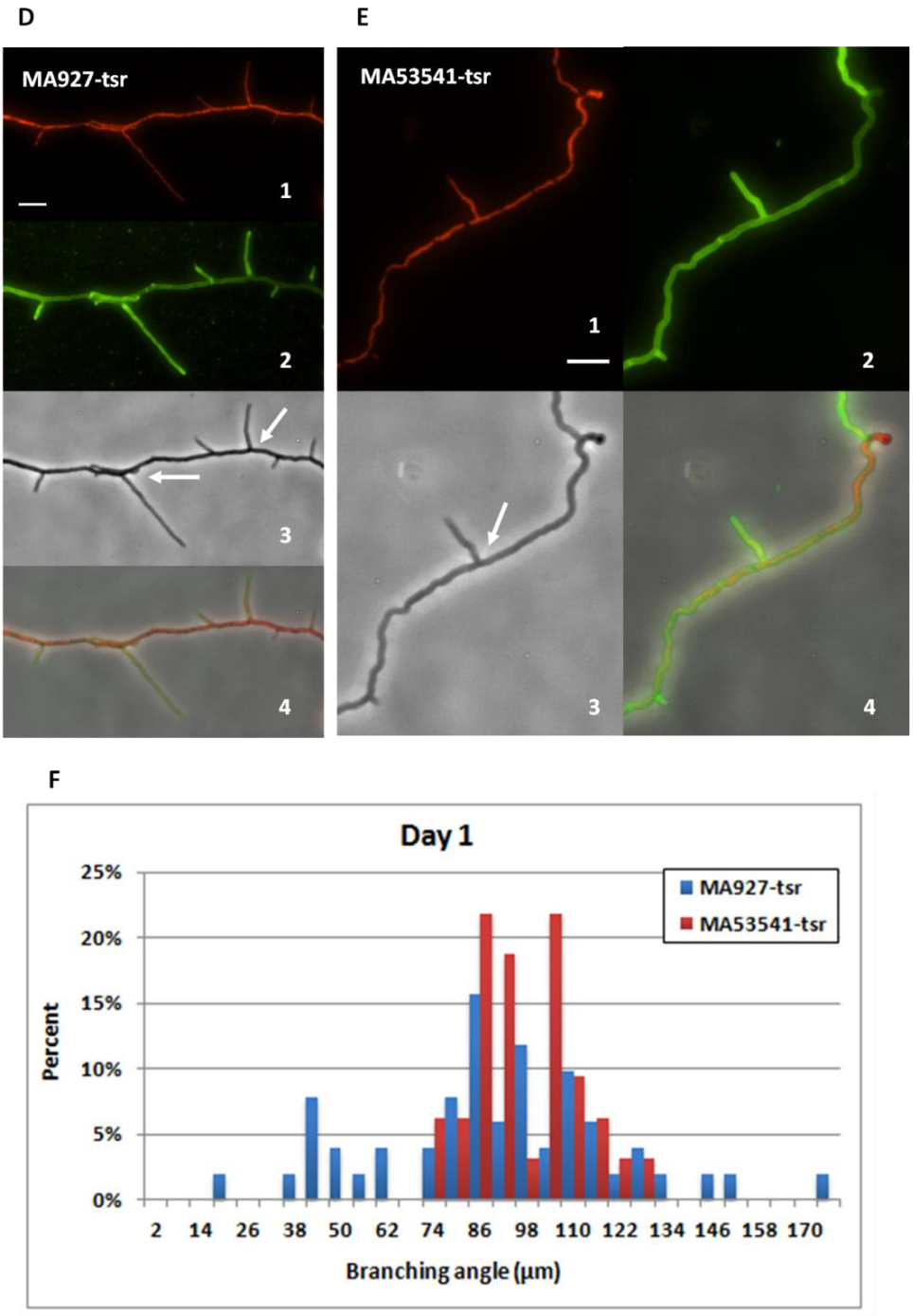

Figure 6-6: Morphological investigation of changing *pgsA* expression on the branch angle in the absence of thiostrepton after one day of growth.

Representative images of MA927 (D) and MA53541 (E) showing DNA stained with PI-TRITC (1); cell walls stained with WGA-FITC (2); bright field image examined by phase contrast microscopy (3); composite image where all channels were merged (4). Strains grown on coverslips inserted at 45° angles into SFM agar. Quantitative analysis of branching angle was carried out on the two treatments (F). The data was divided into bins of 6° as a percentage of the total number of measurements and is displayed as a histogram (n=51, MA927; n=32, MA53541). White scale bar is 5µm.

After two days of growth, we can observe that the general view after one day of growth was broadly similar with the MA53541 (+tsr) branch angles increasing, for instance with ~24% and ~19% in 98° and 105° range. The mean±SD of the branching angles was 92.3°±17.9º. Examples of phase contrast and fluorescence microscopy images showed similar effect with growth after one day (data not shown). Also, we observed that, on average, the branch angle in MA927 (+tsr) was between 50° and 115◦ (Figure 6.7A), although there was a wide distributed of measured values. The actual mean±SDdetermined was 74.8º± 30.6°. With no addition of tsr the majority of branch angles fell within the range of 62-134° for both untreated strains (Figure 6.7B), with mean±SD of 79.9º±37.3° and 94.5º±25.0° for MA927 and MA53541 respectively. In both treated and untreated strains, the difference between branching angles were statistically significant [p = 0.003 (95% CI = -28.62°, -6.37°) for treated strains and p = 0.012 (95% CI = -25.89°, -3.32°) for untreated strains]. This analysis shows that increasing expression of the *pgsA* operon leads to more consistent branching angle and is consistent with the role of PG as a precursor to CL (Sandoval-Calderon et al., 2009), as increased production of CL leads to increased branching in *S. coelicolor* (Jyothikumar et al., 2012).

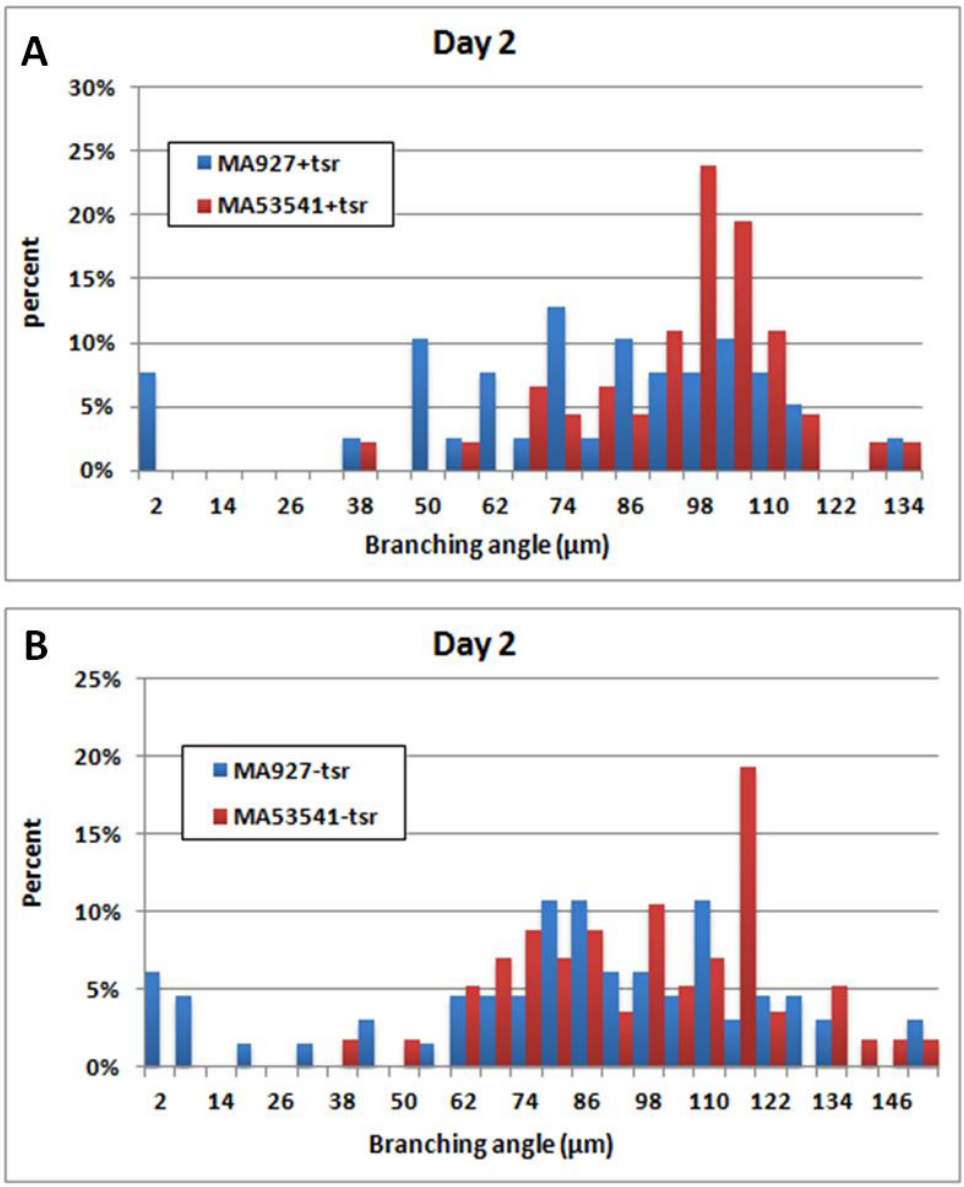

Figure 6-7: Quantitative analysis of branching angles in the strains MA53541 (+ tsr) and MA927 (+ tsr) (A) and MA53541 (-tsr) and MA927 (-tsr) (B) after two days of growth.

The data was divided into bins of 6° as a percentage of the total number of measurements and is displayed as a histogram (n= 39 for MA927 (+tsr), 46 for MA53541 (+tsr), 65 for MA927 (-tsr) and 57 for MA53541 (-tsr).

6.6 Morphological analysis of altering *pgsA* expression on interbranch distance of *S.coelicolor*

Again in this study we investigated the changes in expression of *pgsA* operon genes during the first and second day of growth on interbranch distance. The schematic diagram also was followed in (Figure 6.1) for microscopy and quantitative analysis. The staining pattern with PI and WGA showed in the panel 1, 2, 3 and 4 of the (Figure 6.8A, B, Figure 6.9D, and E). For Examples, panel 1 illustrates hyphae with DNA stained with PI (red), panel 2 is cell walls stained with WGA (green), panel 3 is a phase contrast image and panel 4 is a multiprobe image where all filters are merged. Overall, the pattern of growth at day one for both treated and untreated strains was similar (Figure 6.8C & Figure 6.9F), although MA53541 (+tsr) showed a higher percentage of shorter interbranch distances at 4 μm. This strain showed a higher percentage of interbranch distances within the range 7, 10 and 13 μm with 16% and 20% (Figure 6.8C). Under normal conditions of growth, we can see a similar pattern in both strains. MA927 (-tsr) showed a slightly higher percentage of interbranch distances in the range 19 and 28 μm. Analysis of the data using Minitab gave mean±SD interbranch distances as 13.67±7.80 μm and 10.9±11.4 μm for MA927 (+tsr) and MA53541 (+tsr) respectively. Given that the distribution of the data was significantly different from a Gausian one and normality assumptions could not hold, further analysis was done using the Mann-Whitney test. This test gave median values as 10.916 μm and 9.091 μm for MA927 (+tsr) and MA53541 (+tsr) respectively, and showed that the two samples were significantly different at p = 0.0476 and 95% CI of 0.011—7.108 μm. MA927 (-tsr) also showed some interbranch distances that were longer than those of MA53541 (-tsr), reaching a distance of 23μm (Figure 6.9F). The mean±SD interbranch distances were 9.06±6.53 μm and 8.47±4.83 μm for MA927 (-tsr) and MA53541 (-tsr) respectively, and their median values were 7.250 vs 7.221 μm with no statistically significant difference between them (p = 1.0000, 95% CI = -1.968, 2.126 μm) after the Mann-Whitney test. Therefore, we observed that in the presence of tsr, many of the interbranch distances in MA927 (+tsr) are significantly longer, whilst MA53541 (+tsr) develop in shorter interbranch distances (Figure 6.8 A, B white arrows). But in the absence of tsr,

interbranch distances were similar to the treated strains; with both strains showing long interbranch distances over the range 19 μm (Figure 6.9D, E white arrows).

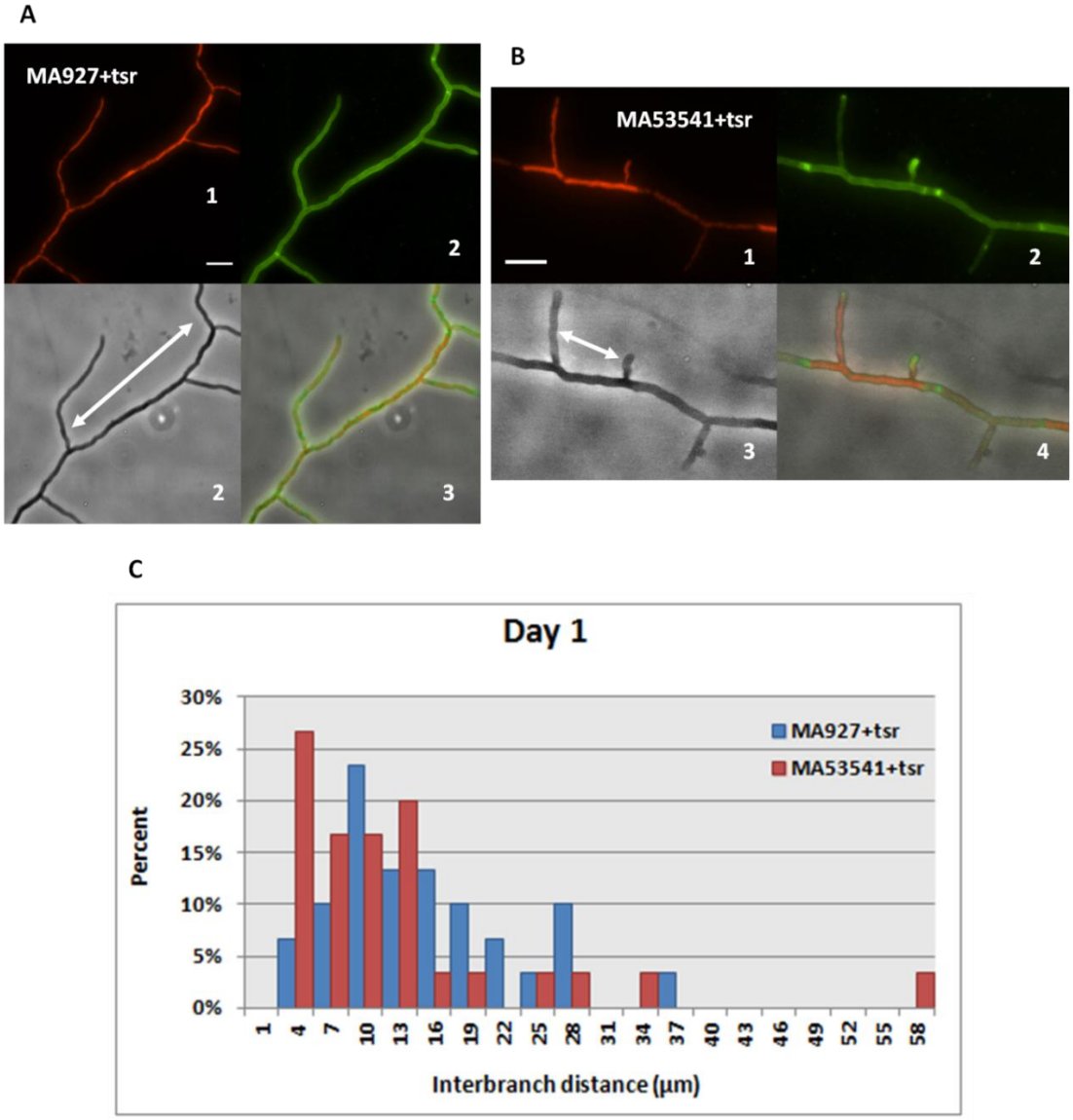

Figure 6-8: Morphological investigation of changing *pgsA* expression on the interbranch distance in the presence of thiostrepton after one day of growth.

Representative images of MA927 +tsr (A) and MA53541+tsr (B) showing DNA stained with PI-TRITC (1); cell walls stained with WGA-FITC (2); bright field image examined by phase contrast microscopy (3); composite image where all filters were merged (4). White arrows in A3 and B3 images indicate the difference in distance between two branches in both strains. Quantitative analysis (C) of interbranch distances in the strains MA53541 (+tsr) and MA927 (+tsr), after one day of growth. The data was divided into bins of 3µm as a percentage of the total number of measurements and is displayed as a histogram. n= 30 for MA927 (+tsr) and 30 for MA53541 (+tsr). White scale bar is 5µm.

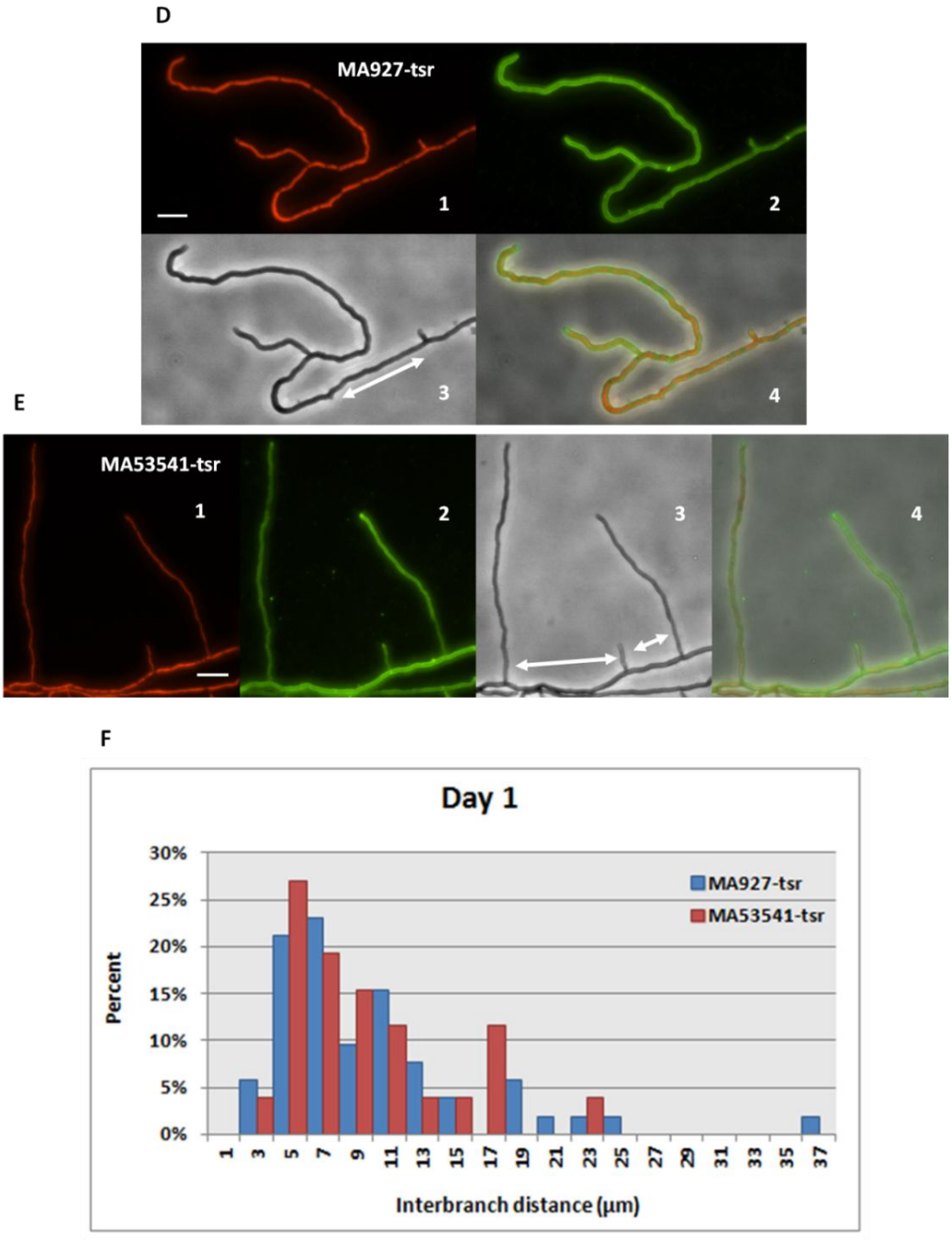

Figure 6-9: Morphological investigation of changing *pgsA* expression on the interbranch distance in the absence of thiostrepton after one day of growth.

Representative images of MA927 (D) and MA53541 (E) showing DNA stained with PI-TRITC (1); cell walls stained with WGA-FITC (2); bright field image examined by phase contrast microscopy (3); composite image where all filters were merged (4). White arrows in D3 and E3 images indicate the difference in distance between two branches in both strains. Quantitative analysis (F) of interbranch distances in the strains MA53541 and MA927, after one day of growth. The data was divided into bins of 3µm as a percentage of the total number of measurements and is displayed as a histogram. n= 52 for MA927 and 26 for MA53541. White scale bar is 5µm.

After two days of growth, the overall pattern of growth for both treated and untreated strains were similar; although MA53541 (+tsr) and MA53541 (-tsr) compared to MA927 (+tsr) and MA927 (-tsr) showed more short interbranch distances especially at the range distance of 4 and 8μm (Figures 6.10). The means ±SDs of the interbranch distances were 14.1±11.4 μm and 7.05±5.69 μm for MA927 (+tsr) and MA53541 (+tsr) respectively, and 6.65± 6.11 μm and 4.90± 3.14 μm for MA927 (-tsr) and MA53541 (-tsr) respectively. These values were all found to be statistically significant for both treated and untreated strains with p-values (95% CI) of 0.002 (2.84, 11.20 μm) and 0.015 (0.342, 3.1434 μm) respectively. Again this is consistent with the earlier analysis that showed that over-expression of the *pgsA* operon resulted in higher levels of branching, thereby decreasing the mean interbranch distance in MA53541 (+tsr) strains. However, the fact that the untreated strains showed significantly different interbranch distances after 2 days of growth might indicate that the observed effect in the treated strains might have been coincidental; although this may be partly due to some other factors in the experiement. It would be necessary to check if these values can be reproduced.

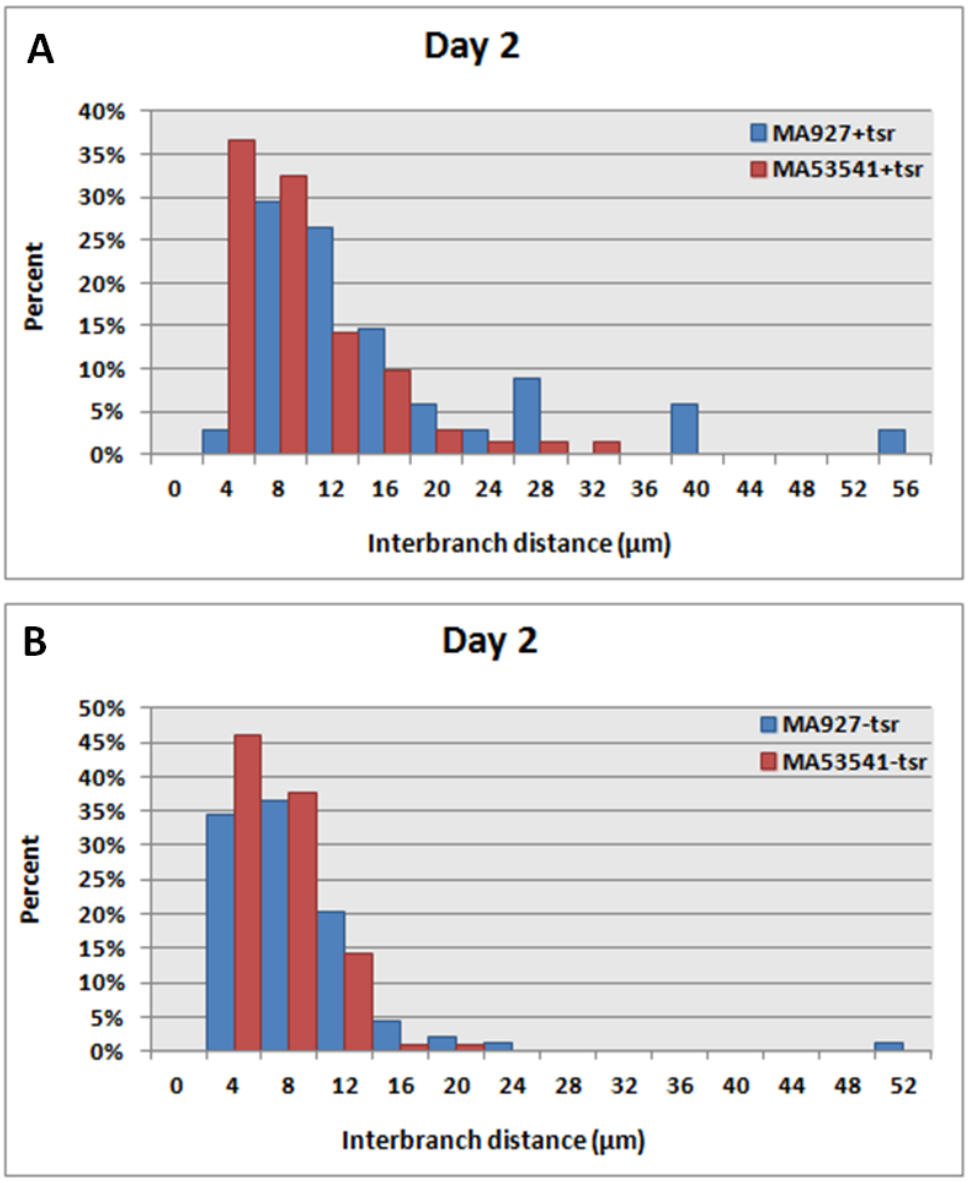

Figure 6-10: Quantitative analysis of interbranch distances in the strains MA53541 (+ tsr) and MA927 (+ tsr) (A) and MA53541 (-tsr) and MA927 (-tsr) (B) after two days of growth.

The data was divided into bins of 4µm as a percentage of the total number of measurements and is displayed as a histogram. n= 34 for MA927 (+tsr), 71 for MA53541 (+tsr), 93 for MA927 (-tsr) and 98 for MA53541 (-tsr).

6.7 Morphological analysis of altering *pgsA* expression on the cross wall distance of *S.coelicolor*

After three days of growth, the effect of changing *pgsA* gene expression on the cross wall distance was examined in aerial hyphae. Measurements were based on the schematic diagram of cross wall distance measurements in (Figure 6.11). The staining pattern with PI and WGA showed in the panel 1, 2, 3 and 4 of the (Figure 6.12A, B, Figure 6.13D and E). For example, panel 1 illustrates hyphae with DNA stained with PI (red), panel 2 is cell walls stained with WGA (green), panel 3 is phase contrast image and panel 4 is a multiprobe image where all filters were merged. We can observe that MA53541 (+tsr) showed a higher percentage of larger cross wall distances than MA927 (+tsr) in the range distance of 1.1, 1.45 and 2.15 µm with 50 %, ~37 % and ~5% (Figure 6.12C). The means±SDs of the cross wall distances were 1.124±0.374 µm and 1.163±0.480 µm for MA927 (+tsr) and MA53541 (+tsr) respectively. Under normal growth, MA927 (-tsr) showed a greater percentage of cross wall distance within the range 1.1-1.45 µm while MA53541 (-tsr) showed higher percentage than MA927 (-tsr) at the distance ranges of 1.8, 2.15 and 2.5 µm (Figure 6.13F). In this case, the means±SDs of the cross wall distances were 1.212±0.439 µm and 1.408±0.449 µm for MA927 (-tsr) and MA53541 (-tsr) respectively. There was no statistically significant difference in cross wall difference between the two strains in the treatment group ($p = 0.345$, 95% CI = -0.1211, 0.0424 µm), although this was statistically significant in the untreated strains ($p = 0.000$, 95% CI = -0.2731, -0.1182 µm). These results suggest that treatment did not induce the mutant strain to develop longer or shorter cross wall distances in comparison to the wild strain. Instead, they suggest that lack of this treatment caused the wild and mutant strains to behave differently, with the latter developing significantly shorter cross wall distances relative to the former. Based on these averages, however, we can observe that both in the presence and absence of tsr, MA53541 showed a slightly greater cross wall distance than MA927 and perhaps suggest that the laying down of crosswalls in aerial hyphae is inhibited by increasing production of PG.

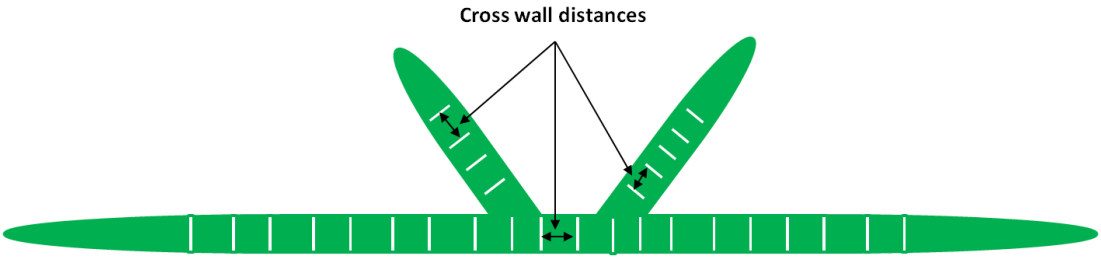

Figure 6-11: Schematic diagram for cross wall measurements in aerial hyphae.

The measurement of cross wall distances was the length between adjacent cross walls.

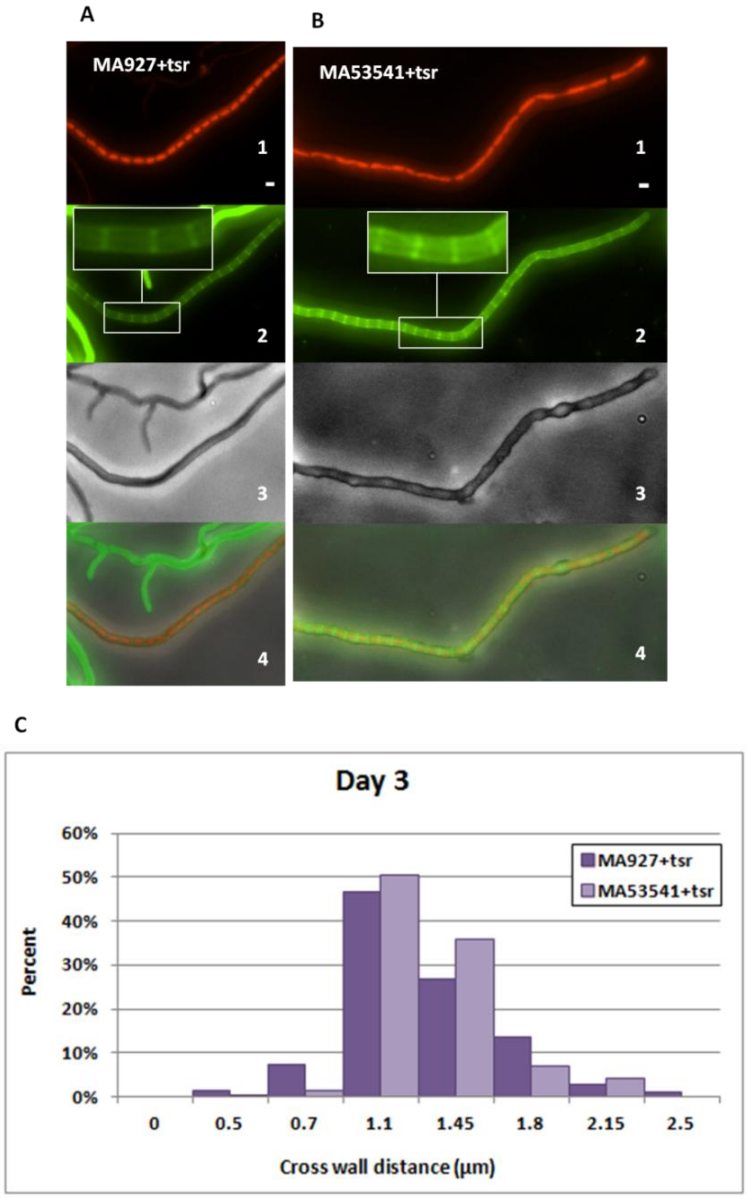

Figure 6-12: Morphological investigation of changing *pgsA* expression on the cross wall distance in the presence of thiostrepton.

All Panels 1,2 ,3 ,4 represent the staining that was used as follows: 1 indicates DNA stained with PI-TRITC (red); 2 is cell wall stained with WGA-FITC (green); 3 is bright field image examined by phase contrast microscopy; 4 is a composite images where all channels are merged. Phase contrast and fluorescence microscopy images (x100 magnification) of *S. coelicolor* spores from MA927 (+tsr) (A) and MA53541 (+tsr) (B). Strains were grown on coverslips inserted at 45° angles into SFM agar. Insets in A2 and B2 images indicate the cross wall in the hypha. Quantitative analysis of cross wall distance in the strains MA927 (+tsr) and MA53541 (+tsr) after the third day of growth (C). The data was divided into bins of 0.35µm as a percentage of the total number of measurements and is displayed as a histogram. n= 208 for MA927 (+tsr) and 218 for MA53541 (+tsr). White scale bar is 1µm.

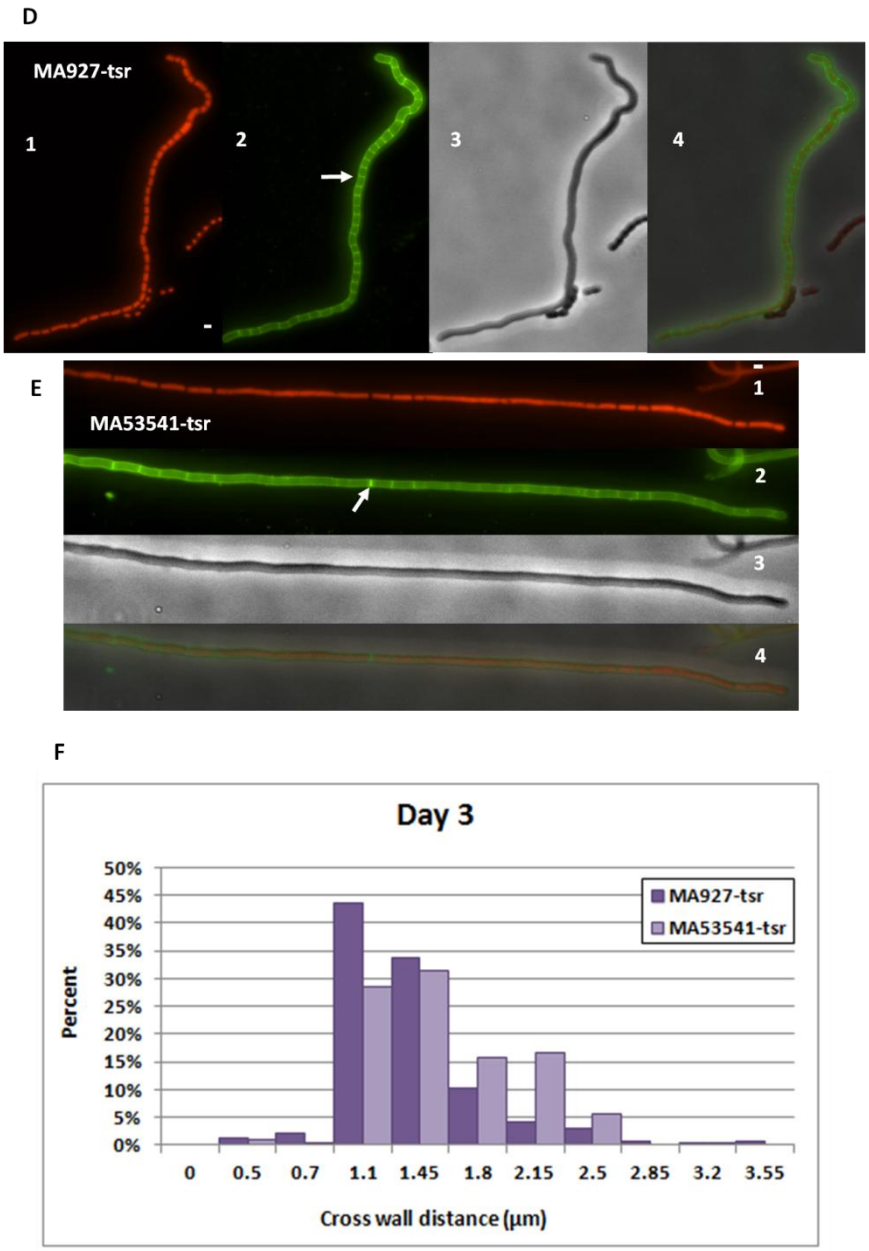

Figure 6-13: Morphological investigation of changing *pgsA* expression on the cross wall distance in the absence of thiostrepton.

All Panels 1,2 ,3 ,4 represent the staining that was used as followes: 1 indicates DNA stained with PI-TRITC (red); 2 is cell wall stained with WGA-FITC (green); 3 is bright field image examined by phase contrast microscopy; 4 is a composite images where all channels are merged. Phase contrast and fluorescence microscopy images (x100 magnification) of *Streptomyces* spores from MA927 (D) and MA53541 (E). Strains were grown on coverslips inserted at 45° angles into SFM agar White arrows in D2 and E2 images indicate cross walls in the hyphae. Quantitative analysis of cross wall distance in the strains MA927 and MA53541 after the third day of growth (F). The data was divided into bins of 0.35µm as a percentage of the total number of measurements and is displayed as a histogram. n= 290 for MA927 and 227 for MA53541. White scale bar is 1µm.

6.8 Morphological analysis of altering *pgsA* expression on the spore width of *S. coelicolor*

Alteration of *pgsA* operon expression on the spore width was investigated in this study after four days of growth. Measurements were based on the schematic diagram of spore width measurements in (Figure 6.14). The staining pattern with PI and WGA showed in the panel 1, 2, 3 and 4 of the (Figure 6.15A, B and Figure 6.16D, and E). For example, panel 1 illustrates hyphae with DNA stained with PI (red), panel 2 is cell walls stained with WGA (green), panel 3 is phase contrast image and panel 4 is multiprobe image where all channels were merged. We can observe that the majority of spore widths fell within the range of 0.65-1.25 µm for all treated strains. However, the MA53541 (+tsr) revealed a greater percentage of spore width at 0.8, 0.85 and 0.90 µm. The mean ±SD of the spore widths were 0.980±0.202 µm and 0.913±0.219 µm for MA927 (+tsr) and MA53541 (+tsr) respectively. The patterns of growth for both strains showed reduced percentages in the width range of 0.95 µm (Figure 6.15C). Under normal growth conditions, the trend of untreated strains showed various distributions of spore width percentages. For instance, we can see that at the spore width range of 0.65-0.85, MA53541 (-tsr) has higher percentages than MA927 (-tsr); whereas at a range of 0.95-1.25 MA927 (-tsr) has higher percentages than MA53541 (-tsr) (Figure 6.16F**)**. The overall mean ±SD values of the spore widths were 0.949±0.210 µm and 0.774±0.201 µm for MA927 (-tsr) and MA53541 (-tsr) respectively. There were statistically significant differences in spore widths between the two strains in the treated group ($p = 0.000$, 95% CI = 0.0388, 0.0955 µm) and untreated group ($p = 0.000$, 95% CI = 0.1476, 0.2016 µm) respectively. Both in the treated and untreated groups, the MA927 strain develops significantly wider spores that the wild strain MA53541. Thus in addition to there being differences in the cross wall distance (see previous section), there appears to be some manifestions of changes in spore diameter in response to increased expression of the *pgsA* operon under tsr treatment. But only after these results have been reproduced in a separate experiment can these results lead to firm interpretations. Thus further experiments to support these data are required.

It was further be observed in Figures 6-15 and 6-16 that there appears to be a subpopulation of small spores in *S. coelicolor*. Reponen et al. (1998) have shown that actinomycete spore sizes vary widely depending on such variables as the species producing them and sampling flow rate. However this was observed among three actinomycetes *Streptomyces albus*, *Micromonospora halophytica* and *Thermoactinomyces vulgaris* but has not been previously reported in *S. coelicolor* (Sutcliffe et al., 2012).

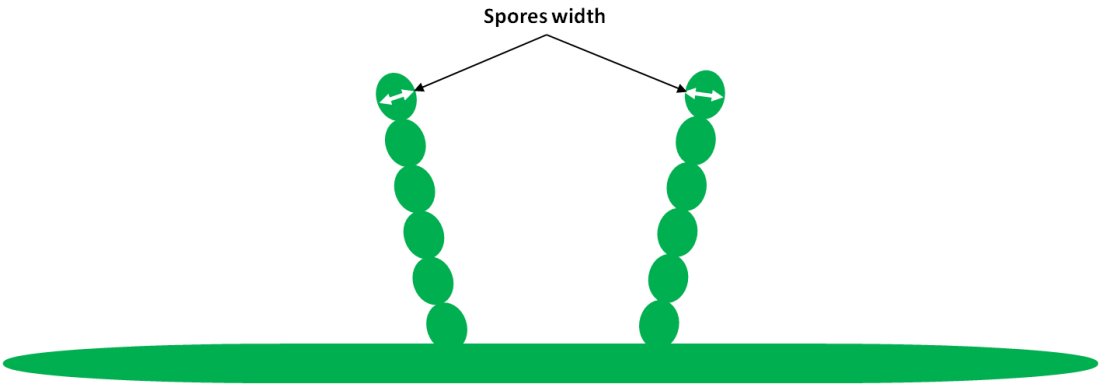

Figure 6-14: Schematic diagram for spore width measurements.

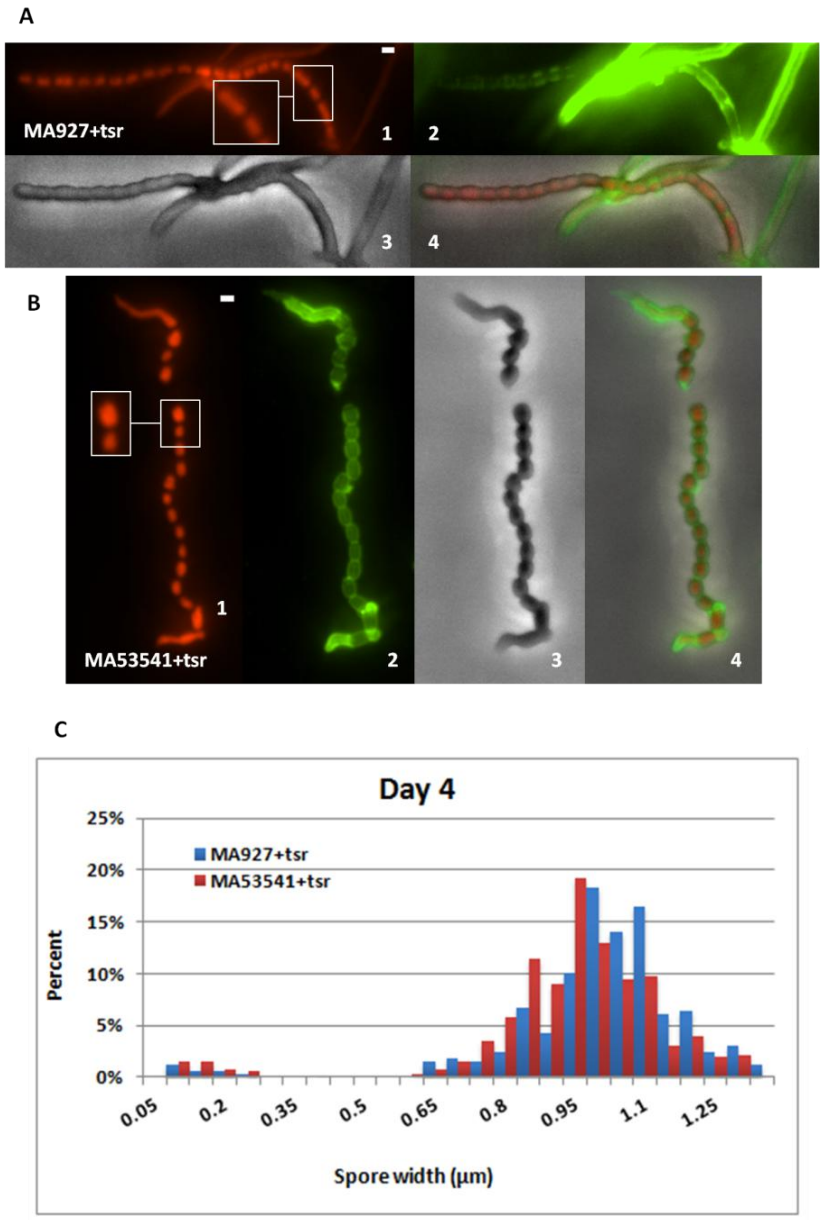

Figure 6-15: Morphological investigation of changing *pgsA* expression on the spore width in the presence of thiostrepton after one day of growth.

All Panels 1, 2, 3, 4 represent the staining that used as follows: 1 indicates DNA stained with PI-TRITC (red); 2 is cell wall stained with WGA-FITC (green); 3 is bright field image examined by phase contrast microscopy; 4 is a composite images where all channels merged. Phase contrast and fluorescence microscopy images (x100 magnification) of *Streptomyces* spore suspensions of MA927 (+tsr) (A) and MA53541 (+tsr) (B). Strains were grown on coverslips inserted at 45° angles into SFM agar. Insets in A1 and B1 images indicate the spore in the sporulating aerial hypha. Quantitative analysis (C) of spore width in the strains MA927 (+tsr) and MA53541 (+tsr) after the fourth day of growth. The data was divided into bins of 0.05µm as a percentage of the total number of measurements and is displayed as a histogram. n= 328 for MA927 (+tsr) and 574 for MA53541 (+tsr). White Scale bar is 1µm.

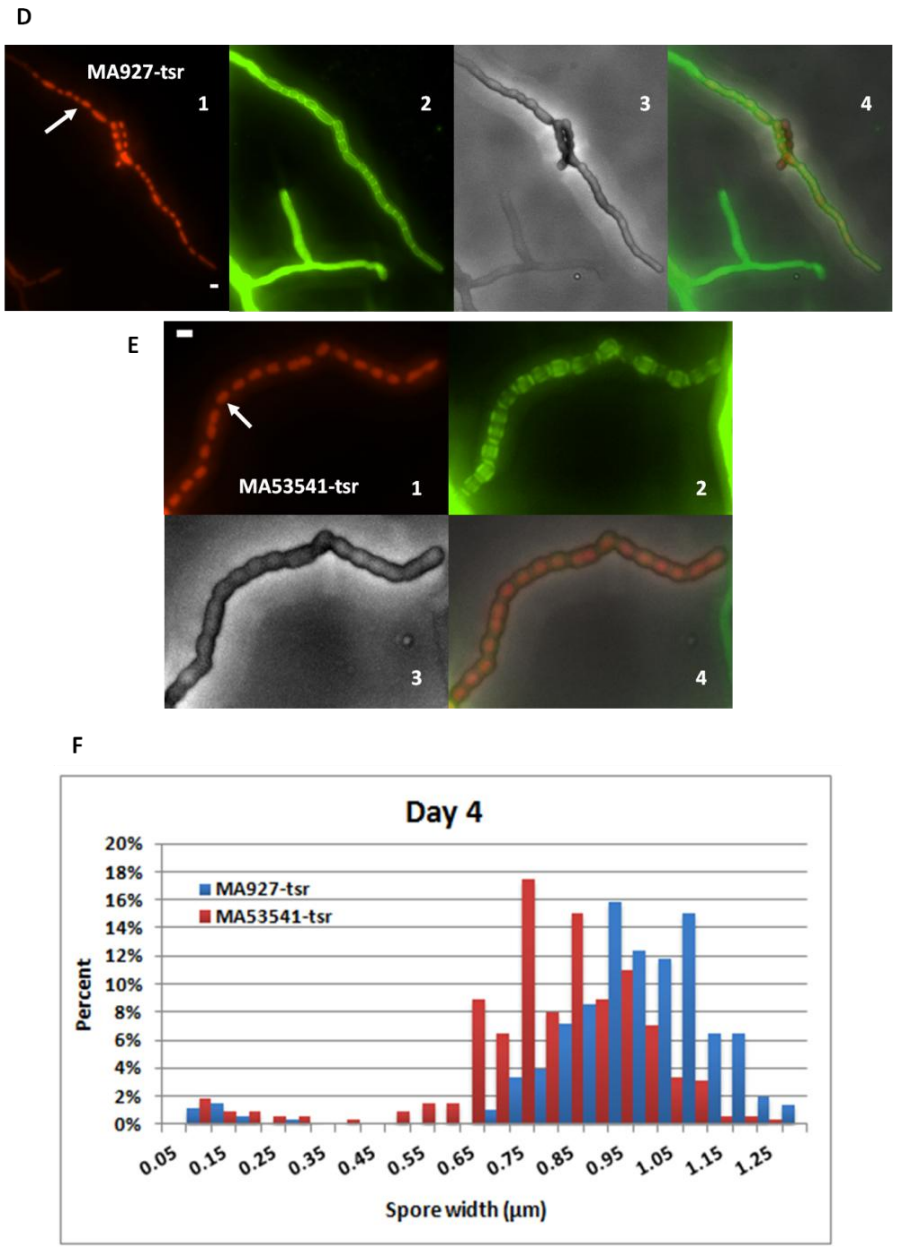

Figure 6-16: Morphological investigation of changing *pgsA* expression on the spore width in the absence of thiostrepton after four days of growth.

All Panels 1, 2, 3, 4 represent the staining that used as follows: 1 indicates DNA stained with PI-TRITC (red); 2 is cell wall stained with WGA-FITC (green); 3 is bright field image examined by phase contrast microscopy; 4 is a composite images where all channels merged. Phase contrast and fluorescence microscopy images (x100 magnification) of *Streptomyces* spore suspensions of MA927 (D) and MA53541 (E). Strains were grown on coverslips inserted at 45° angles into SFM agar. White arrows in D1 and E1 images indicate the spore in the sporulating hypha. Quantitative analysis (F) of spore width in the strains MA927 and MA53541 after the fourth day of growth. The data was divided into bins of 0.05µm as a percentage of the total number of measurements and is displayed as a histogram. n= 670 for MA927 and 327 for MA53541. White Scale bar is 1µm.

6.9 Discussion of Chapter 6

In recent years, bacterial cell membranes are found to produce domains with particular lipid roles and components. By the means of specific fluorescent cell membrane binding dyes, lipid spiral forms elongating along the extended axis of the cell were revealed in *B. subtilis*. These spiral structures were missing when the PG biosynthetic genes were disrupted, proposing that the enrichment in anionic PLs leads to lipid spirals (Barák et al., 2008). Investigations into *Streptomyces* have revealed that the DivIVA protein is involved in tip extension after analysis by fluorescence microscopy. However, a molecular understanding of the precise systems causing growth polarity will not only highlight characteristic of *Streptomyces* but also reveal conserved basic functions of cell membranes in bacteria (Flärdh, 2003).

Cell Morphogenesis in bacteria can be controlled by actin homologue MreB proteins, which form a helical pattern and allow cell elongation to form a rod shape cell wall. However other rod shaped bacteria such as *Corynebacterium glutamicum*, a relative of *Streptomyces*, are found not to undergo cell extension by the MreB system; these bacteria use a completely different system which is based on polar growth that originated from the division mechanism. These findings were important as they provide an insight into the various molecular approaches utilised by bacteria to direct their cellular morphology and propose systems in which these strategies could affect growth proportions and cell envelope formation (Daniel and Errington, 2003).

Fundamental to this chapter is the application of fluorescence microscopy to study the functions of the PG on *Streptomyces* growth and development following our studies on the role of PG in osmotolerance. We have used the application of fluorescent dyes like WGA and PI from still images of *S. coelicolor*. By altering *pgsA* operon expression we could analyse the mycelial architecture through the measurement of distances of apical tip, inter-branching and branching angle measurements after the first and second day of growth. Subsequently, analysis was continued on cross wall distance and spore width after the third and fourth day of growth respectively. Results from image analysis showed that after one day of

addition of tsr, apical tip length changed compared to the control strain resulting in shorter tip to branch distance. Taken together this suggests that increased expression of the *pgsA* operon leads to branching closer to the hyphal tip. On branching angle analysis, in the presence of tsr, the effects of altering *pgsA* expression was only observed at the second day of growth. This is consistent with the role of PG as a precursor to CL (Sandoval-Calderon et al., 2009), as increased production of CL leads to increased branching in *S. coelicolor* (Jyothikumar et al., 2012). Similar observations were seen on interbranch distance analysis; at the second day of incubation, changes in *pgsA* operon expression showed a significant reduction in interbranch length compared to normal expression levels, particularly in the distance range of 4 µm for MA53541 (+tsr) observed on the first and second days of growth. After the third day of incubation, we observed that changes of *pgsA* operon expression have no significant effect on the cross wall distance compared to the control strain. The analysis of spore width was also conducted to study the effect of altering *pgsA* expression on spore width. The result revealed that changing of *pgsA* expression causes significant reduction in spore size.

With regards to all above observations, we believe that the role of *pgsA* in changing branching in *S. coelicolor* is consistent with the involvement of DivIVA (Hempel et al., 2008, Flärdh, 2003). Our data suggests that increasing the content of PG in the mycelium might affect branching, potentially though the role of this PL as a precursor of CL that is known to influence branching in this organism (Jyothikumar et al., 2012). In addition, the cell division protein FtsZ converts multinucleoidal aerial hyphae into uninucleoidal spores in chains and, as such, plays a significant role in regulating phase of cellular development (Schwedock et al., 1997, McCormick, 2009). The fact that increasing expression of the *pgsA* operon shows an increase in cross wall distance suggests that PG may play a role in the localization of FtsZ rings in *S. coelicolor* aerial hyphae. In most other bacteria proteins of the Min system are involved in the correct positioning of FtsZ rings; recent research indicated that MinD undergoes dynamic oligomerization on the membrane surfaces mediated through interactions with membrane lipids; this discovery is important because it expands the extent of lipid association in development (Mileykovskaya and Dowhan, 2005). It is

important to state however, that there is no structural homologue of MinD encoded by the *S. coelicolor* genome.

It has been found that CL interacts with several proteins like FtsZ, FtsW, DnaA and perhaps MinD (Barák et al., 2008). Future studies could investigate the interaction of these different cell division proteins by different staining techniques for fluorescent microscopy.

Chapter 7:

General Discussion

7. General Discussion

In this project we have focused on the gene *SCO5753* (*pgsA*) from the model organism *S. coelicolor,* whose product is predicted to synthesize PG the precursor of CL. In order to study the gene *SCO5753*, the characterization of downstream genes such as *SCO5755* was also investigated as this gene is speculated to regulate *SCO5753*. The function of *SCO5752* and *SCO5753* are unknown, although there is genetic evidence that at least one may be essential for growth and development of *S. coelicolor* (Bellier and Mazodier, 2004).

Our initial study of mutational analysis was conducted on these genes *SCO5751*, *SCO5752, SCO5753* and *SCO5755* to decipher their significance in *Streptomyces.* Using disrupted genes in the transposed cosmids SC7C7.2.F05, SC7C7.2.B06, SC7C7.2.B07 and SC7C7.A02, we showed that it was not possible to obtain any disruptions of these genes. This failure to disrupt these genes suggested that allelic transfer could not occur or each gene is essential for *Streptomyces* growth.

We had several attempts to construct strains of the *pgsA* operon under the control of the tsr inducible promoter at the start of this project, but eventually we successfully placed elements of the operon under the control of *ptipA* in pPM927 and pIJ6902. Thus we could determine if one or more of these genes were toxic if over expressed in *S. coelicolor*. For instance, in *B. subtilis* it was found that six unknown proteins could protect the bacteria against metabolites, endogenous toxic proteins, or other intermediates (Commichau et al., 2013). The complementation result of the strain MA53541 into the cosmid SC7C.B07 by conjugation showed that *SCO5753* could not be disrupted with Tn*5062*. This indicates that this gene might be essential for *S. coelicolor* growth and development. There was considerable difficulty in constructing strains during this project; essential genes are hard to investigate genetically due to the fact that mutants of these genes are not readily achievable as these genes could have a significant role in the growth of the organisms (Herring and Blattner, 2004, Koonin, 2000, Mushegian, 1999). We have observed that the strains MA53541 (harbouring *SCO5753*) and MA55B (harbouring *SCO5755*) are different

from *S. coelicolor* containing the empty vectors MA927 and MA6902 alone. This was especially apparent when they were grown on R5 media.

Analysis of *S. coelicolor* PLs by TLC shows that PG increased when the organism was grown in media containing high concentrations of KCl. This suggests that there is an involvement of PG in the development of *S. coelicolor* during growth in severe environmental conditions.This was observed on PG spots of MA53541 at 0.20M of KCl after 24 and 48 hours of growth. Also, TLC analysis of PLs was performed on strains carrying mutations in the osmoregulatory genes *osaA, osaB, osaC* and *osaD* at 24 hours (Bishop et al., 2004). We found that *osaB* and *osaC* mutants displayed a small increase in the intensity of PG spots in the presence of 0.20M KCl that was similar to *S. coelicolor* wild-type. This effect was not seen in the *osaA* and *osaD* mutants and suggests that the latter two mutants are unable to regulate increases in PG production during hyper-osmotic shock. After 48 hours of growth, we observed that the *osaA* mutant responded to hyperosmotic shock in the same way as the control strains. On the other hand the *osaC* and *osaD* mutants were unaffected at 0.20M of KCl. Taken together this suggests that *OsaD* is perhaps the regulatory protein that governs transmission of signals of hyperosmotic shock to the up regulation of PG production.

The recent development of probes in lipid localization experiments has demonstrated that several proteins correlate with particular domains of the membrane. This has resulted in the discovery of lipid domains in bacteria (Barak and Muchova, 2013). Based on our fluorescence microscopy analyses, we noticed that in the presence of tsr MA53541 developed into many branches of apical tips with average tip distance of 9 µm, whereas the control strain MA927 grew with longer apical tip distances. Also the branch angle of MA53541 in the presence of tsr appears to be closer to 90° compared to MA927 which branched with more acute angles. Furthermore, we observed that in the presence of tsr, interbranch distances in MA53541 were shorter in comparison with the control strain. Although we could observe some small changes in the distances between cross walls in aerial hyphae, this did not manifest itself in significant changes in spore size or morphology. As a result, it is unlikely

that PG plays a role in the positioning of the proteins that dictate the location of rings of FtsZ that determine the site of cross wall formation. Proteins that ae responsible for the position of FtsZ rings include SsgA (van Wezel et al., 2000), SsgB (Willemse et al., 2011) and CrgA (Del Sol et al., 2006).

In conclusion, this study has provided us with an overview of the role of the anionic phospholipids (PG) in *Streptomyces* growth and development. For instance, we have observed that there is an increase in PG content which is promoted by addition of or tsr. The MA55B strain (harbouring *clgR)* was seen to produce the lowest amount of phospholipids based on TLC spot intensities. This might be due to overexpression of *clgR* which has been reported to induce a delay in the development of *S.coelicolor* (Bellier and Mazodier, 2004). Alternatively, the low levels of PLs observed could be due to the difficulty in their extraction or incomplete resolution from each other by TLC. *clsA* (cardiolipin synthase; *SCO1389*) has been previously reported to be essential in *S. coelicolor* where increasing CL production resulted in increased branching (Jyothikumar et al., 2012). This project suggests that *pgsA* could be as essential in *S. coelicolor* given the role PG plays as a precursor to CL synthesis (Sandoval-Calderon et al., 2009).

Chapter 8:

References

8. References

ADAMS, D. W. & ERRINGTON, J. 2009. Bacterial cell division: assembly, maintenance and disassembly of the Z ring. *Nature Reviews Microbiology,* 7**,** 642-653.

AGGARWAL, A. K., RODGERS, D. W., DROTTAR, M., PTASHNE, M. & HARRISON, S. C. 1988. Recognition of a DNA operator by the repressor of phage 434: a view at high resolution. *Science,* 242**,** 899-907.

AINSA, J., RYDING, N., HARTLEY, N., FINDLAY, K., BRUTON, C. & CHATER, K. 2000. WhiA, a Protein of Unknown Function Conserved among Gram-Positive Bacteria, Is Essential for Sporulation in *Streptomyces coelicolor* A3 (2). *Journal of Bacteriology,* 182**,** 5470-5478.

AÍNSA, J. A., BIRD, N., RYDING, N. J., FINDLAY, K. C. & CHATER, K. F. 2010. The complex *whiJ* locus mediates environmentally sensitive repression of development of *Streptomyces coelicolor* A3 (2). *Antonie Van Leeuwenhoek,* 98**,** 225-236.

AÍNSA, J. A., PARRY, H. D. & CHATER, K. F. 1999. A response regulator-like protein that functions at an intermediate stage of sporulation in *Streptomyces coelicolor* A3 (2). *Molecular Microbiology,* 34**,** 607-619.

ALAM, M. T., MERLO, M. E., TAKANO, E. & BREITLING, R. 2010. Genome-based phylogenetic analysis of *Streptomyces* and its relatives. *Molecular Phylogenetics and Evolution,* 54**,** 763-772.

ALI, N., HERRON, P. R., EVANS, M. C. & DYSON, P. J. 2002. Osmotic regulation of the *Streptomyces lividans* thiostrepton-inducible promoter, *ptipA*. *Microbiology,* 148**,** 381-390.

ALMIRON, M., LINK, A. J., FURLONG, D. & KOLTER, R. 1992. A novel DNA-binding protein with regulatory and protective roles in starved *Escherichia coli*. *Genes and Development,* 6**,** 2646-2654.

ANANTHARAMAN, V., KOONIN, E. V. & ARAVIND, L. 2001. TRAM, a predicted RNA-binding domain, common to tRNA uracil methylation and adenine thiolation enzymes. *FEMS Microbiology Letters,* 197**,** 215-221.

ANDERSON, A. S. & WELLINGTON, E. M. 2001. The taxonomy of *Streptomyces* and related genera. *International Journal of Systematic and Evolutionary Microbiology,* 51**,** 797-814.

ANON. 2015. *LIPID Metabolites and Pathways Strategy (LIPID MAPS)* [Online]. National Institute of General Medical Sciences. Available: http://www.lipidmaps.org/.

ANTON, B. P., RUSSELL, S. P., VERTREES, J., KASIF, S., RALEIGH, E. A., LIMBACH, P. A. & ROBERTS, R. J. 2010. Functional characterization of the YmcB and YqeV tRNA methylthiotransferases of *Bacillus subtilis*. *Nucleic Acids Research,* 38**,** 6195-6205.

ANTON, B. P., SALEH, L., BENNER, J. S., RALEIGH, E. A., KASIF, S. & ROBERTS, R. J. 2008. RimO, a MiaB-like enzyme, methylthiolates the universally conserved Asp88 residue of ribosomal protein S12 in *Escherichia coli*. *Proceedings of the National Academy of Sciences,* 105**,** 1826-1831.

ARAVIND, L., ANANTHARAMAN, V., BALAJI, S., BABU, M. M. & IYER, L. M. 2005. The many faces of the helix-turn-helix domain: transcription regulation and beyond. *FEMS Mcrobiology Reviews,* 29**,** 231-262.

ARIGONI, F., TALABOT, F., PEITSCH, M., EDGERTON, M. D., MELDRUM, E., ALLET, E., FISH, R., JAMOTTE, T., CURCHOD, M.-L. & LOFERER, H. 1998. A genome-based approach for the identification of essential bacterial genes. *Nature Biotechnology,* 16**,** 851-856.

ARIÖZ, C., GÖTZKE, H., LINDHOLM, L., ERIKSSON, J., EDWARDS, K., DALEY, D. O., BARTH, A. & WIESLANDER, Å. 2014. Heterologous overexpression of a monotopic glucosyltransferase (MGS) induces fatty acid remodeling in *Escherichia coli* membranes. *Biochimica et Biophysica Acta (BBA)-Biomembranes,* 1838**,** 1862-1870.

ARIÖZ, C., YE, W., BAKALI, A., GE, C., LIEBAU, J., GÖTZKE, H. R., BARTH, A., WIESLANDER, Å. & MÄLER, L. 2013. Anionic lipid binding to the foreign protein MGS provides a tight coupling between phospholipid synthesis and protein overexpression in *Escherichia coli*. *Biochemistry,* 52**,** 5533-5544.

ARRAGAIN, S., GARCIA-SERRES, R., BLONDIN, G., DOUKI, T., CLEMANCEY, M., LATOUR, J.-M., FOROUHAR, F., NEELY, H., MONTELIONE, G. T., HUNT, J. F., MULLIEZ, E., FONTECAVE, M. & ATTA, M. 2010. Post-translational modification of ribosomal proteins: structural and functional characterization of RimO from Thermotoga maritima, a radical *S*-adenosylmethionine methylthiotransferase. *Journal of Biological Chemistry,* 285**,** 5792-5801.

ATTA, M., MULLIEZ, E., ARRAGAIN, S., FOROUHAR, F., HUNT, J. F. & FONTECAVE, M. 2010. *S*-Adenosylmethionine-dependent radical-based modification of biological macromolecules. *Current Opinion in Structural Biology,* 20**,** 684-692.

AUSMEES, N., WAHLSTEDT, H., BAGCHI, S., ELLIOT, M. A., BUTTNER, M. J. & FLÄRDH, K. 2007. SmeA, a small membrane protein with multiple functions in *Streptomyces* sporulation including targeting of a SpoIIIE/FtsK-like protein to cell division septa. *Molecular Microbiology,* 65**,** 1458-1473.

BARAK, I. & MUCHOVA, K. 2013. The role of lipid domains in bacterial cell processes. *International Journal of Molecular Sciences,* 14**,** 4050-4065.

BARÁK, I., MUCHOVÁ, K., WILKINSON, A. J., O'TOOLE, P. J. & PAVLENDOVÁ, N. 2008. Lipid spirals in *Bacillus subtilis* and their role in cell division. *Molecular Microbiology,* 68**,** 1315-1327.

BARRETEAU, H., KOVAČ, A., BONIFACE, A., SOVA, M., GOBEC, S. & BLANOT, D. 2008. Cytoplasmic steps of peptidoglycan biosynthesis. *FEMS Mcrobiology Reviews,* 32**,** 168-207.

BATH, J., WU, L. J., ERRINGTON, J. & WANG, J. C. 2000. Role of *Bacillus subtilis* SpoIIIE in DNA transport across the mother cell-prespore division septum. *Science,* 290**,** 995-997.

BEIRAS-FERNANDEZ, A., VOGT, F., SODIAN, R. & WEIS, F. 2010. Daptomycin: a novel lipopeptide antibiotic against Gram-positive pathogens. *Infection and Drug Resistance,* 3**,** 95-101.

BELLIER, A., GOMINET, M. & MAZODIER, P. 2006. Post-translational control of the *Streptomyces lividans* ClgR regulon by ClpP. *Microbiology,* 152**,** 1021-1027.

BELLIER, A. & MAZODIER, P. 2004. ClgR, a novel regulator of clp and lon expression in *Streptomyces* . *Journal of Bacteriology,* 186**,** 3238-3248.

BENJDIA, A., SUBRAMANIAN, S., LEPRINCE, J., VAUDRY, H., JOHNSON, M. K. & BERTEAU, O. 2010. Anaerobic sulfatase-maturating enzyme–A mechanistic link with glycyl radical-activating enzymes? *FEBS Journal,* 277**,** 1906-1920.

BENNETT, J. A., AIMINO, R. M. & MCCORMICK, J. R. 2007. *Streptomyces coelicolor* genes *ftsL* and *divIC* play a role in cell division but are dispensable for colony formation. *Journal of Bacteriology,* 189**,** 8982-8992.

BENNETT, J. A., YARNALL, J., CADWALLADER, A. B., KUENNEN, R., BIDEY, P., STADELMAIER, B. & MCCORMICK, J. R. 2009. Medium-dependent phenotypes of *Streptomyces coelicolor* with mutations in *ftsI* or *ftsW*. *Journal of Bacteriology,* 191**,** 661-664.

BENSON, A. A. & MARUO, B. 1958. Piant phospholipids. I. Identification of the phosphatidyl glycerols. *Biochimica Biophysica Acta,* 27**,** 189-195.

BENTLEY, S., CHATER, K., CERDENO-TARRAGA, A.-M., CHALLIS, G., THOMSON, N., JAMES, K., HARRIS, D., QUAIL, M., KIESER, H. & HARPER, D. 2002. Complete genome sequence of the model actinomycete *Streptomyces coelicolor* A3 (2). *Nature,* 417**,** 141-147.

BERTEAU, O., GUILLOT, A., BENJDIA, A. & RABOT, S. 2006. A new type of bacterial sulfatase reveals a novel maturation pathway in prokaryotes. *Journal of Biological Chemistry,* 281**,** 22464-22470.

BIBB, M. J., MOLLE, V. & BUTTNER, M. J. 2000. σ^{BldN}, an extracytoplasmic function RNA polymerase sigma factor required for aerial mycelium formation in *Streptomyces coelicolor* A3 (2). *Journal of Bacteriology,* 182**,** 4606-4616.

BIGNELL, D. R., TAHLAN, K., COLVIN, K. R., JENSEN, S. E. & LESKIW, B. K. 2005. Expression of *ccaR*, encoding the positive activator of cephamycin C and clavulanic acid production in *Streptomyces clavuligerus*, is dependent on *bldG*. *Antimicrobial Agents and Chemotherapy,* 49**,** 1529-1541.

BIGNELL, D. R., WARAWA, J. L., STRAP, J. L., CHATER, K. F. & LESKIW, B. K. 2000. Study of the bldG locus suggests that an anti-anti-sigma factor and an anti-sigma factor may be involved in *Streptomyces coelicolor* antibiotic production and sporulation. *Microbiology,* 146**,** 2161-2173.

BIGOT, S., CORRE, J., LOUARN, J. M., CORNET, F. & BARRE, F. X. 2004. FtsK activities in Xer recombination, DNA mobilization and cell division involve overlapping and separate domains of the protein. *Molecular Microbiology,* 54**,** 876-886.

BIGOT, S., SIVANATHAN, V., POSSOZ, C., BARRE, F. X. & CORNET, F. 2007. FtsK, a literate chromosome segregation machine. *Molecular Microbiology,* 64**,** 1434-1441.

BIMBOIM, H. & DOLY, J. 1979. A rapid alkaline extraction procedure for screening recombinant plasmid DNA. *Nucleic Acids Research,* 7**,** 1513-1523.

BISHOP, A., FIELDING, S., DYSON, P. & HERRON, P. 2004. Systematic insertional mutagenesis of a streptomycete genome: a link between osmoadaptation and antibiotic production. *Genome Research,* 14**,** 893-900.

BLIGH, E. G. & DYER, W. J. 1959. A rapid method of total lipid extraction and purification. *Canadian Journal of Biochemistry and Physiology,* 37**,** 911-917.

BOKHOVE, M., CLAESSEN, D., DE JONG, W., DIJKHUIZEN, L., BOEKEMA, E. J. & OOSTERGETEL, G. T. 2013. Chaplins of *Streptomyces coelicolor* self-assemble into two distinct functional amyloids. *Journal of Structural Biology,* 184**,** 301-309.

BORODINA, I., KRABBEN, P. & NIELSEN, J. 2005. Genome-scale analysis of *Streptomyces coelicolor* A3(2) metabolism. *Genome Research,* 15**,** 820-829.

BOUHSS, A., TRUNKFIELD, A. E., BUGG, T. D. & MENGIN-LECREULX, D. 2008. The biosynthesis of peptidoglycan lipid-linked intermediates. *FEMS Mcrobiology Reviews,* 32**,** 208-233.

BRANA, A. F., MANZANAL, M. B. & HARDISSON, C. 1982. Mode of cell wall growth of *Streptomyces* antibioticus. *FEMS Microbiology Letters,* 13**,** 231-235.

BREAKER, R. R. 2012. Riboswitches and the RNA world. *Cold Spring Harbor Perspectives in Biology,* 4**,** a003566.

BRENNAN, R. G. & MATTHEWS, B. W. 1989. The helix-turn-helix DNA binding motif. *The Journal of Biological Chemistry,* 264**,** 1903-1906.

BROWN, N. L., STOYANOV, J. V., KIDD, S. P. & HOBMAN, J. L. 2003. The MerR family of transcriptional regulators. *FEMS Mcrobiology Reviews,* 27**,** 145-163.

BUDDELMEIJER, N. & BECKWITH, J. 2004. A complex of the *Escherichia coli* cell division proteins FtsL, FtsB and FtsQ forms independently of its localization to the septal region. *Molecular Microbiology,* 52**,** 1315-1327.

BURGER, A., SICHLER, K., KELEMEN, G., BUTTNER, M. & WOHLLEBEN, W. 2000. Identification and characterization of the *mre* gene region of *Streptomyces coelicolor* A3 (2). *Molecular and General Genetics MGG,* 263**,** 1053-1060.

BURNE, R. A., WEN, Z. T., CHEN, Y.-Y. M. & PENDERS, J. E. 1999. Regulation of expression of the fructan hydrolase gene of *Streptococcus mutans* GS-5 by induction and carbon catabolite repression. *Journal of Bacteriology,* 181**,** 2863-2871.

BUSH, M. J., BIBB, M. J., CHANDRA, G., FINDLAY, K. C. & BUTTNER, M. J. 2013. Genes required for aerial growth, cell division, and chromosome segregation are targets of WhiA before sporulation in *Streptomyces venezuelae*. *MBio,* 4**,** e00684-13.

BYSTRYKH, L. V., FERNANDEZ-MORENO, M. A., HERREMA, J. K., MALPARTIDA, F., HOPWOOD, D. A. & DIJKHUIZEN, L. 1996. Production of actinorhodin-related "blue pigments" by *Streptomyces coelicolor* A3(2). *Journal of Bacteriology,* 178**,** 2238-2244.

CABEEN, M. T. & JACOBS-WAGNER, C. 2005. Bacterial cell shape. *Nature Reviews Microbiology,* 3**,** 601-610.

CAPSTICK, D. S., JOMAA, A., HANKE, C., ORTEGA, J. & ELLIOT, M. A. 2011. Dual amyloid domains promote differential functioning of the chaplin proteins during *Streptomyces* aerial morphogenesis. *Proceedings of the National Academy of Sciences,* 108**,** 9821-9826.

CAPSTICK, D. S., WILLEY, J. M., BUTTNER, M. J. & ELLIOT, M. A. 2007. SapB and the chaplins: connections between morphogenetic proteins in *Streptomyces coelicolor*. *Molecular Microbiology,* 64**,** 602-613.

CARBALLIDO-LOPEZ, R. 2006. The bacterial actin-like cytoskeleton. *Microbiology and Molecular Biology Reviews,* 70**,** 888-909.

CASTUMA, C., CROOKE, E. & KORNBERG, A. 1993. Fluid membranes with acidic domains activate DnaA, the initiator protein of replication in *Escherichia coli*. *Journal of Biological Chemistry,* 268**,** 24665-24668.

CHALLIS, G. L. & HOPWOOD, D. A. 2003. Synergy and contingency as driving forces for the evolution of multiple secondary metabolite production by *Streptomyces* species. *Proceedings of the National Academy of Sciences,* 100**,** 14555-14561.

CHAMPNESS, W. C. 1988. New loci required for *Streptomyces coelicolor* morphological and physiological differentiation. *Journal of Bacteriology,* 170**,** 1168-1174.

CHATER, K. 1972. A morphological and genetic mapping study of white colony mutants of *Streptomyces coelicolor*. *Journal of General Microbiology,* 72**,** 9-28.

CHATER, K. 1975. Construction and phenotypes of double sporulation deficient mutants in *Streptomyces coelicolor* A3 (2). *Journal of General Microbiology,* 87**,** 312-325.

CHATER, K. F. 1998. Taking a genetic scalpel to the *Streptomyces* colony. *Microbiology,* 144**,** 1465-1478.

CHATER, K. F. 2001. Regulation of sporulation in *Streptomyces coelicolor* A3 (2): a checkpoint multiplex? *Current Opinion in Microbiology,* 4**,** 667-673.

CHATER, K. F. 2011. Differentiation in *Streptomyces*: the properties and programming of diverse cell-types. *Streptomyces: Molecular Biology and Biotechnology,* 3**,** 43-86.

CHATER, K. F., BRUTON, C. J., PLASKITT, K. A., BUTTNER, M. J., MÉNDEZ, C. & HELMANN, J. D. 1989. The developmental fate of *S. coelicolor* hyphae depends upon a gene product homologous with the motility σ factor of *B. subtilis*. *Cell,* 59**,** 133-143.

CHATER, K. F. & CHANDRA, G. 2006. The evolution of development in *Streptomyces* analysed by genome comparisons. *FEMS Mcrobiology Reviews,* 30**,** 651-672.

CHATER, K. F. & CHANDRA, G. 2008. The use of the rare UUA codon to define "expression space" for genes involved in secondary metabolism, development and environmental adaptation in *Streptomyces* . *The Journal of Microbiology,* 46**,** 1-11.

CHATER, K. F. & HORINOUCHI, S. 2003. Signalling early developmental events in two highly diverged *Streptomyces* species. *Molecular Microbiology,* 48**,** 9-15.

CHATTERJEE, S. & CHAUDHURI, K. 2012. Gram-negative bacteria: The cell membranes. *Outer Membrane Vesicles of Bacteria.* Springer.15-34

CHENG, S. C., HUANG, M. Z. & SHIEA, J. 2011. Thin layer chromatography/mass spectrometry. *Journal of Chromatography A,* 1218**,** 2700-2711.

CHIU, M., FOLCHER, M., GRIFFIN, P., HOLT, T., KLATT, T. & THOMPSON, C. 1996. Characterization of the covalent binding of thiostrepton to a thiostrepton-induced protein from *Streptomyces lividans*. *Biochemistry,* 35**,** 2332-2341.

CHIU, M. L., FOLCHER, M., KATOH, T., PUGLIA, A. M., VOHRADSKY, J., YUN, B.-S., SETO, H. & THOMPSON, C. J. 1999. Broad Spectrum Thiopeptide Recognition Specificity of the *Streptomyces lividans* TipAL Protein and Its Role in Regulating Gene Expression. *Journal of Biological Chemistry,* 274**,** 20578-20586.

CHRISTIE, W. W. 2014. Phosphatidylglycerol and related lipids. The AOCS Lipid Library, 2,1-7.

CLAESSEN, D., RINK, R., DE JONG, W., SIEBRING, J., DE VREUGD, P., BOERSMA, F. H., DIJKHUIZEN, L. & WÖSTEN, H. A. 2003. A novel class of secreted hydrophobic proteins is involved in aerial hyphae formation in *Streptomyces coelicolor* by forming amyloid-like fibrils. *Genes and Development,* 17**,** 1714-1726.

CLAESSEN, D., STOKROOS, I., DEELSTRA, H. J., PENNINGA, N. A., BORMANN, C., SALAS, J. A., DIJKHUIZEN, L. & WÖSTEN, H. A. 2004. The formation of the rodlet layer of streptomycetes is the result of the interplay between rodlins and chaplins. *Molecular Microbiology,* 53**,** 433-443.

CLAESSEN, D., WÖSTEN, H. A., KEULEN, G. V., FABER, O. G., ALVES, A. M., MEIJER, W. G. & DIJKHUIZEN, L. 2002. Two novel homologous proteins of *Streptomyces coelicolor* and *Streptomyces lividans* are involved in the formation of the rodlet layer and mediate attachment to a hydrophobic surface. *Molecular Microbiology,* 44**,** 1483-1492.

CLAMP, M., CUFF, J., SEARLE, S. M. & BARTON, G. J. 2004. The Jalview Java alignment editor. *Bioinformatics,* 20**,** 426- 427.

CLARK, D., LIGHTNER, V., EDGAR, R., MODRICH, P., CRONAN, J. E., JR. & BELL, R. M. 1980. Regulation of phospholipid biosynthesis in *Escherichia coli*. Cloning of the structural gene for the biosynthetic *sn*-glycerol-3-phosphate dehydrogenase. *Journal of Biological Chemistry,* 255**,** 714-717.

COLE, S., BROSCH, R., PARKHILL, J., GARNIER, T., CHURCHER, C., HARRIS, D., GORDON, S., EIGLMEIER, K., GAS, S. & BARRY, C. R. 1998. Deciphering the biology of *Mycobacterium tuberculosis* from the complete genome sequence. *Nature,* 393**,** 537-544.

COMBA, S., MENENDEZ-BRAVO, S., ARABOLAZA, A. & GRAMAJO, H. 2013. Identification and physiological characterization of phosphatidic acid phosphatase enzymes involved in triacylglycerol biosynthesis in *Streptomyces coelicolor*. *Microb Cell Fact,* 12.

COMMICHAU, F. M., PIETACK, N. & STÜLKE, J. 2013. Essential genes in *Bacillus subtilis*: a re-evaluation after ten years. *Molecular BioSystems,* 9**,** 1068-1075.

COT, M., RAY, A., GILLERON, M., VERCELLONE, A., LARROUY-MAUMUS, G., ARMAU, E., GAUTHIER, S., TIRABY, G., PUZO, G. & NIGOU, J. 2011. Lipoteichoic acid in *Streptomyces hygroscopicus*: structural model and immunomodulatory activities. *PloS one,* 6**,** e26316.

D'COSTA, V. M., MUKHTAR, T. A., PATEL, T., KOTEVA, K., WAGLECHNER, N., HUGHES, D. W., WRIGHT, G. D. & DE PASCALE, G. 2012. Inactivation of the lipopeptide antibiotic daptomycin by hydrolytic mechanisms. *Antimicrobial Agents and Chemotherapy,* 56**,** 757-764.

DA COSTA, M. S., ALBUQUERQUE, L., NOBRE, M. F. & WAIT, R. 2011. The Identification of Polar Lipids in Prokaryotes. *Methods in Microbiology.* Elsevier Ltd, 38,165-181.

DANIEL, R. A. & ERRINGTON, J. 2003. Control of cell morphogenesis in bacteria: two distinct ways to make a rod-shaped cell. *Cell,* 113**,** 767-776.

DAVIS, N. & CHATER, K. 1990. Spore colour in *Streptomyces Streptomyces coelicolor* A3 (2) involves the developmentally regulated synthesis of a compound biosynthetically related to polyketide antibiotics. *Molecular Microbiology,* 4**,** 1679-1691.

DAVIS, N. & CHATER, K. 1992. The *Streptomyces coelicolor whiB* gene encodes a small transcription factor-like protein dispensable for growth but essential for sporulation. *Molecular and General Genetics MGG,* 232**,** 351-358.

DE JONG, W., WÖSTEN, H. A., DIJKHUIZEN, L. & CLAESSEN, D. 2009. Attachment of *Streptomyces coelicolor* is mediated by amyloidal fimbriae that are anchored to the cell surface via cellulose. *Molecular Microbiology,* 73**,** 1128-1140.

DE ROSA, M., GAMBACORTA, A. & GLIOZZI, A. 1986. Structure, biosynthesis, and physicochemical properties of archaebacterial lipids. *Microbiological Reviews,* 50**,** 70-80.

DEL SOL, R., MULLINS, J. G., GRANTCHAROVA, N., FLARDH, K. & DYSON, P. 2006. Influence of CrgA on assembly of the cell division protein FtsZ during development of *Streptomyces coelicolor*. *Journal of Bacteriology,* 188**,** 1540-1550.

DEN HENGST, C. D., TRAN, N. T., BIBB, M. J., CHANDRA, G., LESKIW, B. K. & BUTTNER, M. J. 2010. Genes essential for morphological development and antibiotic production in *Streptomyces coelicolor* are targets of BldD during vegetative growth. *Molecular Microbiology,* 78**,** 361-379.

DI BERARDO, C., CAPSTICK, D. S., BIBB, M. J., FINDLAY, K. C., BUTTNER, M. J. & ELLIOT, M. A. 2008. Function and redundancy of the chaplin cell surface proteins in aerial hypha formation, rodlet assembly, and viability in *Streptomyces coelicolor*. *Journal of Bacteriology,* 190**,** 5879-5889.

DILLON, D. A., WU, W.-I., RIEDEL, B., WISSING, J. B., DOWHAN, W. & CARMAN, G. M. 1996. The *Escherichia coli pgpB* gene encodes for a diacylglycerol pyrophosphate phosphatase activity. *Journal of Biological Chemistry,* 271**,** 30548-30553.

DITKOWSKI, B., HOLMES, N., RYDZAK, J., DONCZEW, M., BEZULSKA, M., GINDA, K., KĘDZIERSKI, P., ZAKRZEWSKA-CZERWIŃSKA, J., KELEMEN, G. H. & JAKIMOWICZ, D. 2013. Dynamic interplay of ParA with the polarity protein, Scy, coordinates the growth with chromosome segregation in *Streptomyces coelicolor*. *Open Biology,* 3**,** 130006.

DOWER, W. J., MILLER, J. F. & RAGSDALE, C. W. 1988. High efficiency transformation of *E. coli* by high voltage electroporation. *Nucleic Acids Research,* 16**,** 6127-6145.

DRAMSI, S., MAGNET, S., DAVISON, S. & ARTHUR, M. 2008. Covalent attachment of proteins to peptidoglycan. *FEMS Microbiology Reviews,* 32, 307-320.

DUONG, A., CAPSTICK, D. S., DI BERARDO, C., FINDLAY, K. C., HESKETH, A., HONG, H. J. & ELLIOT, M. A. 2012. Aerial development in *Streptomyces coelicolor* requires sortase activity. *Molecular Microbiology,* 83**,** 992-1005.

DYSON, P. 2009. *Streptomyces* . *In:* SCHAECHTER, M. (ed.) *Encyclopedia of Molecular Microbiology.* Oxford: Elsevier, 318-332.

ECCLESTON, M., ALI, R. A., SEYLER, R., WESTPHELING, J. & NODWELL, J. 2002. Structural and genetic analysis of the BldB protein of *Streptomyces coelicolor*. *Journal of Bacteriology,* 184**,** 4270-4276.

EGAN, A. J. & VOLLMER, W. 2013. The physiology of bacterial cell division. *Annals of the New York Academy of Sciences,* 1277**,** 8-28.

EIAMPHUNGPORN, W. & HELMANN, J. D. 2008. The *Bacillus subtilis* σ^M regulon and its contribution to cell envelope stress responses. *Molecular Microbiology,* 67**,** 830-848.

ELLIOT, M. A., BIBB, M. J., BUTTNER, M. J. & LESKIW, B. K. 2001. BldD is a direct regulator of key developmental genes in *Streptomyces coelicolor* A3 (2). *Molecular Microbiology,* 40**,** 257-269.

ELLIOT, M. A., BUTTNER, M. J. & NODWELL, J. R. 2008. Multicellular Development in *Streptomyces*. *In:* WHITWORTH, D. E. (ed.) *Mycobacteria: Multicellularity and Differentiation.* Washington, D.C.: ASM Press,419-439.

ELLIOT, M. A., KAROONUTHAISIRI, N., HUANG, J., BIBB, M. J., COHEN, S. N., KAO, C. M. & BUTTNER, M. J. 2003. The chaplins: a family of hydrophobic cell-surface proteins involved in aerial mycelium formation in *Streptomyces coelicolor*. *Genes and Development,* 17**,** 1727-1740.

ENGUITA, F. J., DE LA FUENTE, J. L., MARTÍN, J. F. & LIRAS, P. 1996. An inducible expression system of histidine-tagged proteins in *Streptomyces lividans* for one-step purification by Ni^{2+} affinity chromatography. *FEMS Microbiology Letters,* 137**,** 135-140.

ERRINGTON, J., DANIEL, R. A. & SCHEFFERS, D. J. 2003. Cytokinesis in bacteria. *Microbiology and Molecular Biology Reviews,* 67**,** 52-65, table of contents.

FACEY, P., HITCHINGS, M., SAAVEDRA-GARCIA, P., FERNANDEZ-MARTINEZ, L., DYSON, P. & DEL SOL, R. 2009. *Streptomyces coelicolor* Dps-like proteins: differential dual roles in response to stress during vegetative growth and in nucleoid condensation during reproductive cell division. *Molecular Microbiology,* 73**,** 1186-1202.

FAHY, E., COTTER, D., SUD, M. & SUBRAMANIAM, S. 2011. Lipid classification, structures and tools. *Biochimica et Biophysica Acta,* 1811**,** 637-647.

FAHY, E., SUBRAMANIAM, S., BROWN, H. A., GLASS, C. K., MERRILL, A. H., JR., MURPHY, R. C., RAETZ, C. R., RUSSELL, D. W., SEYAMA, Y., SHAW, W., SHIMIZU, T., SPENER, F., VAN MEER, G., VANNIEUWENHZE, M. S., WHITE, S. H., WITZTUM, J. L. & DENNIS, E. A. 2005. A comprehensive classification system for lipids. *Journal of Lipid Research,* 46**,** 839-861.

FAHY, E., SUBRAMANIAM, S., MURPHY, R. C., NISHIJIMA, M., RAETZ, C. R., SHIMIZU, T., SPENER, F., VAN MEER, G., WAKELAM, M. J. & DENNIS, E. A. 2009. Update of the LIPID MAPS comprehensive classification system for lipids. *Journal of Lipid Research,* 50**,** S9-14.

FAN, J., JIANG, D., ZHAO, Y., LIU, J. & ZHANG, X. C. 2014. Crystal structure of lipid phosphatase *Escherichia coli* phosphatidylglycerophosphate phosphatase B. *Proceedings of the National Academy of Sciences,* 111**,** 7636-7640.

FERNANDEZ-MARTINEZ, L., DEL SOL, R., EVANS, M., FIELDING, S., HERRON, P., CHANDRA, G. & DYSON, P. 2011. A transposon insertion single-gene knockout library and new ordered cosmid library for the model organism *Streptomyces coelicolor* A3 (2). *Antonie Van Leeuwenhoek,* 99**,** 515-522.

FINN, R. D., BATEMAN, A., CLEMENTS, J., COGGILL, P., EBERHARDT, R. Y., EDDY, S. R., HEGER, A., HETHERINGTON, K., HOLM, L., MISTRY, J., SONNHAMMER, E. L., TATE, J. & PUNTA, M. 2014. Pfam: the protein families database. *Nucleic Acids Research,* 42**,** D222-D230.

FISHOV, I. & WOLDRINGH, C. L. 1999. Visualization of membrane domains in *Escherichia coli*. *Molecular Microbiology,* 32**,** 1166-1172.

FLARDH, K. 2003. Growth polarity and cell division in *Streptomyces* . *Current Opinion in Microbiology,* 6**,** 564-571.

FLÄRDH, K. 2003. Essential role of DivIVA in polar growth and morphogenesis in *Streptomyces coelicolor* A3 (2). *Molecular Microbiology,* 49**,** 1523-1536.

FLÄRDH, K. 2010. Cell polarity and the control of apical growth in *Streptomyces* . *Current Opinion in Microbiology,* 13**,** 758-765.

FLÄRDH, K. & BUTTNER, M. J. 2009. *Streptomyces* morphogenetics: dissecting differentiation in a filamentous bacterium. *Nature Reviews Microbiology,* 7**,** 36-49.

FLÄRDH, K., FINDLAY, K. C. & CHATER, K. F. 1999. Association of early sporulation genes with suggested developmental decision points in *Streptomyces coelicolor* A3 (2). *Microbiology,* 145**,** 2229-2243.

FLÄRDH, K., LEIBOVITZ, E., BUTTNER, M. J. & CHATER, K. F. 2000. Generation of a non-sporulating strain of *Streptomyces coelicolor* A3 (2) by the manipulation of a developmentally controlled *ftsZ* promoter. *Molecular Microbiology,* 38**,** 737-749.

FLOROVA, G., KAZANINA, G. & REYNOLDS, K. A. 2002. Enzymes involved in fatty acid and polyketide biosynthesis in *Streptomyces glaucescens*: role of FabH and FabD and their acyl carrier protein specificity. *Biochemistry,* 41**,** 10462-10471.

FRENKIEL-KRISPIN, D., BEN-AVRAHAM, I., ENGLANDER, J., SHIMONI, E., WOLF, S. G. & MINSKY, A. 2004. Nucleoid restructuring in stationary-state bacteria. *Molecular Microbiology,* 51**,** 395-405.

FREY, P. A., HEGEMAN, A. D. & RUZICKA, F. J. 2008. The Radical SAM Superfamily. *Critical Reviews in Biochemistry and Molecular Biology,* 43**,** 63-88.

FUCHINO, K., BAGCHI, S., CANTLAY, S., SANDBLAD, L., WU, D., BERGMAN, J., KAMALI-MOGHADDAM, M., FLARDH, K. & AUSMEES, N. 2013. Dynamic gradients of an intermediate filament-like cytoskeleton are recruited by a polarity landmark during apical growth. *Proceedings of the National Academy of Sciences,* 110**,** E1889-E1897.

FUKUDA, A., MATSUYAMA, S., HARA, T., NAKAYAMA, J., NAGASAWA, H. & TOKUDA, H. 2002. Aminoacylation of the N-terminal cysteine is essential for Lol-dependent release of lipoproteins from membranes but does not depend on lipoprotein sorting signals. *Journal of Biological Chemistry,* 277**,** 43512-43518.

FUNK, C. R., ZIMNIAK, L. & DOWHAN, W. 1992. The pgpA and pgpB genes of *Escherichia coli* are not essential: evidence for a third phosphatidylglycerophosphate phosphatase. *Journal of Bacteriology,* 174**,** 205-213.

GAGO, G., DIACOVICH, L., ARABOLAZA, A., TSAI, S. C. & GRAMAJO, H. 2011. Fatty acid biosynthesis in actinomycetes. *FEMS Microbiology Reviews,* 35**,** 475-497.

GALLAGHER, L. A., RAMAGE, E., JACOBS, M. A., KAUL, R., BRITTNACHER, M. & MANOIL, C. 2007. A comprehensive transposon mutant library of *Francisella novicida*, a bioweapon surrogate. *Proceedings of the National Academy of Sciences,* 104**,** 1009-1014.

GEHRING, A. M., NODWELL, J. R., BEVERLEY, S. M. & LOSICK, R. 2000. Genomewide insertional mutagenesis in *Streptomyces coelicolor* reveals additional genes involved in morphological differentiation. *Proceedings of the National Academy of Sciences,* 97**,** 9642-9647.

GEIGER, O., LOPEZ-LARA, I. M. & SOHLENKAMP, C. 2013. Phosphatidylcholine biosynthesis and function in bacteria. *Biochimica et Biophysica Acta,* 1831**,** 503-513.

GERDES, S. Y., SCHOLLE, M. D., CAMPBELL, J. W., BALAZSI, G., RAVASZ, E., DAUGHERTY, M. D., SOMERA, A. L., KYRPIDES, N. C., ANDERSON, I., GELFAND, M. S., BHATTACHARYA, A., KAPATRAL, V., D'SOUZA, M., BAEV, M. V., GRECHKIN, Y., MSEEH, F., FONSTEIN, M. Y., OVERBEEK, R., BARABASI, A. L., OLTVAI, Z. N. & OSTERMAN, A. L. 2003. Experimental determination and system level analysis of essential genes in *Escherichia coli* MG1655. *Journal of Bacteriology,* 185**,** 5673-5684.

GOPALAKRISHNAN, A. S., CHEN, Y.-C., TEMKIN, M. & DOWHAN, W. 1986. Structure and expression of the gene locus encoding the

phosphatidylglycerophosphate synthase of *Escherichia coli*. *Journal of Biological Chemistry,* 261**,** 1329-1338.

GORYSHIN, I. Y. & REZNIKOFF, W. S. 1998. Tn*5 in vitro* transposition. *Journal of Biological Chemistry,* 273**,** 7367-7374.

GOULIAN, M. 2010. Two-component signaling circuit structure and properties. *Current Opinion in Microbiology,* 13**,** 184-189.

GRANT, C. E., BAILEY, T. L. & NOBLE, W. S. 2011. FIMO: scanning for occurrences of a given motif. *Bioinformatics,* 27**,** 1017-1018.

GRANT, S. G., JESSEE, J., BLOOM, F. R. & HANAHAN, D. 1990. Differential plasmid rescue from transgenic mouse DNAs into *Escherichia coli* methylation-restriction mutants. *Proceedings of the National Academy of Sciences,* 87**,** 4645-4649.

GRANTCHAROVA, N., LUSTIG, U. & FLARDH, K. 2005. Dynamics of FtsZ assembly during sporulation in *Streptomyces coelicolor* A3(2). *Journal of Bacteriology,* 187**,** 3227-3237.

GRAY, D. I., GOODAY, G. W. & PROSSER, J. I. 1990. Apical hyphal extension in *Streptomyces coelicolor* A3(2). *Journal of General Microbiology,* 136**,** 1077-1084.

GUIJARRO, J., SANTAMARIA, R., SCHAUER, A. & LOSICK, R. 1988. Promoter determining the timing and spatial localization of transcription of a cloned *Streptomyces coelicolor* gene encoding a spore-associated polypeptide. *Journal of Bacteriology,* 170**,** 1895-1901.

GUST, B., CHALLIS, G. L., FOWLER, K., KIESER, T. & CHATER, K. F. 2003. PCR-targeted *Streptomyces* gene replacement identifies a protein domain needed for biosynthesis of the sesquiterpene soil odor geosmin. *Proceedings of the National Academy of Sciences,* 100**,** 1541-1546.

GUST, B., KIESER, T. & CHATER, K. 2002. PCR targeting system in *Streptomyces coelicolor* A3 (2). Online: John Innes Centre, 1-39.

GUYET, A., GOMINET, M., BENAROUDJ, N. & MAZODIER, P. 2013. Regulation of the *clpP1clpP2* operon by the pleiotropic regulator AdpA in *Streptomyces lividans*. *Archives of Microbiology,* 195**,** 831-841.

HACHMANN, A.-B., ANGERT, E. R. & HELMANN, J. D. 2009. Genetic analysis of factors affecting susceptibility of *Bacillus subtilis* to daptomycin. *Antimicrobial Agents and Chemotherapy,* 53**,** 1598-1609.

HAISER, H. J., YOUSEF, M. R. & ELLIOT, M. A. 2009. Cell wall hydrolases affect germination, vegetative growth, and sporulation in *Streptomyces coelicolor*. *Journal of Bacteriology,* 191**,** 6501-6512.

HALL, B. G. 2013. Building phylogenetic trees from molecular data with MEGA. *Molecular Biology and Evolution,* 30**,** 1229-1235.

HAMOEN, L. W., MEILE, J. C., DE JONG, W., NOIROT, P. & ERRINGTON, J. 2006. SepF, a novel FtsZ-interacting protein required for a late step in cell division. *Molecular Microbiology,* 59**,** 989-999.

HANAHAN, D. 1983. Studies on transformation of *Escherichia coli* with plasmids. *Journal of Molecular Biology,* 166**,** 557-580.

HANZELMANN, P. & SCHINDELIN, H. 2006. Binding of 5'-GTP to the C-terminal FeS cluster of the radical *S*-adenosylmethionine enzyme MoaA provides insights into its mechanism. *Proceedings of the National Academy of Sciences,* 103**,** 6829-6834.

HÄNZELMANN, P. & SCHINDELIN, H. 2004. Crystal structure of the *S*-adenosylmethionine-dependent enzyme MoaA and its implications for molybdenum cofactor deficiency in humans. *Proceedings of the National Academy of Sciences,* 101**,** 12870-12875.

HARRISON, C. J. & LANGDALE, J. A. 2006. A step by step guide to phylogeny reconstruction. *The Plant Journal,* 45**,** 561-572.

HAVERKATE, F., HOUTSMULLER, U. & VAN DEENEN, L. 1962. The enzymic hydrolysis and structure of phosphatidyl glycerol. *Biochimica et Biophysica Acta,* 63**,** 547-549.

HAWTHORNE, J. N. & ANSELL, G. B. 1982. *Phospholipids: New Comprehensive Biochemistry,* Amsterdam, Elsevier Biomedical Press.

HEACOCK, P. N. & DOWHAN, W. 1987. Construction of a lethal mutation in the synthesis of the major acidic phospholipids of *Escherichia coli*. *Journal of Biological Chemistry,* 262**,** 13044-13049.

HEERMANN, R. & JUNG, K. 2004. Structural features and mechanisms for sensing high osmolarity in microorganisms. *Current Opinion in Microbiology,* 7**,** 168-174.

HEICHLINGER, A., AMMELBURG, M., KLEINSCHNITZ, E.-M., LATUS, A., MALDENER, I., FLÄRDH, K., WOHLLEBEN, W. & MUTH, G. 2011. The MreB-like protein Mbl of *Streptomyces coelicolor* A3 (2) depends on MreB for proper localization and contributes to spore wall synthesis. *Journal of Bacteriology,* 193**,** 1533-1542.

HELMANN, J. 1991. Alternative sigma factors and the regulation of flagellar gene expression. *Molecular Microbiology,* 5**,** 2875-2882.

HEMPEL, A. M., CANTLAY, S., MOLLE, V., WANG, S.-B., NALDRETT, M. J., PARKER, J. L., RICHARDS, D. M., JUNG, Y.-G., BUTTNER, M. J. & FLÄRDH, K. 2012. The Ser/Thr protein kinase AfsK regulates polar growth and hyphal branching in the filamentous bacteria *Streptomyces*. *Proceedings of the National Academy of Sciences,* 109**,** E2371-E2379.

HEMPEL, A. M., WANG, S.-B., LETEK, M., GIL, J. A. & FLÄRDH, K. 2008. Assemblies of DivIVA mark sites for hyphal branching and can establish new zones of cell wall growth in *Streptomyces coelicolor*. *Journal of Bacteriology,* 190**,** 7579-7583.

HERAI, S., HASHIMOTO, Y., HIGASHIBATA, H., MASEDA, H., IKEDA, H., OMURA, S. & KOBAYASHI, M. 2004. Hyper-inducible expression system for streptomycetes. *Proceedings of the National Academy of Sciences,* 101**,** 14031-14035.

HERRING, C. D. & BLATTNER, F. R. 2004. Conditional lethal amber mutations in essential *Escherichia coli* genes. *Journal of Bacteriology,* 186**,** 2673-2681.

HERRON, P. R., EVANS, M. C. & DYSON, P. J. 1999. Low target site specificity of an IS6100-based mini-transposon, Tn1792, developed for transposon mutagenesis of antibiotic-producing *Streptomyces*. *FEMS Microbiology Letters,* 171**,** 215-221.

HERRON, P. R., HUGHES, G., CHANDRA, G., FIELDING, S. & DYSON, P. J. 2004. Transposon Express, a software application to report the identity of insertions obtained by comprehensive transposon mutagenesis of sequenced genomes: analysis of the preference for *in vitro* Tn*5* transposition into GC-rich DNA. *Nucleic Acids Research,* 32**,** e113-e113.

HOISCHEN, C., GURA, K., LUGE, C. & GUMPERT, J. 1997a. Lipid and fatty acid composition of cytoplasmic membranes from *Streptomyces hygroscopicus* and its stable protoplast-type L form. *Journal of Bacteriology,* 179**,** 3430-3436.

HOISCHEN, C., IHN, W., GURA, K. & GUMPERT, J. 1997b. Structural characterization of molecular phospholipid species in cytoplasmic membranes of the cell wall-less *Streptomyces hygroscopicus* L form by use of electrospray ionization coupled with collision-induced dissociation mass spectrometry. *Journal of Bacteriology,* 179**,** 3437-3442.

HOLMES, D. J., CASO, J. L. & THOMPSON, C. J. 1993. Autogenous transcriptional activation of a thiostrepton-induced gene in *Streptomyces lividans*. *EMBO Journal,* 12**,** 3183-3191.

HOLMES, N. A., WALSHAW, J., LEGGETT, R. M., THIBESSARD, A., DALTON, K. A., GILLESPIE, M. D., HEMMINGS, A. M., GUST, B. & KELEMEN, G. H. 2013. Coiled-coil protein Scy is a key component of a multiprotein assembly controlling polarized growth in *Streptomyces* . *Proceedings of the National Academy of Sciences,* 110**,** E397-E406.

HÖLTJE, J.-V. 1998. Growth of the stress-bearing and shape-maintaining murein sacculus of *Escherichia coli*. *Microbiology and Molecular Biology Reviews,* 62**,** 181-203.

HOMEROVA, D., SEVCIKOVA, B., REZUCHOVA, B. & KORMANEC, J. 2012. Regulation of an alternative sigma factor σ^{I} by a partner switching mechanism with an anti-sigma factor PrsI and an anti-anti-sigma factor ArsI in *Streptomyces coelicolor* A3 (2). *Gene,* 492**,** 71-80.

HONG, H. J., PAGET, M. S. & BUTTNER, M. J. 2002. A signal transduction system in *Streptomyces coelicolor* that activates the expression of a putative cell wall glycan operon in response to vancomycin and other cell wall-specific antibiotics. *Molecular Microbiology,* 44**,** 1199-1211.

HOPWOOD, D., WILDERMUTH, H. & PALMER, H. M. 1970. Mutants of *Streptomyces coelicolor* defective in sporulation. *Journal of General Microbiology,* 61**,** 397-408.

HOPWOOD, D. A. 1999. Forty years of genetics with *Streptomyces* : from in vivo through in vitro to in silico. *Microbiology,* 145**,** 2183-2202.

HOPWOOD, D. A. 2006. Soil to genomics: the *Streptomyces* chromosome. *Annual Review of Genetics,* 40**,** 1-23.

HOSKISSON, P. A. & HUTCHINGS, M. I. 2006. MtrAB–LpqB: a conserved three-component system in actinobacteria? *Trends in microbiology,* 14**,** 444-449.

HOSKISSON, P. A. & RIGALI, S. 2009. Variation in form and function: the helix-turn-helix regulators of the GntR superfamily. *Advances in Applied Microbiology,* 69**,** 1-22.

HUANG, C. H., LIN, Y. S., YANG, Y. L., HUANG, S. W. & CHEN, C. W. 1998. The telomeres of *Streptomyces* chromosomes contain conserved palindromic sequences with potential to form complex secondary structures. *Molecular Microbiology,* 28**,** 905-916.

HUANG, J., SHI, J., MOLLE, V., SOHLBERG, B., WEAVER, D., BIBB, M. J., KAROONUTHAISIRI, N., LIH, C. J., KAO, C. M. & BUTTNER, M. J. 2005. Cross-regulation among disparate antibiotic biosynthetic pathways of *Streptomyces coelicolor*. *Molecular Microbiology,* 58**,** 1276-1287.

HUGHES, K. T. & MATHEE, K. 1998. The anti-sigma factors. *Annual Reviews in Microbiology,* 52**,** 231-286.

HUNT, A. C., SERVÍN-GONZÁLEZ, L., KELEMEN, G. H. & BUTTNER, M. J. 2005. The *bldC* developmental locus of *Streptomyces coelicolor* encodes a member of a family of small DNA-binding proteins related to the DNA-binding domains of the MerR family. *Journal of Bacteriology,* 187**,** 716-728.

HUTCHINGS, M. I., HONG, H. J., LEIBOVITZ, E., SUTCLIFFE, I. C. & BUTTNER, M. J. 2006. The sigma(E) cell envelope stress response of *Streptomyces coelicolor* is influenced by a novel lipoprotein, CseA. *Journal of Bacteriology,* 188**,** 7222-7229.

HUTCHINGS, M. I., HOSKISSON, P. A., CHANDRA, G. & BUTTNER, M. J. 2004. Sensing and responding to diverse extracellular signals? Analysis of the sensor kinases and response regulators of *Streptomyces coelicolor* A3 (2). *Microbiology,* 150**,** 2795-2806.

HUTCHINGS, M. I., PALMER, T., HARRINGTON, D. J. & SUTCLIFFE, I. C. 2009. Lipoprotein biogenesis in Gram-positive bacteria: knowing when to hold ‘em, knowing when to fold ‘em. *Trends in Microbiology,* 17**,** 13-21.

ISHIDA, Y., KITAGAWA, K., NAKAYAMA, A. & OHTANI, H. 2006. Complementary analysis of lipids in whole bacteria cells by thermally assisted hydrolysis and methylation-GC and MALDI-MS combined with on-probe sample pretreatment. *Journal of Analytical and Applied Pyrolysis,* 77**,** 116-120.

JACKSON, B. & KENNEDY, E. 1983. The biosynthesis of membrane-derived oligosaccharides. A membrane-bound phosphoglycerol transferase. *Journal of Biological Chemistry,* 258**,** 2394-2398.

JACOBS, M. A., ALWOOD, A., THAIPISUTTIKUL, I., SPENCER, D., HAUGEN, E., ERNST, S., WILL, O., KAUL, R., RAYMOND, C. & LEVY, R. 2003. Comprehensive transposon mutant library of *Pseudomonas aeruginosa*. *Proceedings of the National Academy of Sciences,* 100**,** 14339-14344.

JAKIMOWICZ, D. & CHATER, K. 2002. The ParB protein of *Streptomyces coelicolor* A3 (2) recognizes a cluster of *parS* sequences within the origin-proximal region of the linear chromosome. *Molecular Microbiology,* 45**,** 1365-1377.

JAKIMOWICZ, D., GUST, B., ZAKRZEWSKA-CZERWINSKA, J. & CHATER, K. F. 2005. Developmental-stage-specific assembly of ParB complexes in *Streptomyces coelicolor* hyphae. *Journal of Bacteriology,* 187**,** 3572-3580.

JAKIMOWICZ, D., MAJKA, J., MESSER, W., SPECK, C., FERNANDEZ, M., MARTIN, M. C., SANCHEZ, J., SCHAUWECKER, F., KELLER, U. &

SCHREMPF, H. 1998. Structural elements of the *Streptomyces oriC* region and their interactions with the DnaA protein. *Microbiology,* 144**,** 1281-1290.

JAKIMOWICZ, D., MOUZ, S., ZAKRZEWSKA-CZERWIŃSKA, J. & CHATER, K. F. 2006. Developmental control of a *parAB* promoter leads to formation of sporulation-associated ParB complexes in *Streptomyces coelicolor*. *Journal of Bacteriology,* 188**,** 1710-1720.

JAKIMOWICZ, D. & VAN WEZEL, G. P. 2012. Cell division and DNA segregation in *Streptomyces* : how to build a septum in the middle of nowhere? *Molecular Microbiology,* 85**,** 393-404.

JAKIMOWICZ, D., ŻYDEK, P., KOIS, A., ZAKRZEWSKA-CZERWIŃSKA, J. & CHATER, K. F. 2007. Alignment of multiple chromosomes along helical ParA scaffolding in sporulating *Streptomyces* hyphae. *Molecular Microbiology,* 65**,** 625-641.

JI, Y., ZHANG, B., VAN, S. F., WARREN, P., WOODNUTT, G., BURNHAM, M. K. & ROSENBERG, M. 2001. Identification of critical *staphylococcal* genes using conditional phenotypes generated by antisense RNA. *Science,* 293**,** 2266-2269.

JORDAN, S., HUTCHINGS, M. I. & MASCHER, T. 2008. Cell envelope stress response in Gram-positive bacteria. *FEMS Mcrobiology Reviews,* 32**,** 107-146.

JYOTHIKUMAR, V., KLANBUT, K., TIONG, J., ROXBURGH, J. S., HUNTER, I. S., SMITH, T. K. & HERRON, P. R. 2012. Cardiolipin synthase is required for *Streptomyces coelicolor* morphogenesis. *Molecular Microbiology,* 84**,** 181-197.

JYOTHIKUMAR, V., TILLEY, E. J., WALI, R. & HERRON, P. R. 2008. Time-lapse microscopy of *Streptomyces Streptomyces coelicolor* growth and sporulation. *Applied and Environmental Microbiology,* 74**,** 6774-6781.

KAIMER, C. & GRAUMANN, P. L. 2010. *Bacillus subtilis* CinA is a stationary phase-induced protein that localizes to the nucleoid and plays a minor role in competent cells. *Archives in Microbiology,* 192**,** 549-557.

KANEDA, T. 1991. Iso-and anteiso-fatty acids in bacteria: biosynthesis, function, and taxonomic significance. *Microbiological Reviews,* 55**,** 288-302.

KATO, J.-Y., FUNA, N., WATANABE, H., OHNISHI, Y. & HORINOUCHI, S. 2007. Biosynthesis of γ-butyrolactone autoregulators that switch on secondary metabolism and morphological development in *Streptomyces* . *Proceedings of the National Academy of Sciences,* 104**,** 2378-2383.

KAWAI, F., SHODA, M., HARASHIMA, R., SADAIE, Y., HARA, H. & MATSUMOTO, K. 2004. Cardiolipin domains in *Bacillus subtilis* marburg membranes. *Journal of Bacteriology,* 186**,** 1475-1483.

KEIJSER, B. J., VAN WEZEL, G. P., CANTERS, G. W. & VIJGENBOOM, E. 2002. Developmental regulation of the *Streptomyces lividans* ram genes: involvement of RamR in regulation of the *ramCSAB* operon. *Journal of Bacteriology,* 184**,** 4420-4429.

KELEMEN, G. H., BRIAN, P., FLÄRDH, K., CHAMBERLIN, L., CHATER, K. F. & BUTTNER, M. J. 1998. Developmental regulation of transcription of *whiE,* a locus specifying the polyketide spore pigment in *Streptomyces coelicolor* A3 (2). *Journal of Bacteriology,* 180**,** 2515-2521.

KELEMEN, G. H., BROWN, G. L., KORMANEC, J., POTÚČKOVA, L., CHATER, K. F. & BUTTNER, M. J. 1996. The positions of the sigma-factor genes, *whiG* and *sigF,* in the hierarchy controlling the development of spore chains in the aerial hyphae of *Streptomyces coelicolor* A3 (2). *Molecular Microbiology,* 21**,** 593-603.

KELEMEN, G. H. & BUTTNER, M. J. 1998. Initiation of aerial mycelium formation in *Streptomyces* . *Current Opinion in Microbiology,* 1**,** 656-662.

KELEMEN, G. H., VIOLLIER, P. H., TENOR, J., MARRI, L., BUTTNER, M. J. & THOMPSON, C. J. 2001. A connection between stress and development in the multicellular prokaryote *Streptomyces coelicolor* A3 (2). *Molecular Microbiology,* 40**,** 804-814.

KELLEY, L. A., MEZULIS, S., YATES, C. M., WASS, M. N. & STERNBERG, M. J. 2015. The Phyre2 web portal for protein modeling, prediction and analysis. *Nature Protocols,* 10**,** 845-858.

KIESER, T., BIBB, M., BUTTNER, M., CHATER, K. & HOPWOOD, D. 2000. *Practical Streptomyces Genetics,* Norwich, England, John Innes Foundation.

KIKUCHI, S., SHIBUYA, I. & MATSUMOTO, K. 2000. Viability of an *Escherichia coli pgsA*Null Mutant Lacking Detectable Phosphatidylglycerol and Cardiolipin. *Journal of Bacteriology,* 182**,** 371-376.

KIM, D.-W., CHATER, K., LEE, K.-J. & HESKETH, A. 2005. Changes in the extracellular proteome caused by the absence of the *bldA* gene product, a developmentally significant tRNA, reveal a new target for the pleiotropic regulator AdpA in *Streptomyces coelicolor*. *Journal of Bacteriology,* 187**,** 2957-2966.

KIM, E.-S., HONG, H.-J., CHOI, C.-Y. & COHEN, S. N. 2001. Modulation of actinorhodin biosynthesis in *Streptomyces lividans* by glucose repression of *afsR2* gene transcription. *Journal of Bacteriology,* 183**,** 2198-2203.

KIM, H.-J., CALCUTT, M. J., SCHMIDT, F. J. & CHATER, K. F. 2000. Partitioning of the linear chromosome during sporulation of *Streptomyces*

coelicolor A3 (2) involves an *oriC*-linked *parAB* locus. *Journal of Bacteriology,* 182**,** 1313-1320.

KIM, I. K., KIM, M. K., LEE, C. J., YIM, H. S., CHA, S. S. & KANG, S. O. 2004. Crystallization and preliminary X-ray crystallographic analysis of the DNA-binding domain of BldD from *Streptomyces coelicolor* A3(2). *Acta Crystallographica,* 60**,** 1115-1117.

KIM, I. K., LEE, C. J., KIM, M. K., KIM, J. M., KIM, J. H., YIM, H. S., CHA, S. S. & KANG, S. O. 2006. Crystal structure of the DNA-binding domain of BldD, a central regulator of aerial mycelium formation in *Streptomyces coelicolor* A3(2). *Molecular Microbiology,* 60**,** 1179-1193.

KLEINSCHNITZ, E. M., HEICHLINGER, A., SCHIRNER, K., WINKLER, J., LATUS, A., MALDENER, I., WOHLLEBEN, W. & MUTH, G. 2011. Proteins encoded by the *mre* gene cluster in *Streptomyces coelicolor* A3(2) cooperate in spore wall synthesis. *Molecular Microbiology,* 79**,** 1367-1379.

KOBAYASHI, K., EHRLICH, S. D., ALBERTINI, A., AMATI, G., ANDERSEN, K., ARNAUD, M., ASAI, K., ASHIKAGA, S., AYMERICH, S. & BESSIERES, P. 2003. Essential *Bacillus subtilis* genes. *Proceedings of the National Academy of Sciences,* 100**,** 4678-4683.

KODANI, S., HUDSON, M. E., DURRANT, M. C., BUTTNER, M. J., NODWELL, J. R. & WILLEY, J. M. 2004. The SapB morphogen is a lantibiotic-like peptide derived from the product of the developmental gene *ramS* in *Streptomyces coelicolor*. *Proceedings of the National Academy of Sciences,* 101**,** 11448-11453.

KOONIN, E. V. 2000. How Many Genes Can Make a Cell: The Minimal-Gene-Set Concept 1. *Annual Review of Genomics and Human Genetics,* 1**,** 99-116.

KOPPELMAN, C. M., AARSMAN, M. E., POSTMUS, J., PAS, E., MUIJSERS, A. O., SCHEFFERS, D. J., NANNINGA, N. & DEN BLAAUWEN, T. 2004. R174 of *Escherichia coli* FtsZ is involved in membrane interaction and protofilament bundling, and is essential for cell division. *Molecular Microbiology,* 51**,** 645-657.

KORMANEC, J., HOMEROVA, D., POTUCKOVA, L., NOVAKOVA, R. & REZUCHOVA, B. 1996. Differential expression of two sporulation specific sigma factors of *Streptomyces aureofaciens* correlates with the developmental stage. *Gene,* 181**,** 19-27.

KWAK, J., DHARMATILAKE, A. J., JIANG, H. & KENDRICK, K. E. 2001. Differential regulation of *ftsZ* transcription during septation of *Streptomyces griseus. Journal of Bacteriology,* 183**,** 5092-5101.

LABISCHINSKI, H. & MAIDHOF, H. C. 1994. Bacterial peptidoglycan: overview and evolving concepts. *New Comprehensive Biochemistry,* 27**,** 23-38.

LANDGRAF, B. J., ARCINAS, A. J., LEE, K. H. & BOOKER, S. J. 2013. Identification of an intermediate methyl carrier in the radical *S*-adenosylmethionine methylthiotransferases RimO and MiaB. *Journal of the American Chemical Society,* 135**,** 15404-15416.

LEE, E.-J., KAROONUTHAISIRI, N., KIM, H.-S., PARK, J.-H., CHA, C.-J., KAO, C. M. & ROE, J.-H. 2005. A master regulator sigmaB governs osmotic and oxidative response as well as differentiation via a network of sigma factors in *Streptomyces coelicolor*. *Molecular Microbiology,* 57**,** 1252-1264.

LEE, E. J., CHO, Y. H., KIM, H. S. & ROE, J. H. 2004. Identification of sigmaB-dependent promoters using consensus-directed search of *Streptomyces coelicolor* genome. *Journal of Microbiology,* 42**,** 147-151.

LEE, K.-H., SALEH, L., ANTON, B. P., MADINGER, C. L., BENNER, J. S., IWIG, D. F., ROBERTS, R. J., KREBS, C. & BOOKER, S. J. 2009. Characterization of RimO, a new member of the methylthiotransferase subclass of the radical SAM superfamily. *Biochemistry,* 48**,** 10162-10174.

LEONARD, T. A., MØLLER-JENSEN, J. & LÖWE, J. 2005. Towards understanding the molecular basis of bacterial DNA segregation. *Philosophical Transactions of the Royal Society B: Biological Sciences,* 360**,** 523-535.

LEZHAVA, A., MIZUKAMI, T., KAJITANI, T., KAMEOKA, D., REDENBACH, M., SHINKAWA, H., NIMI, O. & KINASHI, H. 1995. Physical map of the linear chromosome of *Streptomyces griseus*. *Journal of Bacteriology,* 177**,** 6492-6498.

LI, L., STORM, P., KARLSSON, O. P., BERG, S. & WIESLANDER, Å. 2003. Irreversible binding and activity control of the 1, 2-diacylglycerol 3-glucosyltransferase from *Acholeplasma laidlawii* at an anionic lipid bilayer surface. *Biochemistry,* 42**,** 9677-9686.

LI, W., WU, J., TAO, W., ZHAO, C., WANG, Y., HE, X., CHANDRA, G., ZHOU, X., DENG, Z. & CHATER, K. F. 2007. A genetic and bioinformatic analysis of *Streptomyces coelicolor* genes containing TTA codons, possible targets for regulation by a developmentally significant tRNA. *FEMS Microbiology Letters,* 266**,** 20-28.

LIMAN, R., FACEY, P. D., VAN KEULEN, G., DYSON, P. J. & DEL SOL, R. 2013. A laterally acquired galactose oxidase-like gene is required for aerial development during osmotic stress in *Streptomyces coelicolor*. *PloS one,* 8**,** e54112.

LIMONET, M., SAFFROY, S., MAUJEAN, F., LINDER, M. & DELAUNAY, S. 2007. A comparison of disruption procedures for the analysis of phospholipids from *Streptomyces pristinaespiralis*. *Process Biochemistry,* 42**,** 700-703.

LIN, Y. S., KIESER, H. M., HOPWOOD, D. A. & CHEN, C. W. 1993. The chromosomal DNA of *Streptomyces lividans* 66 is linear. *Molecular Microbiology,* 10**,** 923-933.

LIND, J., RAMO, T., KLEMENT, M. L., BARANY-WALLJE, E., EPAND, R. M., EPAND, R. F., MALER, L. & WIESLANDER, A. 2007. High cationic charge and bilayer interface-binding helices in a regulatory lipid glycosyltransferase. *Biochemistry,* 46**,** 5664-5677.

LIU, G., CHATER, K. F., CHANDRA, G., NIU, G. & TAN, H. 2013. Molecular regulation of antibiotic biosynthesis in *Streptomyces* . *Microbiology and Molecular Biology Reviews,* 77**,** 112-143.

LOPEZ, C. S., ALICE, A. F., HERAS, H., RIVAS, E. A. & SANCHEZ-RIVAS, C. 2006. Role of anionic phospholipids in the adaptation of *Bacillus subtilis* to high salinity. *Microbiology,* 152**,** 605-616.

LOPEZ, C. S., HERAS, H., GARDA, H., RUZAL, S., SANCHEZ-RIVAS, C. & RIVAS, E. 2000. Biochemical and biophysical studies of *Bacillus subtilis* envelopes under hyperosmotic stress. *International Journal of Food Microbiology,* 55**,** 137-142.

LUO, Y., ASAI, K., SADAIE, Y. & HELMANN, J. D. 2010. Transcriptomic and phenotypic characterization of a *Bacillus subtilis* strain without extracytoplasmic function σ factors. *Journal of Bacteriology,* 192**,** 5736-5745.

LUSSIER, F.-X., DENIS, F. & SHARECK, F. 2010. Adaptation of the highly productive T7 expression system to *Streptomyces lividans*. *Applied and Environmental Microbiology,* 76**,** 967-970.

LUTKENHAUS, J. 2007. Assembly dynamics of the bacterial MinCDE system and spatial regulation of the Z ring. *Annual Review of Biochemistry,* 76**,** 539-562.

MACGILVRAY, M. E., LAPEK, J. D., JR., FRIEDMAN, A. E. & QUIVEY, R. G., JR. 2012. Cardiolipin biosynthesis in *Streptococcus mutans* is regulated in response to external pH. *Microbiology,* 158**,** 2133-2143.

MANTECA, A., JUNG, H. R., SCHWAMMLE, V., JENSEN, O. N. & SANCHEZ, J. 2010. Quantitative proteome analysis of *Streptomyces coelicolor* nonsporulating liquid cultures demonstrates a complex differentiation process comparable to that occurring in sporulating solid cultures. *Journal of Proteome Research,* 9**,** 4801-4811.

MARGOLIN, W. 2005. FtsZ and the division of prokaryotic cells and organelles. *Nature Reviews Molecular and Cell Biology,* 6**,** 862-871.

MARGOLIN, W. 2009. Sculpting the bacterial cell. *Current Biology,* 19**,** R812-R822.

MARIJUÁN, P. C., NAVARRO, J. & DEL MORAL, R. 2010. On prokaryotic intelligence: strategies for sensing the environment. *Biosystems,* 99**,** 94-103.

MARTIN, B., GARCIA, P., CASTANIE, M. P. & CLAVERYS, J. P. 1995. The *recA* gene of *Streptococcus pneumoniae* is part of a competence-induced operon and controls lysogenic induction. *Molecular Microbiology,* 15**,** 367-379.

MARTÍNEZ, L. F., BISHOP, A., PARKES, L., DEL SOL, R., SALERNO, P., SEVCIKOVA, B., MAZURAKOVA, V., KORMANEC, J. & DYSON, P. 2009. Osmoregulation in *Streptomyces coelicolor*: modulation of SigB activity by OsaC. *Molecular Microbiology,* 71**,** 1250-1262.

MATSUMOTO, K. 2001. Dispensable nature of phosphatidylglycerol in *Escherichia coli*: dual roles of anionic phospholipids. *Molecular Microbiology,* 39**,** 1427-1433.

MATSUMOTO, K., KUSAKA, J., NISHIBORI, A. & HARA, H. 2006. Lipid domains in bacterial membranes. *Molecular Microbiology,* 61**,** 1110-1117.

MATTHEWS, B. W., OHLENDORF, D. H., ANDERSON, W. F. & TAKEDA, Y. 1982. Structure of the DNA-binding region of *lac* repressor inferred from its homology with *cro* repressor. *Proceedings of the National Academy of Sciences,* 79**,** 1428-1432.

MAZZA, P., NOENS, E. E., SCHIRNER, K., GRANTCHAROVA, N., MOMMAAS, A. M., KOERTEN, H. K., MUTH, G., FLARDH, K., VAN WEZEL, G. P. & WOHLLEBEN, W. 2006. MreB of *Streptomyces coelicolor* is not essential for vegetative growth but is required for the integrity of aerial hyphae and spores. *Molecular Microbiology,* 60**,** 838-852.

MCCORMICK, J. R. 2009. Cell division is dispensable but not irrelevant in *Streptomyces* . *Current Opinion in Microbiology,* 12**,** 689-698.

MCCORMICK, J. R. & FLÄRDH, K. 2012. Signals and regulators that govern *Streptomyces* development. *FEMS Mcrobiology Reviews,* 36**,** 206-231.

MCCORMICK, J. R. & LOSICK, R. 1996. Cell division gene *ftsQ* is required for efficient sporulation but not growth and viability in *Streptomyces coelicolor* A3(2). *Journal of Bacteriology,* 178**,** 5295-5301.

MCCORMICK, J. R., SU, E. P., DRIKS, A. & LOSICK, R. 1994. Growth and viability of *Streptomyces coelicolor* mutant for the cell division gene *ftsZ*. *Molecular Microbiology,* 14**,** 243-254.

MELZOCH, K., DE MATTOS, M. T. & NEIJSSEL, O. M. 1997. Production of acthinorhodin by *Streptomyces coelicolor* A3 (2) grown in chemostat culture. *Biotechnology and Bioengineering,* 54**,** 577-582.

MENON, S. K. & LAWRENCE, C. M. 2013. *Brenner's Encyclopedia of Genetics*, Elsevier Inc, 412-415

MEYER, P. & DWORKIN, J. 2007. Applications of fluorescence microscopy to single bacterial cells. *Research in Microbiology,* 158**,** 187-194.

MILEYKOVSKAYA, E. & DOWHAN, W. 2000. Visualization of phospholipid domains in *Escherichia coli* by using the cardiolipin-specific fluorescent dye 10-*N*-nonyl acridine orange. *Journal of Bacteriology,* 182**,** 1172-1175.

MILEYKOVSKAYA, E. & DOWHAN, W. 2005. Role of membrane lipids in bacterial division-site selection. *Current Opinion in Microbiology,* 8**,** 135-142.

MILEYKOVSKAYA, E. & DOWHAN, W. 2009. Cardiolipin membrane domains in prokaryotes and eukaryotes. *Biochimica et Biophysica Acta,* 1788**,** 2084-2091.

MILEYKOVSKAYA, E., SUN, Q., MARGOLIN, W. & DOWHAN, W. 1998. Localization and function of early cell division proteins in filamentous *Escherichia coli* cells lacking phosphatidylethanolamine. *Journal of Bacteriology,* 180**,** 4252-4257.

MINGYAR, E., SEVCIKOVA, B., REZUCHOVA, B., HOMEROVA, D., NOVAKOVA, R. & KORMANEC, J. 2014. The sigma(F)-specific anti-sigma factor RsfA is one of the protein kinases that phosphorylates the pleiotropic anti-anti-sigma factor BldG in *Streptomyces coelicolor* A3(2). *Gene,* 538**,** 280-287.

MIYAZAKI, C., KURODA, M., OHTA, A. & SHIBUYA, I. 1985. Genetic manipulation of membrane phospholipid composition in *Escherichia coli*: *pgsA* mutants defective in phosphatidylglycerol synthesis. *Proceedings of the National Academy of Sciences,* 82**,** 7530-7534.

MOHAMMADI, T., VAN DAM, V., SIJBRANDI, R., VERNET, T., ZAPUN, A., BOUHSS, A., DIEPEVEEN-DE BRUIN, M., NGUYEN-DISTECHE, M., DE KRUIJFF, B. & BREUKINK, E. 2011. Identification of FtsW as a transporter of lipid-linked cell wall precursors across the membrane. *EMBO Journal,* 30**,** 1425-1432.

MOLLE, V., PALFRAMAN, W. J., FINDLAY, K. C. & BUTTNER, M. J. 2000. WhiD and WhiB, homologous proteins required for different stages of sporulation in *Streptomyces coelicolor* A3(2). *Journal of Bacteriology,* 182**,** 1286-1295.

MORTIER-BARRIERE, I., DE SAIZIEU, A., CLAVERYS, J. P. & MARTIN, B. 1998. Competence-specific induction of *recA* is required for full recombination proficiency during transformation in *Streptococcus pneumoniae*. *Molecular Microbiology,* 27**,** 159-170.

MOSER, R., AKTAS, M. & NARBERHAUS, F. 2014. Phosphatidylcholine biosynthesis in *Xanthomonas campestris* via a yeast-like acylation pathway. *Molecular Microbiology,* 91**,** 736-750.

MUCHOVA, K., JAMROSKOVIC, J. & BARAK, I. 2010. Lipid domains in *Bacillus subtilis* anucleate cells. *Research Microbiology,* 161**,** 783-790.

MUCHOVA, K., WILKINSON, A. J. & BARAK, I. 2011. Changes of lipid domains in *Bacillus subtilis* cells with disrupted cell wall peptidoglycan. *FEMS Microbiology Letters,* 325**,** 92-98.

MURAKAMI, T., HOLT, T. G. & THOMPSON, C. J. 1989. Thiostrepton-induced gene expression in *Streptomyces lividans*. *Journal of Bacteriology,* 171**,** 1459-1466.

MUSHEGIAN, A. 1999. The minimal genome concept. *Current Opinion in Genetics and Development,* 9**,** 709-714.

NAIR, S. & FINKEL, S. E. 2004. Dps protects cells against multiple stresses during stationary phase. *Journal of Bacteriology,* 186**,** 4192-4198.

NGUYEN, K. T., WILLEY, J. M., NGUYEN, L. D., NGUYEN, L. T., VIOLLIER, P. H. & THOMPSON, C. J. 2002. A central regulator of morphological differentiation in the multicellular bacterium *Streptomyces coelicolor*. *Molecular Microbiology,* 46**,** 1223-1238.

NIE, J., HAO, X., CHEN, D., HAN, X., CHANG, Z. & SHI, Y. 2010. A novel function of the human CLS1 in phosphatidylglycerol synthesis and remodeling. *Biochimica et Biophysica Acta,* 1801**,** 438-445.

NODWELL, J. R. & LOSICK, R. 1998. Purification of an extracellular signaling molecule involved in production of aerial mycelium by *Streptomyces coelicolor*. *Journal of Bacteriology,* 180**,** 1334-1337.

NODWELL, J. R., MCGOVERN, K. & LOSICK, R. 1996. An oligopeptide permease responsible for the import of an extracellular signal governing aerial mycelium formation in *Streptomyces coelicolor*. *Molecular Microbiology,* 22**,** 881-893.

NOENS, E. E., MERSINIAS, V., TRAAG, B. A., SMITH, C. P., KOERTEN, H. K. & VAN WEZEL, G. P. 2005. SsgA-like proteins determine the fate of peptidoglycan during sporulation of *Streptomyces coelicolor*. *Molecular Microbiology,* 58**,** 929-944.

NOGLY, P., GUSHCHIN, I., REMEEVA, A., ESTEVES, A. M., BORGES, N., MA, P., ISHCHENKO, A., GRUDININ, S., ROUND, E. & MORAES, I. 2014. X-ray structure of a CDP-alcohol phosphatidyltransferase membrane enzyme and insights into its catalytic mechanism. *Nature Communications,* 5.

NORRIS, V. & AMAR, P. 2012. Chromosome replication in *Escherichia coli*: life on the scales. *Life,* 2**,** 286-312.

O'CONNOR, T. J. & NODWELL, J. R. 2005. Pivotal roles for the receiver domain in the mechanism of action of the response regulator RamR of *Streptomyces coelicolor*. *Journal of Molecular Biology,* 351**,** 1030-1047.

OHLENDORF, D. H., ANDERSON, W. F., FISHER, R. G., TAKEDA, Y. & MATTHEWS, B. W. 1982. The molecular basis of DNA-protein recognition inferred from the structure of cro repressor. *Nature,* 298**,** 718-723.

OHNISHI, Y., KAMEYAMA, S., ONAKA, H. & HORINOUCHI, S. 1999. The A-factor regulatory cascade leading to streptomycin biosynthesis in *Streptomyces griseus* : identification of a target gene of the A-factor receptor. *Molecular Microbiology,* 34**,** 102-111.

OKESLI, A., COOPER, L. E., FOGLE, E. J. & VAN DER DONK, W. A. 2011. Nine post-translational modifications during the biosynthesis of cinnamycin. *Journal of the American Chemical Society,* 133**,** 13753-13760.

PABO, C. O. & SAUER, R. T. 1984. Protein-DNA recognition. *Annual Review of Biochemisty,* 53**,** 293-321.

PAGET, M. S., LEIBOVITZ, E. & BUTTNER, M. J. 1999. A putative two-component signal transduction system regulates σE, a sigma factor required for normal cell wall integrity in *Streptomyces coelicolor* A3 (2). *Molecular Microbiology,* 33**,** 97-107.

PAGET, M. S., MOLLE, V., COHEN, G., AHARONOWITZ, Y. & BUTTNER, M. J. 2001. Defining the disulphide stress response in *Streptomyces coelicolor* A3(2): identification of the sigmaR regulon. *Molecular Microbiology,* 42**,** 1007-1020.

PALOMINO, M. M., ALLIEVI, M. C., GRUNDLING, A., SANCHEZ-RIVAS, C. & RUZAL, S. M. 2013. Osmotic stress adaptation in *Lactobacillus casei* BL23 leads to structural changes in the cell wall polymer lipoteichoic acid. *Microbiology,* 159**,** 2416-2426.

PANDZA, K., PFALZER, G., CULLUM, J. & HRANUELI, D. 1997. Physical mapping shows that the unstable oxytetracycline gene cluster of *Streptomyces rimosus* lies close to one end of the linear chromosome. *Microbiology,* 143**,** 1493-1501.

PARADKAR, A., TREFZER, A., CHAKRABURTTY, R. & STASSI, D. 2003. *Streptomyces* genetics: a genomic perspective. *Critical Reviews in Biotechnology,* 23**,** 1-27.

PARASHAR, A., COLVIN, K. R., BIGNELL, D. R. & LESKIW, B. K. 2009. BldG and SCO3548 interact antagonistically to control key developmental processes in *Streptomyces coelicolor*. *Journal of Bacteriology,* 191**,** 2541-2550.

PARISH, T. & STOKER, N. G. 1997. Development and use of a conditional antisense mutagenesis system in *mycobacteria*. *FEMS Microbiology Letters,* 154**,** 151-157.

PARSONS, J. B. & ROCK, C. O. 2011. Is bacterial fatty acid synthesis a valid target for antibacterial drug discovery? *Current Opinion Microbioogy,* 14**,** 544-549.

PARSONS, J. B. & ROCK, C. O. 2013. Bacterial lipids: metabolism and membrane homeostasis. *Progress in Lipid Research,* 52**,** 249-276.

PENG, Q., YANG, M., WANG, W., HAN, L., WANG, G., WANG, P., ZHANG, J. & SONG, F. 2014. Activation of gab cluster transcription in *Bacillus thuringiensis* by γ-aminobutyric acid or succinic semialdehyde is mediated by the Sigma 54-dependent transcriptional activator GabR. *BMC Microbiology,* 14**,** 306.

PIERREL, F., BJORK, G. R., FONTECAVE, M. & ATTA, M. 2002. Enzymatic modification of tRNAs: MiaB is an iron-sulfur protein. *Journal of Biological Chemistry,* 277**,** 13367-13370.

PLUSCHKE, G., HIROTA, Y. & OVERATH, P. 1978. Function of phospholipids in *Escherichia coli*. Characterization of a mutant deficient in cardiolipin synthesis. *Journal of Biological Chemistry*, 253**,** 5048-5055.

POPE, M. K., GREEN, B. & WESTPHELING, J. 1998. The *bldB* Gene Encodes a Small Protein Required for Morphogenesis, Antibiotic Production, and Catabolite Control in *Streptomyces coelicolor*. *Journal of Bacteriology,* 180**,** 1556-1562.

POTÚČKOVÁ, L., KELEMEN, G. H., FINDLAY, K. C., LONETTO, M. A., BUTTNER, M. J. & KORMANEC, J. 1995. A new RNA polymerase sigma factor, σ^F is required for the late stages of morphological differentiation in *Streptomyces* spp. *Molecular Microbiology,* 17**,** 37-48.

POWELL, D., DUCKWORTH, M. & BADDILEY, J. 1974. An acylated mannan in the membrane of *Micrococcus lysodeikticus*. *FEBS Letters,* 41**,** 259-263.

PROSSER, J. I. & TOUGH, A. J. 1991. Growth mechanisms and growth kinetics of filamentous microorganisms. *Critical Reviews in Biotechnology,* 10**,** 253-274.

RAHMAN, M. M., KOLLI, V. S., KAHLER, C. M., SHIH, G., STEPHENS, D. S. & CARLSON, R. W. 2000. The membrane phospholipids of *Neisseria meningitidis* and *Neisseria gonorrhoeae* as characterized by fast atom bombardment mass spectrometry. *Microbiology,* 146**,** 1901-1911.

RAHMAN, O., CUMMINGS, S. P. & SUTCLIFFE, I. C. 2009a. Phenotypic variation in *Streptomyces* sp. DSM 40537, a lipoteichoic acid producing actinomycete. *Letters in Applied Microbiology,* 48**,** 226-229.

RAHMAN, O., DOVER, L. G. & SUTCLIFFE, I. C. 2009b. Lipoteichoic acid biosynthesis: two steps forwards, one step sideways? *Trends in Microbiology,* 17**,** 219-225.

RANA, F. R., SULTANY, C. M. & BLAZYK, J. 1991. Determination of the lipid composition of *Salmonella typhimurium* outer membranes by 31 P NMR. *Journal of Microbiological Methods,* 14**,** 41-51.

REDENBACH, M., KIESER, H. M., DENAPAITE, D., EICHNER, A., CULLUM, J., KINASHI, H. & HOPWOOD, D. 1996a. A set of ordered cosmids and a detailed genetic and physical map for the 8 Mb *Streptomyces coelicolor* A3 (2) chromosome. *Molecular Microbiology,* 21**,** 77-96.

REMENTZIS, J. & SAMELIS, J. 1996. Rapid GC analysis of cellular fatty acids for characterizing *Lactobacillus sake* and *Lact. curvatus* strains of meat origin. *Letters in Applied Microbiology,* 23**,** 379-384.

REVILL, W. P., BIBB, M. J. & HOPWOOD, D. A. 1995. Purification of a malonyltransferase from *Streptomyces coelicolor* A3(2) and analysis of its genetic determinant. *Journal of Bacteriology,* 177**,** 3946-3952.

REVILL, W. P., BIBB, M. J. & HOPWOOD, D. A. 1996. Relationships between fatty acid and polyketide synthases from *Streptomyces coelicolor* A3(2): characterization of the fatty acid synthase acyl carrier protein. *Journal of Bacteriology,* 178**,** 5660-5667.

REVILL, W. P., BIBB, M. J., SCHEU, A. K., KIESER, H. J. & HOPWOOD, D. A. 2001. Beta-ketoacyl acyl carrier protein synthase III (FabH) is essential for fatty acid biosynthesis in *Streptomyces coelicolor* A3(2). *Journal of Bacteriology,* 183**,** 3526-3530.

REYES-LAMOTHE, R., WANG, X. & SHERRATT, D. 2008. *Escherichia coli* and its chromosome. *Trends Microbiology,* 16**,** 238-245.

RIGALI, S., DEROUAUX, A., GIANNOTTA, F. & DUSART, J. 2002. Subdivision of the helix-turn-helix GntR family of bacterial regulators in the FadR, HutC, MocR, and YtrA subfamilies. *Journal of Biological Chemistry,* 277**,** 12507-12515.

RIOSERAS, B., LÓPEZ-GARCÍA, M. T., YAGÜE, P., SÁNCHEZ, J. & MANTECA, Á. 2014. Mycelium differentiation and development of *Streptomyces coelicolor* in lab-scale bioreactors: programmed cell death, differentiation, and lysis are closely linked to undecylprodigiosin and actinorhodin production. *Bioresource Technology,* 151**,** 191-198.

ROBICHON, C., VIDAL-INGIGLIARDI, D. & PUGSLEY, A. P. 2005. Depletion of apolipoprotein *N*-acyltransferase causes mislocalization of outer membrane lipoproteins in *Escherichia coli*. *Journal of Biological Chemistry,* 280**,** 974-983.

RODRÍGUEZ-GARCÍA, A., COMBES, P., PÉREZ-REDONDO, R., SMITH, M. C. & SMITH, M. C. 2005. Natural and synthetic tetracycline-inducible promoters for use in the antibiotic-producing bacteria *Streptomyces* . *Nucleic Acids Research,* 33**,** e87-e87.

ROMANTSOV, T., BATTLE, A. R., HENDEL, J. L., MARTINAC, B. & WOOD, J. M. 2010. Protein localization in *Escherichia coli* cells: comparison of the cytoplasmic membrane proteins ProP, LacY, ProW, AqpZ, MscS, and MscL. *Journal of Bacteriology,* 192**,** 912-924.

ROMANTSOV, T., HELBIG, S., CULHAM, D. E., GILL, C., STALKER, L. & WOOD, J. M. 2007. Cardiolipin promotes polar localization of osmosensory transporter ProP in *Escherichia coli*. *Molecular Microbiology,* 64**,** 1455-1465.

ROMANTSOV, T., STALKER, L., CULHAM, D. E. & WOOD, J. M. 2008. Cardiolipin controls the osmotic stress response and the subcellular location of transporter ProP in *Escherichia coli*. *Journal of Biological Chemistry,* 283**,** 12314-12323.

ROTHFIELD, L., TAGHBALOUT, A. & SHIH, Y. L. 2005. Spatial control of bacterial division-site placement. *Nature Reviews Microbiology,* 3**,** 959-968.

RUBAN-OSMIALOWSKA, B., JAKIMOWICZ, D., SMULCZYK-KRAWCZYSZYN, A., CHATER, K. F. & ZAKRZEWSKA-CZERWINSKA, J. 2006. Replisome localization in vegetative and aerial hyphae of *Streptomyces coelicolor*. *Journal of Bacteriology,* 188**,** 7311-7316.

RUDOLPH, M. M., VOCKENHUBER, M. P. & SUESS, B. 2013. Synthetic riboswitches for the conditional control of gene expression in *Streptomyces coelicolor*. *Microbiology,* 159**,** 1416-1422.

RUIZ, N. & SILHAVY, T. J. 2005. Sensing external stress: watchdogs of the *Escherichia coli* cell envelope. *Current Opinion in Microbiology,* 8**,** 122-126.

RYDING, N. J., KELEMEN, G. H., WHATLING, C. A., FLARDH, K., BUTTNER, M. J. & CHATER, K. F. 1998. A developmentally regulated gene encoding a repressor-like protein is essential for sporulation in *Streptomyces coelicolor* A3(2). *Molecular Microbiology,* 29**,** 343-357.

SAITOU, N. & NEI, M. 1987. The neighbor-joining method: a new method for reconstructing phylogenetic trees. *Molecular Biology and Evolution,* 4**,** 406-425.

SAKURAI, I., HAGIO, M., GOMBOS, Z., TYYSTJÄRVI, T., PAAKKARINEN, V., ARO, E.-M. & WADA, H. 2003. Requirement of phosphatidylglycerol for maintenance of photosynthetic machinery. *Plant Physiology,* 133**,** 1376-1384.

SALERNO, P., LARSSON, J., BUCCA, G., LAING, E., SMITH, C. P. & FLÄRDH, K. 2009. One of the two genes encoding nucleoid-associated HU proteins in *Streptomyces coelicolor* is developmentally regulated and specifically involved in spore maturation. *Journal of Bacteriology,* 191**,** 6489-6500.

SAMBROOK, J. & RUSSELL, D. W. 2001. *Molecular Cloning: A Laboratory Manual,* Cold Spring Harbor, New York, Cold Spring Harbor Laboratory Press.

SANDOVAL-CALDERON, M., GEIGER, O., GUAN, Z., BARONA-GOMEZ, F. & SOHLENKAMP, C. 2009. A Eukaryote-like Cardiolipin Synthase Is Present in *Streptomyces coelicolor* and in Most Actinobacteria. *Journal of Biological Chemistry* 284**,** 17383–17390.

SAUER, R. T., YOCUM, R. R., DOOLITTLE, R. F., LEWIS, M. & PABO, C. O. 1982. Homology among DNA-binding proteins suggests use of a conserved super-secondary structure. *Nature,* 298**,** 447-451.

SAWYER, E. B., CLAESSEN, D., GRAS, S. L. & PERRETT, S. 2012. Exploiting amyloid: how and why bacteria use cross-*β* fibrils. *Biochemical Society Transactions,* 40**,** 728-734.

SAWYER, E. B., CLAESSEN, D., HAAS, M., HURGOBIN, B. & GRAS, S. L. 2011. The assembly of individual chaplin peptides from *Streptomyces coelicolor* into functional amyloid fibrils. *PloS one,* 6**,** e18839.

SCHAUNER, C., DARY, A., LEBRIHI, A., LEBLOND, P., DECARIS, B. & GERMAIN, P. 1999. Modulation of lipid metabolism and spiramycin biosynthesis in *Streptomyces ambofaciens* unstable mutants. *Applied and Environmental Microbiology,* 65**,** 2730-2737.

SCHEFFERS, D. J. & PINHO, M. G. 2005. Bacterial cell wall synthesis: new insights from localization studies. *Microbiology and Molecular Biology Reviews,* 69**,** 585-607.

SCHLAME, M., RUA, D. & GREENBERG, M. L. 2000. The biosynthesis and functional role of cardiolipin. *Progress in Lipid Research,* 39**,** 257-288.

SCHLEIFER, K. H. & KANDLER, O. 1972. Peptidoglycan types of bacterial cell walls and their taxonomic implications. *Bacteriology Review,* 36**,** 407-477.

SCHMIDTKE, P., LE GUILLOUX, V., MAUPETIT, J. & TUFFERY, P. 2010. fpocket: online tools for protein ensemble pocket detection and tracking. *Nucleic Acids Research,* 38**,** 582-589.

SCHWEDOCK, J., MCCORMICK, J. R., ANGERT, E. R., NODWELL, J. R. & LOSICK, R. 1997. Assembly of the cell division protein FtsZ into ladder-like structures in the aerial hyphae of *Streptomyces coelicolor*. *Molecular Microbiology,* 25**,** 847-858.

SCHWIENTEK, P., SZCZEPANOWSKI, R., RUCKERT, C., STOYE, J. & PUHLER, A. 2011. Sequencing of high G+C microbial genomes using the ultrafast pyrosequencing technology. *Journal of Biotechnology,* 155**,** 68-77.

SCIARA, G., CLARKE, O. B., TOMASEK, D., KLOSS, B., TABUSO, S., BYFIELD, R., COHN, R., BANERJEE, S., RAJASHANKAR, K. R. & SLAVKOVIC, V. 2014. Structural basis for catalysis in a CDP-alcohol phosphotransferase. *Nature Communications,* 5,4068.

SEDDON, A. M., LORCH, M., CES, O., TEMPLER, R. H., MACRAE, F. & BOOTH, P. J. 2008. Phosphatidylglycerol lipids enhance folding of an α helical membrane protein. *Journal of Molecular Biology,* 380**,** 548-556.

SELTMANN, G. & HOLST, O. 2002. *The bacterial cell wall,* Springer Science & Business Media,9-102.

SEVCIKOVA, B., BENADA, O., KOFRONOVA, O. & KORMANEC, J. 2001. Stress-response sigma factor sigma(H) is essential for morphological differentiation of *Streptomyces coelicolor* A3(2). A*rchives of Microbiology,* 177**,** 98-106.

SEVCIKOVA, B., REZUCHOVA, B., HOMEROVA, D. & KORMANEC, J. 2010. The anti-anti-sigma factor BldG is involved in activation of the stress response sigma factor sigma(H) in *Streptomyces coelicolor* A3(2). *Journal of Bacteriology,* 192**,** 5674-5681.

SHIMKETS, L. J. 2014. *Development, Prokaryotic: Variety and Versatility,* Athens, GA, Elsevier Inc.

SHIN, S. C., AHN DO, H., KIM, S. J., LEE, H., OH, T. J., LEE, J. E. & PARK, H. 2013. Advantages of Single-Molecule Real-Time Sequencing in High-GC Content Genomes. *PloS one,* 8**,** e68824.

SIEVERS, S., M ERNST, C., GEIGER, T., HECKER, M., WOLZ, C., BECHER, D. & PESCHEL, A. 2010. Changing the phospholipid composition of *Staphylococcus aureus* causes distinct changes in membrane proteome and membrane-sensory regulators. *Proteomics,* 10**,** 1685-1693.

SILHAVY, T. J., KAHNE, D. & WALKER, S. 2010. The Bacterial Cell Envelope. *Cold Spring Harbor perspectives in biology,* 2**,** a000414.

SLEATOR, R. D. & HILL, C. 2002. Bacterial osmoadaptation: the role of osmolytes in bacterial stress and virulence. *FEMS Microbiology Reviews,* 26**,** 49-71.

SMOKVINA, T., MAZODIER, P., BOCCARD, F., THOMPSON, C. J. & GUERINEAU, M. 1990. Construction of a series of pSAM2-based integrative vectors for use in actinomycetes. *Gene,* 94**,** 53-59.

SOFIA, H. J., CHEN, G., HETZLER, B. G., REYES-SPINDOLA, J. F. & MILLER, N. E. 2001. Radical SAM, a novel protein superfamily linking unresolved steps in familiar biosynthetic pathways with radical mechanisms: functional characterization using new analysis and information visualization methods. *Nucleic Acids Research,* 29**,** 1097-1106.

SOHLENKAMP, C. & GEIGER, O. 2015. Bacterial membrane lipids: diversity in structures and pathways. *FEMS Mcrobiology Reviews***,** fuv008, 1-27.

SOLIVERI, J., BROWN, K. L., BUTTNER, M. J. & CHATER, K. F. 1992. Two promoters for the whiB sporulation gene of *Streptomyces coelicolor* A3(2) and their activities in relation to development. *Journal of Bacteriology,* 174**,** 6215-6220.

STEENBERGEN, J. N., ALDER, J., THORNE, G. M. & TALLY, F. P. 2005. Daptomycin: a lipopeptide antibiotic for the treatment of serious Gram-positive infections. *Journal of Antimicrobial Chemotherapy,* 55**,** 283-288.

STRAUS, S. K. & HANCOCK, R. E. 2006. Mode of action of the new antibiotic for Gram-positive pathogens daptomycin: comparison with cationic antimicrobial peptides and lipopeptides. *Biochimica et Biophysica Acta,* 1758**,** 1215-1223.

SUMMERS, R. G., ALI, A., SHEN, B., WESSEL, W. A. & HUTCHINSON, C. R. 1995. Malonyl-coenzyme A:acyl carrier protein acyltransferase of *Streptomyces glaucescens*: a possible link between fatty acid and polyketide biosynthesis. *Biochemistry,* 34**,** 9389-9402.

SUN, J., KELEMEN, G. H., FERNANDEZ-ABALOS, J. M. & BIBB, M. J. 1999. Green fluorescent protein as a reporter for spatial and temporal gene expression in *Streptomyces coelicolor* A3(2). *Microbiology,* 145**,** 2221-2227.

SUTCLIFFE, I. C. 2010. A phylum level perspective on bacterial cell envelope architecture. *Trends in Microbiology,* 18**,** 464-470.

SUTCLIFFE, I. C., HARRINGTON, D. J. & HUTCHINGS, M. I. 2012. A phylum level analysis reveals lipoprotein biosynthesis to be a fundamental property of bacteria. *Protein Cell,* 3**,** 163-170.

SUTCLIFFE, I. C. & SHAW, N. 1991. Atypical lipoteichoic acids of Gram-positive bacteria. *Journal of Bacteriology,* 173**,** 7065-7069.

SUZUKI, M., HARA, H. & MATSUMOTO, K. 2002. Envelope disorder of *Escherichia coli* cells lacking phosphatidylglycerol. *Journal of Bacteriology,* 184**,** 5418-5425.

SUZUKI, N., OKAI, N., NONAKA, H., TSUGE, Y., INUI, M. & YUKAWA, H. 2006. High-throughput transposon mutagenesis of *Corynebacterium glutamicum* and construction of a single-gene disruptant mutant library. *Applied and Environmental Microbiology,* 72**,** 3750-3755.

TAKANO, E., WHITE, J., THOMPSON, C. J. & BIBB, M. J. 1995. Construction of thiostrepton-inducible, high-copy-number expression vectors for use in *Streptomyces* spp. *Gene,* 166**,** 133-137.

TAKEDA, Y., OHLENDORF, D. H., ANDERSON, W. F. & MATTHEWS, B. W. 1983. DNA-binding proteins. *Science,* 221, 1020-1026.

TALBOT, N. J. 2003. Aerial morphogenesis: enter the chaplins. *Current Biology,* 13**,** R696-R698.

TAN, B. K., BOGDANOV, M., ZHAO, J., DOWHAN, W., RAETZ, C. R. & GUAN, Z. 2012. Discovery of a cardiolipin synthase utilizing phosphatidylethanolamine and phosphatidylglycerol as substrates. *Proceedings of the National Academy of Sciences,* 109**,** 16504-16509.

TANOUE, R., KOBAYASHI, M., KATAYAMA, K., NAGATA, N. & WADA, H. 2014. Phosphatidylglycerol biosynthesis is required for the development of embryos and normal membrane structures of chloroplasts and mitochondria in *Arabidopsis*. *FEBS Letters,* 588**,** 1680-1685.

THANBICHLER, M. & SHAPIRO, L. 2008. Getting organized--how bacterial cells move proteins and DNA. *Nature Reviews Microbiology,* 6**,** 28-40.

THOMPSON, B. J., WIDDICK, D. A., HICKS, M. G., CHANDRA, G., SUTCLIFFE, I. C., PALMER, T. & HUTCHINGS, M. I. 2010. Investigating lipoprotein biogenesis and function in the model Gram-positive bacterium *Streptomyces coelicolor*. *Molecular Microbiology,* 77**,** 943-957.

TIAN, Y., FOWLER, K., FINDLAY, K., TAN, H. & CHATER, K. F. 2007. An unusual response regulator influences sporulation at early and late stages in *Streptomyces coelicolor*. *Journal of Bacteriology,* 189**,** 2873-2885.

TOUCHSTONE, J. C. 1995. Thin-layer chromatographic procedures for lipid separation. *Journal of Chromatography B: Biomedical Sciences and Applications,* 671**,** 169-195.

TOUZÉ, T., BLANOT, D. & MENGIN-LECREULX, D. 2008. Substrate specificity and membrane topology of *Escherichia coli* PgpB, an undecaprenyl pyrophosphate phosphatase. *Journal of Biological Chemistry,* 283**,** 16573-16583.

TRAAG, B. A. & VAN WEZEL, G. P. 2008. The SsgA-like proteins in actinomycetes: small proteins up to a big task. *Antonie Van Leeuwenhoek,* 94**,** 85-97.

TREUNER-LANGE, A. & SOGAARD-ANDERSEN, L. 2014. Regulation of cell polarity in bacteria. *The Journal of Cell Biology,* 206**,** 7-17.

TSCHOWRI, N., SCHUMACHER, M. A., SCHLIMPERT, S., CHINNAM, N. B., FINDLAY, K. C., BRENNAN, R. G. & BUTTNER, M. J. 2014. Tetrameric c-di-GMP mediates effective transcription factor dimerization to control *Streptomyces* development. *Cell,* 158**,** 1136-1147.

UCHIYAMA, J., SASAKI, Y., NAGAHAMA, H., ITOU, A., MATSUOKA, S., MATSUMOTO, K. & HARA, H. 2010. Accumulation of σ^S due to enhanced synthesis and decreased degradation in acidic phospholipid-deficient *Escherichia coli* cells. *FEMS Microbiology Letters,* 307**,** 120-127.

USUI, M., SEMBONGI, H., MATSUZAKI, H., MATSUMOTO, K. & SHIBUYA, I. 1994. Primary structures of the wild-type and mutant alleles encoding the phosphatidylglycerophosphate synthase of *Escherichia coli*. *Journal of Bacteriology,* 176**,** 3389-3392.

VAN WEZEL, G. P., VAN DER MEULEN, J., KAWAMOTO, S., LUITEN, R. G., KOERTEN, H. K. & KRAAL, B. 2000. ssgA is essential for sporulation of *Streptomyces Streptomyces coelicolor* A3(2) and affects hyphal development by stimulating septum formation. *Journal of Bacteriology,* 182**,** 5653-5662.

VANCE, D. E. & VANCE, J. E. 2008. *Biochemistry of Lipids, Lipoproteins and Membranes,* Amsterdam, The Netherlands, Elsevier.

VIOLLIER, P. H., KELEMEN, G. H., DALE, G. E., NGUYEN, K. T., BUTTNER, M. J. & THOMPSON, C. J. 2003a. Specialized osmotic stress response systems involve multiple SigB-like sigma factors in *Streptomyces coelicolor*. *Molecular Microbiology,* 47**,** 699-714.

VIOLLIER, P. H., WEIHOFEN, A., FOLCHER, M. & THOMPSON, C. J. 2003b. Post-transcriptional regulation of the *Streptomyces coelicolor* stress responsive sigma factor, SigH, involves translational control, proteolytic processing, and an anti-sigma factor homolog. *Journal of Molecular Biology,* 325**,** 637-649.

VOLLMER, W. & BERTSCHE, U. 2008. Murein (peptidoglycan) structure, architecture and biosynthesis in *Escherichia coli*. *Biochimica et Biophysica Acta,* 1778**,** 1714-1734.

VOLLMER, W., BLANOT, D. & DE PEDRO, M. A. 2008a. Peptidoglycan structure and architecture. *FEMS Microbiology Reviews,* 32**,** 149-167.

VOLLMER, W., JORIS, B., CHARLIER, P. & FOSTER, S. 2008b. Bacterial peptidoglycan (murein) hydrolases. *FEMS Microbiology Reviews,* 32**,** 259-286.

WALLACE, K. K., ZHAO, B., MCARTHUR, H. A. & REYNOLDS, K. A. 1995. In vivo analysis of straight-chain and branched-chain fatty acid biosynthesis in three actinomycetes. *FEMS Microbiol Letters,* 131**,** 227-234.

WANG, L., YU, Y., HE, X., ZHOU, X., DENG, Z., CHATER, K. F. & TAO, M. 2007. Role of an FtsK-like protein in genetic stability in *Streptomyces Streptomyces coelicolor* A3(2). *Journal of Bacteriology,* 189**,** 2310-2318.

WATERHOUSE, A. M., PROCTER, J. B., MARTIN, D. M., CLAMP, M. & BARTON, G. J. 2009. Jalview Version 2--a multiple sequence alignment editor and analysis workbench. *Bioinformatics,* 25**,** 1189-1191.

WHITE, J. & BIBB, M. 1997. *bldA* dependence of undecylprodigiosin production in *Streptomyces coelicolor* A3(2) involves a pathway-specific regulatory cascade. *Journal of Bacteriology,* 179**,** 627-633.

WHITE, S. W., ZHENG, J., ZHANG, Y. M. & ROCK 2005. The structural biology of type II fatty acid biosynthesis. *Annual Review of Biochemistry,* 74**,** 791-831.

WHITWORTH, D. E. & COCK, P. J. 2009. Evolution of prokaryotic two-component systems: insights from comparative genomics. *Amino Acids,* 37**,** 459-466.

WIDDICK, D. A., HICKS, M. G., THOMPSON, B. J., TSCHUMI, A., CHANDRA, G., SUTCLIFFE, I. C., BRULLE, J. K., SANDER, P., PALMER, T. & HUTCHINGS, M. I. 2011. Dissecting the complete lipoprotein biogenesis pathway in *Streptomyces scabies*. *Molecular Microbiology,* 80**,** 1395-1412.

WILDERMUTH, H. & HOPWOOD, D. A. 1970. Septation during sporulation in *Streptomyces coelicolor*. *Journal of General Microbiology,* 60**,** 51-59.

WILLEMSE, J., BORST, J. W., DE WAAL, E., BISSELING, T. & VAN WEZEL, G. P. 2011. Positive control of cell division: FtsZ is recruited by SsgB during sporulation of *Streptomyces* . *Genes and Developmen*t, 25**,** 89-99.

WILLEY, J., SANTAMARIA, R., GUIJARRO, J., GEISTLICH, M. & LOSICK, R. 1991. Extracellular complementation of a developmental mutation implicates a small sporulation protein in aerial mycelium formation by *S. coelicolor*. *Cell,* 65**,** 641-650.

WILLEY, J., SCHWEDOCK, J. & LOSICK, R. 1993. Multiple extracellular signals govern the production of a morphogenetic protein involved in aerial mycelium formation by *Streptomyces coelicolor*. *Genes and Development,* 7**,** 895-903.

WILLEY, J. M., WILLEMS, A., KODANI, S. & NODWELL, J. R. 2006. Morphogenetic surfactants and their role in the formation of aerial hyphae in *treptomyces coelicolor*. *Molecular Microbiology,* 59**,** 731-742.

WITTMANN, A. & SUESS, B. 2012. Engineered riboswitches: Expanding researchers' toolbox with synthetic RNA regulators. *FEBS Letters,* 586**,** 2076-2083.

WOLDRINGH, C. L., JENSEN, P. R. & WESTERHOFF, H. V. 1995. Structure and partitioning of bacterial DNA: determined by a balance of compaction and expansion forces? *FEMS Microbiology Letters,* 131**,** 235-242.

WOLGEMUTH, C. W., IGOSHIN, O. & OSTER, G. 2003. The motility of mollicutes. *Biophysical Journal,* 85**,** 828-842.

XU, H., CHATER, K. F., DENG, Z. & TAO, M. 2008. A cellulose synthase-like protein involved in hyphal tip growth and morphological differentiation in *Streptomyces* . *Journal of Bacteriology,* 190**,** 4971-4978.

YAGUE, G., SEGOVIA, M. & VALERO-GUILLEN, P. L. 1997. Acyl phosphatidylglycerol: a major phospholipid of *Corynebacterium amycolatum*. *FEMS Microbiol Letters,* 151**,** 125-130.

YAGUE, P., LOPEZ-GARCIA, M. T., RIOSERAS, B., SANCHEZ, J. & MANTECA, A. 2012. New insights on the development of *Streptomyces* and their relationships with secondary metabolite production. *Current Trends Microbiology,* 8**,** 65-73.

YANG, C. C., HUANG, C. H., LI, C. Y., TSAY, Y. G., LEE, S. C. & CHEN, C. W. 2002. The terminal proteins of linear *Streptomyces* chromosomes and plasmids: a novel class of replication priming proteins. *Molecular Microbiology,* 43**,** 297-305.

YANISCH-PERRON, C., VIEIRA, J. & MESSING, J. 1985. Improved M13 phage cloning vectors and host strains: nucleotide sequences of the M13mp18 and pUC19 vectors. *Gene,* 33**,** 103-119.

YU, T. W. & HOPWOOD, D. A. 1995. Ectopic expression of the *Streptomyces coelicolor whiE* genes for polyketide spore pigment synthesis and their interaction with the act genes for actinorhodin biosynthesis. *Microbiology,* 141**,** 2779-2791.

ZAKRZEWSKA-CZERWINSKA, J., MAJKA, J. & SCHREMPF, H. 1995. Minimal requirements of the *Streptomyces lividans* 66 *oriC* region and its transcriptional and translational activities. *Journal of Bacteriology,* 177**,** 4765-4771.

ZHANG, L., FAN, F., PALMER, L. M., LONETTO, M. A., PETIT, C., VOELKER, L. L., JOHN, A. S., BANKOSKY, B., ROSENBERG, M. & MCDEVITT, D. 2000. Regulated gene expression in *Staphylococcus aureus* for identifying conditional lethal phenotypes and antibiotic mode of action. *Gene,* 255**,** 297-305.

ZHANG, Q., VAN DER DONK, W. A. & LIU, W. 2012. Radical-mediated enzymatic methylation: a tale of two SAMS. *Accounts of Chemical Research*, 45**,** 555-564.

ZHANG, Y. M. & ROCK, C. O. 2008. Membrane lipid homeostasis in bacteria. *Nature Reviews Microbiology*, 6**,** 222-233.

ZHOU, P., FLOROVA, G. & REYNOLDS, K. A. 1999. Polyketide synthase acyl carrier protein (ACP) as a substrate and a catalyst for malonyl ACP biosynthesis. *Chemistry and Biology*, 6**,** 577-584.